

Electronic Thesis and Dissertation Repository

4-26-2019 2:00 PM

Applications of Phosphotyrosine Superbinding SH2 Domain Variants

Xuguang Liu, *The University of Western Ontario*

Supervisor: Li, Shawn, *The University of Western Ontario*

A thesis submitted in partial fulfillment of the requirements for the Doctor of Philosophy degree in Biochemistry

© Xuguang Liu 2019

Follow this and additional works at: <https://ir.lib.uwo.ca/etd>



Part of the [Biotechnology Commons](#)

Recommended Citation

Liu, Xuguang, "Applications of Phosphotyrosine Superbinding SH2 Domain Variants" (2019). *Electronic Thesis and Dissertation Repository*. 6200.

<https://ir.lib.uwo.ca/etd/6200>

This Dissertation/Thesis is brought to you for free and open access by Scholarship@Western. It has been accepted for inclusion in Electronic Thesis and Dissertation Repository by an authorized administrator of Scholarship@Western. For more information, please contact wlsadmin@uwo.ca.

Abstract

Protein tyrosine kinases (PTKs, or TKs) have emerged as one of the most intensively pursued targets in the development of anti-cancer therapeutics, due to their critical roles in the phosphotyrosine (pTyr)-mediated signaling network that regulates many cancer-related cellular activities. The TKs, tyrosine phosphorylation phosphatases (PTPs) and pTyr recognition SH2 proteins are intensively tyrosine phosphorylated, which play a pivotal role in determining the signaling outcome of this network. More than 50% of all human proteins are tyrosine phosphorylated and many of these TK substrates have been proven functional in TK regulated cellular activities. Therefore, proteomics studies of tyrosine phosphorylation are of great value for expanding our understanding of this network and its role in tumorigenesis.

Taking advantage an engineered SH2 domain with superb pTyr binding affinity, an SH2-affinity purification mass spectrometry (SH2-AP-MS) assay was developed and optimized for global TK status profiling by determining the abundance of functionally significant TK pTyr peptides including the activation loops. Multiple known TK biomarkers were identified by this assay from a minute amount of protein extracts from cultured cells or clinical leukemia or solid tumor samples. In the quantitative AP-MS study of cancer cells treated by targeted therapeutics, differential TK responses were monitored. The receptor c-Kit was found to be dramatically upregulated with long-term trastuzumab treatment which contributed to acquired trastuzumab resistance in the SK-BR-3 breast cancer cells. These results revealed the potential applications of SH2-AP-MS in the discovery of novel TK biomarkers and examination of TK positive cancers in the clinical setting. In addition, a SH2 superbinder modified yeast two hybrid (Y2H) system was developed that is potentially capable of identifying TK substrate in a high-precision and high-throughput manner. This system consisted of an SH2-superbinder-fused bait that greatly promoted the reporter gene readout, a TK substrate prey or cDNA library preys, and a co-expressed TK under the control of a conditional promoter that allowed for reverse screen to eliminate false positives. In a medium-scale cDNA library screening for Src kinase substrates, 94 positive colonies were isolated representing 48 unique in-frame proteins or protein fragments, of which at least 9 proteins are known Src substrates or direct Src interactors.

Keywords

Tyrosine kinase, phosphorylation, superbinder SH2 domain, cancer, biomarker, affinity purification mass spectrometry, HER2 breast cancer, trastuzumab, drug resistance, yeast two hybrid, Src kinase substrate

Co-Authorship Statement

All chapters of this dissertation were written by Xuguang Liu and edited by Dr. Shawn Li, Dr. Ran Wei, Wen Qin and Courtney Voss.

Unless indicated otherwise where applicable, the experimental results and analysis presented in this dissertation were completed by Xuguang Liu.

The data presented in Chapter 2 is in preparation for publication, except for Table.2.1 and Figure.2.2 that were previously published. Dr. Tomonori Kaneko assisted in making the covalently-conjugated SH2 superbinder beads and optimizing the SH2-AP-MS workflow. Dr. Lei Li assisted in the MS data analysis. The RNA sequencing and data extraction were carried out by Dr. Lyugao Qin and Dr. Xiaoling Liu.

The data presented in Chapter 3 is in preparation for publication. Wen Qin assisted in the cDNA library screening and GAL4-AD immunoprecipitation.

Acknowledgments

First and foremost, I would like to express my sincere gratitude to my supervisor Dr. Shawn Li for his unwavering support of my graduate study and research through the years, and for his patience, motivation, and guidance.

I would like to thank my graduate advisory committee members Dr. David Litchfield, Dr. Patrick O'Donoghue and Dr. Stephen Ferguson for their advices and support.

Many thanks go to all Li lab members, especially Ms. Courtney Voss, Dr. Huadong Liu and Dr. Tomonori Kaneko for their help and friendship.

Finally, I would like to thank my parents Jianchu Liu and Kanglin Huang, and my wife Ran Wei for their understanding, encouragement and support through my years as a graduate student.

Table of Contents

Abstract	ii
Keywords	iii
Co-Authorship Statement.....	iv
Acknowledgments.....	v
Table of Contents	vi
List of Figures and Tables.....	ix
List of Abbreviations	xi
Chapter 1	1
1 General Introduction	1
1.1 TK inhibition drugs in cancer therapy	5
1.2 TKI resistance and TK signaling network complexity	8
1.2.1 Multi-functional components.....	9
1.2.2 Functional redundancy.....	11
1.3 Discovery of the SH2 Superbinder	15
1.4 Potential applications of the SH2 superbinder.....	17
1.5 References.....	19
Chapter 2.....	28
2 SH2 superbinder-AP-MS for Examining TK Activation in Cancer Samples.....	28
2.1 Abstract	28
2.2 Introduction.....	29
2.2.1 Limitations of conventional TK examination assays.....	29
2.2.2 Mass spectrometry	32
2.2.3 Affinity purification of modified peptides	39
2.2.4 SH2-AP-MS	40

2.3	Materials and Methods.....	42
2.3.1	Cell culture.....	42
2.3.2	SH2 superbinder purification and immobilization.....	42
2.3.3	Free peptide and on-membrane peptide synthesis	43
2.3.4	Far Western blot of peptide array membrane	44
2.3.5	Protein tryptic digestion and pTyr peptide enrichment.....	45
2.3.6	Mass spectrometric analysis	46
2.3.7	Cell proliferation assay	47
2.3.8	mRNA isolation and RNA-seq	47
2.4	Results.....	48
2.4.1	Abundance of TK phosphorylated peptides indicate TK activity.....	48
2.4.2	Selection of TK phosphorylated peptides for targeted proteomics.....	60
2.4.3	Identification of TK biomarkers in tumor tissues	67
2.4.4	Tracking kinome dynamics in response to targeted therapeutic	72
2.4.5	Deciphering the mechanism of acquired trastuzumab resistance	75
2.5	Discussion.....	78
2.6	References.....	81
2.7	Supplemental data.....	92
Chapter 3	147
3	SH2 Superbinder Modified Yeast Two Hybrid System for Identifying Tyrosine Kinase Substrates	147
3.1	Abstract.....	147
3.2	Introduction.....	148
3.3	Materials and Methods.....	150
3.3.1	Cloning and transformation	150
3.3.2	Optimization of Src kinase expression in yeast	151

3.3.3	Quantification of MEL1 reporter gene expression	151
3.3.4	Human cDNA library screening	152
3.3.5	SH2-AP-MS identification of AD insertions	152
3.4	Results.....	154
3.4.1	Design of the SH2 superbinder modified Y2H system.....	154
3.4.2	System evaluation with known peptide substrates of Src kinase.....	158
3.4.3	cDNA library screening for Src kinase substrate.....	160
3.4.4	SH2-AP-MS for after-screening prey identification.....	163
3.5	Discussion.....	164
3.6	References.....	166
3.7	Supplemental data.....	169
Chapter 4	173
4	Summary and Perspectives	173
4.1	References.....	178
Curriculum Vitae	182

List of Figures and Tables

Figure 1.1 Schematic of ErbB RTK activation.....	14
Figure 2.1 Nomenclature for peptide fragmentation.....	37
Figure 2.2 SH2-AP-MS detects active TKs that drive cell proliferation.....	53
Figure 2.3 The linearities of Src_419 and GSK3 α _279 in MRM.....	66
Figure 2.4 PRM analysis of fast frozen breast cancer tissues.....	68
Figure 2.5 PRM analysis of PBMCs and formalin-fixed solid tumor specimens.....	71
Figure 2.6 Tracking kinome reprogramming in SK-BR-3 cells.....	74
Figure 2.7 c-Kit is responsible for trastuzumab resistance in SK-BR-3 cells.....	77
Figure 3.1 SH2 superbinder based Y2H for validating TK-substrate pairing.....	156
Figure 3.2 Evaluation of the Y2H system in recognizing Src kinase substrates.....	159
Table 2.1 Activation loop phosphorylation profiles determined by SH2-AP-MS.....	50
Table 2.2 TK pTyr peptide profiles in four breast cancer cell lines.....	56
Table 2.3 A comparison of TK profiles in SH2-AP-MS and RNA-seq.....	58
Table 2.4 Tryptic-digested TK activation loops.....	63
Table 3.1 Library-scale screening for Src kinase substrates.....	161
Table 3.2 Selected Src substrates and functional partners in candidate positives.....	162
Suppl. 2.1 Alignment of activation loop regions of human TKs.....	92
Suppl. 2.2 Far-Western blots of TK pTyr sites by SH2 superbinder and antibody.....	94
Suppl. 2.3 TK pTyr sites and their relative blot intensities to the superbinder.....	95
Suppl. 2.4 Loop panel for PRM.....	118
Suppl. 2.5 Full panel for MRM.....	120

Suppl. 3.1 Yeast toxicity and self-activation tests	169
Suppl. 3.2 SH2 binding affinities of selected Src phosphorylated peptides	170
Suppl. 3.3 AD insertion amplification in eight candidate positives	171
Suppl. 3.4 Protein IDs of candidate positive colonies	172

List of Abbreviations

Abbreviation	Full Name
4G10	anti-phosphotyrosine antibody, clone 4G10
ACN	acetonitrile
AD	GAL4 transcription factor transcription activation domain
AP-MS	affinity-purification mass spectrometry
Co-IP	co-immunoprecipitation
CTK	cytosol tyrosine kinase
DB	GAL4 transcription factor DNA binding domain
DMEM	Dulbecco's modified eagle medium
DMSO	dimethyl sulfoxide
DTT	dithiothreitol
ECL	enhanced chemiluminescence
EGF	epidermal growth factor
EGFR	epidermal growth factor receptor
ErbB2/HER2	human epidermal growth factor 2
Erk	extracellular signal-regulated kinases
FBS	fetal bovine serum
Fmoc	9-fluorenylmethyloxycarbonyl
FP	fluorescent polarization
GFP	green fluorescent protein
GSH	glutathione
GST	glutathione s-transferase
HPLC	high-performance liquid chromatography
IMAC	immobilized metal affinity chromatography
IPTG	isopropyl β -D-a-thiogalactopyranoside
Kd	dissociation constant
LB	lysogeny broth medium
LC	liquid chromatography
MAPK	mitogen-activated protein kinase
MEL1	reporter gene encodes α -galactosidase

MEM	minimum essential media
-His	amino acid source (yeast medium) without Histidine
-Leu	amino acid source (yeast medium) without Leucine
-Trp	amino acid source (yeast medium) without Tryptophan
MRM	multiple reaction monitoring
MS	mass spectrometry
MS/MS	tandem mass spectrometry
NSCLC	non-small cell lung cancer
PBS	phosphate buffered saline
pen/strep	penicillin/streptomycin antibiotics
PI3K	phosphatidylinositol-4,5-bisphosphate 3-kinase
PPI	protein-protein interaction
PRM	parallel reaction monitoring
PTK	protein tyrosine kinase
PTM	post-translational modification
PTP	protein tyrosine phosphatase
pTyr	phosphotyrosine
RPMI	Roswell Park Memorial Institute
RTK	receptor tyrosine kinase
SDS	sodium dodecyl sulphate
SH2	Src homology 2
sMRM	scheduled multiple reaction monitoring
SPE	solid phase extraction
sPRM	scheduled parallel reaction monitoring
TFA	trifluoroacetic acid
TIPS	tri-isopropylsilane
TK	tyrosine kinase
TKI	tyrosine kinase inhibitor
Tris	trisaminomethane
TrM	SH2 triple mutant or superbinder
WT	wild-type
Y2H	yeast two hybrid

Chapter 1

1 General Introduction

Proteins are fundamental biomolecules in the cell that participate in all cellular activities. One well known function of proteins in the cell is as enzymes, which catalyze biochemical reactions, including the processes of assembly and degradation of proteins. The human genome harbours approximately 20,000 genes, and the proteins encoded by more than 18,000 genes have been identified in at least one human tissue (Wilhelm et al., 2014). Typically in a human cell, around 10,000 to 13,000 genes together express a few billion protein molecules, with the most abundant proteins each consisting of several million copies (Milo, 2013). In a HeLa cell of 400 picogram in dry weight, the protein content is approximately 300 picograms (Finka and Goloubinoff, 2013; Volpe and Eremenko-Volpe, 1970).

The complexity of the proteome, the complement of all proteins, modified or not, in an organism is thought to be increase with the number of genes. For example, viruses may contain only a few genes, yeast and *E. coli*, in contrast, have about 5,000 genes (Bassett et al., 1996; Blattner et al., 1997), while mice and humans have over 20,000 genes (Lander et al., 2001; Mouse Genome Sequencing et al., 2002). Some species have exceptionally large genomes. For example, Arabidopsis (*Arabidopsis thaliana*) has approximately the same number of genes as humans (Arabidopsis Genome, 2000), and rice (*Oryza Sativa*) has a genome twice the size of the human genome with over 40,000 genes (Goff et al., 2002). However, plant genomes are usually less heterogeneous, which is likely evolved along with polyploidy (Van de Peer et al., 2017). Rice and wheat are naturally polyploid, Arabidopsis is diploid but have many polyploid cell types, such as the pavement cells which could be up to 128-ploid (Lee et al., 2013). Besides the number of genes, post-translational modifications (PTMs) on proteins make large contributions to the complexity of the human proteome, which generate variants of protein molecules that may behave differentially *in vivo* (Hunter, 2007; Jungblut et al., 2008). Phosphorylation is one of the most common and studied reversible protein PTM. Protein kinases catalyze this process by transferring a γ -phosphate group to the substrate protein, principally on serine, threonine or tyrosine residues, while phosphatases are responsible for removing the phosphate group from these

amino acid residues (Johnson and Lewis, 2001). Humans have evolved a highly complicated protein PTM system, with about one thousand genes being directly involved in protein phosphorylation, for example (Sharma et al., 2014). In contrast, yeast and plants which have a much less sophisticated protein PTM system, lack kinases for tyrosine phosphorylation (Lim and Pawson, 2010).

Pioneering studies on protein phosphorylation were carried out in the 1950s, with serine/threonine phosphorylation first described in 1954 (Burnett and Kennedy, 1954; Fischer and Krebs, 1955; Krebs and Fischer, 1956). Likely due to the much lower occurrence and stability of tyrosine phosphorylation *in vivo* (Manning et al., 2002; Ushiro and Cohen, 1980), the phosphorylation of tyrosine was reported almost 25 years later, even though *in vitro* synthesis of phosphotyrosine in 1933 already revealed the theoretical possibility of tyrosine phosphorylation (Eckhart et al., 1979; Levene and Schormuller, 1933; Sefton et al., 1980). The first isolated kinase, protein kinase A (PKA) was reported in 1968 (Walsh et al., 1968) and the first isolated tyrosine kinase, Src, was reported in 1979 (Oppermann et al., 1979). The human genome encodes about 400 serine/threonine kinases (STKs) but only 90 protein tyrosine kinases (PTKs, or TKs) (Manning et al., 2002), suggesting that serine/threonine phosphorylation is dominant. Indeed, STKs are responsible for about 95% of all amino acid phosphorylation (Ushiro and Cohen, 1980). It was initially estimated that one-third of human proteins are substrates of protein kinases (Cohen, 2000), however, with the advancement of modified-peptide enrichment and mass spectrometry (MS) technologies, the numbers of reported protein phosphorylation and other modification sites are increasing at an exponential rate (Sharma et al., 2014). Even the less abundant tyrosine phosphorylation has been identified in approximately 10, 000 sites from half of all human proteins, according to the ProteomeScout database (Matlock et al., 2015). Our preliminary phosphotyrosine proteomics study, employing a new tyrosine-phosphorylated peptide enrichment strategy which will be introduced in this thesis, reported over 3, 000 novel tyrosine phosphorylation sites identified from nine lab-cultured cancer cell lines (Bian et al., 2016).

Phosphorylation plays an important role in the regulation of protein functions. It has been implicated in mediating many signal transduction pathways and cellular activities (Adams, 2001; Johnson and Lewis, 2001). Since the phosphate group is charged and hydrophilic in

the physiological environment, phosphorylation and de-phosphorylation could result in protein conformational changes, thereby altering the protein function directly. However, tyrosine phosphorylation is somehow distinct from serine or threonine phosphorylation. In many cases, phosphorylation of tyrosine alters protein-protein interactions instead of directly altering protein conformation. On a serine or threonine residue, the phosphate group is attached to the β -OH group on the amino acid side chain. However, on a tyrosine residue, the phosphate group is linked to the O4 position of the phenolic ring, which is located much further away from the amino acid backbone. From a biophysical perspective, the phosphate on a tyrosine residue will result in less impact to the charge status and hydrodynamics of nearby amino acids. This distinct structure likely provides a more recognizable site for specific binding, thereby allowing the evolution of highly specific tyrosine phosphorylation regulating modules including TKs, pTyr binding domains/proteins and tyrosine phosphorylation phosphatases (PTPs) (Hunter, 2014). In addition, at the cellular level, unlike the serine or threonine phosphatases, PTPs typically maintain a highly active status, therefore resulting in a very short half-life for tyrosine phosphorylation (minutes or even seconds in many cases) (Kleiman et al., 2011; Tonks, 2006). This dynamic nature greatly facilitates a pTyr modulating role in signal transduction, which relies on fast changes of component status (Hunter, 2014). Indeed, with 90 TKs, 107 PTPs and 120 pTyr-recognition Src Homolog 2 (SH2)-containing proteins (Liu et al., 2012; Liu et al., 2006; Liu et al., 2011), humans have evolved a complex regulatory network that precisely tunes the dynamics of tyrosine phosphorylation on over 10,000 sites throughout the proteome. This, in turn, mediates a number of key cellular activities *in vivo*, including the aberrant stimulation of the MAPK pathway (cell proliferation) and PI3K-Akt pathway (cell survival) in tumorigenesis and cancer malignance (Lim and Pawson, 2010).

TKs are generally classified into two families according to their distinct sub-cellular localizations. The membrane-localized receptor tyrosine kinase (RTK) family has 58 members distributed into 20 subfamilies (ALK; AXL; DDR; EPH; ErbB; FGFR; INSR; MET; MUSK; PDGFR; PTK7; RET; ROR; ROS; RYK; TIE; TRK; VEGFR; AATYK), and the cytosol-localized protein tyrosine kinase (CTK) family has 32 members distributed into 10 subfamilies (ABL; ACK; CSK; FAK; FES; FRK; JAK; SRC; TEC; SYK) (Robinson et al., 2000). Despite the relatively small gene family size, it must be noted that

aberrant activation of TKs, especially RTKs, have been reported as a pivotal driver of tumorigenesis and cancer malignancy in a multitude of cancer types and at least twenty TKs have been verified as oncogenes or proto-oncogenes (Gharwan and Groninger, 2016; Hunter, 2009; Wu et al., 2015), including the first described oncogene Src that was reported in 1979 (Oppermann et al., 1979; Sefton et al., 1980; Stehelin et al., 1977). Presently, more than half of the approved targeted therapeutics (precision medicines) in cancer treatment are either small molecule TK inhibitors or RTK inhibition antibodies (Bhullar et al., 2018; Gharwan and Groninger, 2016; Twomey et al., 2017; Wu et al., 2015; Zhang et al., 2009). As a result, tyrosine phosphorylation and its mediated signal transduction are among the hottest topics in both cancer biology research and therapeutic development for the past two decades.

1.1 TK inhibition drugs in cancer therapy

The discovery that the viral protein v-Src with TK activity transformed human cells immediately suggested that TKs and tyrosine phosphorylation might be a significant mechanism of transformation (Hunter and Sefton, 1980; Sefton et al., 1980). Later, an investigation into human oncogenes quickly revealed a fusion of the BCR protein and ABL tyrosine kinase (BCR-ABL) was essential and sufficient for the malignant transformation of CML (chronic myelogenous leukemia), and was responsible for the phenotypic abnormalities of CML that identified as Philadelphia chromosome positive (Ph+) (Daley and Baltimore, 1988; Daley et al., 1990). Philadelphia chromosome is the hallmark of CML and found in over 90% of CML patients (Nowell, 1962), which arises from a t(9;22)(q34;q11) reciprocal translocation in chromosomes (Rowley, 1973). The molecular consequence of this translocation is the replacement of the first ABL exon by a fragment from the BCR gene, resulting in the fusion protein BCR-ABL that has deregulated kinase activity (Ben-Neriah et al., 1986). These findings lead to further investigation focusing on BCR-ABL fusion and finally the approval of the first targeted anti-cancer therapeutic imatinib (Gleevec®, Novartis) (Buchdunger et al., 1996; Druker and Lydon, 2000). Unlike most other small molecule TK inhibitors (TKIs) that are ATP (nucleoside triphosphate) mimics, imatinib binds close to the ABL ATP binding site and locks it in a self-inhibited conformation, thereby, inhibiting the kinase activity semi-competitively. Imatinib is highly effective in clinical application, and generally well tolerated in most patients with Ph+ CML. The overall survival rate remains high after 5 years of follow-up, and historical comparison to other treatments also indicates greatly improved survival outcome (Moen et al., 2007). In the long term, a recent study reports a striking 83.3% overall survival rate at 10 years of CML patients receiving imatinib treatment (Hochhaus et al., 2017).

Following the milestone approval of imatinib, kinases, especially TKs, quickly emerged as the most intensively pursued targets in both cancer biology research and anti-cancer therapeutic development. To date, many TKs have been proven as oncogenes or proto-oncogenes in research labs, and over twenty TKs are already validated as biomarkers in many different cancer types (Kannaiyan and Mahadevan, 2018; Levitzki, 2013; Wu et al., 2015). Tens of TK inhibition molecules have been clinically approved, making up more

than half of all approved targeted therapeutics in cancer therapy (Bhullar et al., 2018; Gharwan and Groninger, 2016; Twomey et al., 2017; Wu et al., 2015; Zhang et al., 2009).. Following the great success of imatinib, several other small molecule inhibitors have been clinically approved that target ABL and its fusion variants, including bosutinib (Bosulif®, Pfizer), dasatinib (Sprycel®, Bristol-Myers Squibb), nilotinib (Tasigna®, Novartis) and ponatinib (Iclusig®, Takeda), which are significantly more potent or overcome imatinib resistance (Quintas-Cardama et al., 2007; Rossari et al., 2018). Additionally, the application of imatinib has also been expanded to the treatment of Ph+ acute lymphocytic leukemia (ALL), gastrointestinal stromal tumors (GIST), systemic mastocytosis, and myelodysplastic syndrome (Rossari et al., 2018).

Like that of BCR-ABL, fusion TKs with deregulated kinase activity is a common oncogenic mechanism (Medves and Demoulin, 2012). The RTK anaplastic lymphoma kinase (ALK), also known as CD246 (cluster of differentiation 246), was also first described in a chromosomal translocation as a fusion TK (NPM-ALK) in anaplastic large-cell non-Hodgkin's lymphoma (ALCL), though it was not initially described as an oncogene (Morris et al., 1994; Shiota et al., 1994). In 2008, ALK was identified as a biomarker in neuroblastoma, a most intractable pediatric cancer (Chen et al., 2008; Janoueix-Lerosey et al., 2008). It should be noted that the ALK inhibitor crizotinib (Xalkori®, Pfizer) was clinically approved two years after these reports, which set a record time from biomarker discovery to clinical approval in the development of targeted therapeutics. Although not fully elucidated, ALK appears to be localized in a frequent translocation region of the chromosome, and it has been reported that ALK forms over 30 oncogenic fusions with at least 22 fusion partners in different cancer types (Hallberg and Palmer, 2013). In addition to these fusion TKs, amplification of TK genes, overexpression of TKs, truncation of TK proteins, constitutively active TK mutants and abnormalities of TK regulators are also very common in many different cancer types which drives tumorigenesis and cancer malignancy via similar pathways (Du and Lovly, 2018). For instance, in breast cancer, approximately 15%~30% of patients have tumors that exhibit overexpression, amplification, or both of the RTK ErbB2 (HER2, human epidermal growth factor receptor 2) (Cameron et al., 2017; Seidman et al., 2008; Vogel et al., 2002). This subtype is termed as HER2 positive breast cancer, and the use of the humanized ErbB2

inhibition antibody trastuzumab (Herceptin®, GenenTech), is now the standard of care for these patients (Cameron et al., 2017; Seidman et al., 2008; Vogel et al., 2002).

Two major types of TK inhibition molecules have been developed as therapeutics for TK positive cancers: humanized monoclonal antibodies against the RTK extra-cellular region and small molecule inhibitors (Kannaiyan and Mahadevan, 2018; Wu et al., 2015). The antibodies bind to the RTK extracellular region in the extracellular matrix, which either blocks the binding of ligands (growth factors) or disturbs the ligand-stimulated dimerization of the extracellular region, both of which are required for full RTK activation and the subsequent stimulation of cell proliferation and survival signals. The small molecule inhibitors simply penetrate cell membrane and bind to the TK kinase domain to directly inhibit kinase activity.

1.2 TKI resistance and TK signaling network complexity

Cellular signal transduction could rely on the spatiotemporal dynamics of macromolecules, for example reversible modifications on receptors (Bergeron et al., 2016). Among all these PTMs, tyrosine phosphorylation, as well as pTyr-mediated signal transduction, have been extensively studied due to their significance in numerous cellular activities, including differentiation, proliferation, motility and apoptosis, that are closely related to tumorigenesis and cancer malignancy (Hunter, 2009; Lim and Pawson, 2010; Seet et al., 2006). As introduced earlier, the human genome encodes 90 TKs, 107 PTPs and 120 SH2-containing proteins, which serve as the writer, eraser and reader modules respectively in the pTyr toolkit (Lim and Pawson, 2010). Even with this relatively simple toolkit, the pTyr-mediated signaling network is a highly-complicated and multilayer-regulatory network, which also contains many functionally redundant and promiscuous components (Yarden and Sliwkowski, 2001). Despite the tens of thousands of related research papers that have been published, there is still a lack of comprehensive understanding of this network and its consequences in normal cellular activities and tumorigenesis. For instance, the constitutive stimulation by nerve growth factor (NGF) triggers rat PC12 pheochromocytoma cell differentiation, but transient stimulation only promotes cell proliferation. Under both conditions, the NGF growth factor specifically binds to tropomyosin receptor kinase A (TrkA) and sequentially stimulate the MAPK signaling pathway, which is required for both the cell differentiation and proliferation (Klesse et al., 1999).

The complexity of the pTyr-mediated signaling network seems essential for fine-tuning the phosphorylation on over 10,000 sites using just a few hundred TKs, PTPs and SH2 proteins. However, the frequent functional redundancy, cross talking and signal feedback also means that the network may have difficulty recovering once disturbed, as is seen in cancer cells. In the clinic, this may also increase the difficulty for treating TK positive cancer, especially when the TK biomarker is not the dominant driver of tumorigenesis and malignance. In the application of TK inhibition drugs, both intrinsic and acquired drug resistance are widely observed across different cancer types (Levitcki, 2013; Lovly and Shaw, 2014). ErbB2 (HER2) is a biomarker diagnosed in up to 30% of breast cancer patients (Cameron et al., 2017; Seidman et al., 2008; Vogel et al., 2002), and it was validated that ErbB2 alone was

sufficient for tumor formation and maintenance in HER2 breast cancer (Drebin et al., 1985). However, only about 30% of HER2 positive patients are sensitive to the targeted therapeutic trastuzumab, and the duration of drug response only ranges from 5 to 9 months in many cases (Seidman et al., 2008). Resistance and short-term effects are also found in the application of many other anti-cancer targeted therapeutics (Levitzki, 2013; Lovly and Shaw, 2014). To date, different theories have been made to explain the resistance of targeted therapeutics, although most of these studies are non-systematic and based on laboratory models. However, it is obvious that many theories are related to the plasticity of the pTyr-mediated signaling network in both intrinsic and drug-induced resistances. Even if the on-target TK biomarkers are inhibited, the network might self-adjust to maintain the activation of oncogenic signals. The deregulation of non-target TKs was observed in many cases, which could bypass the inhibition of on-target TK to stimulate cell proliferation and survival (Du and Lovly, 2018; Levitzki, 2013; Lovly and Shaw, 2014). Due to the difficulties in collecting and analyzing patient-derived samples, there is still a lack of large-scale studies that could comprehensively decipher the drug resistance mechanism, even for a given targeted therapeutic in a specific cancer type. A recent review summarized some clinic-based studies on drug resistance in non-small-cell lung cancer (NSCLC) that is positive for EGFR or ALK (Lin and Shaw, 2016). It is estimated that up to 70% of drug resistance cases, in both EGFR and ALK-positive NSCLC, are likely related to the retention of TK activity, either by introducing additional mutations in on-target TKs that abolishes drug binding and increases kinase activity, or deregulation of non-target TKs that compensates for the loss of on-target TK activity by drug inhibition.

1.2.1 Multi-functional components

The mix and match of functionalities in these “writer, eraser and reader” proteins contribute to the regulation of the pTyr-mediated signaling network. The “writer-reader” type TKs, “eraser-reader” type PTPs are very common in this network because many TKs and PTPs also contain SH2 domains. These proteins are also direct TK substrates and highly tyrosine phosphorylated *in vivo* (Hornbeck et al., 2015; Matlock et al., 2015). Over 1000 pTyr sites have been identified in only 90 TKs, which are produced by either intramolecular phosphorylation or intermolecular phosphorylation. The regulation of Src kinase is a good

example exhibiting complicated but fine-tuned regulation caused by the mix and match nature of “writer, eraser and reader” functionalities, as well as some other factors. As introduced above, Src is the first described proto-oncogene, and aberrant activation of Src can drive the transformation of normal cells into cancerous cells (Oppermann et al., 1979; Sefton et al., 1980; Stehelin et al., 1977). From the N- to C-terminus, the Src protein contains a 14-carbon myristoyl group attached to an SH4 domain, a Unique domain, an SH3 domain, an SH2 domain, an SH2-kinase linker, a tyrosine kinase domain, and a carboxy-terminus regulatory tail (Roskoski, 2004). The Src kinase is highly tyrosine-phosphorylated *in vivo* and contains at least 11 pTyr sites (Y93, Y134, Y139, Y187, Y216, Y232, Y338, Y419, Y439, Y522, Y530) (Hornbeck et al., 2015), of which phosphorylation on Y419 and Y530 (Y416 and Y527 in chicken Src) are most abundant and play a pivotal role in the regulation of Src activity (Roskoski, 2004; Roskoski, 2005). At the protein level, the full activation of Src kinase requires phosphorylation of Y419 and de-phosphorylation of Y530. Y419 is in the highly-conserved activation loop within the kinase domain, whose autophosphorylation displaces the activation loop away from the substrate binding pocket to set the kinase domain in an open status. Y530 is more critical in the regulation of Src activation. Once phosphorylated, it binds to the intramolecular SH2 domain and this conformation completely blocks substrate access to the kinase domain regardless of the Y419 phosphorylation status. A similar regulatory mechanism is also observed in other Src family members which share a highly conserved structure and sequence (Thomas and Brugge, 1997). Y530 in Src is phosphorylated by Csk (c-terminal Src kinase) and Csk-homologous kinase, and de-phosphorylated primarily by PTP1B (protein tyrosine phosphatase 1B) (Bjorge et al., 2000). It is intriguing that PTP1B specifically localizes to the cytosolic face of the endoplasmic reticulum (ER) system while Src is a cytosolic kinase mainly associating to the cell membrane (Frangioni et al., 1992; Resh, 1994), which indicates that the PTP1B mediated Src dephosphorylation is spatiotemporally regulated at the subcellular level. A microscopy-based cell biology study exhibited the co-localization of Src and PTP1B scattered throughout the ER system (Monteleone et al., 2012), demonstrating that subcellular distribution might involve in the regulation of Src activity as well. In addition to the intramolecular pTyr site, the Src SH2 domain also directly binds to pTyr sites in other proteins *in vivo*, such as the phosphorylated Y397 in the focal

adhesion kinase (FAK), or protein tyrosine kinase 2 (PTK2) (Xing et al., 1994). The consequence of this binding is further phosphorylation at multiple sites in FAK and the formation of Src-FAK complex, which in turn phosphorylates a number of cytoskeleton-associated proteins to regulate cell motility (Mitra and Schlaepfer, 2006).

Besides the writer-readers or eraser-readers, it is common that other SH2-containing enzymes are also directly involved in the regulation of the pTyr-mediated signaling network. The SH2-containing E3 ligase Cbl family, including Cbl, Cbl-b and Cbl-c in mammals, have emerged as dominant negative regulators of many RTKs by ubiquitinating active RTKs for internalization, which either results in RTK removal from the cell membrane or degradation via the lysosome (Liyasova et al., 2015; Mohapatra et al., 2013; Sorkin and Von Zastrow, 2002). It has also been reported that Cbl family proteins may play a positive role in pTyr-mediated signal transduction by acting as adaptor proteins to recruit other signaling molecules to active RTKs (Scott et al., 2005; Waterman et al., 2002).

Previous work in our lab also reveals an orthogonal regulatory mechanism to this network. We found that the pTyr-binding adaptor protein Numb might also generally function in the internalization of RTKs by recruiting endocytosis-related proteins (Wei et al., 2018). In this process, two Numb isoforms tend to behave in opposing ways in directing ALK to distinct post-endocytic trafficking destinations (Wei et al., 2019). The Numb isoforms bind to the same ALK intracellular region but recruit different endocytic proteins. One Numb isoform mainly directs ALK from the early endosome to late endosome which ultimately degrade in the lysosome. In contrast, a second Numb isoform could promote ALK recycling from the early endosome to the cell membrane therefore only temporarily regulating the on-membrane ALK abundance.

1.2.2 Functional redundancy

The pTyr-mediated signaling network exhibits a clear multi-layered structure (Yarden and Sliwkowski, 2001). From the extracellular matrix to the cytoplasm, this network consists of growth factors that initiate signal transduction, RTKs that transfer signaling through the cell membrane, SH2 domain-containing proteins and cytosol TKs that amplify signaling, and downstream effectors that alter cellular activities accordingly. Functional redundancy,

cross-talk and promiscuity seem highly frequent in this network, likely due to structural and functional conservation among components within the same layer.

Our understanding of this network is largely based on studies of the ErbB RTK subfamily (Fig.1.2). ErbBs serve as an entry portal to transduce a signal from the extracellular matrix into the cytoplasm (Holbro and Hynes, 2004). Intriguingly, the downstream signaling outcome is somehow flexible even when the signal transduction is via the same ErbB members (Yarden and Sliwkowski, 2001). There are at least three major regulatory layers together deciding the signaling outcome: 1) Growth factors. The human genome encodes four ErbB family members, EGFR (ErbB1), ErbB2 (HER2), ErbB3 and ErbB4. The ErbB proteins, like most other RTKs, share an identical molecular architecture, made up of an ectodomain (extracellular domain, ECD), a short and single transmembrane region, an intracellular tyrosine kinase domain and a flexible C-terminal tail with multiple pTyr sites. There are 11 different ligands in total, and all generated from extracellular cleavage of other transmembrane proteins that can bind to and activate at least one ErbB member. These include EGF (epidermal growth factor) (Cohen, 1962, 1964), TGF- α (transforming growth factor alpha) (Derynck et al., 1984; Marquardt et al., 1984), HB-EGF (Heparin-binding EGF-like growth factor) (Higashiyama et al., 1991), amphiregulin (Shoyab et al., 1989), betacellulin (Sasada et al., 1993; Shing et al., 1993), epigen (Strachan et al., 2001), epiregulin (Jones et al., 1999; Toyoda et al., 1995), NRG1 (neuregulin-1) (Peles et al., 1992), NRG2 (neuregulin-2) (Chang et al., 1997), NRG3 (neuregulin-3) (Zhang et al., 1997) and NRG4 (neuregulin-4) (Harari et al., 1999). All ErbB members exhibit ligand preference, and none of these members can bind to all ligands (Fuller et al., 2008; Linggi and Carpenter, 2006); 2) Homo- and hetero-dimerization occur among ErbB members. Dimerization takes place between any two ErbB protein molecules upon the ligand binding. Among all ErbB molecules, the homo-dimerization of ErbB2 and its subsequent activation seems least dependent on the ligand, which has the capacity to dimerize in the absence of ligand binding and overexpression of ErbB2 alone is able to promote ErbB2 homo-dimerization and transform cells (Lemmon, 2009); 3). Four ErbB members generate at least 61 pTyr sites, which bind to tens of SH2 domain-containing proteins *in vitro* and *in vivo*, and a variety of SH2 domain-containing proteins may compete for binding to the same pTyr sites *in vivo* (Jones et al., 2006). Some SH2 containing proteins, such as Shc adaptor

protein, could be phosphorylated upon binding to the active ErbB or other RTKs, which in turn recruits more SH2 domain-containing proteins to amplify signaling further or introduce additional regulators (Good et al., 2011). Upon EGF stimulation, the Shc scaffold protein could undergo multiple waves of phosphorylation that couple with distinct signaling modules thereby resulting in differential signaling outcomes (Zheng et al., 2013). Therefore, all these components together yield a highly versatile phosphorylation status among the four ErbB members and adaptor proteins, which in turn trigger a multitude of signals (Yarden and Sliwkowski, 2001).

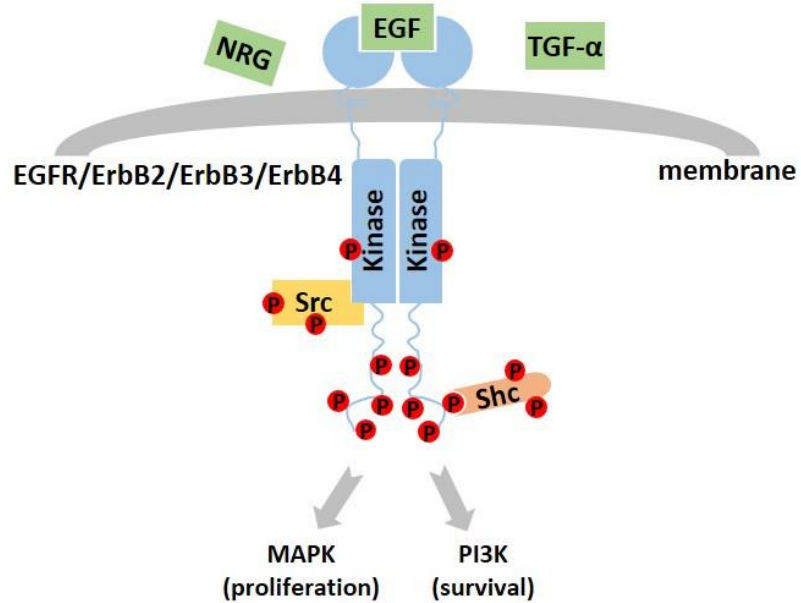


Figure 1.1 Schematic of ErbB RTK activation

The RTK ErbB proteins consist of an ectodomain, a single transmembrane region, an intracellular tyrosine kinase domain and a flexible C-terminus tail with multiple pTyr sites. Upon the binding of extracellular growth factors, two ErbB protein molecules dimerize to come together and activate the intracellular kinase domains. The active kinase domains phosphorylate multiple intracellular tyrosine residues which in turn recruit downstream effectors such as Src kinase and Shc scaffold adaptor protein to stimulate the MAPK cell proliferation signaling and PI3K cell survival signaling.

1.3 Discovery of the SH2 Superbinder

The SH2 (Src Homology 2) domain is a structurally conserved noncatalytic protein domain that specifically binds to phosphorylated tyrosine residues, first described in the Src family kinases (Sadowski et al., 1986). SH2 is the largest family of pTyr-binding modules, and the human genome encodes ~120 SH2 domains in ~110 proteins (Liu et al., 2006). Regarding the structure, all SH2 domains are comprised of about 100 amino acids and share an identical structure with a central seven-stranded beta sheet flanked by two alpha helices (Kuriyan and Cowburn, 1997; Waksman et al., 1992; Waksman et al., 2004). Generally, SH2 domains only bind to phosphorylated tyrosine residues (Songyang et al., 1993; Songyang et al., 1994), with a few exceptions (Kaneko et al., 2012b; Liu et al., 2006; Pawson, 2004). The pTyr-SH2 binding typically has a moderate affinity, with equilibrium dissociation constants (Kd) ranging from 0.1 μ M to 10 μ M in many cases (Jones et al., 2006; Ladbury and Arold, 2011; Ladbury et al., 1995). This relatively weak binding allows rapid association and disassociation between SH2 modules and phosphotyrosine so that the signal from an active tyrosine kinase is promptly transmitted to the downstream proteins and the pTyr-mediated signaling network can adapt to stimuli effectively. The structure of SH2 domains in complex with phosphotyrosine-containing peptides reveals two major binding pockets on the surface responsible for binding: 1) a conserved pTyr-binding pocket provides basal binding affinity and specificity; 2) a secondary binding pocket with preference for the amino acids C-terminal of the pTyr residue in the ligand, which enhances the SH2-pTyr binding specificity. It has been previously reported that the pTyr residue only contributes around half of the binding free energy (ΔG°) of a pTyr ligand to an SH2 domain (Waksman et al., 2004). The typical pTyr-binding pocket is comprised of around a dozen residues, which makes it practical to screen for high-affinity mutants in directed evolution via phage display. Previously, Dr. Kaneko in our lab, together with our collaborators, created a library of mutant Fyn SH2 domains, in which the 15 pTyr-binding pocket residues (R1-K2-A3-R4-S5-E6-T7-T8-A9-S10-L11-S12-K13-H14-K15) were randomized to generate over 10^{10} unique mutants. The SH2 mutant library was expressed on the M13 bacteriophage which was then enriched for binding to pTyr peptides derived from *in vivo* tyrosine phosphorylation proteins. The bacteriophage clones with high binding affinity were sequenced to reveal the mutated residues contributing to enhanced SH2

binding affinity. It was revealed that not all residues in the pocket are equally evolvable. Some residues are resistant to substitution, such as R4, a residue that is conserved in all natural human SH2 domains and crucial for pTyr binding (Bradshaw et al., 1999). At physiological pH, the positively charged arginine could directly bind to the negatively charged phosphate from tyrosine residue. Three hydrophilic residues (T8/S10/K15) are highly evolvable and had the highest substitution frequencies. Substitution of the three hydrophilic residues by hydrophobic residues were identified in most high affinity bacteriophage clones. A triple mutant, T8V/S10A/K15L, was named “superbinder” because it exhibited greatly enhanced binding affinity for pTyr peptides both *in vitro* and *in vivo*. For some native pTyr peptides that bind to the wild-type Fyn SH2 domain in the micromolar (μM) K_d scale, their binding affinities to the superbinder are comparable to typical antibody-antigen binding affinity, with K_d in the low nanomolar (nM) range (Kaneko et al., 2012b). Because the pTyr-binding pocket is highly conserved across the SH2 domains, the same mutations introduced into other SH2 domains, such as those from Src and Grb2, also created superbinders (Huang et al., 2017; Kaneko et al., 2012a). More importantly, the T8V/S10A/K15L mutant is readily expressed in *E.Coli*, and this recombinant protein exhibits great solubility and stability, making it an ideal pTyr-binding reagent.

1.4 Potential applications of the SH2 superbinder

Taking advantage of this enhanced pTyr-binding SH2 domain, we are set out to develop a series of SH2-based assays that could be applied in fields with emerging significance but face a lack of specialized research tools due to the complex and promiscuous nature of the pTyr-mediated signaling network.

Primarily, a SH2-based pTyr peptide affinity purification mass-spectrometry (SH2-AP-MS) assay was developed for comprehensively profiling TK active status *in vivo* by determining the abundance of TK phosphorylated peptides, since phosphorylation is essential for the activation and regulation of many TKs. Conventionally, a similar strategy using anti-pTyr antibodies has been employed in phosphotyrosine proteomics studies. In the SH2-AP-MS strategy, the antibody was replaced by an engineered SH2 superbinder. Compared to antibodies, the superbinder is easily manufactured in bulk with minimal cost and stays stable for months at 4 °C, which make it applicable in large-scale and long-term studies. In addition, the SH2-AP-MS has several advantages compared to conventional TK activity assays and bears the potential to be further optimized for the examination of TK biomarkers in clinical samples. For this thesis study, the workflow of SH2 affinity purification was optimized to improve the efficiency of pTyr peptide enrichment. Moreover, the superbinder was further engineered by mutating two non-functional cysteine residues within the SH2 domain while an additional cysteine residue was introduced to the C-terminus (by Courtney Voss), which allows the covalent immobilization to iodoacetate group-coated resin without disturbing pTyr binding. In addition, the affinity purification buffer was modified to eliminate non-specific electrostatic binding of peptides rich in aspartic acid and/or glutamic acid (assisted by Dr. Tomonori Kaneko). With the optimized assay, known TK biomarkers were successfully detected from a minute amount of protein samples purified from either lab cultured cancer cells or clinical samples, including solid tumor FFPE slides prepared for standard IHC (immunohistochemistry) examination in the clinic. This assay also exhibited great expandability and could be used for the profiling of PTPs, immune-receptor tyrosine-based regulatory motifs and a variety of different TK substrates. In principle, once integrated with the well-developed phosphor-serine/threonine

enrichment strategy, the SH2-AP-MS strategy could be adapted for global profiling of the protein phosphotome.

A SH2 superbinder modified yeast two hybrid (Y2H) system was also designed to identify TK substrates. Due to the complex and promiscuous nature of the pTyr-mediated signaling network, conventional assays, such as the *in vitro* kinase assay and mass spectrometry-based *in vivo* assay, are not necessarily reliable in identifying direct TK substrates. Despite the fact that the number of reported pTyr sites has exploded in recent years, profiling of TK-substrate pairings is severely lagging. The modified Y2H is based on a strategy reported in previous Y2H studies (Clark and Peterson, 2002; Grossmann et al., 2015), in which a TK, a GAL4 DNA binding domain-fused SH2 (bait) and a substrate-fused GAL4 transcription activation domain (prey) were co-expressed in the yeast. Once the substrate is phosphorylated, it can bind to the SH2 to indirectly connect the GAL4 DNA binding domain and transcription activation domain, thereby forming a fully functional GAL4 transcription factor to trigger reporter gene expression. By replacing the natural SH2 with the superbinder mutant and introducing reverse screening, the sensitivity and accuracy of this modified Y2H system was greatly improved. This modified Y2H is capable of profiling TK-substrate pairing in a high-throughput and high-precision manner. In a middle-scale screen against a human cDNA library of 170,000 mated cells, 9 known Src kinase substrates were recapitulated from a total of 48 positive candidates.

Overall, this thesis work has revealed a variety of applications of the SH2 superbinder in proteomics and molecular biology. The SH2-AP-MS also bears great potential to be further adapted for examining TK active cancer and monitoring TK inhibition efficacy in clinical specimens.

1.5 References

- Adams, J.A. (2001). Kinetic and catalytic mechanisms of protein kinases. *Chem Rev* *101*, 2271-2290.
- Arabidopsis Genome, I. (2000). Analysis of the genome sequence of the flowering plant *Arabidopsis thaliana*. *Nature* *408*, 796-815.
- Bassett, D.E., Jr., Basrai, M.A., Connelly, C., Hyland, K.M., Kitagawa, K., Mayer, M.L., Morrow, D.M., Page, A.M., Resto, V.A., Skibbens, R.V., *et al.* (1996). Exploiting the complete yeast genome sequence. *Current opinion in genetics & development* *6*, 763-766.
- Ben-Neriah, Y., Daley, G.Q., Mes-Masson, A.M., Witte, O.N., and Baltimore, D. (1986). The chronic myelogenous leukemia-specific P210 protein is the product of the bcr/abl hybrid gene. *Science* *233*, 212-214.
- Bergeron, J.J., Di Guglielmo, G.M., Dahan, S., Dominguez, M., and Posner, B.I. (2016). Spatial and Temporal Regulation of Receptor Tyrosine Kinase Activation and Intracellular Signal Transduction. *Annu Rev Biochem* *85*, 573-597.
- Bhullar, K.S., Lagaron, N.O., McGowan, E.M., Parmar, I., Jha, A., Hubbard, B.P., and Rupasinghe, H.P.V. (2018). Kinase-targeted cancer therapies: progress, challenges and future directions. *Mol Cancer* *17*, 48.
- Bian, Y., Li, L., Dong, M., Liu, X., Kaneko, T., Cheng, K., Liu, H., Voss, C., Cao, X., Wang, Y., *et al.* (2016). Ultra-deep tyrosine phosphoproteomics enabled by a phosphotyrosine superbinder. *Nat Chem Biol* *12*, 959-966.
- Bjorge, J.D., Pang, A., and Fujita, D.J. (2000). Identification of protein-tyrosine phosphatase 1B as the major tyrosine phosphatase activity capable of dephosphorylating and activating c-Src in several human breast cancer cell lines. *J Biol Chem* *275*, 41439-41446.
- Blattner, F.R., Plunkett, G., 3rd, Bloch, C.A., Perna, N.T., Burland, V., Riley, M., Collado-Vides, J., Glasner, J.D., Rode, C.K., Mayhew, G.F., *et al.* (1997). The complete genome sequence of *Escherichia coli* K-12. *Science* *277*, 1453-1462.
- Bradshaw, J.M., Mitaxov, V., and Waksman, G. (1999). Investigation of phosphotyrosine recognition by the SH2 domain of the Src kinase. *J Mol Biol* *293*, 971-985.
- Buchdunger, E., Zimmermann, J., Mett, H., Meyer, T., Muller, M., Druker, B.J., and Lydon, N.B. (1996). Inhibition of the Abl protein-tyrosine kinase in vitro and in vivo by a 2-phenylaminopyrimidine derivative. *Cancer Res* *56*, 100-104.
- Burnett, G., and Kennedy, E.P. (1954). The enzymatic phosphorylation of proteins. *J Biol Chem* *211*, 969-980.
- Cameron, D., Piccart-Gebhart, M.J., Gelber, R.D., Procter, M., Goldhirsch, A., de Azambuja, E., Castro, G., Jr., Untch, M., Smith, I., Gianni, L., *et al.* (2017). 11 years' follow-up of trastuzumab after adjuvant chemotherapy in HER2-positive early breast cancer: final analysis of the HERceptin Adjuvant (HERA) trial. *Lancet* *389*, 1195-1205.

- Chang, H., Riese, D.J., 2nd, Gilbert, W., Stern, D.F., and McMahan, U.J. (1997). Ligands for ErbB-family receptors encoded by a neuregulin-like gene. *Nature* *387*, 509-512.
- Chen, Y., Takita, J., Choi, Y.L., Kato, M., Ohira, M., Sanada, M., Wang, L., Soda, M., Kikuchi, A., Igarashi, T., *et al.* (2008). Oncogenic mutations of ALK kinase in neuroblastoma. *Nature* *455*, 971-974.
- Clark, D.D., and Peterson, B.R. (2002). Rapid detection of protein tyrosine kinase activity in recombinant yeast expressing a universal substrate. *J Proteome Res* *1*, 207-209.
- Cohen, P. (2000). The regulation of protein function by multisite phosphorylation--a 25 year update. *Trends Biochem Sci* *25*, 596-601.
- Cohen, S. (1962). Isolation of a mouse submaxillary gland protein accelerating incisor eruption and eyelid opening in the new-born animal. *J Biol Chem* *237*, 1555-1562.
- Cohen, S. (1964). Isolation and Biological Effects of an Epidermal Growth-Stimulating Protein. *Natl Cancer Inst Monogr* *13*, 13-37.
- Daley, G.Q., and Baltimore, D. (1988). Transformation of an interleukin 3-dependent hematopoietic cell line by the chronic myelogenous leukemia-specific P210bcr/abl protein. *Proc Natl Acad Sci U S A* *85*, 9312-9316.
- Daley, G.Q., Van Etten, R.A., and Baltimore, D. (1990). Induction of chronic myelogenous leukemia in mice by the P210bcr/abl gene of the Philadelphia chromosome. *Science* *247*, 824-830.
- Derynck, R., Roberts, A.B., Winkler, M.E., Chen, E.Y., and Goeddel, D.V. (1984). Human transforming growth factor- α : precursor structure and expression in *E. coli*. *Cell* *38*, 287-297.
- Drebin, J.A., Link, V.C., Stern, D.F., Weinberg, R.A., and Greene, M.I. (1985). Down-modulation of an oncogene protein product and reversion of the transformed phenotype by monoclonal antibodies. *Cell* *41*, 697-706.
- Druker, B.J., and Lydon, N.B. (2000). Lessons learned from the development of an abl tyrosine kinase inhibitor for chronic myelogenous leukemia. *J Clin Invest* *105*, 3-7.
- Du, Z., and Lovly, C.M. (2018). Mechanisms of receptor tyrosine kinase activation in cancer. *Mol Cancer* *17*, 58.
- Eckhart, W., Hutchinson, M.A., and Hunter, T. (1979). An activity phosphorylating tyrosine in polyoma T antigen immunoprecipitates. *Cell* *18*, 925-933.
- Finka, A., and Goloubinoff, P. (2013). Proteomic data from human cell cultures refine mechanisms of chaperone-mediated protein homeostasis. *Cell Stress Chaperones* *18*, 591-605.
- Fischer, E.H., and Krebs, E.G. (1955). Conversion of phosphorylase b to phosphorylase a in muscle extracts. *J Biol Chem* *216*, 121-132.

- Frangioni, J.V., Beahm, P.H., Shifrin, V., Jost, C.A., and Neel, B.G. (1992). The nontransmembrane tyrosine phosphatase PTP-1B localizes to the endoplasmic reticulum via its 35 amino acid C-terminal sequence. *Cell* 68, 545-560.
- Fuller, S.J., Sivarajah, K., and Sugden, P.H. (2008). ErbB receptors, their ligands, and the consequences of their activation and inhibition in the myocardium. *J Mol Cell Cardiol* 44, 831-854.
- Gharwan, H., and Groninger, H. (2016). Kinase inhibitors and monoclonal antibodies in oncology: clinical implications. *Nat Rev Clin Oncol* 13, 209-227.
- Goff, S.A., Ricke, D., Lan, T.H., Presting, G., Wang, R., Dunn, M., Glazebrook, J., Sessions, A., Oeller, P., Varma, H., *et al.* (2002). A draft sequence of the rice genome (*Oryza sativa* L. ssp. *japonica*). *Science* 296, 92-100.
- Good, M.C., Zalatan, J.G., and Lim, W.A. (2011). Scaffold proteins: hubs for controlling the flow of cellular information. *Science* 332, 680-686.
- Grossmann, A., Benlasfer, N., Birth, P., Hegele, A., Wachsmuth, F., Apelt, L., and Stelzl, U. (2015). Phospho-tyrosine dependent protein-protein interaction network. *Molecular systems biology* 11, 794.
- Hallberg, B., and Palmer, R.H. (2013). Mechanistic insight into ALK receptor tyrosine kinase in human cancer biology. *Nat Rev Cancer* 13, 685-700.
- Harari, D., Tzahar, E., Romano, J., Shelly, M., Pierce, J.H., Andrews, G.C., and Yarden, Y. (1999). Neuregulin-4: a novel growth factor that acts through the ErbB-4 receptor tyrosine kinase. *Oncogene* 18, 2681-2689.
- Higashiyama, S., Abraham, J.A., Miller, J., Fiddes, J.C., and Klagsbrun, M. (1991). A heparin-binding growth factor secreted by macrophage-like cells that is related to EGF. *Science* 251, 936-939.
- Hochhaus, A., Larson, R.A., Guilhot, F., Radich, J.P., Branford, S., Hughes, T.P., Baccarani, M., Deininger, M.W., Cervantes, F., Fujihara, S., *et al.* (2017). Long-Term Outcomes of Imatinib Treatment for Chronic Myeloid Leukemia. *N Engl J Med* 376, 917-927.
- Holbro, T., and Hynes, N.E. (2004). ErbB receptors: directing key signaling networks throughout life. *Annu Rev Pharmacol Toxicol* 44, 195-217.
- Hornbeck, P.V., Zhang, B., Murray, B., Kornhauser, J.M., Latham, V., and Skrzypek, E. (2015). PhosphoSitePlus, 2014: mutations, PTMs and recalibrations. *Nucleic Acids Res* 43, D512-520.
- Huang, H., Kaneko, T., Sidhu, S.S., and Li, S.S. (2017). Creation of Phosphotyrosine Superbinders by Directed Evolution of an SH2 Domain. *Methods Mol Biol* 1555, 225-254.
- Hunter, T. (2007). The age of crosstalk: phosphorylation, ubiquitination, and beyond. *Mol Cell* 28, 730-738.

- Hunter, T. (2009). Tyrosine phosphorylation: thirty years and counting. *Curr Opin Cell Biol* 21, 140-146.
- Hunter, T. (2014). The genesis of tyrosine phosphorylation. *Cold Spring Harb Perspect Biol* 6, a020644.
- Hunter, T., and Sefton, B.M. (1980). Transforming gene product of Rous sarcoma virus phosphorylates tyrosine. *Proc Natl Acad Sci U S A* 77, 1311-1315.
- Janoueix-Lerosey, I., Lequin, D., Brugieres, L., Ribeiro, A., de Pontual, L., Combaret, V., Raynal, V., Puisieux, A., Schleiermacher, G., Pierron, G., *et al.* (2008). Somatic and germline activating mutations of the ALK kinase receptor in neuroblastoma. *Nature* 455, 967-970.
- Johnson, L.N., and Lewis, R.J. (2001). Structural basis for control by phosphorylation. *Chem Rev* 101, 2209-2242.
- Jones, J.T., Akita, R.W., and Sliwkowski, M.X. (1999). Binding specificities and affinities of egf domains for ErbB receptors. *FEBS Lett* 447, 227-231.
- Jones, R.B., Gordus, A., Krall, J.A., and MacBeath, G. (2006). A quantitative protein interaction network for the ErbB receptors using protein microarrays. *Nature* 439, 168-174.
- Jungblut, P.R., Holzhutter, H.G., Apweiler, R., and Schluter, H. (2008). The speciation of the proteome. *Chem Cent J* 2, 16.
- Kaneko, T., Huang, H., Cao, X., Li, X., Li, C., Voss, C., Sidhu, S.S., and Li, S.S. (2012a). Superbinder SH2 domains act as antagonists of cell signaling. *Sci Signal* 5, ra68.
- Kaneko, T., Joshi, R., Feller, S.M., and Li, S.S. (2012b). Phosphotyrosine recognition domains: the typical, the atypical and the versatile. *Cell Commun Signal* 10, 32.
- Kannaiyan, R., and Mahadevan, D. (2018). A comprehensive review of protein kinase inhibitors for cancer therapy. *Expert Rev Anticancer Ther* 18, 1249-1270.
- Kleiman, L.B., Maiwald, T., Conzelmann, H., Lauffenburger, D.A., and Sorger, P.K. (2011). Rapid phospho-turnover by receptor tyrosine kinases impacts downstream signaling and drug binding. *Mol Cell* 43, 723-737.
- Klesse, L.J., Meyers, K.A., Marshall, C.J., and Parada, L.F. (1999). Nerve growth factor induces survival and differentiation through two distinct signaling cascades in PC12 cells. *Oncogene* 18, 2055-2068.
- Krebs, E.G., and Fischer, E.H. (1956). The phosphorylase b to a converting enzyme of rabbit skeletal muscle. *Biochim Biophys Acta* 20, 150-157.
- Kuriyan, J., and Cowburn, D. (1997). Modular peptide recognition domains in eukaryotic signaling. *Annu Rev Biophys Biomol Struct* 26, 259-288.
- Ladbury, J.E., and Arold, S.T. (2011). Energetics of Src homology domain interactions in receptor tyrosine kinase-mediated signaling. *Methods Enzymol* 488, 147-183.

- Ladbury, J.E., Lemmon, M.A., Zhou, M., Green, J., Botfield, M.C., and Schlessinger, J. (1995). Measurement of the binding of tyrosyl phosphopeptides to SH2 domains: a reappraisal. *Proc Natl Acad Sci U S A* 92, 3199-3203.
- Lander, E.S., Linton, L.M., Birren, B., Nusbaum, C., Zody, M.C., Baldwin, J., Devon, K., Dewar, K., Doyle, M., FitzHugh, W., *et al.* (2001). Initial sequencing and analysis of the human genome. *Nature* 409, 860-921.
- Lee, E., Liu, X., Eglit, Y., and Sack, F. (2013). FOUR LIPS and MYB88 conditionally restrict the G1/S transition during stomatal formation. *J Exp Bot* 64, 5207-5219.
- Lemmon, M.A. (2009). Ligand-induced ErbB receptor dimerization. *Exp Cell Res* 315, 638-648.
- Levene, P.A., and Schormuller, A. (1933). The synthesis of tyrosinephosphoric acid. *Journal of Biological Chemistry* 100, 583-587.
- Levitzki, A. (2013). Tyrosine kinase inhibitors: views of selectivity, sensitivity, and clinical performance. *Annu Rev Pharmacol Toxicol* 53, 161-185.
- Lim, W.A., and Pawson, T. (2010). Phosphotyrosine signaling: evolving a new cellular communication system. *Cell* 142, 661-667.
- Lin, J.J., and Shaw, A.T. (2016). Resisting Resistance: Targeted Therapies in Lung Cancer. *Trends Cancer* 2, 350-364.
- Linggi, B., and Carpenter, G. (2006). ErbB receptors: new insights on mechanisms and biology. *Trends Cell Biol* 16, 649-656.
- Liu, B.A., Engelmann, B.W., and Nash, P.D. (2012). The language of SH2 domain interactions defines phosphotyrosine-mediated signal transduction. *FEBS Lett* 586, 2597-2605.
- Liu, B.A., Jablonowski, K., Raina, M., Arcé, M., Pawson, T., and Nash, P.D. (2006). The Human and Mouse Complement of SH2 Domain Proteins—Establishing the Boundaries of Phosphotyrosine Signaling. In *Molecular Cell*, pp. 851-868.
- Liu, B.A., Shah, E., Jablonowski, K., Stergachis, A., Engelmann, B., and Nash, P.D. (2011). The SH2 domain-containing proteins in 21 species establish the provenance and scope of phosphotyrosine signaling in eukaryotes. *Sci Signal* 4, ra83.
- Liyasova, M.S., Ma, K., and Lipkowitz, S. (2015). Molecular pathways: cbl proteins in tumorigenesis and antitumor immunity—opportunities for cancer treatment. *Clin Cancer Res* 21, 1789-1794.
- Lovly, C.M., and Shaw, A.T. (2014). Molecular pathways: resistance to kinase inhibitors and implications for therapeutic strategies. *Clin Cancer Res* 20, 2249-2256.
- Manning, G., Whyte, D.B., Martinez, R., Hunter, T., and Sudarsanam, S. (2002). The protein kinase complement of the human genome. *Science* 298, 1912-1934.

- Marquardt, H., Hunkapiller, M.W., Hood, L.E., and Todaro, G.J. (1984). Rat transforming growth factor type 1: structure and relation to epidermal growth factor. *Science* 223, 1079-1082.
- Matlock, M.K., Holehouse, A.S., and Naegle, K.M. (2015). ProteomeScout: a repository and analysis resource for post-translational modifications and proteins. *Nucleic Acids Res* 43, D521-530.
- Medves, S., and Demoulin, J.B. (2012). Tyrosine kinase gene fusions in cancer: translating mechanisms into targeted therapies. *J Cell Mol Med* 16, 237-248.
- Milo, R. (2013). What is the total number of protein molecules per cell volume? A call to rethink some published values. *Bioessays* 35, 1050-1055.
- Mitra, S.K., and Schlaepfer, D.D. (2006). Integrin-regulated FAK-Src signaling in normal and cancer cells. *Curr Opin Cell Biol* 18, 516-523.
- Moen, M.D., McKeage, K., Plosker, G.L., and Siddiqui, M.A. (2007). Imatinib: a review of its use in chronic myeloid leukaemia. *Drugs* 67, 299-320.
- Mohapatra, B., Ahmad, G., Nadeau, S., Zutshi, N., An, W., Scheffe, S., Dong, L., Feng, D., Goetz, B., Arya, P., *et al.* (2013). Protein tyrosine kinase regulation by ubiquitination: critical roles of Cbl-family ubiquitin ligases. *Biochim Biophys Acta* 1833, 122-139.
- Monteleone, M.C., Gonzalez Wusener, A.E., Burdisso, J.E., Conde, C., Caceres, A., and Arregui, C.O. (2012). ER-bound protein tyrosine phosphatase PTP1B interacts with Src at the plasma membrane/substrate interface. *PLoS One* 7, e38948.
- Morris, S.W., Kirstein, M.N., Valentine, M.B., Dittmer, K.G., Shapiro, D.N., Saltman, D.L., and Look, A.T. (1994). Fusion of a kinase gene, ALK, to a nucleolar protein gene, NPM, in non-Hodgkin's lymphoma. *Science* 263, 1281-1284.
- Mouse Genome Sequencing, C., Waterston, R.H., Lindblad-Toh, K., Birney, E., Rogers, J., Abril, J.F., Agarwal, P., Agarwala, R., Ainscough, R., Alexandersson, M., *et al.* (2002). Initial sequencing and comparative analysis of the mouse genome. *Nature* 420, 520-562.
- Nowell, P.C. (1962). The minute chromosome (Ph1) in chronic granulocytic leukemia. *Blut* 8, 65-66.
- Oppermann, H., Levinson, A.D., Varmus, H.E., Levintow, L., and Bishop, J.M. (1979). Uninfected vertebrate cells contain a protein that is closely related to the product of the avian sarcoma virus transforming gene (src). *Proc Natl Acad Sci U S A* 76, 1804-1808.
- Pawson, T. (2004). Specificity in signal transduction: from phosphotyrosine-SH2 domain interactions to complex cellular systems. *Cell* 116, 191-203.
- Peles, E., Bacus, S.S., Koski, R.A., Lu, H.S., Wen, D., Ogden, S.G., Levy, R.B., and Yarden, Y. (1992). Isolation of the neu/HER-2 stimulatory ligand: a 44 kd glycoprotein that induces differentiation of mammary tumor cells. *Cell* 69, 205-216.
- Quintas-Cardama, A., Kantarjian, H., and Cortes, J. (2007). Flying under the radar: the new wave of BCR-ABL inhibitors. *Nat Rev Drug Discov* 6, 834-848.

- Resh, M.D. (1994). Myristylation and palmitoylation of Src family members: the fats of the matter. *Cell* 76, 411-413.
- Robinson, D.R., Wu, Y.M., and Lin, S.F. (2000). The protein tyrosine kinase family of the human genome. *Oncogene* 19, 5548-5557.
- Roskoski, R. (2004). Src protein-tyrosine kinase structure and regulation. In *Biochemical and Biophysical Research Communications*, pp. 1155-1164.
- Roskoski, R., Jr. (2005). Src kinase regulation by phosphorylation and dephosphorylation. *Biochem Biophys Res Commun* 331, 1-14.
- Rossari, F., Minutolo, F., and Orciuolo, E. (2018). Past, present, and future of Bcr-Abl inhibitors: from chemical development to clinical efficacy. *J Hematol Oncol* 11, 84.
- Rowley, J.D. (1973). Letter: A new consistent chromosomal abnormality in chronic myelogenous leukaemia identified by quinacrine fluorescence and Giemsa staining. *Nature* 243, 290-293.
- Sadowski, I., Stone, J.C., and Pawson, T. (1986). A noncatalytic domain conserved among cytoplasmic protein-tyrosine kinases modifies the kinase function and transforming activity of Fujinami sarcoma virus P130gag-fps. *Mol Cell Biol* 6, 4396-4408.
- Sasada, R., Ono, Y., Taniyama, Y., Shing, Y., Folkman, J., and Igarashi, K. (1993). Cloning and expression of cDNA encoding human betacellulin, a new member of the EGF family. *Biochem Biophys Res Commun* 190, 1173-1179.
- Scott, R.P., Eketjall, S., Aineskog, H., and Ibanez, C.F. (2005). Distinct turnover of alternatively spliced isoforms of the RET kinase receptor mediated by differential recruitment of the Cbl ubiquitin ligase. *J Biol Chem* 280, 13442-13449.
- Seet, B.T., Dikic, I., Zhou, M.M., and Pawson, T. (2006). Reading protein modifications with interaction domains. *Nat Rev Mol Cell Biol* 7, 473-483.
- Sefton, B.M., Hunter, T., Beemon, K., and Eckhart, W. (1980). Evidence that the phosphorylation of tyrosine is essential for cellular transformation by Rous sarcoma virus. *Cell* 20, 807-816.
- Seidman, A.D., Berry, D., Cirrincione, C., Harris, L., Muss, H., Marcom, P.K., Gipson, G., Burstein, H., Lake, D., Shapiro, C.L., *et al.* (2008). Randomized phase III trial of weekly compared with every-3-weeks paclitaxel for metastatic breast cancer, with trastuzumab for all HER-2 overexpressors and random assignment to trastuzumab or not in HER-2 nonoverexpressors: final results of Cancer and Leukemia Group B protocol 9840. *J Clin Oncol* 26, 1642-1649.
- Sharma, K., D'Souza, R.C., Tyanova, S., Schaab, C., Wisniewski, J.R., Cox, J., and Mann, M. (2014). Ultradeep human phosphoproteome reveals a distinct regulatory nature of Tyr and Ser/Thr-based signaling. *Cell Rep* 8, 1583-1594.
- Shing, Y., Christofori, G., Hanahan, D., Ono, Y., Sasada, R., Igarashi, K., and Folkman, J. (1993). Betacellulin: a mitogen from pancreatic beta cell tumors. *Science* 259, 1604-1607.

Shiota, M., Fujimoto, J., Semba, T., Satoh, H., Yamamoto, T., and Mori, S. (1994). Hyperphosphorylation of a novel 80 kDa protein-tyrosine kinase similar to Ltk in a human Ki-1 lymphoma cell line, AMS3. *Oncogene* 9, 1567-1574.

Shoyab, M., Plowman, G.D., McDonald, V.L., Bradley, J.G., and Todaro, G.J. (1989). Structure and function of human amphiregulin: a member of the epidermal growth factor family. *Science* 243, 1074-1076.

Songyang, Z., Shoelson, S.E., Chaudhuri, M., Gish, G., Pawson, T., Haser, W.G., King, F., Roberts, T., Ratnofsky, S., Lechleider, R.J., *et al.* (1993). SH2 domains recognize specific phosphopeptide sequences. *Cell* 72, 767-778.

Songyang, Z., Shoelson, S.E., McGlade, J., Olivier, P., Pawson, T., Bustelo, X.R., Barbacid, M., Sabe, H., Hanafusa, H., Yi, T., *et al.* (1994). Specific motifs recognized by the SH2 domains of Csk, 3BP2, fps/fes, GRB-2, HCP, SHC, Syk, and Vav. *Mol Cell Biol* 14, 2777-2785.

Sorkin, A., and Von Zastrow, M. (2002). Signal transduction and endocytosis: close encounters of many kinds. *Nat Rev Mol Cell Biol* 3, 600-614.

Stehelin, D., Fujita, D.J., Padgett, T., Varmus, H.E., and Bishop, J.M. (1977). Detection and enumeration of transformation-defective strains of avian sarcoma virus with molecular hybridization. *Virology* 76, 675-684.

Strachan, L., Murison, J.G., Prestidge, R.L., Sleeman, M.A., Watson, J.D., and Kumble, K.D. (2001). Cloning and biological activity of epigen, a novel member of the epidermal growth factor superfamily. *J Biol Chem* 276, 18265-18271.

Thomas, S.M., and Brugge, J.S. (1997). Cellular functions regulated by Src family kinases. *Annu Rev Cell Dev Biol* 13, 513-609.

Tonks, N.K. (2006). Protein tyrosine phosphatases: from genes, to function, to disease. *Nat Rev Mol Cell Biol* 7, 833-846.

Toyoda, H., Komurasaki, T., Uchida, D., Takayama, Y., Isobe, T., Okuyama, T., and Hanada, K. (1995). Epiregulin. A novel epidermal growth factor with mitogenic activity for rat primary hepatocytes. *J Biol Chem* 270, 7495-7500.

Twomey, J.D., Brahme, N.N., and Zhang, B. (2017). Drug-biomarker co-development in oncology - 20 years and counting. *Drug Resist Updat* 30, 48-62.

Ushiro, H., and Cohen, S. (1980). Identification of phosphotyrosine as a product of epidermal growth factor-activated protein kinase in A-431 cell membranes. *J Biol Chem* 255, 8363-8365.

Van de Peer, Y., Mizrachi, E., and Marchal, K. (2017). The evolutionary significance of polyploidy. *Nat Rev Genet* 18, 411-424.

Vogel, C.L., Cobleigh, M.A., Tripathy, D., Gutheil, J.C., Harris, L.N., Fehrenbacher, L., Slamon, D.J., Murphy, M., Novotny, W.F., Burchmore, M., *et al.* (2002). Efficacy and safety of trastuzumab as a single agent in first-line treatment of HER2-overexpressing metastatic breast cancer. *J Clin Oncol* 20, 719-726.

- Volpe, P., and Eremenko-Volpe, T. (1970). Quantitative studies on cell proteins in suspension cultures. *Eur J Biochem* *12*, 195-200.
- Waksman, G., Kominos, D., Robertson, S.C., Pant, N., Baltimore, D., Birge, R.B., Cowburn, D., Hanafusa, H., Mayer, B.J., Overduin, M., *et al.* (1992). Crystal structure of the phosphotyrosine recognition domain SH2 of v-src complexed with tyrosine-phosphorylated peptides. *Nature* *358*, 646-653.
- Waksman, G., Kumaran, S., and Lubman, O. (2004). SH2 domains: role, structure and implications for molecular medicine. *Expert Rev Mol Med* *6*, 1-18.
- Walsh, D.A., Perkins, J.P., and Krebs, E.G. (1968). An adenosine 3',5'-monophosphate-dependant protein kinase from rabbit skeletal muscle. *J Biol Chem* *243*, 3763-3765.
- Waterman, H., Katz, M., Rubin, C., Shtiegman, K., Lavi, S., Elson, A., Jovin, T., and Yarden, Y. (2002). A mutant EGF-receptor defective in ubiquitylation and endocytosis unveils a role for Grb2 in negative signaling. *EMBO J* *21*, 303-313.
- Wei, R., Kaneko, T., Liu, X., Liu, H., Li, L., Voss, C., Liu, E., He, N., and Li, S.S. (2018). Interactome Mapping Uncovers a General Role for Numb in Protein Kinase Regulation. *Mol Cell Proteomics* *17*, 2216-2228.
- Wei, R., Liu, X., Voss, C., Qin, W., Dagnino, L., Li, L., Vigny, M., and Li, S.S. (2019). NUMB regulates the endocytosis and activity of the anaplastic lymphoma kinase in an isoform-specific manner. *J Mol Cell Biol*.
- Wilhelm, M., Schlegl, J., Hahne, H., Gholami, A.M., Lieberenz, M., Savitski, M.M., Ziegler, E., Butzmann, L., Gessulat, S., Marx, H., *et al.* (2014). Mass-spectrometry-based draft of the human proteome. *Nature* *509*, 582-587.
- Wu, P., Nielsen, T.E., and Clausen, M.H. (2015). FDA-approved small-molecule kinase inhibitors. *Trends Pharmacol Sci* *36*, 422-439.
- Xing, Z., Chen, H.C., Nowlen, J.K., Taylor, S.J., Shalloway, D., and Guan, J.L. (1994). Direct interaction of v-Src with the focal adhesion kinase mediated by the Src SH2 domain. *Mol Biol Cell* *5*, 413-421.
- Yarden, Y., and Sliwkowski, M.X. (2001). Untangling the ErbB signalling network. *Nat Rev Mol Cell Biol* *2*, 127-137.
- Zhang, D., Sliwkowski, M.X., Mark, M., Frantz, G., Akita, R., Sun, Y., Hillan, K., Crowley, C., Brush, J., and Godowski, P.J. (1997). Neuregulin-3 (NRG3): a novel neural tissue-enriched protein that binds and activates ErbB4. *Proc Natl Acad Sci U S A* *94*, 9562-9567.
- Zhang, J., Yang, P.L., and Gray, N.S. (2009). Targeting cancer with small molecule kinase inhibitors. *Nat Rev Cancer* *9*, 28-39.
- Zheng, Y., Zhang, C., Croucher, D.R., Soliman, M.A., St-Denis, N., Pasculescu, A., Taylor, L., Tate, S.A., Hardy, W.R., Colwill, K., *et al.* (2013). Temporal regulation of EGF signalling networks by the scaffold protein Shc1. *Nature* *499*, 166-171.

Chapter 2

2 SH2 superbinder-AP-MS for Examining TK Activation in Cancer Samples

2.1 Abstract

The human genome harbors 90 TK genes. Over 20 of these have been characterized as biomarkers across a wide variety of cancers and more than half of all approved anti-cancer targeted therapeutics are TK inhibition molecules. Many TKs are functionally redundant and stimulate the same oncogenic signaling pathways, therefore the retention of (on-target or non-target) TK activity becomes one of the major influences on the efficacy of TK inhibition therapy. The examination of TK biomarkers mainly relies on the gold standard IHC and FISH assays, which are low-multiplexing and incapable of profiling TK activity systematically due to the limitations of visual perception. Next generation sequencing has recently been approved for screening genomic alterations in cancer, but gene amplification/mutation are not direct indicators of TK activity. Here we have developed a superbinder SH2 enabled AP-MS assay for evaluating TK activity by targeting functional pTyr sites on 87 TKs. This assay combines a highly efficient pTyr affinity purification afforded by the superbinder SH2 and MS analysis. In the examination of clinical samples, the activation loop peptides of known TK biomarkers were identified from both leukemia whole blood and solid tumors tissues, even from a minute amount of protein recovered from a few FFPE (formalin-fixed, paraffin-embedded) slides. In cell models of drug resistance, TK reprogramming was monitored in the SK-BR-3 breast cancer cells treated with trastuzumab, and the deregulation of c-Kit receptor tyrosine kinase was shown to be responsible for acquired trastuzumab resistance. The SH2-AP-MS approach bears great potential for discovering TK biomarkers and deciphering resistance mechanism to targeted therapeutics. This assay has potential to be applied either independently or as a complementary approach to IHC/FISH, as it can be used to analyze the same FFPE tissue specimens.

2.2 Introduction

Along with the great success of anti-cancer targeted therapeutics, the biomarker-based classification of cancer subtypes has become crucial for guiding the design of therapy in the clinic, particularly for the treatment of advanced stage cancer (Mabert et al., 2014). The identification of selected TKs, as well as other types of biomarkers, have become routine examinations for many cancer types in clinical laboratory (Pavlou et al., 2013). As introduced earlier, ErbB2 (HER2) is a TK biomarker in breast cancer. The analysis of ErbB2, estrogen receptor (ER) and progesterone receptor (PR) are already widely accepted for classifying breast cancer (Gradishar et al., 2018). Conventionally, examination of protein or gene biomarkers all employ the same strategies and techniques: immunohistochemistry (IHC) assays for evaluating protein abundance and *in situ* hybridization assays (ISH) for detecting gene fusion or amplification. These robust assays are relatively sensitive and accurate and have been used in both research and clinic laboratories for decades. Until now there are still massive efforts underway to develop these gold standard examination tools to match the continuous discovery of new biomarkers in different diseases including cancer. However, with the emergence of the personal/precision medicine concept, these conventional tools are being challenged by more comprehensive and quantitative omics techniques (Collins et al., 2017; Jung, 2016; Tanase et al., 2016).

2.2.1 Limitations of conventional TK examination assays

Several limitations can impede the application of conventional assays in comprehensive evaluation of TK activity in cancer.

1) Low multiplexing capability. Conventional biomarker diagnostic assays rely on the specific interaction between biomarkers and probes and generally follow the same strategy: staining the biopsy tissue section with probes and then visualizing the probe/biomarker by microscopy. Theoretically the probes, either specific antibodies or complementary nucleic acid fragments, are highly selective, therefore it is possible to apply multiple probes to detect their corresponding biomarkers simultaneously. However, multiplexing is greatly limited by the visual perception adopted in all these assays. In a high-end fluorescence microscope, combinations of different excitation sources and emission filters may visualize

four to five spectrally distinct fluorochromes simultaneously. It is possible to precisely excite more fluorochromes with different laser sources, but the wide emission spectra (typically 40~50 nm with broad tails) can result in severe spectral overlapping in the narrow blue-to-red spectral window, which means the emission from a given fluorochrome contributes to the signal of multiple emission channels. Currently quadruplex IHC seems to be the highest level of multiplexing IHC that can be potentially applied in FFPE examination in the clinic (Dixon et al., 2015). Some of our preliminary data already reveals that cancer cells may co-express multiple TKs in relatively high levels, for which only a cocktail of corresponding TK inhibitors can effectively inhibit cell proliferation (Bian et al., 2016). Clearly, quadruplex IHC is incapable of revealing the complexity of TK activation in some cancers. Over 20 TKs have been identified as biomarkers in various cancer types and it is likely that more TKs and TK associated proteins will be added to the list of potential therapeutic targets in the future (Kannaiyan and Mahadevan, 2018; Levitzki, 2013; Wu et al., 2015). Using a different strategy of microscopic detection may improve the technique. For instance, characterizing photostability or Raman scattering can distinguish spectra-overlapping fluorochromes and greatly increase the multiplexing level (Orth et al., 2018; Wei et al., 2017). However, none of these microscopy technologies have been applied in biopsy examination in the clinic to date, and technically speaking, multi-probe staining is not a practical assay.

2) Compromised data reproducibility. It is believed that different labs or pathologists may have slightly different criteria to determine TK status, especially when the TK abundance or amplification are not strongly positive or negative (Handorf et al., 2013). The classic IHC assay and fluorescent *in situ* hybridization (FISH) assay both have a complicated sample preparation process consisting of tens of steps including tissue fixation, dehydration, paraffin embedding, sectioning and re-hydration, all before incubation with antibody or nucleic acid probes. Days of bench work will be required for obtaining the raw data. Even though highly stringent protocols have been established for these assays, the batch-to-batch variation is still hardly eliminated or minimized to a certain level consistently. The inherent heterogeneity in the distribution of TK positive cells within the tumor may pose another problem. It was previously estimated that more than 10% of HER2-positive breast cancer diagnosis yield inaccurate results, falsely reporting HER2

status (Paik et al., 2002; Perez et al., 2006; Sauter et al., 2009; Sui et al., 2009; Wolff et al., 2007). Taking advantage of rapidly-developing artificial intelligence (AI, or deep learning) technology, some attempts have been made to automate image analysis to increase the accuracy of microscopy-based analysis and help reduce human error (Khosravi et al., 2017). However, image analysis AI platforms are still frequently unreliable, often unable to distinguish dogs from cats, for example.

3) Less quantitative reporting. In HER2 biopsy examination by IHC or FISH, the status of HER2 is classified as 0 degree (HER2 negative), +1 degree (HER2 positive, marginal), +2 degree and highest +3 degree (HER2 positive). A noticeable problem of HER2 examination is its accuracy or the value in guiding therapy design. Based on clinical trials and subsequent statistical studies, the degree of HER2 activation determined by IHC/FISH did not correlate well with response to treatment with HER2 inhibition antibody trastuzumab (Denkert et al., 2013; Vassilakopoulou et al., 2014; Xu et al., 2016). In fact, approximately 70% of breast patients diagnosed as HER2 positive do not respond to trastuzumab treatment at all (Perez et al., 2010; Seidman et al., 2008). Using the same assays, the MCF7 cell line is defined as HER2 0 degree or +1 degree because HER2 expression is detectable but relatively less-abundant in MCF7. In contrast, the SK-BR-3 or BT-474 cell lines are HER2 +3 degree as they are known cell lines expressing high levels of HER2. Quantitatively, SK-BR-3 or BT-474 cells express 100~150-fold higher HER2 protein compared to MCF7 cells (Bian et al., 2016; Holliday and Speirs, 2011; Subik et al., 2010). It could be anticipated a quantitative and comprehensive report would provide more invaluable guidance for physicians to design the strategy of treatment and decide the dose of therapeutics precisely. As will be presented in this thesis, ErbB2 (HER2) is the dominant RTK in SK-BR-3 and BT-474, while multiple RTKs are co-deregulated in MCF7 including ErbB2, DDR1 (Epithelial discoidin domain-containing receptor) and IGF-1R/INSR (Insulin receptors). None of these RTKs are extremely active in MCF7 cells, but their expression profiles are all relatively abundant among nine cancer cell lines examined (Bian et al., 2016). It is intriguing that only a combination of inhibitors against ErbB2/DDR1/IGF-1R/INSR exhibited great inhibitory effect on MCF7 cell viability, which was additive and dose-dependent, but individual inhibitors at an identical concentration had little to no effect on MCF7 cell viability.

2.2.2 Mass spectrometry

Mass spectrometry (MS) is an analytical technique that is powerful and widely applied in bio-omics studies (Aebersold and Goodlett, 2001; Vestal, 2011). The basic principle of mass spectrometry is to generate ions from the analyte by applicable ionization methods, to separate the ions by their distinct mass-to-charge (m/z) ratio using mass analyzers, and to determine the abundance of ions qualitatively or quantitatively using ion detectors (Gross, 2004). Regarding the proteomics study, which is largely depending on the analysis of peptides enzymatically digested from proteins, liquid chromatography-electrospray ionization-tandem mass spectrometry (LC-ESI-MS/MS) systems are preferred. These MS systems convert peptides into ions by electrospray ionization, and combine the physical separation capability of LC (or high-performance liquid chromatography, HPLC) with the mass analysis capability of MS. In tandem MS systems with multiple mass analyzers, the mass-selected ions (MS1) are subjected to a second (MS2) or even more rounds of mass spectrometric analysis (MS_n), which exhibits great advantages for the analysis of specific organic compounds in a complex matrix, such as peptides digested from whole cell lysate (McLafferty, 1981). A collision module is typically equipped in tandem MS systems between MS1 and MS2, which allows the collision between ionized analytes and neutral gas atoms (helium, nitrogen or argon). During collision, some energy is converted into internal energy resulting in bond breakages within the analytes. This process is known as collision-induced dissociation (CID) or collision-activated dissociation (CAD) (Jennings, 2000). In a classic tandem MS workflow, the analytes are first ionized, and the target ions are filtered from the matrix in the first mass analyzer. The selected analytes are then fragmented in the collision module, and from the daughter ions the secondary mass analyzer isolates target ions again which are finally quantified in the ion detector (McLafferty, 1981). Theoretically for peptide or protein analyses, the amino acid sequence and modification could be clearly elucidated by analyzing the data combined from MS1 and MS2. In the form of LC-MS/MS, this workflow becomes even more specific when the peptides are pre-separated by chromatography.

2.2.2.1 Mass spectrometry systems used in this study

Two tandem LC-MS systems, the SCIEX triple-quadrupole MS system and the Thermo QExactive quadrupole-orbitrap hybrid MS system, were used in my studies.

The quadrupole is a classic type of mass analyzer (Dawson, 1986; Gross, 2004; Miller and Denton, 1986). A quadrupole analyzer consists of four cylindrical (z-direction) rod electrodes, or even hyperbolically shaped rods (Thermo), that are arranged in a square configuration (xy-plane). The pairs of opposite rods are each connected to radio-frequency (RF) and direct-current (DC) power supplies at the same potential. Once an ion enters the quadrupole via the z-direction, the ion will oscillate in the xy-directions due to the periodic attraction/repulsion forces generated from the RF and DC electrical fields. As the space is limited among the quadrupole in xy-directions, some ions may hit the rods and become neutralized due to over-the-range oscillation amplitudes in xy-directions, while other ions may pass through, thereby selected by the quadrupole MS analyzer. By defining the RF and DC voltage and frequency, a narrow m/z window could be opened for the pass-through of ions with specific m/z values. The triple-quadrupole MS is a tandem mass spectrometer consisting of two quadrupole MS analyzers (MS1/MS2), and a non-mass-selected (RF only) quadrupole (collision cell) between MS1 and MS2 for analyte fragmentation. This design was first developed in late 1970s (Yost and Enke, 1978), is currently the most reliable and robust MS system used in a multitude of research and industrial fields, and is arguably the best choice of equipment for quantitative targeted proteomics.

A major drawback of the triple-quadrupole is the low resolving power (mass resolution). Mass resolution is the degree of separation of analytes with slightly different m/z values and defined as the smallest difference in m/z ($\Delta m/z$) that can be distinguished for a given m/z value: $\text{resolution} = (m/z) / (\Delta m/z)$. Typically, the quadrupole resolution is only a few thousands which restricts its applications to tasks that do not require high resolution. Mass accuracy is another parameter closely related to the mass resolution, which can be calculated as the absolute mass difference (experimental v.s. theoretical) divided by theoretical mass and given in parts per million (ppm). Similarly, a quadrupole does not have excellent mass accuracy, even though mechanical optimization is being continuously developed (Yang et al., 2002). Due to the lower resolution and accuracy, quantitative

proteomics typically require more procedures and additional testing using synthesized peptides in the triple-quadrupole system (Gross, 2004). Multiple rounds of ion selection and parameter optimization for individual synthetic peptides need to be carried out and a standard MS2 spectral library is usually built in this process. In the analysis of bio-materials that are highly complicated and may contain a lot of interfering ions (analytes with similar LC elution timing and close m/z values in MS1/MS2), the MS2 spectrum of a targeted peptide can be searched in the standard spectral library, thereby allowing the selection of genuine daughter ions derived from the target peptides.

The orbitrap is an ion-trap type of mass analyzer employing ion trapping in an electrostatic-only field, which is generated between an outer barrel-like electrode and a coaxial inner spindle-like electrode (Makarov, 2000). In the presence of an RF field (as that in a quadrupole), ions orbit around the coaxial inner electrode that perform harmonic oscillation with frequencies determined by the corresponding m/z values. The image charge induced by the ion motion passing near the conductor (image current) is then recorded and converted to a mass spectrum by Fourier transform (Hu et al., 2005; Makarov, 2000). A great advantage of orbitrap mass analyzer is high mass resolution and mass accuracy. The proto-type orbitrap built in 1990s already reached a resolution of 140,000. Our Thermo QExactive system has a resolution ranging from 17,500 to 140,000. Even with a resolution of 17,500, mass accuracy is typically within 5 ppm for most peptides, which is comparable to decent triple quadrupole systems or even better. In addition, unlike the quadrupole mass analyzer that only selects one ion in one scanning round, the orbitrap analyzer can handle and detect tens of ions simultaneously, making it more practical in discovery proteomics studies.

2.2.2.2 Protein digestion

Even though intact proteins or protein complexes are analyzable in some specialized MS systems, enzymatically digested peptides are still the most common analytes in MS-based proteomics studies, therefore protein digestion using a dedicated protease represents a key procedure in the classic proteomics experiment. The serine protease trypsin is predominantly utilized to cleave proteins, mainly due to its sequence-specificity, high activity, and cost-efficiency. Trypsin was discovered over a century ago and is widely

found in the digestive system of vertebrates where it hydrolyzes food proteins (Rawlings and Barrett, 1994). Trypsin cleaves peptide chains specifically at the carboxy-terminal of the amino acids Arginine (R) and Lysine (K), except when followed by Proline (P). Wild type trypsin undergoes autolysis, which generates pseudotrypsin with broadened cleavage specificity. To eliminate the possible mis-cleavages produced by pseudotrypsin, trypsin is usually modified in lysine residues by reductive methylation (Keil-Dlouha et al., 1971; Rice et al., 1977), yielding an autolysis-resistant trypsin variant that is more suitable for proteomics studies.

The length of tryptic digested peptides typically ranges between 8 and 30 amino acids, which are efficiently separated by LC using reversed-phase chromatography (hydrophobic chromatography) with an octadecyl-carbon chain (C18) bonded silica as the stationary phase, and a mixture of water (polar) and organic solvent (acetonitrile, ACN, non-polar) as the mobile phase. C18 is hydrophobic and has a strong affinity for hydrophobic peptides in the polar mobile phase, which can be eluted from C18 by decreasing the polarity of the solution in the mobile phase. In a mobile phase gradient with decreasing polarity, peptides with increasing hydrophobicity will be eluted sequentially. Following LC separation, tryptic digested peptides are also optimal for ionization in ESI. Arginine and lysine are two of the three positive amino acids. During ionization in the acidic mobile phase, the amine group at the amino-terminus and arginine or lysine at the carboxyl-terminus typically make the peptide +2 charged. If another positive amino acid histidine is included in the sequence, or there is a R/K miscleavage, the peptide ion could be +3 charged. Both +2 and +3 charging, and even +4 charging of most tryptic digested peptides all fall within the appropriate m/z range for MS detection.

2.2.2.3 Peptide fragmentation

Peptide fragmentation and subsequent MS2 analysis is crucial for identifying the peptide sequence and PTMs on specific amino acids. During fragmentation, the flying peptides collide with neutral gas atoms and break into charged fragments (daughter ions). Several daughter ion types may be generated due to the different break sites within the peptides, which is determined by many factors including peptide sequence, charge status, collision energy etc. As shown in Fig.2.1, if a precursor peptide breaks once in the peptide backbone,

six different types of daughter ions may be produced, which are also termed “sequence ions” as they carry an intact amino-terminus or carboxyl-terminus containing fragments of the precursor peptide (Roepstorff and Fohlman, 1984). The fragments with the intact amino-terminus are named as a, b and c ions, whereas their complementary fragments with intact carboxyl-terminus are referred to as x, y and z ions. The distribution of positive (basic) amino acids (R/K/H) and charge status are key factors governing the fragmentation behavior of protonated peptides. Among all ions, b and y type ions are the most common ion types. y ions are most important sequence ions for tryptic peptides and y1 and y2 ions are almost universally present in MS2, while b2 and b3 ions are also present in most MS2 peptide spectrums.

Breakage in the side chain or multiple breakages in the backbone produce additional types of daughter ions. Compared to the sequence ions with intact amino- or carboxyl-termini, these ions are usually less important for proteomics studies. However, in some specific MS applications, detection of non-sequence ions is of great value as well. For instance, a combination of a type and y type cleavages produces immonium ions that carry composition information for amino acids. In the detection of pTyr peptides, the existence of immonium ion at m/z 216.0426 is solid evidence of tyrosine phosphorylation. Because the non-sequencing ions are usually located in the low m/z range and less abundant than sequence ions, their detection and subsequent computational analysis usually require additional effort.

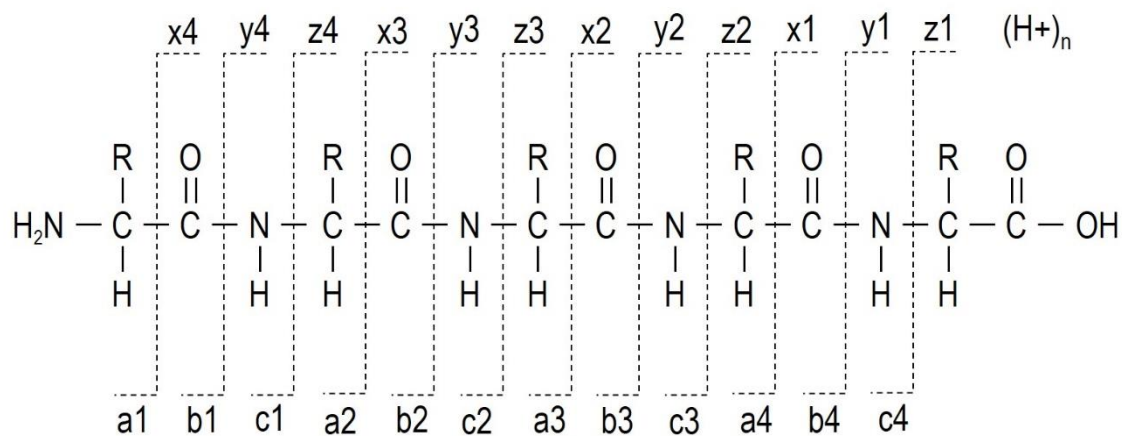


Figure 2.1 Nomenclature for peptide fragmentation

Simplified nomenclature for peptide cleavage within backbone and fragmented ions in collision induced dissociation.

2.2.2.4 Mass spectrometry methods

In MS-based proteomics studies, there are two fundamental strategies: targeted quantification and discovery-based identification. With a targeted quantification, the goal is to monitor a selection of peptides/proteins of interest with high sensitivity, reproducibility and quantitative accuracy. On the other hand, with discovery-based identification, the goal is to identify as many peptides/proteins as possible, and in this case, the abundance of analytes is qualitative only or relatively quantitative (Doerr, 2012, 2014). The targeted strategy of mass spectrometry usually combines tandem MS analyzers with LC to detect a specific analyte at a specific time (LC retention time). There are several MS methods usually applied in the qualification and quantification of peptides: multiple (selected) reaction monitoring (MRM/SRM), parallel reaction monitoring (PRM) and selected ion monitoring (SIM).

MRM is a widely accepted method in quantitative targeted proteomics, performed on the classic triple quadrupole MS system introduced above. The precursor is first isolated in MS1 to enter the collision cell for fragmentation, then a specific daughter ion is isolated again in MS2 to enter the detector. In MRM, the m/z values of both precursor and daughter ions need to be defined and the daughter ions are scanned sequentially. Once the MS2 spectral library and calibration curve are built using standard/synthesized peptides, MRM can quantify the peptide abundance absolutely and accurately.

Both PRM and SIM are newer methods developed along with the application of orbitrap MS analyzer. Because the orbitrap analyzer can analyze all detectable daughter ions in a wide m/z range simultaneously, only the m/z values of precursors are defined in PRM and SIM methods. In our QExactive quadrupole-orbitrap MS system, PRM uses the front-end quadrupole (MS1) analyzer to isolate the precursor, then fragments it in the collision cell and finally detects all daughter ions in the orbitrap (MS2) analyzer. SIM collects the data for daughter ions in the same way as PRM, but also measures the precursor abundance directly without fragmentation in another scanning. Therefore, PRM identifies and quantifies peptides using daughter ion data, while SIM identifies peptides using daughter ion data but quantifies peptides using precursor ion data. Because the fragmentation efficiency is limited, SIM has significant higher sensitivity than PRM. On the other hand,

PRM has an advantage over SIM with improved signal-to-noise ratio rather than absolute signal, especially in the analysis of highly complicated samples (Gallien et al., 2012). Taking advantage of the high resolving power of orbitrap, both PRM and SIM provide high selectivity and high sensitivity for confident peptide confirmation, and therefore are extremely suitable for identifying a large number of peptides in complicated samples. With proper parameter optimization, even hundreds of peptides could be quantified in a single test (Kuhlmann et al., 2018). Due to the inherent nature of the orbitrap analyzer, PRM and SIM are less quantitative compared to MRM, and require internal standards for proper quantification.

2.2.3 Affinity purification of modified peptides

Even though protein phosphorylation is a very abundant PTM within the proteome and two-thirds of all human proteins are phosphorylated on multiple sites (Sharma et al., 2014), phosphorylated peptides only make up a small portion of all peptides digested from the cell lysate. Theoretically, the MS should be able to directly isolate and detect phosphorylated peptides from the matrix. However, this is highly impractical, even with the highest-end MS systems, because of the overwhelming signals from much more abundant non-phosphorylated peptides. The signal for most phosphorylated peptides could be easily masked by non-phosphorylated peptides with close m/z values. Therefore, affinity purification (AP) of phosphorylated peptides, as well as any other modified peptides, is an essential step in sample preparation for MS-based PTM studies (Fila and Honys, 2012). Most enrichment strategies are based on affinity chromatography or immunoprecipitation to isolate modified peptides with enhanced affinities to the matrix or PTM-specific antibodies. Titanium dioxide (TiO₂) and immobilized metal ion affinity chromatography (IMAC) are able to capture phosphorylated peptides effectively (de Graaf et al., 2014; Sharma et al., 2014; Zhou et al., 2013), but they are only used for enriching pSer and pThr peptides. The much less abundant pTyr peptides are usually enriched using anti-pTyr antibodies (Rikova et al., 2007; Tinti et al., 2012; Zhang et al., 2005).

We developed an engineered SH2 superbinder as an ideal reagent for affinity purification of pTyr peptides and subsequent MS analysis (Bian et al., 2016). From the study of nine lab-cultured cancer cell lines, the SH2-AP-MS approach led to the identification of around

10,000 unique pTyr sites, of which over 3,000 sites are novel. Compared to the most commonly used 4G10 anti-pTyr antibody, the superbinder has a comparable pTyr enriching ability at the same molar amount. The superbinder and 4G10 exhibit differential specificity since each method can identify a large portion of unique pTyr peptides. However, when 20-fold molar excess amount of the SH2 superbinder was applied, it was able to capture almost all pTyr peptides captured as 4G10, plus numerous others. Therefore, the SH2 superbinder bears great potential to be used as an alternative to anti-pTyr antibodies in AP-MS. More importantly, the superbinder is easily expressed and purified from bacteria at minimal cost and has excellent stability.

2.2.4 SH2-AP-MS

As introduced earlier, TKs are a major type of biomarkers and therapeutic targets in cancer. More than half of the FDA approved anti-cancer targeted drugs are TK inhibition molecules. In addition, immune checkpoint inhibition therapeutics, such as the humanized anti-PD1/PDL1 antibodies, are also designed to interfere with TK activation in immune cells (Wilkinson and Leishman, 2018). A common consequence of these therapies is the change of tyrosine phosphorylation status in either TK or TK substrates, especially on the sites determining kinase activity and signal transduction. This raises the possibility to evaluate TK activity and drug response by tracking the PTM dynamics on functional pTyr sites. Indeed, some conventional IHC based TK examination assays take advantage of the specific anti-pTyr antibodies that only recognize site-specific phosphorylated TK variants, which represent active forms of the corresponding TKs (Mandell, 2008). To meet the emerging requirement for precision medicine, we have developed an SH2-AP-MS assay for simultaneous detection of 79 (PRM) or 157 (MRM) functional pTyr peptides that cover up to 87 TKs, including all known TK biomarkers and additional (proto)oncogenic TKs. High multiplexity is a major advantage of this approach, compared to the gold standard IHC/FISH assays. Since MS is sensitive analytic equipment and the SH2 superbinder affinity purification is highly efficient, this assay only requires tens of micrograms of proteins, or even less, which can be easily extracted from cultured cells, fast frozen (FF) tumor tissues, or even biopsy FFPE specimens that have been examined in the clinical laboratory.

A variety of different patient-derived samples from both solid tumors and leukemia were analyzed by this assay, including breast cancer, lung cancer, bile duct cancer, acute myelogenous leukemia and chronic lymphocytic leukemia. Several known TK biomarkers in these cancer types, such as ALK, BTK and FGFR, were detected with solid MS/MS data. This assay was also applied to assess transient TK kinome reprogram in cultured SK-BR-3 HER2 breast cancer cells treated with the HER2 inhibitor lapatinib. Lapatinib inhibition caused acute EGFR/ErbB2/Src activity loss. ErBB2 activity was recovered between 24 to 48 hours but both EGFR and Src retained low-level activity. In addition, the mechanism of acquired drug was investigated, which is common in the clinic and one of the main reasons for compromised efficiency of targeted therapies. Due to difficulty in obtaining patient-derived samples before and after targeted therapy, a trastuzumab resistant model was established in SK-BR-3 cells, which were continuously exposed to a low dose of trastuzumab for over six months in the lab. The SH2-AP-MS analysis revealed a dramatic increase in the phosphorylation of c-Kit at the activation loop tyrosine residue in the resistant clone, consistent with the findings from transcriptome sequencing. The c-Kit inhibitor imatinib alone had little effect on cell viability, however, it re-sensitized the resistant cells to trastuzumab treatment, indicating the activation of c-Kit compensated for the loss of HER2 activity and contributed to trastuzumab resistance in SK-BR-3 cells. Overall, these data have revealed the potential value of the SH2-AP-MS assay in both research and clinic applications.

2.3 Materials and Methods

2.3.1 Cell culture

All breast cancer cell lines used in this study were grown in Roswell Park Memorial Institute (RPMI) 1640 medium supplemented with 10% FBS, 100 $\mu\text{g/ml}$ penicillin, 100 $\mu\text{g/ml}$ streptomycin and 2 mg/ml L-Glutamine. Cells were incubated at 37 °C in a humidified atmosphere containing 5% carbon dioxide.

2.3.2 SH2 superbinder purification and immobilization

The SH2 superbinder engineered from human Src tyrosine kinase was integrated into the pETM-30 vector for GST (glutathione S-transferase) fusion, or the pETM-11 for His (poly-histidine) fusion (by Courtney Voss). The plasmids were transformed into the BL21 strain of *Escherichia coli*. Positive colonies were isolated by antibiotic resistance and grown in liquid Lysogeny Broth (LB) medium (10 g/L tryptone, 5 g/L yeast extract and 10 g/L sodium chloride) to reach OD₆₀₀ 0.6~0.8. The cells were then induced by 0.5 mM IPTG (isopropyl β -D-1-thiogalactopyranoside) for 16~18 hours at 18 °C with slow rotation. Cells were harvested by centrifugation and either processed immediately or stored as a dry pellet at -80 °C.

For GST purification, cells collected from 100 ml culture were resuspended in 10 ml PBS (phosphate-buffered saline) buffer containing 2% (v/v) protease inhibitor cocktail (Sigma), 2% (v/v) Triton X-100, 1 mg/ml lysozyme and 20 units/ml benzonase. The suspension was sonicated for 50 seconds (5 seconds * 10 times) and then incubated for 30 minutes on ice. Next, the lysate was centrifuged at 15,000 g for 30 minutes at 4 °C and the cleared supernatant was flowed through a column with 0.5 ml pre-equilibrated glutathione agarose (GST) beads (GenScript). The beads were then washed by 10 ml PBS buffer and the purified GST-tagged protein was eluted by PBS buffer containing 10 mM Glutathione.

The procedures for His-tagged superbinder purification and subsequent immobilization were optimized by Dr. Kaneko. The expression of His-tagged superbinder was induced in BL21 cells following the same procedures described above. Cells collected from 400 ml culture were suspended in 10 ml lysis buffer (50 mM sodium phosphate, 150 mM NaCl, 20 mM imidazole, 2% (v/v) protease inhibitor cocktail (Sigma), 0.5% (v/v) Triton-X100,

1 mg/ml lysozyme, 20 units/ml benzonase and 0.5 mM TCEP (tris(2-chloroethyl) phosphine), pH 8.0). The suspension was sonicated for 50 seconds (5 seconds \times 10) and then lysed for 30 minutes on ice. Next, the lysate was centrifuged at 15,000 g for 30 minutes at 4 °C and the cleared supernatant was passed through the column with 0.8 ml pre-equilibrated nickel-NTA beads (GenScript). The beads were then washed by 20 ml high-salt washing buffer (50 mM sodium phosphate, 500 mM NaCl, 20 mM imidazole, pH 8.0). The purified His-tagged protein was eluted by 4 ml elution buffer (50 mM sodium phosphate, 150 mM NaCl, 250 mM imidazole, pH 8.0) and the elution was mixed with 4 ml coupling buffer (50 mM sodium phosphate, 150 mM NaCl, 20 mM imidazole, 5 mM EDTA, pH 8.0). The final elution was filtered, and the protein concentration was adjusted to 1 mg/ml by adding coupling buffer.

For immobilization, 15 mg (in 15ml buffer) superbinder was incubated with 5 ml SulfoLink beads (Thermo) for 30 minutes at room temperature, with head-to-toe rotation mixing. The beads were collected by centrifugation and then washed in the column with 20 ml coupling buffer (flow-through). To neutralize un-reacted iodoacetyl groups, the beads were incubated with 15 ml blocking buffer (50 mM cysteine in coupling buffer, filtered) for 45 minutes at room temperature, with occasional re-suspending. Next, the beads were washed in the column with 20 ml washing buffer (50 mM Tris-HCl, 1 M NaCl, pH 8.0, flow-through) and finally re-suspended in storage buffer (50 mM Tris-HCl, 50 mM NaCl, 0.2% sodium azide, pH 7.6). Stocked at 4°C, the SulfoLink-superbinder beads maintain over 90% activity after two months.

2.3.3 Free peptide and on-membrane peptide synthesis

Both free and membrane-bound peptides were synthesized on an automatic Intavis peptide synthesizer, using the solid phase peptide synthesis method (Kent, 1988). All regular and modified (phosphorylated) amino acids were protected by Fmoc (9-fluorenylmethyl-oxycarbonyl) or Boc (tert-butyloxycarbonyl) groups to prevent unwanted reactions among peptide side chains and the amine group. For free peptides that were synthesized as MS standards, Wang-resin conjugated with either arginine (Wang-R) or lysine (Wang-K) were used as the solid support phase, since tryptic digestion used in this study only generated R/K ending peptides. In the first synthesis cycle (coupling), the protection group

(Fmoc/Boc) in R or K was removed with 20% piperidine in DMF (N, N-Dimethylformamide) which released the free amine group for subsequent coupling. The next protected amino acid was attached to this amine group via its carboxyl group, forming an amide bond. All un-occupied amine groups were then blocked (acetylated) with acetic anhydride to avoid any further incorrect amine bonds in following cycles. Next, deprotection was carried out again to generate the free amine group ready for the coupling of next amino acid. At the end of the synthesis, the crude peptides were cleaved from the solid support resin using a mixture containing 95% TFA (trifluoroacetic acid), 3% TIPS (tri-isopropylsilane) and 2% water, which would also remove all other protecting groups on amino acid side chains. On-membrane peptides (peptide-array) were synthesized following similar procedures, however the solid support phase was replaced with a home-made amine-derivative cellulose membrane (filter paper) (Frank, 1992).

To make the amine-derivative cellulose membrane, qualitative filter papers (Whatman) were first treated with 100 ml methanol containing 1.2% (v/v) perchloric acid for 15 minutes, washed with 100 ml 100% ethanol three times and air dried. The filter papers were incubated in a mixture with 72 ml dioxane, 8ml epibromohydrine and 800 μ l of 60% perchloric acid for 3 hours, washed with 100 ml 100% ethanol three times then air dried again. Next, the filter papers were incubated in 100 ml 50% 1, 3 diaminopropane (v/v) in DMF for at least 16 hours with slow rotation. The filter papers were then washed sequentially in 100 ml DMF, 100ml ethanol, 100 ml water and 100ml ethanol, 20 minutes per wash and three times in each solution. The membranes were air-dried following the last wash in ethanol. Finally, the filter papers were incubated in 100 ml 0.5 M MeNa (sodium methoxide) in methanol for 15 minutes, washed in water three times then air-dried. The amine-derivative filter papers were stored at -20 °C and stable for months.

2.3.4 Far Western blot of peptide array membrane

Peptide array membranes were pre-blocked with 5% skim milk (m/v) in TBST buffer (0.1 M Tris-HCl, 150 mM NaCl, and 0.1% Tween 20, pH 7.4) for 1 hour at room temperature, with slow shaking. The 4G10 Platinum anti-pTyr antibody (a mixture of 4G10 and pY20 mouse mAbs, Millipore) was directly added into the blocking solution at 1:1000 ratio to blot the membrane for 1 hour at room temperature, with slow shaking. Then the membranes

were washed with TBST buffer three times, 5 minutes per wash. Next, the membranes were probed with secondary antibody anti-mouse-HRP (1:1000) in 5% (m/v) skim milk in TBST buffer for 1 hour at room temperature followed by the same washing procedures. Finally, the peptide array was visualized using ECL solution in a Bio-Rad imaging system. After the 4G10 Platinum blotting, the peptide array membranes were washed and incubated for 30 minutes at room temperature in stripping buffer (1.5% glycine, 0.1% SDS, 1% tween 20, pH 2.2) (Kaufmann et al., 1987; Kaufmann and Kellner, 1998). The membranes were then blotted with GST-tagged SH2 superbinder and anti-GST-HRP sequentially following the same procedures described above.

2.3.5 Protein tryptic digestion and pTyr peptide enrichment

The total protein was harvested from different materials, including cultured cells, peripheral blood mononuclear cells (PBMCs) isolated from whole blood, fast-frozen and FFPE slides of tumor tissues. The cells were first washed with ice-cold PBS buffer once and directly lysed in 8M urea containing 50 mM Tris-HCl (pH7.6) and complete mammalian cell protease inhibitor cocktail (Sigma). Cell debris was removed by centrifugation, then the supernatant was transferred into a fresh tube and mixed with 5-fold volume of cold precipitation mixture (50% acetone, 50% ethanol and 0.1% acetic acid). The fast-frozen tissues were manually ground with liquid nitrogen then processed in a similar manner as described above. The FFPE slides were first de-waxed by washing in xylene and ethanol sequentially. The tissue specimens were detached from the glass slides then resuspended in 6M GuHCl containing 25 mM DTT and 50mM Tris-HCl (pH7.6). The protein was recovered (de-crosslinked) by heating at 100 °C (boiling water bath) for 30 minutes then 80 °C for 2 hours. Debris and undissolved protein were removed by centrifugation, then the supernatant was transferred into a fresh tube and mixed with 5-fold volume of cold precipitation mixture.

After at least two hours of precipitation in -20 °C, the protein precipitate was collected by centrifugation and washed with 75% ethanol, then dissolved in 100 µl 8 M urea or 6 M GuHCl with sonication in water bath. The protein concentration was determined by the Bradford protein assay (BioRad) with a linear range 200 µg/ml ~ 1400 µg/ml. The protein was reduced using 5 mM 1,4-dithiothreitol (DTT) for one hour and alkylated in 14 mM

iodoacetamide (IAA) in darkness for an additional hour. Unreacted IAA was neutralized by adding 5 mM DTT in excess. Tryptic digestion was carried out at 37 °C overnight with an enzyme-to-protein ratio of 1:20 ~1:40 (w/w) according to the manufacture's protocol (Promega, V5111).

The resulting peptide mixture was desalted using a Strata-X polymeric SPE column (Phenomenex), and then re-suspended in 900 µl modified IAP buffer (50 mM Tris-HCl, 50 mM NaCl, pH 7.6). For affinity purification, 300 µg of on-bead superbinder (100 µl) was used for the enrichment of each sample. The peptide matrix was incubated with the beads for two hours at 4 °C with head-to-toe rotation. Then the beads were washed two times with 1 ml high-salt modified IAP buffer (50 mM Tris-HCl, 200 mM NaCl, pH7.6), and two times with 1ml 50 mM ammonium bicarbonate. In each washing, the mixture was rotated for 1 minute at room temperature. For elution, the beads were incubated with 200 µl 1% TFA for 10 minutes, with occasional re-suspending. The enriched peptide was dried using a speed vacuum, then re-dissolved in 0.1% formic acid (FA) at an appropriate volume for direct MS injection.

2.3.6 Mass spectrometric analysis

The MS experiments were performed on the Thermo QExactive quadrupole-orbitrap hybrid MS system equipped with a Thermo nanoLC 1000, or the SCIEX Qtrap 6500+ triple-quadrupole MS system equipped with a Waters NanoAcquity UPLC. Both LC systems were configured in a two-column (trapping column and analytic column) setting. In the Thermo system, a C18 trapping column (length 3 cm, diameter 75 µm, particle size 3 µm, pore size 100 Å) and a C18 analytic column (length 50 cm, diameter 75 µm, particle size 2 µm, pore size 100 Å, spray tip built in) were used. In the SCIEX system, a C18 trapping column (length 2 cm, diameter 180 µm, particle size 3 µm, pore size 100 Å) and a C18 analytic column (length 20 cm, diameter 75 µm, particle size 1.7 µm, pore size 130 Å) were used. The flow rate was set at 300 nl/min and a 1~2 hours gradient (3% to 35% acetonitrile in 0.1% FA) was used for separating the peptide matrix in both systems.

2.3.7 Cell proliferation assay

Cell viability was evaluated using WST-8 cell counting kit (Cayman). The WST-8 monosodium salt, 2-(2-methoxy-4-nitrophenyl)-3-(4-nitrophenyl)-5-(2,4-disulfophenyl)-2H-tetrazolium, is bio-reducible and produces a water-soluble orange formazan dye in the presence of cellular dehydrogenases. The amount of formazan dye produced is linearly proportional to the number of cells or the overall cell viability. Cells were cultured in 90 μ l culture medium in 96-well tissue culture plates (Sarstedt). 10 μ l of WST-8 working solution was directly added to the culture medium and the plate was then incubated for 30 minutes to 1 hour in the incubation chamber. The absorbance at 460 nm was determined using a plate reader (PerkinElmer).

2.3.8 mRNA isolation and RNA-seq

Cells were cultured in 6-well tissue culture plates (Sarstedt) and total mRNA was isolated by TRIzol following the manufacturer's protocol (Invitrogen). Briefly, cells were washed once with warm PBS buffer, then 0.5 ml TRIzol was added to the culture dish to directly lyse the cells. The lysate was pipetted up and down several times and incubated for 5 minutes for complete lysis. Then, the cells were transferred to a microcentrifuge tube and 0.1 ml of chloroform was added and mixed well by vortex. The mixture was centrifuged at 15,000 g for 15 minutes at 4 °C and the colorless upper aqueous phase was transferred into a fresh microcentrifuge tube. 0.25 ml isopropanol was added into the aqueous phase for precipitating the RNA. cDNA was synthesized by reverse-transcription and then analyzed by next generation sequencing (NGS) performed on the Illumina Miseq system at the London Regional Genomic Center (LRGC).

2.4 Results

2.4.1 Abundance of TK phosphorylated peptides indicate TK activity

We previously established a strategy for systematic identification of pTyr sites by AP-MS using the Src SH2 superbinder (GST-tagged) as the affinity reagent (Bian et al., 2016). In the study of nine cultured cancer cell lines, ~ 10,000 pTyr peptides were identified, of which over 3,000 sites were novel. As expected, a large portion of these pTyr peptides belong to TKs, SH2-containing proteins and PTPs, which are subject to intensive regulation of tyrosine phosphorylation (Hornbeck et al., 2015; Matlock et al., 2015). From the same dataset, tens of phosphorylated kinase activation loop peptides were also identified whose relative abundance closely correlated to the activation status of the corresponding TKs among these cancer cell lines. For example, a high abundance of ErbB2 (HER2) phosphorylated activation loop was detected in BT-474 and SK-BR-3 cells, which are classified as HER2 + 3 breast cancer cells by IHC/FISH.

Even though *in vivo* TK activity can be determined by multiple regulatory mechanisms (Huse and Kuriyan, 2002; Pawson and Scott, 2005), the phosphorylation of tyrosine residues within the kinase activation loop is essential for TK activation in many cases (Feng et al., 1997; Nolen et al., 2004; Rikova et al., 2007; Schindler et al., 2000; Zhang et al., 2000). The activation loop is a short, flexible region within the kinase domain, located close to the catalytic loop in the three-dimensional structure (Knighton et al., 1991; Kornev and Taylor, 2010). In many non-constitutively active TKs, activation loop phosphorylation will counteract the positive charge of the arginine in the catalytic core which then opens for substrate access (Johnson and Lewis, 2001; Kornev and Taylor, 2010; Meng and Roux, 2014; Tokunaga et al., 2014). Similarly, in many serine/threonine kinases, a conserved threonine residue is typically found in the activation loop, and phosphorylation of this residue is required for kinase activation as well. The human genome encodes 90 TKs, which share a highly conserved activation loop region containing one or two conserved tyrosine residues, as aligned in Suppl.2.1. A small portion of serine/threonine kinases have non-classic activation loops, such as the MAPK subfamily that contain a T-D/E-Y motif and require dual phosphorylation in both threonine and tyrosine residues for kinase activation (Cargnello and Roux, 2011). A few phosphorylated MAPK activation loops have

been successfully detected by AP-MS previously (Hornbeck et al., 2015), including MAPK1 (Erk2) and MAPK3 (Erk1) which are master regulators of cell proliferation (Boulton et al., 1991; Jones and Kazlauskas, 2001; Raman et al., 2007; Rubinfeld and Seger, 2005; Squires et al., 2002).

Most TK activation loops are compatible with trypsin digestion, producing peptides suitable in length for LC-MS analysis. Therefore, a hypothesis is formed based on the understanding of these sequentially and functionally conserved kinase activation loops, that protein kinase status might be comprehensively evaluated using AP-MS by determining the abundance of the phosphorylated activation loop peptides. Theoretically, this is feasible since phosphor-peptide enrichment and MS analysis have been well developed. Immobilized Metal Affinity Chromatography (IMAC) is the most widely used method to purify pSer/pThr peptides according to their affinity to specific metal ions (de Graaf et al., 2014; Sharma et al., 2014; Zhou et al., 2013), and the SH2 superbinder has been demonstrated as an excellent reagent for pTyr peptide enrichment as well (Bian et al., 2016). By combining both reagents, it is possible to enrich pTyr and pSer/pThr peptides sequentially from the same sample and profile the activation of all protein kinases in a single experiment.

In a previous study of nine cancer cell lines, 35 TK activation loops were identified in at least one cell line. Label free quantification was used to generate a heatmap of activation loop phosphorylation (Tab.2.1). As expected, different cell lines exhibited differential activation loop phosphorylation patterns, suggesting that tyrosine kinase activation could be cell type specific. Based on the corresponding activation loop phosphorylation, more cytosolic TKs were activated in Jurkat T cells, but not in non-hematopoietic cells. Conversely, numerous RTK activation loops were detected in all but the Jurkat T cells. This suggests that RTKs may be the major type of oncogenic drivers in cancer cells of epithelial origin.

Table 2.1 Activation loop phosphorylation profiles determined by SH2-AP-MS

Family	Proteins	HeLa	BEL7402	HEPG2	MCF10A	MCF7	MB231	bT474	SKBR3	JURKAT	Variance
CTK_ABL	ABL1/2		1.1	0.9	-0.1	-0.2			0.3	1.6	0.53
CTK_ACK	TNK2	1.0	0.3	0.5	-0.1	-0.1	0.5	0.5	0.5	0.3	0.11
CTK_BRK	PTK6	0.8			0.9	0.1	-0.3	1.7	0.5		0.47
CTK_FAK	PTK2	-0.7	0.3	1.0	-0.7	-0.3	-1.0	0.1	-0.3	-0.8	0.41
CTK_FAK	PTK2B	0.7	1.8	0.8	2.1	0.7	-0.4	1.0	1.6	1.3	0.53
CTK_FER	FER						-0.8			-0.1	n.a.
CTK_FER	FES									-0.6	n.a.
CTK_JAK	JAK1	1.1	1.3	1.0	0.2	1.1	0.1	1.1	-0.2	1.3	0.35
CTK_JAK	JAK3									-0.2	n.a.
CTK_SRC	FRK		-0.9		-1.0	1.0		0.9	1.3		1.24
CTK_SRC	HCK/LYN			-1.3	-0.9		-0.1			-0.4	0.29
CTK_SRC	YES/LCK/FYN/SRC		-0.1	-1.1		-0.4	0.0	-0.3	-0.8	0.9	0.41
CTK_SYK	SYK				0.9						n.a.
CTK_SYK	ZAP70	-1.1								1.2	n.a.
CTK_TEC	ITK									1.9	n.a.
CTK_TEC	TEC	-0.3	-1.4		-0.4	-1.1	0.9			-0.2	0.65
RTK_AXL	AXL	-0.2	-0.1	0.1			-0.2				0.03
RTK_AXL	MERTK/TYRO3	-0.6	0.3	-0.2	-0.4			-0.5	-0.9	-0.8	0.15
RTK_DDR	DDR1	1.4	-0.1	0.6	0.4	1.5		0.9	1.4	-0.5	0.57
RTK_EGFR	EGFR	-0.8	-0.1	1.0			1.5		0.3		0.80
RTK_EGFR	ERBB2		1.6	1.4		2.3	-0.4	3.8	3.6		2.45
RTK_EPH	EPHA1					1.4		1.6			n.a.
RTK_EPH	EPHA2	2.4	0.7	1.2		2.1	1.6	0.7	0.9		0.48
RTK_EPH	EPHA3/4/5					0.4	0.9	-1.2		0.6	0.91
RTK_EPH	EPHA7	-0.3				-0.7		-1.2			0.18
RTK_EPH	EPHB2	0.2	1.9	-0.3	0.5	1.2	2.4	1.0	-0.2	-0.1	0.91
RTK_EPH	EPHB3					0.8		1.3	1.5		0.14
RTK_EPH	EPHB4		1.6	1.6	-0.6	2.0	0.5	2.0	1.3		0.92
RTK_INSR	IGF1R/INSR	2.1	0.9	1.0	0.8	1.6	0.9	1.0	0.3	0.2	0.35
RTK_MET	MET	1.6	0.6	1.9	2.2	0.0	0.9	-0.5	0.0	-0.8	1.09
RTK_MET	MST1R	1.6	-0.1	1.1	1.9	-1.2		-0.6	0.7	-0.9	1.39

A heatmap outlining phosphorylation status of TK activation loops in nine cancer cell lines determined by SH2-AP-MS. Raw data was obtained from a full scanning (full MS/data-dependent MS2) performed on a Thermo QExactive. The spectral peak area of MS1 was used for the quantification of peptide abundance and Z-scores of Log2 intensity values were represented. Blank spaces indicate instances for which the corresponding phosphorylated activation loops were not detected. This figure was published and modified from (Bian et al., 2016).

To validate whether the MS data faithfully recapitulated TK phosphorylation status *in vivo*, Western blotting was used to evaluate the phosphorylation status of the activation loops of ErbB2 (pTyr_877) and IGF-1R/INSR (pTyr_1161_1165_1166). Using pTyr site-specific antibodies, four breast cancer cell lines MCF7, BT-474, SK-BR-3 and MDA-MB-231 exhibited distinct ErbB2 and IGF-1R activation loop phosphorylation patterns by western blot. These four cell lines also represent the major breast cancer subtypes (Holliday and Speirs, 2011; Subik et al., 2010): MCF7 is “Luminal A” subtype (ER+, PR+/-, HER2-, or HER2 +1); BT-474 is “Luminal B” subtype (ER+, PE+/-, HER2+); SK-BR-3 is “HER2-enriched” subtype (ER-, PR-, HER2+); and MDA-MB-231 is “Triple-negative” subtype (ER-, PR-, HER2-). ErbB2 was highly expressed and phosphorylated in the activation loop in both BT-474 and SK-BR-3 cells, and IGF-1R was highly expressed and phosphorylated in the activation loop in MCF7 cells (Fig.2.2 A-B). A moderate level of IGF-1R protein expression and activation loop phosphorylation was also observed in BT-474 and MDA-MB-231 cells. These results agree in principle with the activation-loop phosphorylation status profiled by MS (Tab.2.1). To determine whether activation loop phosphorylation predicts kinase activity, activation (phosphorylation)-dependent recruitment of adaptor proteins to ErbB2 and IGF-1R was also examined (Dey et al., 1996; Xie et al., 1995). It is apparent that more Grb2 was recruited by ErbB2 in BT-474 and SK-BR-3 cells and more IRS-1 was recruited by IGF-1R in MCF7 cells (Fig.2.2 A-B).

Because TKs are major drivers of tumorigenesis, selective inhibition of deregulated TK is an effective strategy in cancer therapy. The efficacy of cell proliferation inhibition was tested by applying three TK inhibitors, lapatinib (EGFR/ErBB2), GSK1838705 (IGF-1R/INSR) and DDR1-IN-1(DDR1) in the four cell lines. In the single inhibition test, the HER2 positive BT-474 and SK-BR-3 cells were only sensitive to lapatinib, as expected. MCF7 cells were sensitive to GSK1838705 but not lapatinib or DDR1-IN-1, while MDA-MB-231 cells exhibited no response to any of these inhibitors (Fig.2.2 C-E). This indicates that IGF-1R plays a more important role than EGFR/ErBB2 or DDR1 in promoting MCF7 cell proliferation, even though they were all found in a moderate activation status in MCF7 by SH2-AP-MS. However, a combination of lapatinib and DDR1-IN-1 exhibited an obvious inhibition effect on MCF7 proliferation, which also further sensitized MCF7 cells to the treatment of GSK1838705 (Fig.2.2 F-G). Such an effect was not observed in BT-

474, SK-BR-3 or MDA-MB-231 cells. These data suggest that EGFR/ErbB2 are the dominant drivers of cell proliferation in BT-474 and SK-BR-3 cells. BT-474 and SK-BR-3 have moderate activation of DDR1 and IGF-1R, but neither significantly contributes to cell proliferation. In MCF7 cells, IGF-1R cooperates with EGFR/ErBB2 and DDR1 to promote cell proliferation together. Here, the quantitative kinase activity profiling by SH-AP-MS presents accurate and valuable information regarding global TK activation and may be used to guide cancer treatment by specifically targeting multiple co-activated TKs that have been found common in many clinical cases (Lee et al., 2012; Zhang et al., 2011).

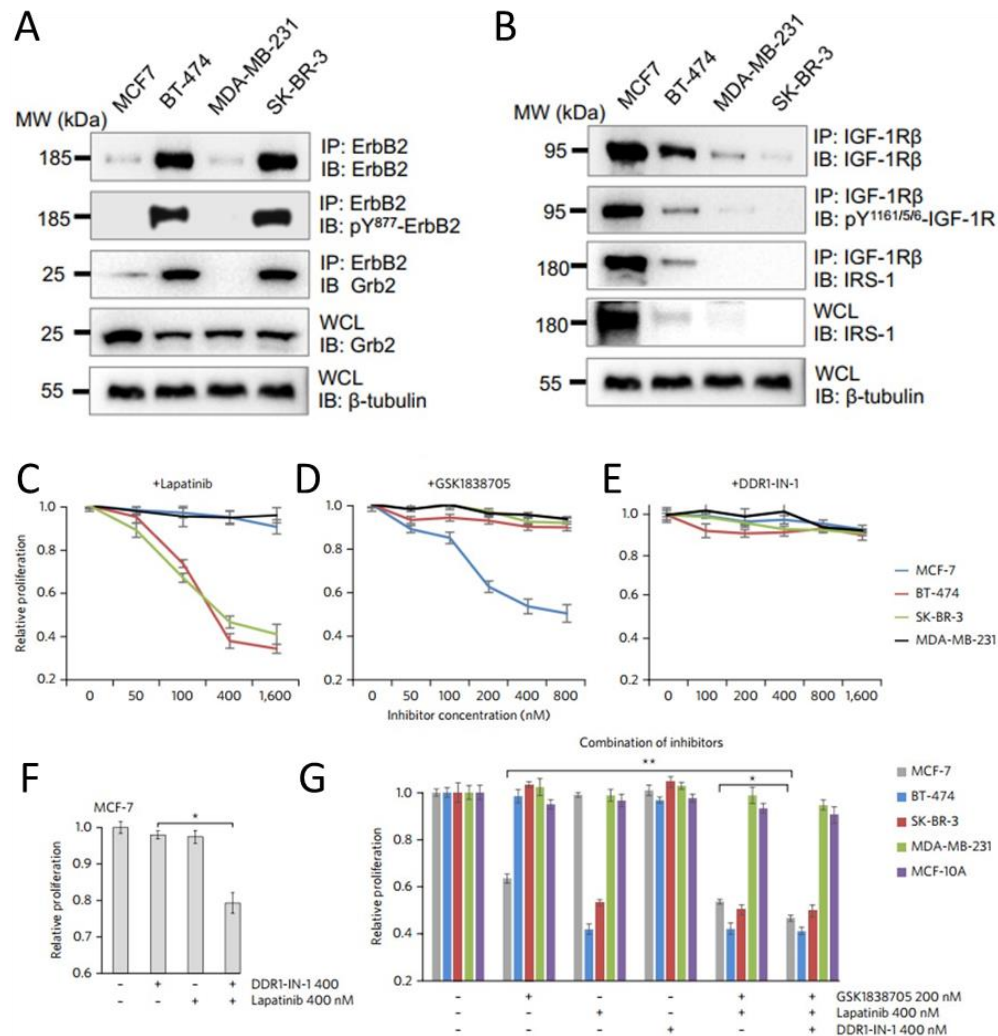


Figure 2.2 SH2-AP-MS detects active TKs that drive cell proliferation

(A-B) ErbB2 and IGF-1R, which showed distinct activation loop phosphorylation patterns in the four breast cancer cell lines (Tab.2.1) were analyzed for protein expression, activation loop phosphorylation (using specific antibodies as indicated) and activation-dependent recruitment of SH2 proteins. High ErbB2 expression, activation loop Y877 phosphorylation and Grb2 recruitment were observed in the BT-474 and SK-BR-3 cells. High IGF-1R expression, activation loop Y1161/1165/1166 phosphorylation and IRS-1 recruitment were observed in MCF7 and BT-474 cells; (C-E) Distinct responses of the breast cancer cell lines MCF7, BT-474, SK-BR-3 and MDA-MB-231 to pharmacological inhibition of ErbB2 (by lapatinib), IGF-1R (by GSK1838705) or DDR1 (by DDR1-IN-1), $n=3$; (F) Combined treatment of MCF-7 cells with lapatinib and DDR1-IN-1 significantly inhibit the cell proliferation. $p < 0.01$, $n = 3$; (G) Triple inhibition of IGF-1R, ErbB2 and DDR1 significantly inhibits proliferation of MCF7 cells compared to double or single inhibition treatment, $p < 0.01$, $n = 4$. These results were published and modified from (Bian et al., 2016)

To investigate the possibility of applying the SH2-AP-MS assay in examining TKs in clinically collected tumor tissues, which are processed using different procedures and typically supplied in a small amount, the entire SH2-AP-MS workflow was thoroughly optimized for maximizing the pTyr peptide recycling and MS discovery rates (assisted by Dr. Tomonori Kaneko). Subsequently, the TK activation status was re-evaluated in MCF7, BT-474, SK-BR-3 and MDA-MB-231 cells.

Because protein tyrosine phosphatases (PTPs) are constitutively active in living cells, tyrosine phosphorylation usually has a short half-life *in vivo*, in many cases just a few minutes or even seconds if it is not protected through binding to an SH2 domain for example (Hunter, 2014; Kleiman et al., 2011). For most TK studies in cancer biology, including the work presented above (Tab.2.1, Fig.2.2), cell pre-treatment by sodium orthovanadate (pervanadate) is a key procedure which globally inhibits PTPs to preserve tyrosine phosphorylation (Huyer et al., 1997). In MS-based proteomics studies, this treatment was crucial for the detection of less-abundant or highly dynamic tyrosine phosphorylation sites. Even though pervanadate is a highly specific PTP inhibitor, the treatment is known to interfere with the pTyr-mediated signaling network. It was reported that pervanadate activated insulin receptors without the presence of insulin in cultured cells (Fantus et al., 1989). From a structural perspective, pervanadate should not act like a ligand to bind or stimulate insulin receptors. In a cell-free system, pervanadate did not alter the phosphorylation status of insulin receptors or interfere with the stimulating effect of insulin at all. In fact, pervanadate indirectly promoted the auto-phosphorylation level of insulin receptors by inhibiting PTPs, and the accumulated auto-phosphorylation in turn self-activated the receptor (Shisheva and Shechter, 1993). Considering many RTKs undergo a similar process of activation, and cross-activation and feed-back loops are common in this signaling network, pervanadate may not simply preserve tyrosine phosphorylation but also alter the phosphorylation differentially on specific sites. Therefore, sample collection procedures were simplified by directly lysing the cells without pervanadate treatment. In order to match the low protein amount collected from patient derived tissues, the cultured cell lysate protein amount was reduced from 5 mg to 300 μ g. In addition, instead of using GST-tagged superbinder (on beads) as the affinity reagent, the superbinder was further engineered by mutating all endogenous cysteine residues and covalently linking the His-

tagged superbinder to SulfoLink Coupling Resin (Thermo) via a single cysteine residue added to the C terminal tail. This covalent-conjugated superbinder out-performed previous versions, as shown in other studies led by Dr. Tomonori Kaneko. Enrichment and MS analysis of the four breast cancer cell lines, MCF7, BT-474, SK-BR3 and MDA-MB-231 were performed using the covalent-conjugated superbinder beads. Not surprisingly, the total number of identified pTyr peptides dropped by 90% and only 200~300 pTyr peptides were identified in each cell line. However, 69 pTyr peptides representing 38 TKs were still detected from 300 μ g lysate, including 64% (16 out of 25) of the activation loops that were detected from 5 mg lysate before. Among the four cell lines, BT-474 and SK-BR-3 cells have the highest abundance of EGFR and ErbB2 peptides, MCF7 cells have the highest abundance of IGF-1R and INSR peptides, and MDA-MB-231 cells have the highest abundance of AXL and EPHA2 peptides (Tab.2.2). These results in general agree with the preliminary data obtained from the larger scale samples (Tab.2.1).

Table 2.2 TK pTyr peptide profiles in four breast cancer cell lines

TK	Position	MCF7	BT474	SKBR3	231	TK	Position	MCF7	BT474	SKBR3	231
AXL (UFO)	702*				21.6	FRK	387*		19.6	17.2	
AXL (UFO)	703*				20.8	FRK	497	19.9	19.8	21.1	
CSF1R	923			14.7		FYN;YES1	213;222	18.6	19	19.7	19.7
DDR1	792	17.4	18.1			FYN;YES1	214;223		18.8		18.1
DDR1	796*	16.6	17	20.1		FYN;YES1;FGR	185;194;180	18.8	21.1	19.5	20.8
DDR1	797*	15.6	17.3	20.1		FYN;YES1;LCK;SRC	420;426;394;419*	19	23.2	21.3	23.2
DDR2	740*			20		IGF1R;INSRR	1161;1185	20.9	18.2		19.1
DDR2	741*			20		IGF1R;INSRR	1165;1189	19.6			18
EGFR	1110		21.8	22.7	21.1	INSRR	1145			16.2	
EGFR	1172		25.9	26.4	22	INSRR	1146			16.2	
EGFR	1197		17.1	17.1		JAK1	1034		20.2	18.2	20.6
EPHA1	781*	18.9	21.9	20.2		JAK2	221			15.5	
EPHA2	588	21.8	22.8	21.3	26.2	LYN	194	17.5			19.6
EPHA2	594	22.8	22.8	23	28	LYN;HCK	397;411*	16.1			
EPHA2	772*	19.2	21.1	21.6	25.6	MET	1234				20
EPHA2	960	15.4	17.2	16.2	19.1	PTK2 (FAK1)	397	18.2	18.8		
EPHA4	602	23.1	21.9		16.9	PTK2 (FAK1)	570		16		
EPHA7	597	19.8	19.4			PTK2 (FAK1)	576*	16.4	18.2	16.9	21.4
EPHA6;EPHA7	830;791*	20.9	19.3			PTK2 (FAK1)	577*	17.8	18.3	17.7	21.2
EPHB1;EPHB2	600;602	19.4	19.8		19.1	PTK2 (FAK1)	861		20.8		21.8
EPHB3	600		19.7	14.7		PTK2 (FAK1)	925				17.8
EPHB3	792*		21.8			PTK2B (FAK2)	579				
EPHB3;EPHB4	608;590	19.7	22.9	17.3	14.9	PTK2B (FAK2)	580				
EPHB3;EPHB4	614;596	22.7	25.6	20.9	19.1	PTK2B (FAK2)	819			16	
EPHB4	774*		19			PTK2B (FAK2)	849		18.5	19.2	
ERBB2	877*	17	27.3	25.8	20.8	PTK6	114		19.1		
ERBB2	1139		20.8	19.7		PTK6	447	17.3	23.2	19.2	17.9
ERBB2	1248	18.6	30	29.3	22.2	RET	900	14.7			
ERBB3	868*		16.8			RET	1096		17.6		
ERBB3	1328	18.3	24.8	23.1		SYK (KSYK)	323	19.2		17.7	
ERBB4	1150		19.1			SYK (KSYK)	352		20.1		
ERBB4	1162		17.3			TNK2 (ACK1)	284*			19.2	
ERBB4	1208	17				TNK2 (ACK1)	518		21		
FER	402	18.1	20.8	18.1	20.8	TNK2 (ACK1)	859		19.1		
FER	714*		17.9		18.3	TYK2	292		16.3		
FGFR4	754		16.1								

* activation loop

A heatmap to exhibit differential phosphorylation status of TK pTyr sites in four cultured breast cancer cell lines determined by SH2-AP-MS. Raw data was obtained from a full scanning (full MS/data-dependent MS2) performed on a Thermo QExactive. The spectral peak area of MS1 was used for the quantification of peptide abundance and Log2 intensity values were represented. Blank spaces indicate instances for which the corresponding phosphorylated peptides were not detected. All detected pTyr sites within TK activation loops were denoted by an asterisk.

The SH2-AP-MS results were further compared to transcriptome sequencing (NGS) data for the four breast cancer cell lines, which was archived in the Expression Atlas Database (Petryszak et al., 2016). Data for all TKs in these cell lines were extracted and ranked by TPM values (transcripts per kilobase million). The 10 most abundant (mRNA) TKs and MS detected pTyr sites in these TKs were summarized in Tab.2.3. Overall, 31 out of 40 TKs were detected in the four cells by SH2-AP-MS, including the activation loops for the most abundant TK in individual cell lines (DDR1 in MCF-7; ErbB2 in BT-474; SK-BR-3; AXL in MDA-MB-231). Consistent with the TK inhibition test (Fig.2.2 C-G), DDR1 (TPM 168) and IGF-1R (TPM 98) ranked 1st and 3rd in MCF7, while ErbB2 ranks 1st in both BT-474 (TPM 1365) and SK-BR-3 (TPM 1811). AXL (TPM 828) ranks 1st and MET (TPM 120) ranks 3rd in MDA-MB-231. Even though the inhibition of AXL or MET was not further investigated in MDA-MB-231 cells in this study, it has been previously reported that their inhibitors suppressed the growth and metastasis of xenografted MDA-MB-231 cells (Holland et al., 2010; Mayer and Krop, 2010; Shen et al., 2018).

Indeed, a few oncogenic TKs, that are relatively abundant in mRNA and functionally significant *in vivo*, were not detected by SH2-AP-MS in both 5 mg and 300 µg samples. In BT-474, 9 out the 10 most abundant TKs were detected in 300 µg lysate, except for ABL, which ranked 2nd. In the data obtained from 5 mg lysate, only a few non-loop pTyr sites were detected in BT-474. However, the ABL activation loop was detected in a few other cell lines (Tab.2.1). Obviously, ABL protein is expressed and functional in BT-474 cells, since specific inhibition of ABL sensitized BT-474 to fulvestrant (breast cancer hormonal therapeutic), reduced cell viability and prevented cell cycle progression by promoting fulvestrant-induced estrogen receptor degradation (Zhao et al., 2011; Zhao et al., 2010). Several reasons might cause this poor ABL activation loop detection in BT-474 cells, including non-optimal LC-MS parameters for this peptide, interference by other peptides in BT-474, or relatively low abundance of ABL phosphorylation *in vivo*. Among all four cell lines, a broad existence of EPH family members was observed. Over 20% of detected TK pTyr sites are from EFHA1/2/4/6/7 and EPHB1/2/3/4 (Tab.2.2), but few studies have suggested any functions of EPH family in oncogenicity to date.

Table 2.3 A comparison of TK profiles in SH2-AP-MS and RNA-seq

MCF7			BT474			SKBR3			MDA-MB-231		
RNA-seq Top10 TK	TPM	Shotgun MS pTyr sites	RNA-seq Top10 TK	TPM	Shotgun MS pTyr sites	RNA-Seq Top10 TK	TPM	Shotgun MS pTyr sites	RNA-seq Top10 TK	TPM	Shotgun MS pTyr sites
DDR1	168	792;796*;797*	ERBB2	1365	877*;1139;1248	ERBB2	1811	877*;1139;1248	AXL	828	702*;703*
EPHB4	125	590;596	ABL1	114	N/A	DDR1	166	796*;797*	EPHA2	396	588;594;602;772*
IGF1R	98	1161;1165*	YES1	110	194;222;223;426*	ERBB3	89	1328	MET	120	1234*
JAK1	92	N/A	ERBB3	88	868;1328	CSK	61	N/A	EGFR	102	1110;1172
ERBB3	68	1328	FGFR4	81	754	JAK1	48	1034*	ABL1	101	N/A
CSK	64	N/A	EPHB4	71	1150;1162	YES1	45	194;222;426*	JAK1	70	1034*
TYK2	50	N/A	DDR1	63	792;796*;797*	EPHB3	41	608;614	YES1	63	194;222;223;426*
RET	48	900	EPHB3	53	600;608;614;792*	EGFR	39	1110;1172	ROR1	54	N/A
ERBB2	46	877*	JAK1	45	1034*	TYK2	35	N/A	FGFR1	50	N/A
EPHA4	44	602	PTK2	44	397;570;576*;577*;861	EPHA2	35	588;594;602;772*	PTK2	47	576*;577*;861;925

The SH2-AP-MS detected TK pTyr sites were summarized with the 10 most abundant (mRNA) TKs in four breast cancer cell lines MCF7, BT-474, SK-BR3 and MDA-MB-231 (Expression Atlas DB). All pTyr sites within activation loops were denoted by an asterisk. Overall, pTyr sites were detected in 31 of 40 TKs. For the most abundant TKs in each cell line, DDR1 in MCF7, ErbB2 in BT-474 and SK-BR-3, AXL in MDA-MB-231, the activation loops were detected.

In conclusion, the SH2-AP-MS assay generally enriched and detected TKs effectively in both the activation loops and other tyrosine phosphorylated sites. Most highly abundant TKs, particularly the validated TK biomarkers, were detectable from a small amount of cell lysate without pervanadate treatment. The MS-determined TK pTyr peptide intensities correlated well with TK mRNA abundance or TK biological function in the four breast cancer cell lines. If a more sensitive targeted MS approach could be established, and introducing internal standards in MS detection, the global TK activation status could be quantitatively profiled in a single experiment using even less total lysate protein, which could be collected from biopsy tissues.

2.4.2 Selection of TK phosphorylated peptides for targeted proteomics

TKs are intensively tyrosine phosphorylated proteins and usually contain multiple pTyr sites. Among the 90 TKs, there are over 1,000 pTyr sites that have been identified at least once before (Hornbeck et al., 2015; Matlock et al., 2015). It is anticipated that the site-specific modifications on TKs would vary in different backgrounds or physiological conditions (Yarden and Sliwkowski, 2001), but some TK pTyr sites including the activation loops seem more abundant and functionally significant. The PhosphoSitePlus database summarizes the number of records in which the modification is determined by either discovery MS studies (HTP, high throughput) or other approaches (LTP, low throughput) (Hornbeck et al., 2015). In the case of Src kinase, pTyr_419 (activation loop) and pTyr_530 (c-tail), which are known as two key regulatory sites for Src activation (Roskoski, 2004; Roskoski, 2005), rank 1st and 2nd in both HTP and LTP. In our preliminary SH2-AP-MS data, both sites are also ranked at the top among all detected Src pTyr sites (Bian et al., 2016). As shown in Tab.2.2, pTyr_419 seems to be the only detected and most abundant Src pTyr site among the four breast cancer cell lines. In the same dataset, three pTyr sites (pTyr_877, pTyr_1129, pTyr_1248) were detected in ErbB2, which ranked 3rd, 5th and 1st in HTP and LTP among 13 ErbB2 pTyr sites. pTyr_877 is located in the activation loop, pTyr_1139 is involved in the stimulation of various ErbB2 downstream events including cell adhesion, cell growth and cell motility (Dankort et al., 2001; Northey et al., 2008), while pTyr_1248 mainly promotes protein stabilization, maintains kinase activity, and generally contributes to all known ErBB2 functions (Dankort et al., 2001; Dittmar et al., 2002; Dong et al., 2017; Heinrich et al., 2010; Northey et al., 2008). Therefore, phosphorylation on both the activation loop and other functional pTyr sites might be used as indicators of TK activity and function. Inclusion of non-loop pTyr sites in the targeted MS detection panel is immediately beneficial to cover TKs that have an activation loop peptide disfavored by either the tryptic digestion or LC-MS detection. A comprehensive detection panel will also make the analysis more insightful and better characterize the global TK status. For example, four members of the Src kinase family share an identical tryptic-digested activation loop (Src_pTyr_419, YES_pTyr_426, FYN_pTyr_420 and LCK_pTyr_394), therefore inclusion of unique non-loop pTyr peptides will help distinguish the Src family members.

The binding between ~1000 human TK pTyr sites and the SH2 superbinder was evaluated by far-western assay to identify the superbinder-favored pTyr sites. Peptides for all known TK pTyr sites were synthesized on nitrocellulose membranes, each peptide containing a phosphor-tyrosine flanked by 7 amino acid residues on each side. Information on site-specific modifications and peptide sequences were extracted from the ProteomeScout database (Matlock et al., 2015). An artificial peptide G₇-pY-G₇ was synthesized as a positive control for relative quantification of binding affinities. The performance of the SH2 superbinder and anti-pTyr antibody 4G10 platinum (mouse monoclonal cocktail IgG2b 4G10 and PY20) were compared for recognizing these ~1000 peptides. In the far Western assay, the membranes were first hybridized with 4G10 platinum and anti-mouse-HRP antibody sequentially, then illuminated by enhanced chemiluminescence (ECL) solution. The same membranes were then stripped for re-probing with GST tagged SH2 superbinder (20 times molar amount compared to 4G10 platinum) and anti-GST-HRP antibody. As shown in Suppl.2.2, both the 4G10 antibody and the GST-tagged SH2 superbinder generally performed well in recognizing ~500 pTyr sites. The binding affinity (equilibrium dissociation constant, K_d) between an antibody and a target antigen is usually in the low nano-molar (nM) range, typically a few nanomolar (Pan et al., 2016). The superbinder has greatly enhanced pTyr-binding affinity compared to its wild type variant, but still retains binding specificity and only has low nano-molar binding affinity to some optimal binding peptides (Kaneko et al., 2012a; Kaneko et al., 2012b). Not surprisingly, the superbinder clearly favored several of these TK pTyr peptides (Suppl.2.2), while the 4G10 platinum antibody exhibited much less variance in blotting intensities. Compared to the positive control peptide G₇-pY-G₇, which bound to the superbinder with 510 nM affinity in solution (Kaneko et al., 2012a), ~76% of TK pTyr peptides exhibited higher blot intensities (suppl.2.3). The ErbB2_877 activation loop peptide displayed weak binding to the superbinder, with about half of the blot intensity on the far Western blot compared to the positive control peptide G₇-pY-G₇, but it was detected in multiple different cell lines in previous SH2-AP-MS studies. Therefore, it is estimated that over 95% of TK pTyr peptides could be captured by a saturating amount of superbinder in the affinity purification, which exhibit stronger binding to the superbinder than the ErbB2_877 peptide on the blot (suppl.2.3).

Tab.2.4 lists 67 trypsin-digested activation loop peptides, which represent 79 TKs, and their relative binding affinities to the superbinder. A few activation loops, such as the ErbB3_866 and LMTK2_295, were not tested in the far Western assay because the two sites were not archived in the ProteomeScout database when the peptide array was prepared. ErbB3 is considered to be a “dead” kinase, which dimerizes with other ErbB members that are solely responsible for ErbB3 intramolecular phosphorylation and subsequent recruitment of SH2 proteins (Yarden and Sliwkowski, 2001). However, some recent studies reveal that ErbB3 is capable of weak autophosphorylation (Shi et al., 2010; Steinkamp et al., 2014). Indeed, phosphorylation on ErbB3_868 and ErbB3_1328 was detected in BT-474 cells (Tab.2.2), with the ErbB3_868 peptide being the predicted activation loop. In another tumor tissue analysis presented below, LMTK2_295 peptides were also detected with reliable MS/MS spectra (Fig.2.4 G-I). Therefore, the 67 activation loops are compatible with superbinder enrichment.

Table 2.4 Tryptic-digested TK activation loops

Protein and site	Sequence	Intensity	Protein and site	Sequence	Intensity
ABL1/2_393/439	LMTGDTY[Pho]TAHAGAK	0.95	INSRR_1145_1146	DVYETDY[Pho]Y[Pho]R	1.26/0.84
ACK1_284	ALPQNDDHY[Pho]VMQEHR	1.83	ITK_512	FVLDDQY[Pho]TSSTGTK	1.97
BLK_389	IIDSEY[Pho]TAQEGAK	0.71	JAK1_1034_1035	EY[Pho]Y[Pho]TVK	2.59/2.20
BMX_566	YVLDDQY[Pho]VSSVGTGK	2.16	JAK3_980_981	DY[Pho]Y[Pho]VVR	3.01/2.92
BTK_551	YVLDEY[Pho]TSSVGSK	2.31	KIT_823	NDSNY[Pho]VVK	2.26
CSF1R_809	DIMNDSNY[Pho]IVK	1.44	KSYK_525_526	ADENY[Pho]Y[Pho]K	2.32/1.14
DDR1_796_797	NLYAGDY[Pho]Y[Pho]R	2.04/1.79	LMTK1_283	EDY[Pho]FVTADQLWVPLR	1.99
DDR2_740_741	NLYSGDY[Pho]Y[Pho]R	3.16/2.25	LMTK2_295	EDY[Pho]IETDDK	NA
EPHA1_781	LLDDFDGTY[Pho]ETQGGK	2.08	LMTK3_296_297	EDY[Pho]Y[Pho]LTPER	2.54/1.75
EPHA2_772	VLEDDPEATY[Pho]TSSGGK	1.09	MERTK/TYRO3_753_754/685_686	IYSGDY[Pho]Y[Pho]R	2.05/1.22
EPHA3/4/5_779/779/883	VLEDDPEAAY[Pho]ITTR	1.35	MET_1234_1235	EY[Pho]Y[Pho]SVHMK	2.59/2.56
EPHA6/7_830/791	VLEDDPEAAY[Pho]ITTTGGK	1.89	MUSK_755_756	NIYSADY[Pho]Y[Pho]K	2.57/1.49
EPHA8_793	VLEDDPEAAY[Pho]ITTTGGK	2	NTRK1_680_681	DIYSTDY[Pho]Y[Pho]R	2.49/2.22
EPHB1_778	YLQDDTSDPTY[Pho]TSSLGK	1.13	NTRK2/3_706_707/709_710	DVYSTDY[Pho]Y[Pho]R	2.4/1.89
EPHB2_780	FLEDDTSDPTY[Pho]TSALGGK	1.81	PGFRA_849	DIMHDSNY[Pho]VSK	1.39
EPHB3_792	FLEDDPSDPTY[Pho]TSSLGK	1.46	PGFRB_857	DSNY[Pho]ISK	1.61
EPHB4_774	FLEENSSDPTY[Pho]TSSLGK	1.5	PTK6_342	EDVY[Pho]LSHDHNIPIYK	1.23
ErbB1(EGFR)_869	EY[Pho]HAEGGK	0.56	PTK7_960_961	DVYNSEY[Pho]Y[Pho]HFR	1.69
ERBB2_877	LLDIDETAY[Pho]HADGGK	0.54	RET_905	DVYEDSY[Pho]VJK	1.38
ERBB3_866	QLLY[Pho]SEAK	NA	RON_1238_1239	EY[Pho]Y[Pho]SVQQHR	3/2.94
ERBB4_875	EY[Pho]NADGGK	0.56	ROR1_645_646	EIYSADY[Pho]Y[Pho]R	2.52/NA
FAK1_576_577	YMEDSTY[Pho]Y[Pho]K	0.95/0.76	ROR2_645_646	EVYAADY[Pho]Y[Pho]K	NA/2.98
FAK2_579_580	YIEDEDY[Pho]Y[Pho]K	1.43/2.24	SRC/YES/FYN/LCK_419/426/420/394	LIEDNEY[Pho]TAR	0.74
FER_714	QEDGGVY[Pho]SSSGLK	1.5	SRMS_380	DDIY[Pho]SPSSSK	1.77
FES_713	EEADGVY[Pho]AASGGLR	1.13	TEC_519	YVLDDQY[Pho]TSSSGAK	1.6
FGFR1_653_654	DIHHIDY[Pho]Y[Pho]K	1.56/1.25	TIE1_1007	GEEVY[Pho]VJK	1.04
FGFR2_656_657	DINNIDY[Pho]Y[Pho]K	1.89/1.46	TIE2_992	GQEVY[Pho]VJK	1.08
FGFR3_647_648	DVHNLDY[Pho]Y[Pho]K	1.37/1.04	TKX_420	YVLDEY[Pho]VSSFGAK	2.28
FGFR4_642_643	GVHHIDY[Pho]Y[Pho]K	1.75/1.16	TYK2_1054_1055	AVPEGHEY[Pho]Y[Pho]R	2.74/2.04
FGR_412	DDEY[Pho]NPCQGSK	0.29	UFO_702_703	IYNGDY[Pho]Y[Pho]R	1.68/1.12
FLT3_842	DIMSDSNY[Pho]VVR	1.59	VGFR1_1053	NPDY[Pho]VJR	0.97
FRK_387	VDNEDIY[Pho]ESR	2.72	VGFR2/3_1059/1068	DPDY[Pho]VJR	1.11
HCK/LYN_411/397	VIEDNEY[Pho]TAR	0.98	ZAP70_492_493	ALGADDSY[Pho]Y[Pho]TAR	0.88/2.55
IGF1R/INSR_1165_1166/1189_1190	DIYETDY[Pho]Y[Pho]R	0.88/1.07	All blot intensities were normalized to the blot intensity of G7-pY-G7 peptide		

A summary of 67 tryptic-digested activation loops representing 79 TKs, and their relative blot intensities to the superbinder as determined by far Western assay. Most activation loops bind to the superbinder with greater affinity than the ErbB2_877 activation loop. The ErbB3_868 and LMTK2_295 activation loops were not tested by the far Western assay but were detected by SH2-AP-MS in different samples (Tab.2.2; Fig.2.4 G-I).

Both PRM and MRM methods were used for the targeted proteomics studies using cell culture models and tumor tissues samples. First, a loop-panel was generated for PRM that included 67 activation loops, as well as 6 functionally significant and relatively abundant non-loop TK pTyr peptides (Suppl.2.4). All candidate peptides were synthesized *in vitro* to represent the tryptic-digested forms. Peptides with cysteine residues were alkylated by iodoacetamide (IAA). In the PRM test carried out on a Thermo QExactive MS system, the loop-panel peptides were found to meet the following criteria: presence of a clearly defined peak, reproducibility of retention time and peak area. The retention time, charge status and optimal collision energy (CE) were then determined individually. In addition to the loop-panel, a more comprehensive full-panel was generated by introducing 1~3 non-loop pTyr peptides for each TK, if available. pTyr sites with high HTP/LTP numbers, good superbinder binding affinities and functions in promoting TK activity or pTyr-mediated signaling were preferred. Similarly, the corresponding peptides were synthesized *in vitro* and tested by MRM on a Qtrap6500+ MS system. Some peptides with relatively poor MS detection were excluded, including a few activation loops that performed significantly worse than non-loop pTyr peptides within the same TKs. For example, EGFR_1172 peptide, which is ranked 2nd among all EGFR pTyr sites in HTP/LTP and characterized as a modification inducing EGFR enzymatic activity, replaced EGFR_867 activation loop as the primary target of EGFR. The final full-panel consists of 60 activation loops and 97 non-loop pTyr peptides that cover 87 TKs (Suppl.2.5), except for EPHAA, LTK and MATK, for which no pTyr sites were identified before or suitable for trypsin digestion. A few non-TK pTyr peptides were also synthesized as controls, including the activation loops of MAPK1 (Erk2) and MAPK3 (Erk1), and the GSK3 α _279 (GSK3 β _216) peptide (GEPNVSpYICSR) which is constitutively phosphorylated in many cell lines (Doble and Woodgett, 2003).

Due to the large number of target peptides, the absence of matrix with diversified pTyr peptides and difficulty to collect patient-derived samples expressing 87 TKs (or at least those validated TK biomarkers), it appears not practical to carry out standard tests for MS-based peptide quantification, such as making the calibration curves, detecting interfering ions or determining the limits of detection/quantification for individual peptides. The MRM linearities of Src_419 and GSK3 α _279 (GSK3 β _216) peptides, shown in Fig.2.3,

were at least 4 orders of magnitude. Although stable isotope labelling provides the most precise target quantification and is least subject to interferences, the cost of high purity standards for all these peptides would also be prohibitive. Additional criteria were applied post-analysis to ensure correct identifications of the signal attributes to each of the target peptides. For all PRM/MRM detected TKs (pTyr peptides) presented in this study, 4~10 transitions attributed to the target peptide were verified co-eluted and displaying identical chromatographic retention and MS/MS spectra to the corresponding synthetic peptide.

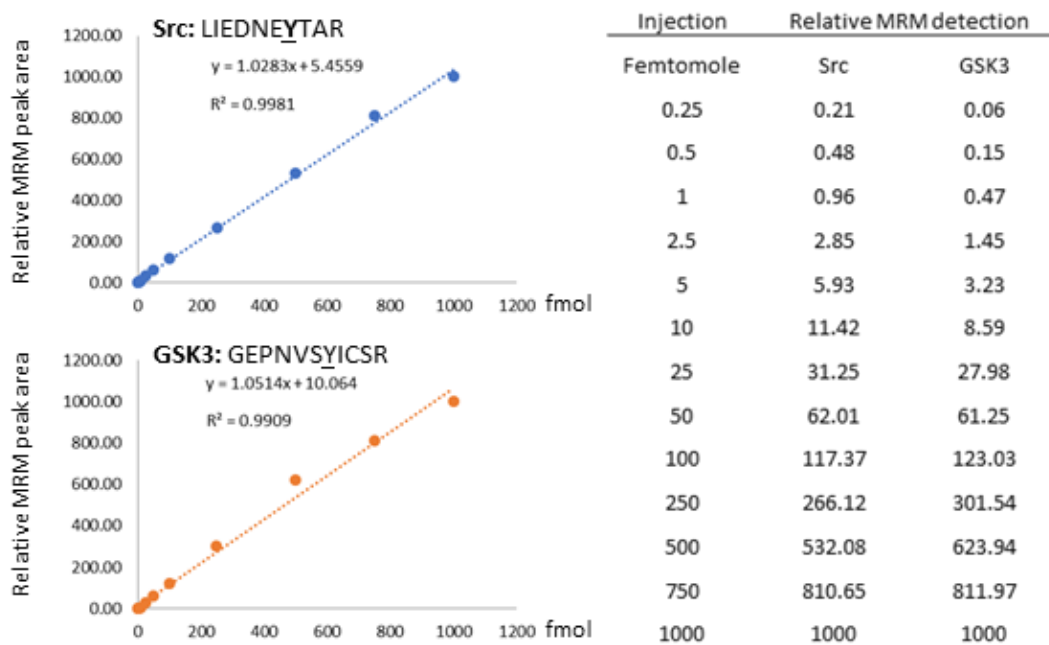


Figure 2.3 The linearities of Src₄₁₉ and GSK3 α ₂₇₉ in MRM

The linearities of Src₄₁₉ and GSK3 α ₂₇₉ peptides, as calculated by relative peak areas determined by MRM. The dynamic range is between 250 picomolar and 1 nanomolar for both peptides.

2.4.3 Identification of TK biomarkers in tumor tissues

The initial PRM investigation was carried out using a few fast-frozen surgical breast tumor tissues (Ontario Tumor Bank). From 50 µg of lysate, multiple TKs and GSK3 were detected with reliable extracted ion chromatogram (XIC) data (Fig.2.4). To evaluate the PRM reproducibility, two biological replicate samples were prepared from the same frozen tissue and two technical PRM replicates were tested for each sample. The GSK3 peptide was detected as the dominant peak in all replicates, however it likely was not the optimal internal control due to the large variance observed across different samples (Fig.2.4 A-B, D-E, G). The variation of GSK3 peak area was approximately 20% between two technical replicates and up to 40% between two biological replicates (Fig.2.4 C), but several folds across different tissues (Fig.2.4 A, D, G). This reproducibility is not ideal and only acceptable for qualitative analysis, considering the possible intratumor heterogeneity and limited accuracy of PRM. Activated CDC42 (ACK1_284) was the only TK peptide detected in sample #1 (Fig.2.4 A-B), which was previously reported as a deregulated TK in some breast cancer cell lines that promoted cell proliferation, invasion and colony forming ability (Wu et al., 2017). In samples #2 and #3, a few oncogenic or protooncogenic TKs were detected, including ALK_1507 (non-loop) (Fig.2.4 D-F), LMTK2_296 (Fig.2.4 G-I) and Src family TKs (SRC_419/YES_426/FYN_420/LCK_394) (Fig.2.4 G-H, J). ALK is natively expressed during the early stages of embryonic development and in neural cells in adults (Iwahara et al., 1997; Morris et al., 1994; Morris et al., 1997). Although not defined as a breast cancer biomarker, ectopic expression of ALK has been identified in both breast cancer cell lines and patient-derived tissues in various reports (Hanna et al., 2015; Kim et al., 2015; Krishnamurthy et al., 2013; Siraj et al., 2015). Tissue #1 and #2 were HER2 positive according to records obtained from the Ontario Tumor Bank (#1 IHC; #2 FISH), however, no phosphorylated ErbB2 peptide was detected in these tissues, while the control experiment using the SK-BR-3 cell line exhibited the highest peak of ErbB2 activation loop among all detected peptides (Fig.2.4 K). Next, ErbB2 protein and phosphorylation levels in these tissue samples were evaluated by Western blot. As shown in Fig.2.4 L, SK-BR-3 exhibited high ErbB2 expression and phosphorylation, while only weak ErbB2 expression was observed in tissue sample #2 and no ErbB2 phosphorylation was detected in any tissue samples.

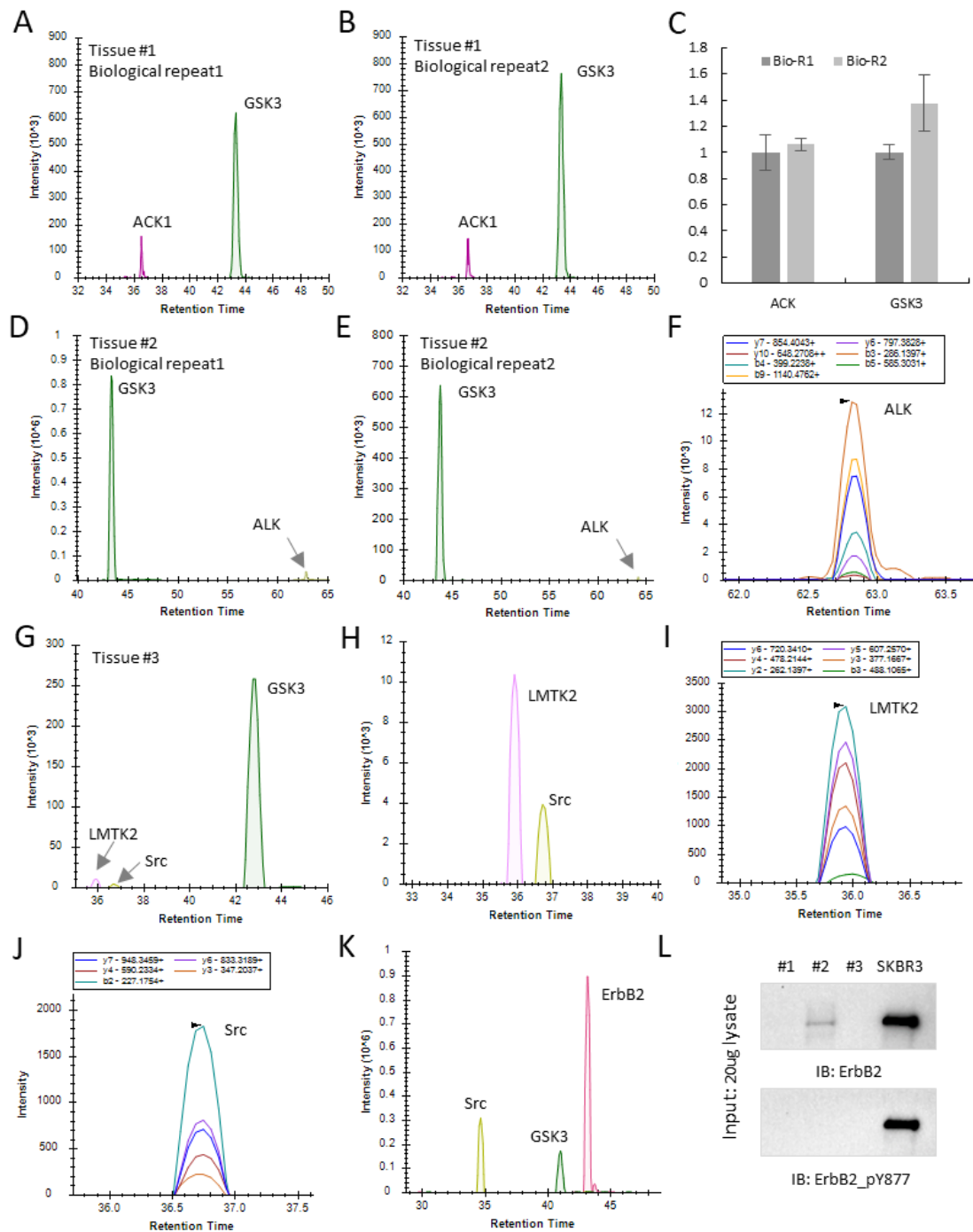


Figure 2.4 PRM analysis of fast frozen breast cancer tissues

SH2-AP-MS (PRM) analysis of fast frozen surgically-resected breast cancer tissues. (A-B) Two PRM biological replicates of 50 μ g protein extracted from a HER2 positive (IHC) breast cancer tissue (#1). GSK3 and ACK were detected in both samples; (C) The data reproducibility of GSK3

and ACK peptides detected in two biological replicates as shown in A-B, n=2; (D-E) Two PRM biological replicates of 50 μ g protein extracted from a HER2 positive (FISH) breast cancer tissue (#2). GSK3, EPHB3 and ALK were detected in both samples; F) XIC of ALK_1507 non-loop pTyr peptide detected in tissue #2; (G-H) The PRM result of 50 μ g protein extracted from a HER2 negative breast cancer tissue (#3). The dominant GSK3 peak was excluded from the spectra to better visualize low-abundant detected TKs; (I) XIC of LMTK2_295 activation loop detected in tissue #3; (J) XIC of Src TK family activation loop detected in tissue #3. The activation loop is conserved in Src, Yes, Fyn and Lck (phosphorylated on Y419/426/420/394); (K) The PRM result of 20 μ g SKBR3 cell lysate (pervanadate treated). The ErbB2 activation loop and Src TK family activation loop were dominant in the spectra; (L) western blot of total protein lysate extracted from tissues and SK-BR-3 cells by anti-ErbB2 and anti-ErbB2_pY877 antibodies. 20 μ g total lysate was loaded for gel electrophoresis. Only weak ErBB2 expression was detected in tissue #2 but no phospho-ErbB2 was detected in any tissues. The positive control SK-BR-3 cells exhibited strong expression and phosphorylation of ErbB2.

Furthermore, PRM was performed on samples collected from other cancer types, including primary peripheral blood mononuclear cells (PBMCs) isolated from acute myeloid leukemia (AML) and chronic lymphocytic leukemia (CLL) whole blood, and FFPE (formalin-fixed paraffin-embedded) slides for lung cancer and biliary cancer tissues. The Src kinase family is known to be highly active in immune cells, while two Src family activation loops, the Src/Yes/Fyn/Lck activation loop and the Hck/Lyn activation loop, were detected in all PBMC samples (Fig.2.5 A-C). A few additional activation loops were detected from 90 μ g AML sample with relatively high abundance (Fig.2.5 B). BTK is a biomarker in chronic lymphocytic leukemia (CLL) but recently validated as potential biomarker in AML as well (Prada-Arismendy et al., 2017; Rushworth et al., 2014). Fes is widely expressed in myeloid cell lineages and required for oncogenic FLT3 signaling in AML (Voisset et al., 2010; Weir et al., 2017). The FFPE slides of lung cancer and biliary cancer each had approximately 1 cm² of 5-micron thickness tissue specimen. Similarly, known and new potential TK biomarkers were detected in both lung cancer and biliary cancer samples, each from 4 specimens on FFPE slides (Fig.2.5 D-E). ALK is a well-defined biomarker in non-small cell lung cancer (NSCLC) and FGFR1 gene amplification has been identified in approximately 23% NSCLC and 6% small cell lung cancer (SCLC) cases (Fig.2.5 D) (Peifer et al., 2012; Thai and Solomon, 2018; Weiss et al., 2010). In biliary cancer, deregulation of FGFR family members and insulin receptors were also reported previously (Fig.2.5 E) (Rizvi and Borad, 2016; Suzuki et al., 2015; Valle et al., 2017). GSK3 was only detected in one PBMC sample but not in fixed lung cancer or biliary cancer tissues.

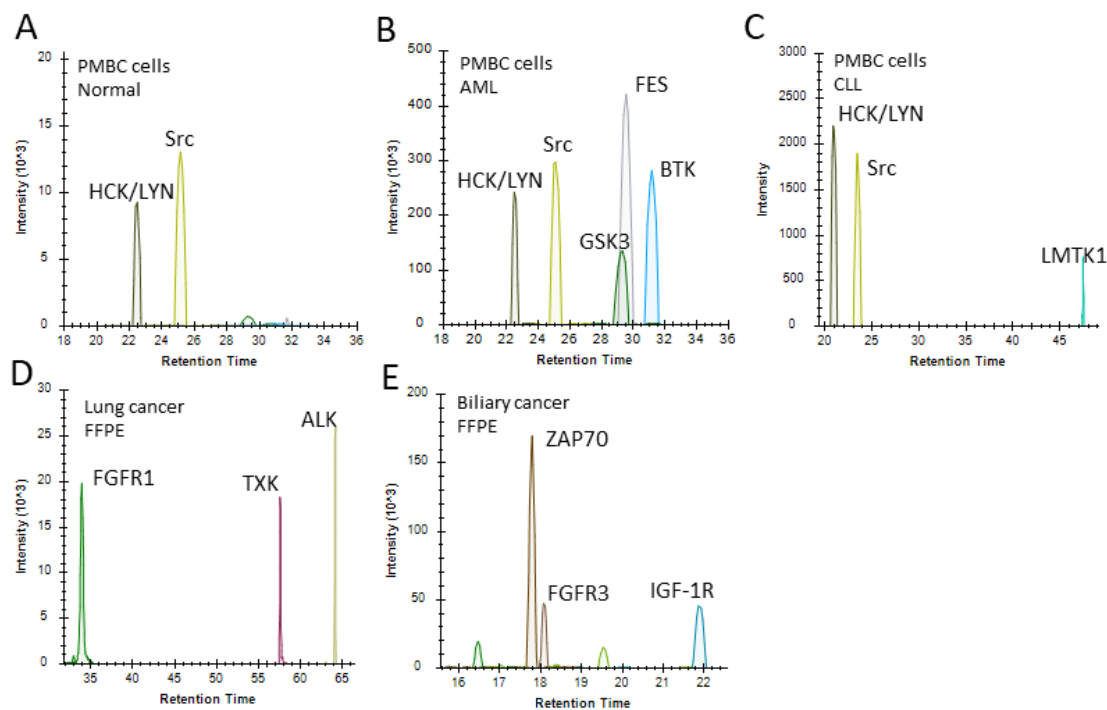


Figure 2.5 PRM analysis of PBMCs and formalin-fixed solid tumor specimens

SH2-AP-MS (PRM) analysis of samples from leukemia, lung cancer and biliary cancer. (A) The activation loops of Src/Yes/Fyn/Lck and Fyn/Hck were detected from PBMC cells isolated from healthy whole blood. The protein amount is less than 20 μg ; (B) The activation loops of BTK, Src/Yes/Fyn/Lck, Fyn/Hck and Fes were detected from PBMC cells isolated from AML whole blood. The protein amount is 90 μg ; (C) The activation loops of Src and LMTK1 were detected from PBMC cells isolated from CLL whole blood. The protein amount is less than 20 μg ; (E) The activation loops of FGFR1 and TXK, and non-loop pTyr peptide of ALK_1507 were detected from lung cancer FFPE slides. The protein amount is less than 20 μg ; (F) The activation loops of ZAP70, FGFR1, FGFR3, IGF-1R/INSR and RET were detected from biliary cancer FFPE slides. The protein amount is 90 μg .

2.4.4 Tracking kinome dynamics in response to targeted therapeutic

Even though a few known and potential TK biomarkers were identified by PRM in different clinically-collected tumor tissues, validation analyses using conventional approaches were generally not practical due to the limited sample size. To further evaluate the accuracy of the SH2-AP-MS assay, MRM was used to track TK kinome dynamics in cultured cells treated with a TK inhibitor. In cancer treatment, the complexity of oncogenic signaling pathways greatly limits the efficacy of component-by-component targeted therapies, therefore it is anticipated that a comprehensive analysis of how oncogenic signaling can be adapted to drugs could provide great opportunity to treat tumors with high specificity and efficacy (Logue and Morrison, 2012). For TKs, especially the oncogenic or proto-oncogenic TKs, a few assays have been developed to globally profile TK activation status for research only. R&D Systems® designed an on-membrane antibody array that could capture and quantify the relative activities of tens of TKs in a single test, and RayBiotech® developed a similar ELISA-based assay. AP-MS has also been tested for profiling the full human kinome including both STKs and TKs. The multiplexed kinase inhibitor (MIB) MS strategy uses low-specificity small molecule kinase inhibitors as affinity reagents to enrich active forms of kinases, which generally bind to ATP-mimicking kinase inhibitors. When compared to next generation sequencing, MIB-AP-MS could identify approximately 50-60% of the expressed kinome. Due to the compromised binding affinities of the kinase inhibitors, MIB-AP-MS typically requires milligram-scale lysate protein for the affinity purification, and kinases must be in a non-denatured, active conformation for binding the affinity reagents (Duncan et al., 2012; Stuhlmiller et al., 2015).

Using SH2-AP-MS, TK kinome profiling was performed on SK-BR-3 cells treated with lapatinib. SK-BR-3 expresses moderate levels of EGFR and high levels of ErbB2, and therefore is sensitive to the EGFR/ErbB2 dual-specificity inhibitor lapatinib (Fig.2.2 C). SK-BR-3 cells were treated with lapatinib for two days and total cell lysate was collected at 0, 2, 6, 12, 24, 48 hours. Samples of 50 µg lysate were analyzed individually by MRM using the full-panel. As shown in Fig.2.6 A-C, a few oncogenic TKs were detected at all time points, including the non-loop peptide EGFR_1172 (Fig.2.6 E), ErbB2_877 activation

loop (Fig.2.6 F) and Src activation loop (Fig.2.6 G), which are among the most abundant TK pTyr peptides in untreated SK-BR-3 (Tab.2.2). SK-BR-3 is known to express all three TKs and respond to their inhibitors, with an IC₅₀ of 15 nM to lapatinib (highly sensitive) and 4.17 μ M to dasatinib (Src inhibitor, moderately sensitive) (Stanley et al., 2017). Phosphorylation of EGFR_1172 and Src_419 was attenuated upon lapatinib treatment for 48 hours (Fig.2.6 G, I). As introduced earlier, phosphorylation on both sites promotes kinase activity, therefore EGFR and Src should be inhibited by lapatinib after 48 hours treatment. In contrast, phosphorylation on ErbB2_877 was more dynamic, which decreased at 24 hours but increased between 24 hours and 48 hours, indicating a re-gaining of ErbB2 kinase activity during the treatment (Fig.2.6 H). The same observations were reported in a previous study of lapatinib treated SK-BR-3 cells, which were validated by both MIB-AP-MS and Western blot (Stuhlmiller et al., 2015).

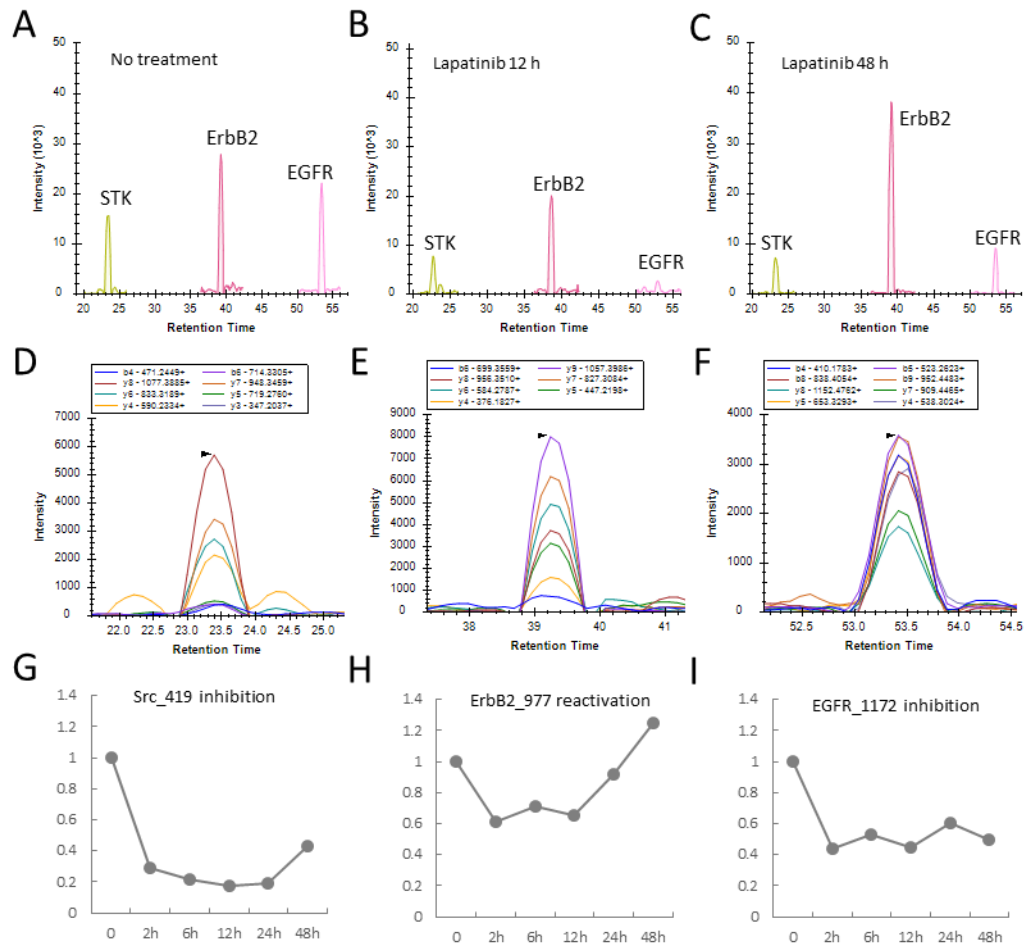


Figure 2.6 Tracking kinome reprogramming in SK-BR-3 cells

SH2-AP-MS (PRM) analysis of SK-BR-3 cells treated with lapatinib for 48 hours. (A-C) EGFR, ErbB2 and Src were detected in 50 μ g cell lysate of SK-BR-3 cells treated with lapatinib for 0 hour, 12 hours and 48 hours; (D) XIC of EGFR_1172 non-loop pTyr peptide; (E) XIC of ErbB2_877 activation loop peptide; (F) XIC of Src activation loop peptide; (G-I) The relative quantification of peak areas of EGFR, ErbB2 and Src peptides in MRM at six time points of lapatinib treatment. For EGFR and Src peptides, phosphorylation was inhibited by lapatinib after 48 hours treatment. For the ErbB2 peptide, phosphorylation was only inhibited by lapatinib for 24 hours and recovered between 24 hours and 48 hours.

2.4.5 Deciphering the mechanism of acquired trastuzumab resistance

In addition to short-term and temporary drug-induced TK kinome reprogramming, the TK kinome may be permanently altered during long-term drug treatment of TK positive cancers. In treating HER2 positive breast cancer, the humanized antibody trastuzumab shows considerable clinical efficacy and extends overall survival (Cameron et al., 2017; Seidman et al., 2008; Vogel et al., 2002). However, in many cases, the trastuzumab-sensitive patients only responded to this therapy for five to nine months when acquired resistance became established. Even though the resistant mechanism could be complex, Trastuzumab resistance has been previously shown to be driven by the deregulation of non-target TKs, including overactivation of EGFR, IGF-1R, Src kinases or overexpression of hepatocyte growth factor (Dua et al., 2010; Lu et al., 2001; Moulder et al., 2001; Nahta et al., 2005; Ritter et al., 2007; Shattuck et al., 2008; Zhang et al., 2011).

Following an established strategy (Zhang et al., 2011), a trastuzumab resistant clone was built in the lab. SK-BR-3 cells were incubated with a low dose (4 $\mu\text{g/ml}$ and 8 $\mu\text{g/ml}$) of trastuzumab for over six months for the selection of resistant cells (Zhang et al., 2011). Compared to the parental cells (SKBR3o), resistant cells (SKBR3r) exhibited little morphological change but were significantly less sensitive to trastuzumab (Fig.2.7 A-B). In the SH2-AP-MS (MRM) analysis, EGFR₁₁₇₂, ErbB2 activation loop and Src activation loop were still the best detected peptides, although their relative abundance was slightly altered in the resistant cells (Fig.2.7 C-E). According to the MRM quantification, EGFR₁₁₇₂ and ErbB2₈₇₇ phosphorylation exhibited little variance, while Src phosphorylation increased by about two-folds in the resistant cells (Fig.2.7 E). The MAPK1 (Erk2) activation loop was detected in both cell lines at a consistent level, indicating that the resistant cells retained a comparable active-status in cell proliferation. It is intriguing that the c-Kit activation loop (NDSNYVVK, c-Kit₈₂₃) was detected in the resistant cells (Fig.2.7 D). c-Kit, also known as mast/stem cell growth factor receptor (SCFR) or CD117, is a proto-oncogenic RTK first described as a cellular homolog of the feline sarcoma viral oncogene v-Kit (Yarden et al., 1987). Like many other oncogenic RTKs, deregulation of c-Kit results in the activation of cell proliferation and survival signaling pathways in various cancer types (Hirota et al., 2002; Lennartsson et al., 2005;

Lennartsson and Ronnstrand, 2012). In transcriptome sequencing, c-Kit was found to be the most up-regulated TK with an 80- fold increase in mRNA abundance in the resistant cells (Fig.2.7 F).

In a previous study of acquired trastuzumab resistance, Src was concluded as a key modulator of the trastuzumab response, which was activated in both intrinsic and acquired resistant HER2 positive cells, including SK-BR-3 (Zhang et al., 2011). Here only a moderate increase of Src phosphorylation was observed. The efficacy of cell proliferation inhibition was further tested by applying three inhibitors, trastuzumab (HER2), imatinib (c-Kit) and SKI-1 (Src) (Fig.2.7 G). The parental cells were only sensitive to trastuzumab, while combining inhibition of c-Kit and Src brought no additional effect to trastuzumab. In contrast, the resistant cells became moderately sensitive to imatinib and the imatinib inhibition sensitized the resistant cells to trastuzumab treatment.

Together these data indicate that ErbB2 is active and a dominant driver of cell proliferation in both parental and resistant SK-RB-3 cells. Both c-Kit expression and activation are significantly up-regulated in the resistant cells, which promotes cell proliferation along with ErbB2.

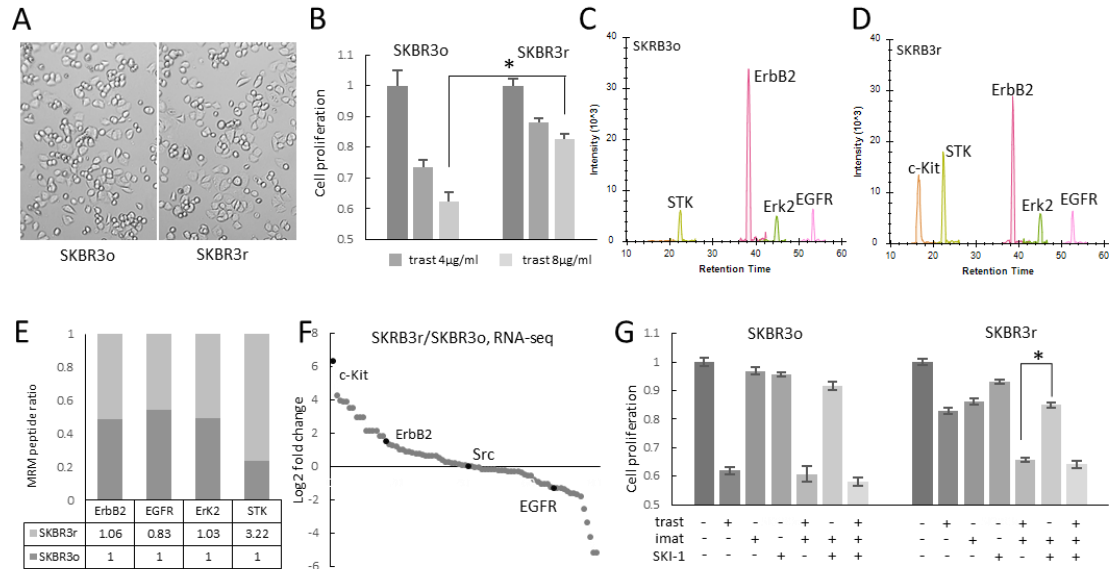


Figure 2.7 c-Kit is responsible for trastuzumab resistance in SK-BR-3 cells

Deregulated c-Kit contributes to the acquired trastuzumab resistance in SK-BR-3 cells, which was established by exposing cultured cells to a low dose of trastuzumab for six months. (A) The morphology of parental (SKBR3o) and resistant (SKBR3r) cells; (B) SKBR3r cells are less sensitive to trastuzumab treatment. Cell proliferation was determined by WST-8 assay, $n=3$, $p<0.05$; (C-D) SH2-AP-MS (MRM) analysis of 50 μg cell lysate of SKBR3o and SKBR3r cells. EGFR_1172, and activation loops of ErbB2, Src and MAPK1(Erk2) were detected in both cells; (E) Ratio of peptide abundance (SKBR3r/SKBR3o) determined by MS; (F) Ratio of TK expression levels (\log_2 value, SKBR3r/SKBR3o) determined by transcriptome sequencing (data by Dr. Lyugao Qin and Dr. Xiaoling Liu). c-Kit is the most upregulated TK with 80-fold increase in transcription; (G) Inhibition of c-Kit but not Src re-sensitized SKBR3r cells for trastuzumab treatment. Inhibitors and concentrations: trastuzumab (HER2), 8 $\mu\text{g}/\text{ml}$; imatinib (c-Kit), 2 μM ; SKI-1 (Src), 1 μM . Cell proliferation was determined by WST-8 assay, $n=3$, $p<0.05$.

2.5 Discussion

The SH2-AP-MS is an orthogonal method for comprehensive evaluation of TK activity, designed for the analysis of TK functional phosphorylation sites that are affinity-purified by the SH2 superbinder. As phosphorylation is essential for TK activation and pTyr-mediated signal transduction in many cases, phosphorylation status on functional tyrosine residues could be a reliable indicator of TK activity. The binding between the superbinder SH2 and around 1000 TK pTyr sites was globally characterized, allowing the selection of superbinder-favored sites for target proteomic studies. In the optimized affinity purification workflow, pTyr peptides were effectively enriched by a saturating amount of the SH2 superbinder. Comparable enrichment efficacy could be reached using anti-pTyr antibodies in theory, however the high cost of antibodies makes this impractical. The SH2-AP-MS has great sensitivity and sample compatibility, and therefore may be further optimized for the TK examination in patient tissues, and even FFPE specimens after IHC/FISH staining. In comparison with IHC/FISH/NGS, the SH2-AP-MS approach detects the active TK forms. Potentially, this assay will be able to eliminate some false positives of conventional methods because gene amplification or protein expression is not well correlated with kinase activity. Even though not as comprehensive as the NGS platform, the MS detection panel could be further expanded to increase the level of multiplexing. Phosphorylation sites on SH2-containing adaptors, scaffold proteins, and the components of PI3K pathways, or other TK activity inhibitory sites could be included to generate the TK signaling panel for MS detection. Since activation loop phosphorylation is typically occurring in serine/threonine kinase activation, it is also possible to integrate IMAC in the affinity purification for sequential isolation pTyr and pSer/pThr peptides, which would allow for systematic analysis of any selected protein kinases and substrate proteins in a single test.

As an analytical technology with high levels of sensitivity and accuracy, MS has been widely used in many fields including clinical laboratories. A gas chromatography (GC)-MS method was first approved for the screening of drugs of abuse in the 1980s (Health and Services, 1988). Since then many additional small molecules were added into the MS detection list in the clinic, including therapeutic drugs, metabolites indicating inborn errors of metabolism and steroid hormones (Jannetto and Fitzgerald, 2016). Even though MS is

capable of detecting a wide range of analytes from small molecules to intact proteins, the MS analysis of biomarkers from a protein matrix is much more challenging for the clinical laboratory, mainly due to regulatory issues, difficulties in sample preparation and running complex analytic systems. With constant technological advancements, MS has begun to transform practices in the clinical laboratory. In 2013, the Biotyper (Bruker) MALDI (Matrix Assisted Laser Desorption/Ionization)-TOF MS system was approved for identifying gram negative bacterial species in the clinic (Clark et al., 2013). In the Biotyper test, intact proteins were directly ionized from the microbes by MALDI and analyzed in a TOF mass analyzer. The spectrums were then matched to a reference library of known clinical strains. This entire workflow only takes approximately 15 minutes, thereby greatly reducing the cost of reagents and labor compared to conventional culture techniques, and brings potential healthcare benefit for rapid pathogen identification (Croxatto et al., 2012; Demirev and Fenselau, 2008).

Due to technical limits, the Biotyper is only capable of identifying the most abundant proteins in microbes, but its design is highly robust and reliable, therefore suitable for clinical practice. In contrast, our SH2-AP-MS detection of TK biomarkers is much more sensitive and precise but requires specific proficiency for sample preparation and MS method development. In addition, the compromised durability (uptime) is a common concern for all complex tandem MS systems. The filter aided sample preparation (FASP) strategy can be tested for improving the SH2 affinity purification (Manza et al., 2005), which may simplify the procedures and further increase the pTyr peptide recycle rate. In the current workflow, multiple steps result in sample loss, including the protein precipitation from raw extraction, C18 desalting and several rounds of resuspending and buffer exchange. By using a filtered column, some of these steps can be merged and carried out in the filter column, and C18 desalting can potentially be omitted. C18 desalting is an important step in sample preparation as salts that ionize during electrospray suppress the signal from peptides, however desalting is a main cause of sample loss, due to incomplete and irreversible peptide binding. Ideally in the proposed FASP-SH2-AP workflow, protein (raw extract) is reduced, alkylated and digested all within the filter column. Next, the tryptic digested peptides are collected by centrifugation while trypsin is trapped by the filter. Then the enrichment is directly performed in the peptide flow-through without buffer

exchange, as the superbinder SH2 is stable and active under high salt conditions (e.g. 2M Urea). Last, the SH2 beads are washed and eluted following the established procedures and the elution is ready for direct LC injection. By using rapid-digest trypsin, the entire process can be finished within 8 hours.

The abundance of pTyr peptides can be absolutely quantified by introducing isotope-labelled peptide standards before the affinity purification. However, this is impractical due to the long list of target peptides and high cost of isotope-labelled peptide synthesis and purification. The GSK3 α _279 was previously thought to be a constitutive phosphorylation site, but it exhibited wide variation among different samples and was even absent in some cases therefore it is not worthwhile to make a few isotope-labelled peptides as universal standards, either. Considering that TKs are usually among the most intensively tyrosine phosphorylated proteins, and the known TK biomarker loops are frequently the most abundant peaks in the corresponding cell lines (Tab.2.1, Tab.2.2), the qualitative or semi-quantitative analysis is still invaluable for identifying TK biomarkers or abnormal TK activation. Future studies may be focused on translating the SH2 superbinder AP-MS approach to the cancer clinic to inform target therapy, starting with commonly occurring cancer types, such as breast cancer and non-small cell lung cancer. The isotope-labelled peptides for key pTyr sites, including ErbB2, ALK, Src and MAPKs, will be introduced for absolute MS quantification. The standard IHC/FISH tests can be carried out simultaneously, to allow comparison of the results obtained from the SH2-AP-MS approach and the conventional tests that are current gold standards in pathology.

2.6 References

Aebersold, R., and Goodlett, D.R. (2001). Mass Spectrometry in Proteomics. *Chemical Reviews* *101*, 269-296.

Bian, Y., Li, L., Dong, M., Liu, X., Kaneko, T., Cheng, K., Liu, H., Voss, C., Cao, X., Wang, Y., *et al.* (2016). Ultra-deep tyrosine phosphoproteomics enabled by a phosphotyrosine superbinder. *Nat Chem Biol* *12*, 959-966.

Boulton, T.G., Nye, S.H., Robbins, D.J., Ip, N.Y., Radziejewska, E., Morgenbesser, S.D., DePinho, R.A., Panayotatos, N., Cobb, M.H., and Yancopoulos, G.D. (1991). ERKs: a family of protein-serine/threonine kinases that are activated and tyrosine phosphorylated in response to insulin and NGF. *Cell* *65*, 663-675.

Cargnello, M., and Roux, P.P. (2011). Activation and function of the MAPKs and their substrates, the MAPK-activated protein kinases. *Microbiol Mol Biol Rev* *75*, 50-83.

Clark, A.E., Kaleta, E.J., Arora, A., and Wolk, D.M. (2013). Matrix-assisted laser desorption ionization-time of flight mass spectrometry: a fundamental shift in the routine practice of clinical microbiology. *Clin Microbiol Rev* *26*, 547-603.

Collins, D.C., Sundar, R., Lim, J.S.J., and Yap, T.A. (2017). Towards Precision Medicine in the Clinic: From Biomarker Discovery to Novel Therapeutics. *Trends Pharmacol Sci* *38*, 25-40.

Croxatto, A., Prod'hom, G., and Greub, G. (2012). Applications of MALDI-TOF mass spectrometry in clinical diagnostic microbiology. *FEMS Microbiol Rev* *36*, 380-407.

Dankort, D., Maslikowski, B., Warner, N., Kanno, N., Kim, H., Wang, Z., Moran, M.F., Oshima, R.G., Cardiff, R.D., and Muller, W.J. (2001). Grb2 and Shc adapter proteins play distinct roles in Neu (ErbB-2)-induced mammary tumorigenesis: implications for human breast cancer. *Mol Cell Biol* *21*, 1540-1551.

Dawson, P.H. (1986). Quadrupole mass analyzers: Performance, design and some recent applications. *Mass Spectrometry Reviews* *5*, 1-37.

de Graaf, E.L., Giansanti, P., Altelaar, A.F., and Heck, A.J. (2014). Single-step enrichment by Ti⁴⁺-IMAC and label-free quantitation enables in-depth monitoring of phosphorylation dynamics with high reproducibility and temporal resolution. *Mol Cell Proteomics* *13*, 2426-2434.

Demirev, P.A., and Fenselau, C. (2008). Mass spectrometry for rapid characterization of microorganisms. *Annu Rev Anal Chem (Palo Alto Calif)* *1*, 71-93.

Denkert, C., Huober, J., Loibl, S., Prinzler, J., Kronenwett, R., Darb-Esfahani, S., Brase, J.C., Solbach, C., Mehta, K., Fasching, P.A., *et al.* (2013). HER2 and ESR1 mRNA expression levels and response to neoadjuvant trastuzumab plus chemotherapy in patients with primary breast cancer. *Breast Cancer Res* *15*, R11.

- Dey, B.R., Frick, K., Lopaczynski, W., Nissley, S.P., and Furlanetto, R.W. (1996). Evidence for the direct interaction of the insulin-like growth factor I receptor with IRS-1, Shc, and Grb10. *Mol Endocrinol* *10*, 631-641.
- Dittmar, T., Husemann, A., Schewe, Y., Nofer, J.R., Niggemann, B., Zanker, K.S., and Brandt, B.H. (2002). Induction of cancer cell migration by epidermal growth factor is initiated by specific phosphorylation of tyrosine 1248 of c-erbB-2 receptor via EGFR. *FASEB J* *16*, 1823-1825.
- Dixon, A.R., Bathany, C., Tsuei, M., White, J., Barald, K.F., and Takayama, S. (2015). Recent developments in multiplexing techniques for immunohistochemistry. *Expert Rev Mol Diagn* *15*, 1171-1186.
- Doble, B.W., and Woodgett, J.R. (2003). GSK-3: tricks of the trade for a multi-tasking kinase. *J Cell Sci* *116*, 1175-1186.
- Doerr, A. (2012). Mass spectrometry-based targeted proteomics. *Nature Methods* *10*, 23.
- Doerr, A. (2014). DIA mass spectrometry. *Nature Methods* *12*, 35.
- Dong, H., Ma, L., Gan, J., Lin, W., Chen, C., Yao, Z., Du, L., Zheng, L., Ke, C., Huang, X., *et al.* (2017). PTPRO represses ERBB2-driven breast oncogenesis by dephosphorylation and endosomal internalization of ERBB2. *Oncogene* *36*, 410-422.
- Dua, R., Zhang, J., Nhonthachit, P., Penuel, E., Petropoulos, C., and Parry, G. (2010). EGFR over-expression and activation in high HER2, ER negative breast cancer cell line induces trastuzumab resistance. *Breast Cancer Res Treat* *122*, 685-697.
- Duncan, J.S., Whittle, M.C., Nakamura, K., Abell, A.N., Midland, A.A., Zawistowski, J.S., Johnson, N.L., Granger, D.A., Jordan, N.V., Darr, D.B., *et al.* (2012). Dynamic reprogramming of the kinome in response to targeted MEK inhibition in triple-negative breast cancer. *Cell* *149*, 307-321.
- Fantus, I.G., Kadota, S., Deragon, G., Foster, B., and Posner, B.I. (1989). Pervanadate [peroxide(s) of vanadate] mimics insulin action in rat adipocytes via activation of the insulin receptor tyrosine kinase. *Biochemistry* *28*, 8864-8871.
- Feng, J., Witthuhn, B.A., Matsuda, T., Kohlhuber, F., Kerr, I.M., and Ihle, J.N. (1997). Activation of Jak2 catalytic activity requires phosphorylation of Y1007 in the kinase activation loop. *Mol Cell Biol* *17*, 2497-2501.
- Fila, J., and Honys, D. (2012). Enrichment techniques employed in phosphoproteomics. *Amino Acids* *43*, 1025-1047.
- Frank, R. (1992). Spot-Synthesis - an Easy Technique for the Positionally Addressable, Parallel Chemical Synthesis on a Membrane Support. *Tetrahedron* *48*, 9217-9232.
- Gallien, S., Duriez, E., Crone, C., Kellmann, M., Moehring, T., and Domon, B. (2012). Targeted proteomic quantification on quadrupole-orbitrap mass spectrometer. *Mol Cell Proteomics* *11*, 1709-1723.

Gradishar, W.J., Anderson, B.O., Balassanian, R., Blair, S.L., Burstein, H.J., Cyr, A., Elias, A.D., Farrar, W.B., Forero, A., Giordano, S.H., *et al.* (2018). Breast Cancer, Version 4.2017, NCCN Clinical Practice Guidelines in Oncology. *J Natl Compr Canc Netw* 16, 310-320.

Gross, J.r.H. (2004). *Mass spectrometry : a textbook* (Berlin ; New York: Springer).

Handorf, C.R., Kulkarni, A., Grenert, J.P., Weiss, L.M., Rogers, W.M., Kim, O.S., Monzon, F.A., Halks-Miller, M., Anderson, G.G., Walker, M.G., *et al.* (2013). A multicenter study directly comparing the diagnostic accuracy of gene expression profiling and immunohistochemistry for primary site identification in metastatic tumors. *Am J Surg Pathol* 37, 1067-1075.

Hanna, M.G., Najfeld, V., Irie, H.Y., Tripodi, J., and Nayak, A. (2015). Analysis of ALK gene in 133 patients with breast cancer revealed polysomy of chromosome 2 and no ALK amplification. *Springerplus* 4, 439.

Health, U.D.o., and Services, H. (1988). Mandatory guidelines for federal workplace drug testing programs. *Federal Register* 53, 11970-11989.

Heinrich, C., Keller, C., Boulay, A., Vecchi, M., Bianchi, M., Sack, R., Lienhard, S., Duss, S., Hofsteenge, J., and Hynes, N.E. (2010). Copine-III interacts with ErbB2 and promotes tumor cell migration. *Oncogene* 29, 1598-1610.

Hirota, S., Nishida, T., Isozaki, K., Taniguchi, M., Nishikawa, K., Ohashi, A., Takabayashi, A., Obayashi, T., Okuno, T., Kinoshita, K., *et al.* (2002). Familial gastrointestinal stromal tumors associated with dysphagia and novel type germline mutation of KIT gene. *Gastroenterology* 122, 1493-1499.

Holland, S.J., Pan, A., Franci, C., Hu, Y., Chang, B., Li, W., Duan, M., Torneros, A., Yu, J., Heckrodt, T.J., *et al.* (2010). R428, a selective small molecule inhibitor of Axl kinase, blocks tumor spread and prolongs survival in models of metastatic breast cancer. *Cancer Res* 70, 1544-1554.

Holliday, D.L., and Speirs, V. (2011). Choosing the right cell line for breast cancer research. *Breast Cancer Res* 13, 215.

Hornbeck, P.V., Zhang, B., Murray, B., Kornhauser, J.M., Latham, V., and Skrzypek, E. (2015). PhosphoSitePlus, 2014: mutations, PTMs and recalibrations. *Nucleic Acids Res* 43, D512-520.

Hu, Q., Noll, R.J., Li, H., Makarov, A., Hardman, M., and Cooks, R.G. (2005). The Orbitrap: a new mass spectrometer. *Journal of Mass Spectrometry* 40, 430-443.

Hunter, T. (2014). The genesis of tyrosine phosphorylation. *Cold Spring Harb Perspect Biol* 6, a020644.

Huse, M., and Kuriyan, J. (2002). The conformational plasticity of protein kinases. *Cell* 109, 275-282.

- Huyer, G., Liu, S., Kelly, J., Moffat, J., Payette, P., Kennedy, B., Tsaprailis, G., Gresser, M.J., and Ramachandran, C. (1997). Mechanism of inhibition of protein-tyrosine phosphatases by vanadate and pervanadate. *J Biol Chem* 272, 843-851.
- Iwahara, T., Fujimoto, J., Wen, D., Cupples, R., Bucay, N., Arakawa, T., Mori, S., Ratzkin, B., and Yamamoto, T. (1997). Molecular characterization of ALK, a receptor tyrosine kinase expressed specifically in the nervous system. *Oncogene* 14, 439-449.
- Jannetto, P.J., and Fitzgerald, R.L. (2016). Effective Use of Mass Spectrometry in the Clinical Laboratory. *Clin Chem* 62, 92-98.
- Jennings, K.R. (2000). The changing impact of the collision-induced decomposition of ions on mass spectrometry. *Int J Mass Spectrom* 200, 479-493.
- Johnson, L.N., and Lewis, R.J. (2001). Structural basis for control by phosphorylation. *Chem Rev* 101, 2209-2242.
- Jones, S.M., and Kazlauskas, A. (2001). Growth-factor-dependent mitogenesis requires two distinct phases of signalling. *Nat Cell Biol* 3, 165-172.
- Jung, K. (2016). Statistical Aspects in Proteomic Biomarker Discovery. *Methods Mol Biol* 1362, 293-310.
- Kaneko, T., Huang, H., Cao, X., Li, X., Li, C., Voss, C., Sidhu, S.S., and Li, S.S. (2012a). Superbinder SH2 domains act as antagonists of cell signaling. *Sci Signal* 5, ra68.
- Kaneko, T., Joshi, R., Feller, S.M., and Li, S.S. (2012b). Phosphotyrosine recognition domains: the typical, the atypical and the versatile. *Cell Commun Signal* 10, 32.
- Kannaiyan, R., and Mahadevan, D. (2018). A comprehensive review of protein kinase inhibitors for cancer therapy. *Expert Rev Anticancer Ther* 18, 1249-1270.
- Kaufmann, S.H., Ewing, C.M., and Shaper, J.H. (1987). The erasable Western blot. *Anal Biochem* 161, 89-95.
- Kaufmann, S.H., and Kellner, U. (1998). Erasure of western blots after autoradiographic or chemiluminescent detection. *Methods Mol Biol* 80, 223-235.
- Keil-Dlouha, V.V., Zylber, N., Imhoff, J., Tong, N., and Keil, B. (1971). Proteolytic activity of pseudotrypsin. *FEBS Lett* 16, 291-295.
- Kent, S.B. (1988). Chemical synthesis of peptides and proteins. *Annu Rev Biochem* 57, 957-989.
- Khosravi, P., Kazemi, E., Imielinski, M., Elemento, O., and Hajirasouliha, I. (2017). Deep Convolutional Neural Networks Enable Discrimination of Heterogeneous Digital Pathology Images. *EBioMedicine*.
- Kim, M.H., Lee, S., Koo, J.S., Jung, K.H., Park, I.H., Jeong, J., Kim, S.I., Park, S., Park, H.S., Park, B.W., *et al.* (2015). Anaplastic lymphoma kinase gene copy number gain in inflammatory breast cancer (IBC): prevalence, clinicopathologic features and prognostic implication. *PLoS One* 10, e0120320.

- Kleiman, L.B., Maiwald, T., Conzelmann, H., Lauffenburger, D.A., and Sorger, P.K. (2011). Rapid phospho-turnover by receptor tyrosine kinases impacts downstream signaling and drug binding. *Mol Cell* 43, 723-737.
- Knighton, D.R., Zheng, J.H., Ten Eyck, L.F., Ashford, V.A., Xuong, N.H., Taylor, S.S., and Sowadski, J.M. (1991). Crystal structure of the catalytic subunit of cyclic adenosine monophosphate-dependent protein kinase. *Science* 253, 407-414.
- Kornev, A.P., and Taylor, S.S. (2010). Defining the conserved internal architecture of a protein kinase. *Biochim Biophys Acta* 1804, 440-444.
- Krishnamurthy, S., Woodward, W., Yang, W., Reuben, J.M., Tepperberg, J., Ogura, D., Niwa, S., Huo, L., Gong, Y., El-Zein, R., *et al.* (2013). Status of the anaplastic lymphoma kinase (ALK) gene in inflammatory breast carcinoma. *Springerplus* 2, 409.
- Kuhlmann, L., Cummins, E., Samudio, I., and Kislinger, T. (2018). Cell-surface proteomics for the identification of novel therapeutic targets in cancer. *Expert Rev Proteomics* 15, 259-275.
- Lee, M.J., Ye, A.S., Gardino, A.K., Heijink, A.M., Sorger, P.K., MacBeath, G., and Yaffe, M.B. (2012). Sequential application of anticancer drugs enhances cell death by rewiring apoptotic signaling networks. *Cell* 149, 780-794.
- Lennartsson, J., Jelacic, T., Linnekin, D., and Shivakrupa, R. (2005). Normal and oncogenic forms of the receptor tyrosine kinase kit. *Stem Cells* 23, 16-43.
- Lennartsson, J., and Ronnstrand, L. (2012). Stem cell factor receptor/c-Kit: from basic science to clinical implications. *Physiol Rev* 92, 1619-1649.
- Levitcki, A. (2013). Tyrosine kinase inhibitors: views of selectivity, sensitivity, and clinical performance. *Annu Rev Pharmacol Toxicol* 53, 161-185.
- Logue, J.S., and Morrison, D.K. (2012). Complexity in the signaling network: insights from the use of targeted inhibitors in cancer therapy. *Genes Dev* 26, 641-650.
- Lu, Y., Zi, X., Zhao, Y., Mascarenhas, D., and Pollak, M. (2001). Insulin-like growth factor-I receptor signaling and resistance to trastuzumab (Herceptin). *J Natl Cancer Inst* 93, 1852-1857.
- Mabert, K., Cojoc, M., Peitzsch, C., Kurth, I., Souchelnytskyi, S., and Dubrovskaya, A. (2014). Cancer biomarker discovery: current status and future perspectives. *Int J Radiat Biol* 90, 659-677.
- Manza, L.L., Stamer, S.L., Ham, A.J., Codreanu, S.G., and Liebler, D.C. (2005). Sample preparation and digestion for proteomic analyses using spin filters. *Proteomics* 5, 1742-1745.
- Makarov, A. (2000). Electrostatic Axially Harmonic Orbital Trapping: A High-Performance Technique of Mass Analysis. *Analytical Chemistry* 72, 1156-1162.
- Mandell, J.W. (2008). Immunohistochemical assessment of protein phosphorylation state: the dream and the reality. *Histochem Cell Biol* 130, 465-471.

- Matlock, M.K., Holehouse, A.S., and Naegle, K.M. (2015). ProteomeScout: a repository and analysis resource for post-translational modifications and proteins. *Nucleic Acids Res* 43, D521-530.
- McLafferty, F.W. (1981). Tandem mass spectrometry. *Science* 214, 280-287.
- Meng, Y., and Roux, B. (2014). Locking the active conformation of c-Src kinase through the phosphorylation of the activation loop. *J Mol Biol* 426, 423-435.
- Miller, P.E., and Denton, M.B. (1986). The quadrupole mass filter: basic operating concepts. *Journal of chemical education* 63, 617.
- Morris, S.W., Kirstein, M.N., Valentine, M.B., Dittmer, K.G., Shapiro, D.N., Saltman, D.L., and Look, A.T. (1994). Fusion of a kinase gene, ALK, to a nucleolar protein gene, NPM, in non-Hodgkin's lymphoma. *Science* 263, 1281-1284.
- Morris, S.W., Naeve, C., Mathew, P., James, P.L., Kirstein, M.N., Cui, X., and Witte, D.P. (1997). ALK, the chromosome 2 gene locus altered by the t(2;5) in non-Hodgkin's lymphoma, encodes a novel neural receptor tyrosine kinase that is highly related to leukocyte tyrosine kinase (LTK). *Oncogene* 14, 2175-2188.
- Moulder, S.L., Yakes, F.M., Muthuswamy, S.K., Bianco, R., Simpson, J.F., and Arteaga, C.L. (2001). Epidermal growth factor receptor (HER1) tyrosine kinase inhibitor ZD1839 (Iressa) inhibits HER2/neu (erbB2)-overexpressing breast cancer cells in vitro and in vivo. *Cancer Res* 61, 8887-8895.
- Nahta, R., Yuan, L.X., Zhang, B., Kobayashi, R., and Esteva, F.J. (2005). Insulin-like growth factor-I receptor/human epidermal growth factor receptor 2 heterodimerization contributes to trastuzumab resistance of breast cancer cells. *Cancer Res* 65, 11118-11128.
- Nolen, B., Taylor, S., and Ghosh, G. (2004). Regulation of protein kinases; controlling activity through activation segment conformation. *Mol Cell* 15, 661-675.
- Northey, J.J., Chmielecki, J., Ngan, E., Russo, C., Annis, M.G., Muller, W.J., and Siegel, P.M. (2008). Signaling through ShcA is required for transforming growth factor beta- and Neu/ErbB-2-induced breast cancer cell motility and invasion. *Mol Cell Biol* 28, 3162-3176.
- Orth, A., Ghosh, R.N., Wilson, E.R., Doughney, T., Brown, H., Reineck, P., Thompson, J.G., and Gibson, B.C. (2018). Super-multiplexed fluorescence microscopy via photostability contrast. *Biomed Opt Express* 9, 2943-2954.
- Paik, S., Bryant, J., Tan-Chiu, E., Romond, E., Hiller, W., Park, K., Brown, A., Yothers, G., Anderson, S., Smith, R., *et al.* (2002). Real-world performance of HER2 testing--National Surgical Adjuvant Breast and Bowel Project experience. *J Natl Cancer Inst* 94, 852-854.
- Pan, Y., Sackmann, E.K., Wypisniak, K., Hornsby, M., Datwani, S.S., and Herr, A.E. (2016). Determination of equilibrium dissociation constants for recombinant antibodies by high-throughput affinity electrophoresis. *Sci Rep* 6, 39774.

Pavlou, M.P., Diamandis, E.P., and Blasutig, I.M. (2013). The long journey of cancer biomarkers from the bench to the clinic. *Clin Chem* 59, 147-157.

Pawson, T., and Scott, J.D. (2005). Protein phosphorylation in signaling--50 years and counting. *Trends Biochem Sci* 30, 286-290.

Peifer, M., Fernandez-Cuesta, L., Sos, M.L., George, J., Seidel, D., Kasper, L.H., Plenker, D., Leenders, F., Sun, R., Zander, T., *et al.* (2012). Integrative genome analyses identify key somatic driver mutations of small-cell lung cancer. *Nat Genet* 44, 1104-1110.

Perez, E.A., Reinholz, M.M., Hillman, D.W., Tenner, K.S., Schroeder, M.J., Davidson, N.E., Martino, S., Sledge, G.W., Harris, L.N., Gralow, J.R., *et al.* (2010). HER2 and chromosome 17 effect on patient outcome in the N9831 adjuvant trastuzumab trial. *J Clin Oncol* 28, 4307-4315.

Perez, E.A., Suman, V.J., Davidson, N.E., Martino, S., Kaufman, P.A., Lingle, W.L., Flynn, P.J., Ingle, J.N., Visscher, D., and Jenkins, R.B. (2006). HER2 testing by local, central, and reference laboratories in specimens from the North Central Cancer Treatment Group N9831 intergroup adjuvant trial. *J Clin Oncol* 24, 3032-3038.

Petryszak, R., Keays, M., Tang, Y.A., Fonseca, N.A., Barrera, E., Burdett, T., Fullgrabe, A., Fuentes, A.M., Jupp, S., Koskinen, S., *et al.* (2016). Expression Atlas update--an integrated database of gene and protein expression in humans, animals and plants. *Nucleic Acids Res* 44, D746-752.

Prada-Arismendy, J., Arroyave, J.C., and Rothlisberger, S. (2017). Molecular biomarkers in acute myeloid leukemia. *Blood Rev* 31, 63-76.

Raman, M., Chen, W., and Cobb, M.H. (2007). Differential regulation and properties of MAPKs. *Oncogene* 26, 3100-3112.

Rawlings, N.D., and Barrett, A.J. (1994). Families of serine peptidases. *Methods Enzymol* 244, 19-61.

Rice, R.H., Means, G.E., and Brown, W.D. (1977). Stabilization of bovine trypsin by reductive methylation. *Biochim Biophys Acta* 492, 316-321.

Rikova, K., Guo, A., Zeng, Q., Possemato, A., Yu, J., Haack, H., Nardone, J., Lee, K., Reeves, C., Li, Y., *et al.* (2007). Global survey of phosphotyrosine signaling identifies oncogenic kinases in lung cancer. *Cell* 131, 1190-1203.

Ritter, C.A., Perez-Torres, M., Rinehart, C., Guix, M., Dugger, T., Engelman, J.A., and Arteaga, C.L. (2007). Human breast cancer cells selected for resistance to trastuzumab in vivo overexpress epidermal growth factor receptor and ErbB ligands and remain dependent on the ErbB receptor network. *Clin Cancer Res* 13, 4909-4919.

Rizvi, S., and Borad, M.J. (2016). The rise of the FGFR inhibitor in advanced biliary cancer: the next cover of time magazine? *J Gastrointest Oncol* 7, 789-796.

Roepstorff, P., and Fohlman, J. (1984). Proposal for a common nomenclature for sequence ions in mass spectra of peptides. *Biomed Mass Spectrom* 11, 601.

Roskoski, R. (2004). Src protein-tyrosine kinase structure and regulation. In *Biochemical and Biophysical Research Communications*, pp. 1155-1164.

Roskoski, R., Jr. (2005). Src kinase regulation by phosphorylation and dephosphorylation. *Biochem Biophys Res Commun* 331, 1-14.

Rubinfeld, H., and Seger, R. (2005). The ERK cascade: a prototype of MAPK signaling. *Mol Biotechnol* 31, 151-174.

Rushworth, S.A., Murray, M.Y., Zaitseva, L., Bowles, K.M., and MacEwan, D.J. (2014). Identification of Bruton's tyrosine kinase as a therapeutic target in acute myeloid leukemia. *Blood* 123, 1229-1238.

Sauter, G., Lee, J., Bartlett, J.M., Slamon, D.J., and Press, M.F. (2009). Guidelines for human epidermal growth factor receptor 2 testing: biologic and methodologic considerations. *J Clin Oncol* 27, 1323-1333.

Schindler, T., Bornmann, W., Pellicena, P., Miller, W.T., Clarkson, B., and Kuriyan, J. (2000). Structural mechanism for STI-571 inhibition of abelson tyrosine kinase. *Science* 289, 1938-1942.

Seidman, A.D., Berry, D., Cirincione, C., Harris, L., Muss, H., Marcom, P.K., Gipson, G., Burstein, H., Lake, D., Shapiro, C.L., *et al.* (2008). Randomized phase III trial of weekly compared with every-3-weeks paclitaxel for metastatic breast cancer, with trastuzumab for all HER-2 overexpressors and random assignment to trastuzumab or not in HER-2 nonoverexpressors: final results of Cancer and Leukemia Group B protocol 9840. *J Clin Oncol* 26, 1642-1649.

Sharma, K., D'Souza, R.C., Tyanova, S., Schaab, C., Wisniewski, J.R., Cox, J., and Mann, M. (2014). Ultradeep human phosphoproteome reveals a distinct regulatory nature of Tyr and Ser/Thr-based signaling. *Cell Rep* 8, 1583-1594.

Shattuck, D.L., Miller, J.K., Carraway, K.L., 3rd, and Sweeney, C. (2008). Met receptor contributes to trastuzumab resistance of Her2-overexpressing breast cancer cells. *Cancer Res* 68, 1471-1477.

Shen, Y., Zhang, W., Liu, J., He, J., Cao, R., Chen, X., Peng, X., Xu, H., Zhao, Q., Zhong, J., *et al.* (2018). Therapeutic Activity of DCC-2036, a Novel Tyrosine Kinase Inhibitor, against Triple-Negative Breast Cancer Patient-Derived Xenografts by Targeting AXL/MET. *Int J Cancer*.

Shi, F., Telesco, S.E., Liu, Y., Radhakrishnan, R., and Lemmon, M.A. (2010). ErbB3/HER3 intracellular domain is competent to bind ATP and catalyze autophosphorylation. *Proc Natl Acad Sci U S A* 107, 7692-7697.

Shisheva, A., and Shechter, Y. (1993). Mechanism of pervanadate stimulation and potentiation of insulin-activated glucose transport in rat adipocytes: dissociation from vanadate effect. *Endocrinology* 133, 1562-1568.

Siraj, A.K., Beg, S., Jehan, Z., Prabhakaran, S., Ahmed, M., A, R.H., Al-Dayel, F., Tulbah, A., Ajarim, D., and Al-Kuraya, K.S. (2015). ALK alteration is a frequent event in aggressive breast cancers. *Breast Cancer Res* 17, 127.

Squires, M.S., Nixon, P.M., and Cook, S.J. (2002). Cell-cycle arrest by PD184352 requires inhibition of extracellular signal-regulated kinases (ERK) 1/2 but not ERK5/BMK1. *Biochem J* 366, 673-680.

Stanley, A., Ashrafi, G.H., Seddon, A.M., and Modjtahedi, H. (2017). Synergistic effects of various Her inhibitors in combination with IGF-1R, C-MET and Src targeting agents in breast cancer cell lines. *Sci Rep* 7, 3964.

Steinkamp, M.P., Low-Nam, S.T., Yang, S., Lidke, K.A., Lidke, D.S., and Wilson, B.S. (2014). erbB3 is an active tyrosine kinase capable of homo- and heterointeractions. *Mol Cell Biol* 34, 965-977.

Stuhlmiller, T.J., Miller, S.M., Zawistowski, J.S., Nakamura, K., Beltran, A.S., Duncan, J.S., Angus, S.P., Collins, K.A., Granger, D.A., Reuther, R.A., *et al.* (2015). Inhibition of Lapatinib-Induced Kinome Reprogramming in ERBB2-Positive Breast Cancer by Targeting BET Family Bromodomains. *Cell Rep* 11, 390-404.

Subik, K., Lee, J.F., Baxter, L., Strzepek, T., Costello, D., Crowley, P., Xing, L., Hung, M.C., Bonfiglio, T., Hicks, D.G., *et al.* (2010). The Expression Patterns of ER, PR, HER2, CK5/6, EGFR, Ki-67 and AR by Immunohistochemical Analysis in Breast Cancer Cell Lines. *Breast Cancer (Auckl)* 4, 35-41.

Sui, W., Ou, M., Chen, J., Wan, Y., Peng, H., Qi, M., Huang, H., and Dai, Y. (2009). Comparison of immunohistochemistry (IHC) and fluorescence in situ hybridization (FISH) assessment for Her-2 status in breast cancer. *World J Surg Oncol* 7, 83.

Suzuki, H., Roa, J.C., Kawamoto, T., Ishige, K., Wistuba, II, Li, D., Thomas, M.B., and Shoda, J. (2015). Expression of insulin-like growth factor I receptor as a biomarker for predicting prognosis in biliary tract cancer patients. *Mol Clin Oncol* 3, 464-470.

Tanase, C., Albulescu, R., and Neagu, M. (2016). Proteomic Approaches for Biomarker Panels in Cancer. *J Immunoassay Immunochem* 37, 1-15.

Thai, A.A., and Solomon, B.J. (2018). Treatment of ALK-positive nonsmall cell lung cancer: recent advances. *Curr Opin Oncol* 30, 84-91.

Tinti, M., Nardoza, A.P., Ferrari, E., Sacco, F., Corallino, S., Castagnoli, L., and Cesareni, G. (2012). The 4G10, pY20 and p-TYR-100 antibody specificity: profiling by peptide microarrays. *N Biotechnol* 29, 571-577.

Tokunaga, Y., Takeuchi, K., Takahashi, H., and Shimada, I. (2014). Allosteric enhancement of MAP kinase p38alpha's activity and substrate selectivity by docking interactions. *Nat Struct Mol Biol* 21, 704-711.

Valle, J.W., Lamarca, A., Goyal, L., Barriuso, J., and Zhu, A.X. (2017). New Horizons for Precision Medicine in Biliary Tract Cancers. *Cancer Discov* 7, 943-962.

Vassilakopoulou, M., Togun, T., Dafni, U., Cheng, H., Bordeaux, J., Neumeister, V.M., Bobos, M., Pentheroudakis, G., Skarlos, D.V., Pectasides, D., *et al.* (2014). In situ quantitative measurement of HER2mRNA predicts benefit from trastuzumab-containing chemotherapy in a cohort of metastatic breast cancer patients. *PLoS One* 9, e99131.

Vestal, M.L. (2011). The future of biological mass spectrometry. *J Am Soc Mass Spectrom* 22, 953-959.

Voisset, E., Lopez, S., Chaix, A., Georges, C., Hanssens, K., Prebet, T., Dubreuil, P., and De Sepulveda, P. (2010). FES kinases are required for oncogenic FLT3 signaling. *Leukemia* 24, 721-728.

Wei, L., Chen, Z., Shi, L., Long, R., Anzalone, A.V., Zhang, L., Hu, F., Yuste, R., Cornish, V.W., and Min, W. (2017). Super-multiplex vibrational imaging. *Nature* 544, 465-470.

Weir, M.C., Hellwig, S., Tan, L., Liu, Y., Gray, N.S., and Smithgall, T.E. (2017). Dual inhibition of Fes and Flt3 tyrosine kinases potently inhibits Flt3-ITD+ AML cell growth. *PLoS One* 12, e0181178.

Weiss, J., Sos, M.L., Seidel, D., Peifer, M., Zander, T., Heuckmann, J.M., Ullrich, R.T., Menon, R., Maier, S., Soltermann, A., *et al.* (2010). Frequent and focal FGFR1 amplification associates with therapeutically tractable FGFR1 dependency in squamous cell lung cancer. *Sci Transl Med* 2, 62ra93.

Wilkinson, R.W., and Leishman, A.J. (2018). Further Advances in Cancer Immunotherapy: Going Beyond Checkpoint Blockade. *Front Immunol* 9, 1082.

Wolff, A.C., Hammond, M.E., Schwartz, J.N., Hagerty, K.L., Allred, D.C., Cote, R.J., Dowsett, M., Fitzgibbons, P.L., Hanna, W.M., Langer, A., *et al.* (2007). American Society of Clinical Oncology/College of American Pathologists guideline recommendations for human epidermal growth factor receptor 2 testing in breast cancer. *Arch Pathol Lab Med* 131, 18-43.

Wu, P., Nielsen, T.E., and Clausen, M.H. (2015). FDA-approved small-molecule kinase inhibitors. *Trends Pharmacol Sci* 36, 422-439.

Wu, X., Zahari, M.S., Renuse, S., Kelkar, D.S., Barbhuiya, M.A., Rojas, P.L., Stearns, V., Gabrielson, E., Malla, P., Sukumar, S., *et al.* (2017). The non-receptor tyrosine kinase TNK2/ACK1 is a novel therapeutic target in triple negative breast cancer. *Oncotarget* 8, 2971-2983.

Xie, Y., Pendergast, A.M., and Hung, M.C. (1995). Dominant-negative mutants of Grb2 induced reversal of the transformed phenotypes caused by the point mutation-activated rat HER-2/Neu. *J Biol Chem* 270, 30717-30724.

Xu, Q.Q., Pan, B., Wang, C.J., Zhou, Y.D., Mao, F., Lin, Y., Guan, J.H., Shen, S.J., Zhang, X.H., Xu, Y.L., *et al.* (2016). HER2 amplification level is not a prognostic factor for HER2-positive breast cancer with trastuzumab-based adjuvant treatment: a systematic review and meta-analysis. *Oncotarget* 7, 63571-63582.

Yang, L., Amad, M.a., Winnik, W.M., Schoen, A.E., Schweingruber, H., Mylchreest, I., and Rudewicz, P.J. (2002). Investigation of an enhanced resolution triple quadrupole mass spectrometer for high - throughput liquid chromatography/tandem mass spectrometry assays. *Rapid Communications in Mass Spectrometry* 16, 2060-2066.

Yarden, Y., Kuang, W.J., Yang-Feng, T., Coussens, L., Munemitsu, S., Dull, T.J., Chen, E., Schlessinger, J., Francke, U., and Ullrich, A. (1987). Human proto-oncogene c-kit: a new cell surface receptor tyrosine kinase for an unidentified ligand. *EMBO J* 6, 3341-3351.

Yarden, Y., and Sliwkowski, M.X. (2001). Untangling the ErbB signalling network. *Nat Rev Mol Cell Biol* 2, 127-137.

Yost, R.A., and Enke, C.G. (1978). Selected ion fragmentation with a tandem quadrupole mass spectrometer. *Journal of the American Chemical Society* 100, 2274-2275.

Zhang, J., Billingsley, M.L., Kincaid, R.L., and Siraganian, R.P. (2000). Phosphorylation of Syk activation loop tyrosines is essential for Syk function. An in vivo study using a specific anti-Syk activation loop phosphotyrosine antibody. *J Biol Chem* 275, 35442-35447.

Zhang, S., Huang, W.C., Li, P., Guo, H., Poh, S.B., Brady, S.W., Xiong, Y., Tseng, L.M., Li, S.H., Ding, Z., *et al.* (2011). Combating trastuzumab resistance by targeting SRC, a common node downstream of multiple resistance pathways. *Nat Med* 17, 461-469.

Zhang, Y., Wolf-Yadlin, A., Ross, P.L., Pappin, D.J., Rush, J., Lauffenburger, D.A., and White, F.M. (2005). Time-resolved mass spectrometry of tyrosine phosphorylation sites in the epidermal growth factor receptor signaling network reveals dynamic modules. *Mol Cell Proteomics* 4, 1240-1250.

Zhao, H., Lo, Y.H., Yu, L., and Wang, S.C. (2011). Overcoming resistance to fulvestrant (ICI182,780) by downregulating the c-ABL proto-oncogene in breast cancer. *Mol Carcinog* 50, 383-389.

Zhao, H., Ou-Yang, F., Chen, I.F., Hou, M.F., Yuan, S.S., Chang, H.L., Lee, Y.C., Plattner, R., Waltz, S.E., Ho, S.M., *et al.* (2010). Enhanced resistance to tamoxifen by the c-ABL proto-oncogene in breast cancer. *Neoplasia* 12, 214-223.

Zhou, H., Ye, M., Dong, J., Corradini, E., Cristobal, A., Heck, A.J., Zou, H., and Mohammed, S. (2013). Robust phosphoproteome enrichment using monodisperse microsphere-based immobilized titanium (IV) ion affinity chromatography. *Nat Protoc* 8, 461-480.

2.7 Supplemental data

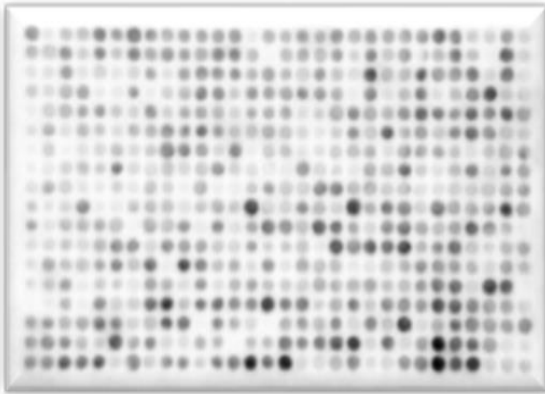
Suppl. 2.1 Alignment of activation loop regions of human TKs

ID	Name	Sequence Alignment
P00519	ABL1	---GD-TYT-----AHAGA-KFPIKWTAPESLA-----YNKFSIKSDVW 423
P42684	ABL2	---GD-TYT-----AHAGA-KFPIKWTAPESLA-----YNTFSIKSDVW 469
Q07912	ACK1	--QNDHYV-----MQEHR-KVPFAWCAPELTK-----TRTFSHASDTW 314
Q9UM73	ALK	--RAS-YZR-----KGGCA-MLPVKWPPEAFM-----EGIFTSKTDTW 1313
P51451	BLK	---DS-EYT-----AQEGA-KFPIKWTAPEAII-----FGVFTIKADVW 419
P51813	BMX	---DD-QYV-----SSVGT-KFPVKWSAPEVFH-----YFKYSSKSDVW 596
Q06187	BTK	---DD-EYT-----SSVGS-KFPVWRSPPEVLM-----YSKFSSKSDIW 581
P07333	CSF1R	---NDSNYI-----VKGNA-RLPVKWMAPESIF-----DCVYTVQSDVW 839
P41240	CSK	-----S-----TQDTG-KLPVKWTAPEALR-----EKKFSTKSDVW 370
Q08345	DDR1	--AGD-YZR-----VQGRA-VLPIRWMAWECIL-----MGKFTTASDVW 827
Q16832	DDR2	--SGD-YZR-----IQGRA-VLPIRWMSWESIL-----LGKFTTASDVW 771
P00533	EGFR	AEEK-EYH-----AEGG-KVPIKWMALESIL-----HRIYTHQSDVW 898
P21709	EPHA1	DFDG-TYE-----TQGG-KIPIRWTAPEAIA-----HRIFTTASDVW 810
P29317	EPHA2	DDPEA-TYT-----TSGG-KIPIRWTAPEAIS-----YRKFTSASDVW 801
P29320	EPHA3	DDPEA-AYT-----TRGG-KIPIRWTSPEAIA-----YRKFTSASDVW 808
P54764	EPHA4	DDPEA-AYT-----TRGG-KIPIRWTAPEAIA-----YRKFTSASDVW 808
P54756	EPHA5	DDPEA-AYT-----TRGG-KIPIRWTAPEAIA-----FRKFTSASDVW 862
Q9UF33	EPHA6	DDPEA-AYT-----TTGG-KIPIRWTAPEAIA-----YRKFTSASDAW 860
Q15375	EPHA7	DDPEA-VYT-----TTGG-KIPVWWTAPEAIQ-----YRKFTSASDVW 820
P29322	EPHA8	DDPDA-AYT-----TTGG-KIPIRWTAPEAIA-----FRTFSSASDVW 822
P54762	EPHB1	DDTSDPTYT-----SSLGG-KIPVWWTAPEAIA-----YRKFTSASDVW 808
P29323	EPHB2	DDTSDPTYT-----SALGG-KIPIRWTAPEAIQ-----YRKFTSASDVW 810
P54753	EPHB3	DDPSDPTYT-----SSLGG-KIPIRWTAPEAIA-----YRKFTSASDVW 822
P54760	EPHB4	ENSSDPTYT-----SSLGG-KIPIRWTAPEAIA-----FRKFTSASDAW 804
O15197	EPHB6	-----PQGP-SCLLRWAAPEVIA-----HGKHTTSSDVW 845
P04626	ERBB2	IDET-EYH-----ADGG-KVPIKWMALESIL-----RRRFTTHQSDVW 906
P21860	ERBB3	PDDK-QLL-----YSEA-KTPIKWMALESIH-----FGKYTHQSDVW 895
Q15303	ERBB4	GDEK-EYN-----ADGG-KMPIKWMALECIH-----YRKFTTHQSDVW 904
Q05397	FAK1	--DST-YYK-----A-SKG-KLPIKWMAPESIN-----FRRFTSASDVW 606
Q14289	FAK2	--DED-YYK-----A-SVT-RLPIKWMSPESIN-----FRRFTTASDVW 609
P16591	FER	---GG-VYS-----S-SGLKQIPIKWTAPEALN-----YGRYSSESVDW 744
P07332	FES	---DG-VYA-----ASGGLRQVPVKWTAPEALN-----YGRYSSESVDW 744
P11362	FGFR1	--HID-YYK-----KTNG-RLPVKWMAPEALF-----DRIYTHQSDVW 684
P21802	FGFR2	--NID-YYK-----KTNG-RLPVKWMAPEALF-----DRVYTHQSDVW 687
P22607	FGFR3	--NLD-YYK-----KTNG-RLPVKWMAPEALF-----DRVYTHQSDVW 678
P22455	FGFR4	--HID-YYK-----KTSNG-RLPVKWMAPEALF-----DRVYTHQSDVW 673
P09769	FGR	---DD-EYN-----PCQGS-KFPIKWTAPEAAL-----FGRFTIKSDVW 442
P36888	FLT3	---SDSNYV-----VRGNA-RLPVKWMAPESLF-----EGIYTIKSDVW 872
P42685	FRK	VDNED-IYE-----SRHEI-KLPVKWTAPEAIR-----SNKFSIKSDVW 417
P06241	FYN	---DN-EYT-----ARQGA-KFPIKWTAPEAAL-----YGRFTIKSDVW 450
P08631	HCK	---DN-EYT-----AREGA-KFPIKWTAPEAIN-----FGSFTIKSDVW 441
P08069	IGF1R	--ETD-YZR-----KGGKG-LLPVRWMSPELTK-----DGVFTTYSVDW 1196
P06213	INSR	--ETD-YZR-----KGGKG-LLPVRWMAPELTK-----DGVFTTSSDMW 1220
P14616	INSRR	--ETD-YZR-----KGGKG-LLPVRWMAPELTK-----DGIFTTHSDVW 1176
Q08881	ITK	---DD-QYT-----SSTGT-KFPVKWASPEVFS-----FSRYSSKSDVW 542
P23458	JAK1	--TDKEYYT-----VKDDR-DSPVFWYAPECLM-----QSKFYIASDVW 1065
O60674	JAK2	--QDKEYYK-----VKEPG-ESPIFWYAPESLT-----ESKFSVASDVW 1038
P52333	JAK3	--LDKDYVY-----VREPG-QSPIFWYAPESLS-----DNIFSRQSDVW 1011

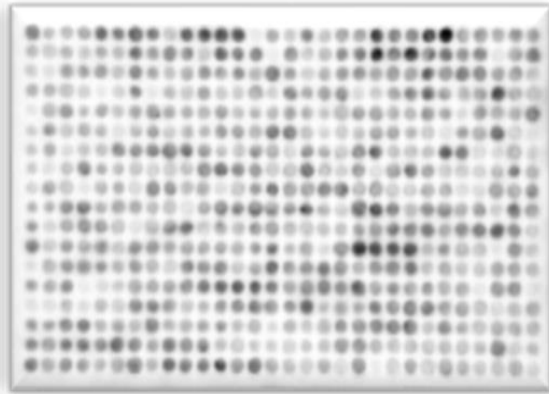
P10721	KIT	---NDSNYV-----VKGNA-RLPVKWMAPESIF-----NCVYTFESDVW 853
P43405	KSYK	A-DEN-YYK-----AQTHG-KWPVKWYAPECIN-----YYKFSSKSDVW 556
P06239	LCK	---DN-EYT-----AREGA-KFPIKWTAPEAIN-----YGTFTIKSDVW 424
Q6ZMQ8	LMTK1	--RED-YFV-----TADQL-WVPLRWIAPELVDEVHSNLLVVDQTKSGNVW 321
Q8IWU2	LMTK2	--KED-YIE-----TDDKK-VFPLRWTAPELVTSFQDRLLTADQTKYSNIW 333
Q96Q04	LMTK3	--KED-YYL-----TPERL-WIPLRWAAPELLGELHGTFMVVDQSRRESNIW 334
P29376	LTK	--RAS-YYR-----RGDRA-LLPVKWPPEAFL-----EGIFTSKTDSW 707
P07948	LYN	---DN-EYT-----AREGA-KFPIKWTAPEAIN-----FGCFTIKSDVW 427
P42679	MATK	-----K-----GLDSS-RLPVKWTAPEALK-----HGKFTSKSDVW 408
Q12866	MERTK	--SGD-YYR-----QGRIAKMPVKWIAIESLA-----DRVYTSKSDVW 784
P08581	MET	--DKE-YYSV-----HNKTGAKLPVKWMALESQ-----TQKFTTKSDVW 1267
O15146	MUSK	--SAD-YYK-----ANEND-AIPIRWMPPEAIF-----YNRYTTESDVW 786
P04629	NTRK1	--STD-YYR-----VGGR-MLPIRWMPPEAIF-----YRKFTTESDVW 711
Q16620	NTRK2	--STD-YYR-----VGHT-MLPIRWMPPEAIF-----YRKFTTESDVW 737
Q16288	NTRK3	--STD-YYRLFNPSGNDFCIWCEVGGHT-MLPIRWMPPEAIF-----YRKFTTESDVW 754
P16234	PGFRA	---HDSNYV-----SKGST-FLPVKWMAPESIF-----DNLYTTLSDVW 879
P09619	PGFRB	---RDSNYI-----SKGST-FLPLKWMAPESIF-----NSLYTTLSDVW 887
Q13882	PTK6	---ED-VYL-----S-HDH-NIPYKWTAPEALS-----RGHYSTKSDVW 371
Q13308	PTK7	---NSEYYH-----FRQA-WVPLRWMSPEAIL-----EGDFSTKSDVW 990
P07949	RET	--EED-SYV-----KRSQG-RIPVKWMAIESLF-----DHIYTTQSDVW 935
Q04912	RON	--DRE-YYSV-----QQHRHARLPVKWMALESQ-----TYRFTTKSDVW 1271
Q01973	ROR1	--SAD-YYR-----VQSKS-LLPIRWMPPEAIM-----YGKFSSSDIWI 676
Q01974	ROR2	--AAD-YYK-----LLGNS-LLPIRWMAPEAIM-----YGKFSSSDIWI 676
P08922	ROS1	--KND-YYR-----KRGE-LLPVRWMAPEAIF-----DGIFTTQSDVW 2145
P34925	RYK	--PMD-YHC-----LGDNENRVPVRWMALESV-----NNEFSSASDVW 523
P12931	SRC	---DN-EYT-----ARQGA-KFPIKWTAPEAAL-----YGRFTIKSDVW 449
Q9H3Y6	SRMS	---DD-IYS-----PSSSS-KIPVKWTAPEAAN-----YRVFSQKSDVW 410
Q6J9G0	STYK1	T--RG-A-----ISSTQTIPLKWLAPERLL-----LRPASIRADVW 310
P42680	TEC	---DD-QYT-----SSGA-KFPVKWCPPEVFN-----YSRFSSKSDVW 549
P35590	TIE1	-----VYV-----KKTMG-RLPVRWMAIESLN-----YSVYTTKSDVW 1037
Q02763	TIE2	-----VYV-----KKTMG-RLPVRWMAIESLN-----YSVYTTNSDVW 1022
Q13470	TNK1	--GARGRYV-----MGGPR-PIPYAWCAPESLR-----HGAFSSASDVW 307
P42681	TXK	---DD-EYV-----SSFGA-KFPIKWPPEVFL-----FNKYSSKSDVW 450
P29597	TYK2	--EGHEYR-----VREDG-DSPVFWYAPECLK-----EYKFYYASDVW 1085
Q06418	TYRO3	--SGD-YYR-----QGCASKLPVKWLALESIA-----DNLYTVQSDVW 716
P30530	UFO	--NGD-YYR-----QGRIAKMPVKWIAIESLA-----DRVYTSKSDVW 733
P17948	VGFR1	---KNPDYV-----RKGDT-RLPLKWMAPESIF-----DKIYSTKSDVW 1083
P35968	VGFR2	---KDPDYV-----RKGDA-RLPLKWMAPETIF-----DRVYTIQSDVW 1089
P35916	VGFR3	---KDPDYV-----RKGSA-RLPLKWMAPESIF-----DKVYTTQSDVW 1098
P07947	YES	---DN-EYT-----ARQGA-KFPIKWTAPEAAL-----YGRFTIKSDVW 456
P43403	ZAP70	A-DDS-YYT-----ARSAG-KWPLKWYAPECIN-----FRKFSSRSDVW 523
		*

Suppl. 2.2 Far-Western blots of TK pTyr sites by SH2 superbinder and antibody

GST-Superbinder



4G10 Platinum



Suppl. 2.3 TK pTyr sites and their relative blot intensities to the superbinder

Protein	Sequence	Site	Intensity	Trypsin digestion
ABL1	CTREPPFpYIITEFMTa	Y312	2.79	Y
ABL1	QGWVPSNpYITPVNSLa	Y115	2.33	Y
ABL1	IITEFMTpYGNLLDYL	Y320	2.2	Y
ABL1	HKLGGGQpYGEVYEGVa	Y253	2.01	Y
ABL1	TAPESLApYNKFSIKSa	Y413	1.85	Y
ABL1	YEGVWKKpYSLTVAVKa	Y264	1.81	Y
ABL1	VSRNAAEpYLLSSGINa	Y139	1.75	Y
ABL1	SLEKHSWpYHGVPVSRNa	Y128	1.65	Y
ABL1	TASDGKLpYVSSESRFa	Y185	1.58	Y
ABL1	GGQYGEVpYEGVWKKYa	Y257	1.42	Y
ABL1	KRNKPTVpYGVSPNYDa	Y226	1.31	Y
ABL1	EGCPEKVpYELMRACWa	Y469	1.31	Y
ABL1	LYTFCVSpYVDSIQQMa	Y1070	1.13	Y
ABL1	VYGVSPNpYDKWEMERa	Y232	1.12	Y
ABL1	LEAGKNLpYTFCVSYVa	Y1064	1	Y
ABL1	RLMTGDTpYTAHAGAKa	Y393	0.95	Y
ABL1	EKLRVLGpYNHNGEWCa	Y93	0.89	Y
ABL2	QGWVPSNpYITPVNSLa	Y161	2.23	Y
ABL2	TTADGKVpYVTAESRFa	Y231	2.21	Y
ABL2	TAPESLApYNTFSIKSa	Y459	2.02	Y
ABL2	VSRSAAEpYLLSSLINa	Y185	1.94	Y
ABL2	SSSSVVpYLPRLPILa	Y568	1.74	Y
ABL2	YVGVWKKpYSLTVAVKa	Y310	1.6	Y
ABL2	HKLGGOOpYGEVYVGVa	Y299	1.55	Y
ABL2	SLEKHSWpYHGVPVRSa	Y174	1.53	Y
ABL2	GGQYGEVpYVGVWKKYa	Y303	1.4	Y
ABL2	KCNKPTVpYGVSPIHDa	Y272	1.15	Y
ABL2	NLVPPKpYGGSFAQRa	Y718	1.15	Y
ABL2	EGCPPKVpYELMRACWa	Y515	1.13	Y
ABL2	EKLRVLGpYQNNGEWSa	Y139	0.99	Y
ABL2	RLMTGDTpYTAHAGAKa	Y439	0.78	Y
ACK1	KKVSSTHpYLLPERPa	Y859	3.45	Y
ACK1	HRNLIRLpYGVVLTTPPa	Y193	3.42	Y
ACK1	SFASDPKpYATPQVIQa	Y827	2.73	Y
ACK1	KVSSTHyYLLPERPSa	Y860	2.63	Y
ACK1	LLPERSpYLERYQRFa	Y868	2.15	Y
ACK1	LPQNDDHpYVMQEHRKa	Y284	1.83	Y
ACK1	GGVKKPTpYDPVSEDQa	Y518	1.48	Y
ALK	QPREPLSpYSRLQRKSa	Y46	1.66	Y
ALK	MELOSPEpYKLSKLRTa	Y1078	1.05	Y
ALK	KNCPGPVpYRIMTQCWa	Y1359	0.86	Y
ALK	MTDYNNPpYCFAGKTSa	Y1096	0.63	Y
ALK	TSLWNPTpYGSWFTEKa	Y1507	0.62	Y

ALK	TSTIMTDpYNPNYCFAa	Y1092	0.59	Y
BLK	VVTKEPlpYIVTEYMAa	Y309	2.99	Y
BLK	CLDEGGYpYISPRITFa	Y188	2.58	Y
BLK	RCLDEGGpYYISPRITa	Y187	2.11	Y
BLK	LVTGREGpYVPSNFVAa	Y107	1.98	Y
BLK	YTATERQpYELOPaaaa	Y501	1.65	Y
BLK	LQALVQHpYSKKGDGLa	Y205	1.02	Y
BLK	PIYIVTEpYMARGCLLa	Y314	0.92	Y
BLK	OIAEGMApYIERMNSIa	Y350	0.91	Y
BLK	ARIIDSEpYTAQEGAKa	Y389	0.71	Y
BMX	RYVLDDQpYVSSVGTKa	Y566	2.16	Y
BMX	NSSQVGMpYTVSLFSKa	Y330	1.42	Y
BMX	LGKWKQpYDVAVKMla	Y440	1.3	Y
BMX	LTKTNLSpYYEYDKMKa	Y40	0.83	Y
BMX	SSTSLAQpYDSNSKKIa	Y216	0.45	Y
BMX	KLYLAENpYCFDSIPKa	Y365	0.42	Y
BTK	RYVLDDepYTSSVGSKa	Y551	2.31	Y
BTK	TVHKLSYpYYEYDFERGa	Y40	2.23	Y
BTK	LKKVVAlpYDYMPMNAa	Y223	1.98	Y
BTK	CSTPQSpYYLAEKHLa	Y344	1.84	Y
BTK	STPQSQYpYLAEKHLFa	Y345	1.74	Y
BTK	PQGVIRHpYVVCSTPQa	Y334	1.67	Y
BTK	DVCEAMEpYLESKQFLa	Y511	1.32	Y
BTK	KVVALYDpYMPMNANDa	Y225	0.96	Y
BTK	HEKLVQLpYGVCTKQRa	Y461	0.8	Y
BTK	IAQGLRLpYRPHLASEa	Y617	0.72	Y
BTK	GLISRLKpYPVVSQONKa	Y375	0.51	Y
CSFIR	EDRRERDpYTNLPSSSa	Y923	1.55	Y
CSFIR	DIMNDSNpYIVKGNARa	Y809	1.44	Y
CSFIR	YKLVKDGpYQMAQPAFa	Y873	1.37	Y
CSFIR	DPEGGVDpYKNIHLEKa	Y699	1.21	Y
CSK	VEEKGLpYIVTEYMAa	Y263	1.86	Y
CSK	DGCPPAVpYEVKNCWVa	Y416	1.55	Y
CSK	EGIIPANpYVQKREGVa	Y64	1.41	Y
CSK	DVCEAMEpYLEGNFVa	Y304	1.35	Y
CSK	EQAERLLpYPPETGLFa	Y97	0.89	Y
CSK	VAAQDEFpYRSGWALNa	Y184	0.85	Y
CSK	AKGSLVDpYLRSRGRSa	Y277	0.84	Y
DDR1	RNLYAGDpYYRVQGRAa	Y796	2.04	Y
DDR1	PACPOGLpYELMLRCWa	Y881	2.04	Y
DDR1	NLYAGDYpYRVQGRAVa	Y797	1.79	Y
DDR1	FGMSRNLpYAGDYRVA	Y792	1.78	Y
DDR1	YRLLLATpYARPPRGPa	Y520	1.43	Y
DDR1	RDQGRQVpYLSRPPACa	Y869	1.43	Y
DDR1	GPREPPPpYQEPRPRGa	Y484	1.25	Y

DDR2	RNLYSGDpYYRIOGRAa	Y740	3.16	Y
DDR2	EQGSNSTpYDRIFPLRa	Y471	2.9	Y
DDR2	SDVRTVSpYTNLKFMAa	Y684	2.84	Y
DDR2	FGMSRNLpYSGDYRla	Y736	2.3	Y
DDR2	IFPLRPDpYQEPSRLJa	Y481	2.26	Y
DDR2	NLYSGDYpYRIOGRAVa	Y741	2.25	Y
DDR2	RDQGRQTpYLPQPAICa	Y813	0.62	Y
EGFR	MARDPQRpYLVIQGDEa	Y978	2.8	Y
EGFR	NMYYENSpYALAVLSNa	Y117	2.21	Y
EGFR	IIRGNMypYENSYALaAa	Y113	2.03	Y
EGFR	STAENAEpYLRVAPQSa	Y1197	1.74	Y
EGFR	ISLDNPDpYQDFFPKa	Y1172	1.72	Y
EGFR	KEILDEApYVMASVDNa	Y764	1.7	Y
EGFR	NCIQCAHpYIDGPHCVa	Y585	1.38	Y
EGFR	SGAFGTvpYKGLWIPeAa	Y727	1.35	Y
EGFR	SPTDSNFpYRALMDEEa	Y998	1.32	Y
EGFR	QIIRGNMypYENSYALa	Y112	1.25	Y
EGFR	PICTIDvpYIMIMVKWa	Y944	1.23	Y
EGFR	GSVQNPvpYHNQPLNPa	Y1110	0.99	Y
EGFR	QIAKGMNpYLEDRRLVa	Y827	0.82	Y
EGFR	LGAEKEpYHAEGGKVa	Y869	0.56	Y
EPHA1	LDDFDGTpYETQGGKla	Y781	2.08	Y
EPHA2	EHFMAAGpYTAIEKVVa	Y930	2.64	Y
EPHA2	ROSPEDVpYFSKSEOLa	Y575	2.24	Y
EPHA2	GHQKRIApYSLGLKDa	Y960	2.17	Y
EPHA2	QLKPLKtpYVDPHTYEa	Y588	1.6	Y
EPHA2	TYVDPHTpYEDPNQAVa	Y594	1.34	Y
EPHA2	EDDPEATpYTTSGGKla	Y772	1.09	Y
EPHA2	ESIKMQQpYTEHFMAAa	Y921	0.94	Y
EPHA2	KYLANMNpYVHRDLAAa	Y735	0.77	Y
EPHA2	TAPEAISpYRKFTSASa	Y791	0.71	Y
EPHA2	PMMIIEpYMENGALDa	Y694	0.64	Y
EPHA2	LEGVISKpYKPMMIITa	Y685	0.33	Y
EPHA2	AGEFGEvYKGMKTSa	Y628	0.32	Y
EPHA3	CKETFNLpYMESEDDDa	Y123	1.68	Y
EPHA3	EDDPEAApYTRGGKla	Y779	1.35	Y
EPHA3	KYLSDMGpYVHRDLAAa	Y742	1.27	Y
EPHA3	TYVDPHTpYEDPTQAVa	Y602	1.14	Y
EPHA3	KLPGLRtpYVDPHTYEa	Y596	1.04	Y
EPHA3	GIASGMKpYLSDMGYVa	Y736	0.97	Y
EPHA3	KETFNLpYMESEDDHa	Y124	0.83	Y
EPHA3	EIFTGVEpYSSCDTIAa	Y937	0.72	Y
EPHA3	IKTLKVgpYTEKQRDa	Y659	0.58	Y
EPHA3	PVMIVTEpYMENGLDa	Y701	0.57	Y
EPHA4	LNQGVRTpYVDPPTYEa	Y596	1.73	Y

EPHA4	TYVDPFTpYEDPNOAVa	Y602	1.57	Y
EPHA4	EDDPEAApYTTRGGKla	Y779	1.44	Y
EPHA4	TAPEAIApYRKFTSASa	Y798	1.17	Y
EPHA5	TYIDPHTpYEDPNQAVa	Y656	2.01	Y
EPHA5	KLPGVRTpYIDPHTYEa	Y650	1.84	Y
EPHA5	KCMCKAGpYEEKNGTCa	Y295	1.28	Y
EPHA5	EDDPEAApYTTRGGKla	Y833	1.13	Y
EPHA5	SPLGSGApYRSVGEWLa	Y967	0.82	Y
EPHA5	KYLSDMGpYVHRDLAAa	Y796	0.8	Y
EPHA5	GISAGMKpYLSDMGYVa	Y790	0.5	Y
EPHA5	IKTLKVGpYTEKQRDa	Y713	0.35	Y
EPHA6	EDDPEAApYTTRGGKla	Y831	1.89	Y
EPHA6	TYIDPDTpYEDPSLAVa	Y612	1.24	Y
EPHA6	KYLSDMGpYVHRDLAAa	Y794	1.07	Y
EPHA6	TAPEAIApYRKFSASa	Y850	0.89	Y
EPHA6	GIASGMKpYLSDMGYVa	Y788	0.83	Y
EPHA6	RFPGIKTPYIDPDYTa	Y606	0.71	Y
EPHA7	EDDPEAVpYTTRGGKla	Y791	2.47	Y
EPHA7	QEGDEELpYFHFKFPGa	Y597	1.98	Y
EPHA7	GIAAGMRpYLADMGYVa	Y748	1.58	Y
EPHA7	RYLADMGpYVHRDLAAa	Y754	1.31	Y
EPHA7	TAPEAIQpYRKFTSASa	Y810	0.95	Y
EPHA7	KFPGTKTPYIDPETYEa	Y608	0.8	Y
EPHA7	TYIDPETpYEDPNRAVa	Y614	0.65	Y
EPHA7	IKTLKVGpYTEKQRDa	Y671	0.53	Y
EPHA8	FYAEPTHpYEEPGRAGa	Y616	2.33	Y
EPHA8	EDDPDAApYTTRGGKla	Y793	2	Y
EPHA8	LAMIVTEpYMENGSLa	Y715	1.19	Y
EPHB1	YSDKLQHpYSTGRGSPa	Y582	1.3	Y
EPHB1	DDTSDPTpYTSLSGGKa	Y778	1.13	Y
EPHB1	GSPGMKIpYIDPFTYEa	Y594	0.96	Y
EPHB1	TAPEAIApYRKFTSASa	Y798	0.8	Y
EPHB1	KYLAEMNpYVHRDLAAa	Y740	0.78	Y
EPHB1	AYSKEAVpYSDKLQHYa	Y575	0.63	Y
EPHB1	IYIDPFTpYEDPNEAVa	Y600	0.56	Y
EPHB1	SDFGLSRpYLQDDTSDa	Y768	0.49	Y
EPHB1	AGEFGEVpYKGRKLKLPa	Y634	0.45	Y
EPHB2	YTDKLQHpYTSGHMTPa	Y584	2.21	Y
EPHB2	LDRITIPpYTSFNTVDa	Y912	2.14	Y
EPHB2	DDTSDPTpYTSALGGKa	Y780	1.81	Y
EPHB2	GRYSGKMpYFQTMTEAa	Y524	1.48	Y
EPHB2	KYLADMNpYVHRDLAAa	Y742	1.42	Y
EPHB2	PVSRSGFpYLAQDYGa	Y175	1.42	Y
EPHB2	MTPGMKIpYIDPFTYEa	Y596	1.4	Y
EPHB2	FERADSEpYTDKLQHYa	Y577	1.11	Y

EPHB2	GIAAGMKpYLADMNYVa	Y736	1.1	Y
EPHB2	IYIDPFTpYEDPNEAVa	Y602	1.07	Y
EPHB2	YEKELSEpYNATAIKSa	Y481	0.96	Y
EPHB2	DDTSDPTpYTSALGGKa	Y781	0.85	Y
EPHB2	IKTLKSGpYTEKQRDa	Y659	0.69	Y
EPHB2	TAPEAIQpYRKFTSASa	Y800	0.53	Y
EPHB2	FYLAFQDpYGGCMSLIa	Y181	0.41	Y
EPHB3	LDRTVDPpYTFTTVGa	Y924	3.78	Y
EPHB3	DDPSDPTpYTSALGGKa	Y792	1.46	Y
EPHB3	YTEKLQQpYIAPGMKVa	Y600	1.22	Y
EPHB3	IAPGMKVpYIDPFTYEa	Y608	1.16	Y
EPHB3	TAPEAIpYRKFTSASa	Y812	1.05	Y
EPHB3	KYLSEMNpYVHRDLAAa	Y754	1.01	Y
EPHB3	RHGSSEpYTEKLQQYa	Y593	0.96	Y
EPHB3	VYIDPFTpYEDPNEAVa	Y614	0.66	Y
EPHB4	AKEIDVSpYVKIEEVIa	Y614	3.97	Y
EPHB4	LDQRQPHpYSAFGSVGa	Y906	2.34	Y
EPHB4	YSDKHGQpYLIGHGTKa	Y581	1.86	Y
EPHB4	ENSSDPTpYTSSLGGKa	Y774	1.5	Y
EPHB4	IGHGTVpYIDPFTYEa	Y590	1.43	Y
EPHB4	GGREDLTpYALRCRECa	Y357	1.14	Y
EPHB4	SNGREAEpYSDKHGQYa	Y574	0.99	Y
EPHB4	TGGPAPQpYaaaaaaaa	Y987	0.98	Y
EPHB4	VYIDPFTpYEDPNEAVa	Y596	0.95	Y
EPHB6	AREVDPApYIKIEEVIa	Y669	3.34	Y
EPHB6	YTEQLQQpYSSPGLGVa	Y635	2.76	Y
EPHB6	SPGLGVKpYYIDPSTYa	Y644	1.82	Y
EPHB6	YYIDPSTpYEDPCQAIa	Y651	1.79	Y
EPHB6	PGLGVKYpYIDPSTYEa	Y645	1.68	Y
ERBB2	SPLDSTFpYRSLEDDa	Y1005	1.95	Y
ERBB2	KEILDEApYVMAGVGSa	Y772	1.74	Y
ERBB2	PTAENPEpYGLDVPVa	Y1248	1.69	Y
ERBB2	SGAFGTVpYKGIWIPDa	Y735	1.29	Y
ERBB2	LDIDETE pYHADGGKVa	Y877	0.54	Y
ERBB3	HQAPHVHpYARLKLRLa	Y1307	2.69	Y
ERBB3	SAFDNPDpYWH SRLFPa	Y1328	1.69	Y
ERBB3	RPRGDSApYHSQRHSLa	Y1132	1.54	Y
ERBB4	MARDPQRpYLVIQGDDa	Y984	3.17	Y
ERBB4	PPKAEDepYVNEPLYLa	Y1202	2.04	Y
ERBB4	EYVNEPLpYLNTFANTa	Y1208	1.92	Y
ERBB4	KAFDNPDpYWNHSLPPa	Y1242	1.89	Y
ERBB4	STLQHPDpYLQEYSTKa	Y1258	1.69	Y
ERBB4	HPDYLQEpYSTKYFYKa	Y1262	1.46	Y
ERBB4	QALDNPEpYHNASNGPa	Y1188	1.41	Y
ERBB4	GHSPPPApYTPMSGNQa	Y1056	1.4	Y

ERBB4	SGAFGTV _p YKGIWVPEa	Y733	1.15	Y
ERBB4	GELDEEG _p YMT _p MRDKa	Y1150	0.99	Y
ERBB4	DQNKFLC _p YADTIHWQa	Y157	0.84	Y
ERBB4	RDKPKQE _p YLN _p VEENa	Y1162	0.8	Y
ERBB4	EDSSTQR _p YSADPTVFa	Y1128	0.74	Y
ERBB4	EQGVSV _p YRAPSTIa	Y1081	0.68	Y
ERBB4	MSGNQFV _p YRDGGFAAa	Y1066	0.68	Y
ERBB4	LEGDEKE _p YNADGGKMa	Y875	0.56	Y
FAK1	DRSNDKV _p YENV _p TGLVa	Y925	3.86	Y
FAK1	ALEKKS _n _p YEVLEKDVa	Y194	3.09	Y
FAK1	KPTLNFF _p YQVKSDYa	Y148	2.65	Y
FAK1	KMKLAQQ _p YVMTSLQQa	Y1007	2.05	Y
FAK1	YQVKSD _p YMLEIADQa	Y155	1.69	Y
FAK1	GDFGLSR _p YMEDSTYYa	Y570	1.35	Y
FAK1	RYMEDST _p YYKASKGKa	Y576	0.95	Y
FAK1	YMEDSTY _p YKASKGKLa	Y577	0.76	Y
FAK1	MTSLQQE _p YKKQMLTAa	Y1016	0.33	Y
FAK2	CQLPPEG _p YVVV _p VKNVa	Y906	3.16	Y
FAK2	EGFFGEV _p YEGVYTNHa	Y440	2.72	Y
FAK2	RYIEDED _p YYKASVTRa	Y579	2.24	Y
FAK2	DRTDDL _v _p YLN _p VMELVa	Y881	2.19	Y
FAK2	GDFGLSR _p YIEDEDYYa	Y573	1.76	Y
FAK2	TPEKEV _G _p YLEFTGPPa	Y849	1.75	Y
FAK2	OKOMVED _p YOWLROEEa	Y819	1.65	Y
FAK2	YIEDEDY _p YKASVTRLa	Y580	1.43	Y
FAK2	VCSLSDV _p YQMEKDIAa	Y683	1.27	Y
FAK2	RRPGGPQ _p YGIAREDVa	Y418	1.1	Y
FAK2	KSLDPMV _p YMNDKSPLa	Y834	0.52	Y
FAK2	PKPSRPK _p YRPP _p QTNa	Y722	0.41	Y
FER	LKGIFDE _p YSQITSLVa	Y229	3.59	Y
FER	SHGKPGE _p YVLSVYSDa	Y492	3	Y
FER	KQQVKKS _p YIGVHQQIa	Y114	2.33	Y
FER	TAPEALN _p YGRYSSESa	Y734	1.82	Y
FER	RQEDGGV _p YSSSGLKQa	Y714	1.5	Y
FER	EPPPVVN _p YEE _p DARSVa	Y402	1.35	Y
FER	GEYVLSV _p YSDGQRRHa	Y497	1.34	Y
FER	EAKILKQ _p YDHPNIVKa	Y615	0.94	Y
FES	RIQPEAE _p YQGFLRQYa	Y261	1.56	Y
FES	TAPEALN _p YGRYSSESa	Y734	1.35	Y
FES	REEADGV _p YAASGGLRa	Y713	1.14	Y
FES	EARILKQ _p YSHPNIVRa	Y614	1.08	Y
FES	SAQAKRK _p YQEASKDKa	Y156	0.6	Y
FGFR1	IGPDNLP _p YVQLKTAa	Y307	3.01	Y
FGFR1	IGGYKVR _p YATWSIIMa	Y210	2.55	Y
FGFR1	MLAGVSE _p YELPEDPRa	Y463	2.07	Y

FGFR1	KDLVSCApYOVARGMEa	Y605	1.77	Y
FGFR1	RDIIHIDpYKKTNGa	Y653	1.56	Y
FGFR1	RRPPGLEpYCYNPSHNa	Y583	1.25	Y
FGFR1	DIHHIDYpYKKTNGRa	Y654	1.25	Y
FGFR1	NRMPVApYWTSPEKMa	Y154	1.18	Y
FGFR1	SKGNLREpYLOARRPPa	Y572	1.06	Y
FGFR1	PPGLEyCpYNPSHNPEa	Y585	0.62	Y
FGFR1	SNCTNELpYMMMRDCWa	Y730	0.61	Y
FGFR1	OVARGMEpYLASKKCIa	Y613	0.53	Y
FGFR1	VEFMCKVpYSDPOPHa	Y280	0.51	Y
FGFR2	RRPPGMEpYSYDINRVa	Y586	2.09	Y
FGFR2	PPGMEYSpYDINRVPEa	Y588	1.92	Y
FGFR2	RDINNIDpYKKTNGa	Y656	1.89	Y
FGFR2	DINNIDYpYKKTNGRa	Y657	1.46	Y
FGFR2	KDLVSTpYQLARGMEa	Y608	1.44	Y
FGFR2	OLARGMEpYLASOKCIa	Y616	0.98	Y
FGFR2	ANCTNELpYMMMRDCWa	Y733	0.55	Y
FGFR3	KDLVSCApYQVARGMEa	Y599	1.6	Y
FGFR3	ANCTHDLpYIMMRECWa	Y724	1.57	Y
FGFR3	RDVHNLDpYKKTNGa	Y647	1.37	Y
FGFR3	DVHNLDYpYKKTNGRa	Y648	1.04	Y
FGFR3	RRPPGLDpYSFDTCkPa	Y577	0.73	Y
FGFR3	QVARGMEpYLASQKCIa	Y607	0.62	Y
FGFR4	RGVHHIDpYKKTNSNGa	Y642	1.75	Y
FGFR4	LLAVSEEpYLDLRLTFa	Y754	1.31	Y
FGFR4	GVHHIDYpYKKTNSNGRa	Y643	1.16	Y
FGR	KLDMGGYpYITTRVQFa	Y209	3.04	Y
FGR	RKLDMGGpYITTRVQa	Y208	2.75	Y
FGR	VTLFIAlpYDYEARTEa	Y86	2.01	Y
FGR	SETTKGApYSLIRDWa	Y180	1.87	Y
FGR	LEGDFRSpYGAADHYGa	Y28	1.1	Y
FGR	SYGAADHpYGPDPKAAa	Y34	0.63	Y
FGR	RLIKDDEpYNPCOGSKa	Y412	0.29	Y
FLT3	VSECPHTpYQNRPFsa	Y969	2.29	Y
FLT3	QKGLDNGpYsIsKFCNa	Y401	2.25	Y
FLT3	SIRNTLLpYTLRRPYFa	Y166	2.18	Y
FLT3	FYVDFREpYEYDLKWEa	Y597	2.09	Y
FLT3	HKHQPEpYIFHAENDa	Y416	1.96	Y
FLT3	VDFREYEpYDLKWEFPa	Y599	1.93	Y
FLT3	KEHNFSFpYPTFOSHpa	Y726	1.59	Y
FLT3	DIMSdSNpYVVRGNARa	Y842	1.59	Y
FLT3	KVMNATApYGIKGTGVa	Y630	1.03	Y
FRK	CTLEDPIpYITELMRa	Y303	4.09	Y
FRK	QSQRHGHPYFVALFDYa	Y46	2.77	Y
FRK	KVDNEDIpYESRHEIKa	Y387	2.72	Y

FRK	SSOOLoGpYIPSNYVAa	Y99	2.52	Y
FRK	LNEFVSHpYTKTSDGLa	Y193	2.27	Y
FRK	YFETDSSpYSDANNFla	Y497	2.15	Y
FRK	YFVALFDpYQARTAEa	Y53	1.97	Y
FRK	QGYIPSNpYVAEDRSLa	Y104	1.94	Y
FRK	LVGEHNpYKVADFLa	Y368	1.76	Y
FRK	PAPFDLSpYKTVDQWEa	Y221	1.37	Y
FRK	RHGSLQEpYLNQNDTGSa	Y317	0.95	Y
FRK	DAEKOLLpYSENKTGsa	Y132	0.9	Y
FYN	VVSEEPpYIVTEYMNa	Y339	3.5	Y
FYN	VTLFVALpYDYEARTEa	Y91	2.61	Y
FYN	RKLDNGGpYYITTRAQa	Y213	2.36	Y
FYN	KLDNGGpYYITTRAQFa	Y214	1.96	Y
FYN	SETTKGApYSLsIRDWa	Y185	1.87	Y
FYN	TAPEAALpYGRFTIKSa	Y440	1.24	Y
FYN	RLIEDNEpYTAROGAKa	Y417	0.81	Y
FYN	RLIEDNEpYTAROGAKa	Y420	0.73	Y
HCK	VVTKEIpYIITEFMAa	Y330	3.77	Y
HCK	TLDNGGFpYISPRSTFa	Y209	3.21	Y
HCK	SETTKGSpYSLsVRDYa	Y180	2.39	Y
HCK	LATRKEGpYIPSNYVAa	Y127	1.98	Y
HCK	RVEDNEpYTAREGAKa	Y411	0.98	Y
IGF1R	QGSFGMVpYEGVAKGVa	Y1014	3.55	Y
IGF1R	GLKPWTOpYAVYVKAVa	Y577	3.41	Y
IGF1R	GWKLFYNpYALVIFEMa	Y115	3.19	Y
IGF1R	IRGWKLFpYNYALVIFa	Y113	2.97	Y
IGF1R	GFREVSFPYSEENKLa	Y1280	2.64	Y
IGF1R	PWTQYAVpYVKAVTLTa	Y580	2.47	Y
IGF1R	FGMTRDpYETDYRKa	Y1161	2.08	Y
IGF1R	FREVSFPYSEENKLPa	Y1281	1.5	Y
IGF1R	DIYETDpYRKGGKGLa	Y1166	1.07	Y
IGF1R	NLKDIGLpYNLRNITRa	Y131	1.04	Y
IGF1R	RDIYETDpYRKGGKGa	Y1165	0.88	Y
IGF1R	SFDERQPpYAHMNGGRa	Y1346	0.52	Y
INSR	YLKIRRSpYALVSLSFa	Y401	4.4	Y
INSR	SLGFKRSpYEEHIPYTa	Y1355	2.78	Y
INSR	FGMTRDpYETDYRKa	Y1185	2.58	Y
INSR	QGSFGMVpYEGNARDIa	Y1038	2.03	Y
INSR	YLLFRVpYGLESLKDa	Y94	1.7	Y
INSR	GLRHFTGpYRIELOACa	Y818	1.59	Y
INSR	RDIYETDpYRKGGKGa	Y1189	1.35	Y
INSR	DIYETDpYRKGGKGLa	Y1190	1.11	Y
INSR	SYEEHIPpYTHMNGGKa	Y1361	0.83	Y
INSRR	QGSFGMVpYEGLARGLa	Y994	2.61	Y
INSRR	RDVYETDpYRKGGKGa	Y1145	1.26	Y

INSRR	GLRHFTE _p YRIDIHACa	Y783	1.08	Y
INSRR	DVYETDY _p YRKGGKGLa	Y1146	0.84	Y
ITK	DSRTAGT _p YTVSVFTKa	Y273	3.23	Y
ITK	SPNNLET _p YEWYNKSIa	Y237	3.11	Y
ITK	DRNGHEG _p YVPSSYLVa	Y220	2.97	Y
ITK	RLASTHV _p YQIMNHCWa	Y588	2.18	Y
ITK	VHDNYLL _p YVFAPDREa	Y90	2.07	Y
ITK	RFVLDDQ _p YTSSTGTKa	Y512	1.97	Y
ITK	EGYVPSS _p YLVEKSPNa	Y225	1.68	Y
ITK	GLVTRLR _p YVPCFGRQa	Y336	1.42	Y
ITK	LTKASLApYFEDRHGKa	Y40	0.53	Y
ITK	ALRRNEE _p YCLLDSSEa	Y198	0.49	Y
ITK	NNSLVPK _p YHPNFWMDa	Y120	0.48	Y
ITK	LATGCAQ _p YDPTKNASa	Y146	0.39	Y
JAK1	FVSLVDG _p YFRLTADAa	Y412	4.01	Y
JAK1	AIETDKE _p YYTVKDDRa	Y1034	2.59	Y
JAK1	PNCPDEV _p YQLMRKCWa	Y1125	2.33	Y
JAK1	IETDKEY _p YTVKDDRDa	Y1035	2.2	Y
JAK1	KDISYKR _p YIPETLNKa	Y220	1.94	Y
JAK1	QICKGMD _p YLGSRQYVa	Y993	1.64	Y
JAK1	AQEWQPV _p YPMQSLFa	Y568	0.92	Y
JAK1	YSGTLM _p YKDDEGTSa	Y605	0.68	Y
JAK2	DQTPLA _p YNSISYKTa	Y201	3.65	Y
JAK2	FVSLIDG _p YYRLTADAa	Y372	3.11	Y
JAK2	IRAKIQD _p YHILTRKRa	Y221	2.77	Y
JAK2	NLKLIME _p YLPYGSLRa	Y931	2.55	Y
JAK2	SPKDFNK _p YFLTFAVEa	Y435	2.55	Y
JAK2	LIMEYLP _p YGSLRDYLa	Y934	2.41	Y
JAK2	AIYNSIS _p YKTFLPKCa	Y206	1.81	Y
JAK2	GSVEMCR _p YDPLQDNTa	Y868	1.74	Y
JAK2	VRREVG _p YDYGOLHETEa	Y570	1.72	Y
JAK2	VSLIDG _p YRLTADAHa	Y373	1.72	Y
JAK2	OICKGME _p YLGTKRYIa	Y966	1.57	Y
JAK2	AGNQTGL _p YVLRCSPKa	Y423	1.27	Y
JAK2	DHIKLLQ _p YTSQICKGa	Y956	1.14	Y
JAK2	KFGSLDT _p YLKKNKNCa	Y637	0.96	Y
JAK2	LTADAHH _p YLCKEVAPa	Y382	0.55	Y
JAK3	LPLDKDY _p YVVREPGQa	Y981	3.01	Y
JAK3	LLPLDKD _p YVVREPGa	Y980	2.92	Y
JAK3	DASRLL _p YSSOICKGa	Y929	1.94	Y
JAK3	SLRLVME _p YLPSCGLRa	Y904	1.62	Y
KIT	SESTNH _p YNSLANCSa	Y936	2.81	Y
KIT	DIKNSN _p YVVKGNARa	Y823	2.26	Y
KIT	RSVRIGS _p YIERDVTPa	Y747	2.12	Y
KIT	DHAEAA _p YKNLLHSKa	Y703	1.92	Y

KIT	KVVEATApYGLIKSDAa	Y609	1.64	Y
KIT	EHAPAEMpYDIMKTCWa	Y900	1.33	Y
KIT	VMILTYKpYLQKPMYEa	Y547	0.95	Y
KIT	GTVECKApYNDVGKTSa	Y494	0.5	Y
KIT	FTDKWEDpYPKSENEsa	Y362	0.45	Y
KSYK	ELRLRNYpYYDVVNaaa	Y630	3.04	Y
KSYK	VLLVTQHpYAKISDFGa	Y507	3	Y
KSYK	LRLRNYpYDVVNaaaa	Y631	2.73	Y
KSYK	STVSFNPpYEPELAPWa	Y323	2.61	Y
KSYK	YAPECINpYKFSKsa	Y546	2.52	Y
KSYK	MQQLDNPpYIVRMIGIa	Y431	2.4	Y
KSYK	ALRADENpYYKAQTHGa	Y525	2.33	Y
KSYK	LWQLVEHpYSYKADGLa	Y244	2.25	Y
KSYK	ERELNGTpYAIAGGRTa	Y74	1.92	Y
KSYK	VELRLRNpYYYDVVNaa	Y629	1.83	Y
KSYK	IISRIKSpYSFPKPGHa	Y296	1.53	Y
KSYK	LLRQSRNpYLGGFALSa	Y47	1.5	Y
KSYK	ARDNNGSpYALCLLHEa	Y203	1.28	Y
KSYK	GKWPVKWpYAPECINYa	Y539	1.25	Y
KSYK	LMWEAFSpYQGKPYRGa	Y568	1.23	Y
KSYK	LRADENpYKAQTHGKa	Y526	1.14	Y
KSYK	QVSMGMKpYLEESNFVa	Y484	0.83	Y
KSYK	EIRPKEVpYLDRLKLLTa	Y364	0.75	Y
LCK	NLDNGGFpYISPRITFa	Y192	2.44	Y
LCK	FGEVWMGpYYNGHTKVa	Y263	1.81	Y
LCK	TAPEAINpYGTFTIKSa	Y414	1.7	Y
LCK	GEVWMGYpYNGHTKVAa	Y264	1.68	Y
LCK	DNCPEELpYQLMRLCwa	Y470	1.67	Y
LCK	LHELVRHpYTNASDGLa	Y209	1.66	Y
LCK	EDRPTFDpYLRSVLEda	Y489	1.45	Y
LCK	FTATEGOpYOPOPaaaa	Y505	1.39	Y
LCK	RLIEDNEpYTAREGAKa	Y394	0.68	Y
LMTK1	HCKYREDpYFVTADOLa	Y283	1.99	Y
LMTK1	SRGLNFEpYKWEAGRGa	Y479	0.52	Y
LMTK2	SWPHSAPpYSRFSISPa	Y1468	2.69	Y
LMTK2	PSLQTSKpYFSPPPAa	Y1448	1.6	Y
LMTK2	TAGSQGSpYRDSAYFSa	Y1100	0.95	Y
LMTK3	HSNYKEDpYYLTPERLa	Y296	2.54	Y
LMTK3	LGEIFSDpYTPAQVVVa	Y156	2.06	Y
LMTK3	SNYKEDpYLTPERLWa	Y297	1.75	Y
LYN	HDKLVRLpYAVVTREEa	Y306	3.47	Y
LYN	SLDNGGYpYISPRITFa	Y173	3.38	Y
LYN	VTREEIpYIITEYMAa	Y316	3.34	Y
LYN	SLDNGGYpYISPRITFa	Y194	3.21	Y
LYN	RSLDNGGpYYISPRITa	Y193	3.2	Y

LYN	FGEVWVGpYYNNSTKV _a	Y265	2.78	Y
LYN	LLYEIVTpYGKIPYPG _a	Y439	2.68	Y
LYN	GEVWVGpYpYYNNSTKV _{Aa}	Y266	2.11	Y
LYN	EGFIPSNpYVAKLNTL _a	Y117	1.63	Y
LYN	ENCPDELpYDIMKMCW _a	Y473	1.41	Y
LYN	RVIEDNEpYTAREGAK _a	Y397	1.09	Y
LYN	PIYIIEpYMAKGSLL _a	Y321	0.83	Y
LYN	RVIEDNEpYTAREGAK _a	Y376	0.79	Y
LYN	MTALSOGpYRMPRVEN _a	Y460	0.74	Y
MERTK	KKIYSGDpYRQGRIA _a	Y753	2.05	Y
MERTK	FGLSKIpYSGDYRQ _a	Y749	1.78	Y
MERTK	DSELVVNpYIAKKSFC _a	Y549	1.39	Y
MERTK	KIYSGDYpYRQGRIA _{Ka}	Y754	1.23	Y
MET	YREDPIVpYEIHPKTS _a	Y745	2.83	Y
MET	RDMYDKEpYYSVHNKT _a	Y1234	2.59	Y
MET	DMYDKEYpYYSVHNKTG _a	Y1235	2.56	Y
MET	EYCPDPLpYEVMLKCW _a	Y1313	2.41	Y
MET	RGHFGCVpYHGTLLDN _a	Y1093	1.96	Y
MET	NTFDITVpYLLQGRRL _a	Y1295	1.28	Y
MET	VSNESVDpYRATFPED _a	Y1003	0.98	Y
MET	SPLVVLpYMKHGDLR _a	Y1159	0.79	Y
MET	RRLQPEpYCPDPLYE _a	Y1307	0.66	Y
MUSK	RNIYSADpYKANEND _a	Y755	2.57	Y
MUSK	RLHPNPMpYORMPLLL _a	Y554	1.83	Y
MUSK	FGLSRNIpYASADYYK _{Aa}	Y751	1.65	Y
MUSK	YPRNNIEpYVRDIGEG _a	Y577	1.63	Y
MUSK	NIYSADYpYKANEND _{Aa}	Y756	1.49	Y
NTRK1	TYGQWPpYQLSNTE _{Aa}	Y729	2.79	Y
NTRK1	RDIYSTDpYRVRGGRT _a	Y674	2.67	Y
NTRK1	RDIYSTDpYRVRGGRT _a	Y680	2.49	Y
NTRK1	DIYSTDYpYRVRGGRT _{Ma}	Y675	2.38	Y
NTRK1	DIYSTDYpYRVRGGRT _{Ma}	Y681	2.22	Y
NTRK1	FGMSRDIpYSTDYRV _a	Y676	1.93	Y
NTRK1	RACPPEVpYAIMRGCW _a	Y757	1.64	Y
NTRK1	RACPPEVpYAIMRGCW _a	Y751	1.57	Y
NTRK1	RACPPEVpYAIMRGCW _a	Y721	1.33	Y
NTRK1	PLLMVFEpYMRHGDLN _a	Y591	1.08	Y
NTRK1	LAQAPPVpYLDVLG _{aaa}	Y791	0.93	Y
NTRK1	MPPESiLpYRKFTTES _a	Y701	0.76	Y
NTRK2	RDVYSTDpYRVRGGHT _a	Y706	2.4	Y
NTRK2	FGMSRDVpYSTDYRV _a	Y702	1.89	Y
NTRK2	DVYSTDYpYRVRGGHT _{Ma}	Y707	1.86	Y
NTRK2	LAKASPVpYLDILG _{aaa}	Y817	1.33	Y
NTRK2	KVFLAECpYNLCPEQD _a	Y558	0.59	Y
NTRK3	RDVYSTDpYYRFLNPS _a	Y709	3.63	Y

NTRK3	AKNPHLR _p YINLSSNR _a	Y131	2.8	Y
NTRK3	DVYSTDY _p YRLFNPSG _a	Y710	2.72	Y
NTRK3	FGMSRDV _p YSTDY _p YRL _a	Y705	2.24	Y
NTRK3	YVEDVNV _p YFSKGRHG _a	Y604	2.09	Y
NTRK3	KPLNHGI _p YVEDVNV _a	Y597	1.7	Y
NTRK3	RVCPKEV _p YDVMLGCW _a	Y800	1.15	Y
NTRK3	PVIENPQ _p YFRQGHNC _a	Y516	1.13	Y
NTRK3	KVFLAEC _p YNLSPTK _D _a	Y558	1.12	Y
PDGFRA	ADESTRS _p YVILSFEN _a	Y720	3.2	Y
PDGFRA	RVDSDNA _p YIGVTYK _N _a	Y988	2.9	Y
PDGFRA	DHATSEV _p YEIMVKCW _a	Y926	2.01	Y
PDGFRA	PEKRPSF _p YHLSEIVE _a	Y944	1.49	Y
PDGFRA	DIMHDSN _p YVSKGSTF _a	Y849	1.39	Y
PDGFRA	KQADTTQ _p YVPMLEK _a	Y742	1.2	Y
PDGFRA	SDIQRSL _p YDRPAS _Y _K _a	Y762	1.16	Y
PDGFRA	KVVEGT _A _p YGLSRSOP _a	Y613	1.05	Y
PDGFRA	NAYIGVT _p YKNEEDK _L _a	Y993	0.82	Y
PDGFRA	ERKEVSK _p YSDIQRSL _a	Y754	0.79	Y
PDGFRA	ENLLPGQ _p YKKS _Y _E _K _I _a	Y958	0.75	Y
PDGFRA	SFENNGD _p YMDMKQAD _a	Y731	0.38	Y
PDGFRA	LYDRPAS _p YKKK _S _M _L _D _a	Y768	0.34	Y
PDGFRB	CTKGGPI _p YIITEYCR _a	Y678	2.75	Y
PDGFRB	AHASDEI _p YEIMQKCW _a	Y934	2.16	Y
PDGFRB	IITEYCR _p YGDLDV _D _L _a	Y686	2.15	Y
PDGFRB	DIMRDSN _p YISKGSTF _a	Y857	1.61	Y
PDGFRB	GEGYKKK _p YQQVDEEF _a	Y970	1.59	Y
PDGFRB	SKDESVD _p YVPM _L _D _M _K _a	Y751	1.5	Y
PDGFRB	PIYIITE _p YCRYGDL _V _a	Y683	1.42	Y
PDGFRB	RYGDLVD _p YLHRNKHT _a	Y692	1.39	Y
PTK6	SEKPSAD _p YVLSVRD _T _a	Y114	3.08	Y
PTK6	RLSSFTS _p YENPT _a _a _a _a	Y447	1.64	Y
PTK6	RLIKEDV _p YLSHDHN _I _a	Y342	1.23	Y
PTK6	SHDHNIP _p YKWTAPE _A _a	Y351	0.58	Y
PTK7	CREAEPH _p YMVLEYV _D _a	Y872	2.6	Y
PTK7	KDVYNSE _p YYHFRQAW _a	Y960	1.69	Y
PTK7	PHYMVLE _p YVDLGD _L _K _a	Y877	1.1	Y
RET	HLKGRAG _p YTTVAVK _M _a	Y752	3.08	Y
RET	RYPNDSV _p YANWMLSP _a	Y1096	2.77	Y
RET	PLLLIVE _p YAKYGSL _R _a	Y806	2.21	Y
RET	FGLSRDV _p YEEDSYV _K _a	Y900	2.14	Y
RET	TWIENKL _p YGRISHAF _a	Y1062	1.82	Y
RET	DVYEEDS _p YVKRSQGR _a	Y905	1.38	Y
RET	TNTGFPR _p YPNDSV _Y _A _a	Y1090	1.19	Y
RET	AQAFPV _S _p YSSSGARR _a	Y687	1.15	Y
RET	SRKVGPG _p YLGSGGS _R _a	Y826	0.98	Y

RET	DNCSEEMpYRLMLOCWa	Y981	0.84	Y
RET	HPHVIKLpYGACSDGg	Y791	0.36	Y
RON	RDILDREpYYSVQQRHa	Y1238	3	Y
RON	DILDREYpYYSVQQRHa	Y1239	2.94	Y
RON	GVVYHGEpYIDQAQNRa	Y1101	1.69	Y
RON	QVARSMEpYLAEQKFVa	Y1198	1.15	Y
ROR1	REIYSADpYYRVQSKSa	Y645	2.52	Y
ROR2	EVYAADYpYKLLGNSLa	Y646	2.98	Y
ROR2	ATRNVLVpYDKLNVKIa	Y624	1.94	Y
ROR2	MAPEAIMpYGKFSIDSa	Y666	0.94	Y
ROS1	KYIIQWKpYAQLLGSWa	Y135	2.36	Y
ROS1	KNREGLNpYMVLAATECa	Y2274	2.28	Y
ROS1	QLLGSWTpYTKTVSRPa	Y144	2.05	Y
ROS1	DISKGCvpYLERMHFa	Y2069	1.56	Y
ROS1	GKPEGLNpYACLTHSGa	Y2334	1.27	Y
ROS1	IOIAVKNpYYSDDPLEHa	Y1535	1.15	Y
RYK	RDLFPMDpYHCLGDNEa	Y492	0.42	Y
SRC	KLDSGGFpYITSRTQFa	Y216	3.19	Y
SRC	VVSEEPpYIVTEYMSa	Y338	2.87	Y
SRC	VTTFVALpYDYESRTEa	Y93	2.56	Y
SRC	AYVERMNpYVHRDLRAa	Y385	2.16	Y
SRC	TAPEAALpYGRFTIKSa	Y439	1.2	Y
SRC	SETTKGApYCLSVSDFa	Y187	1.02	Y
SRC	RLIEDNEpYTAROGAKa	Y419	0.74	Y
SRMS	RLLKDDIpYSPSSSKa	Y380	1.77	Y
STYK1	MTMDGLLpYDLTEKQVa	Y221	1.61	Y
TEC	RLERQEpYLILEKNDa	Y206	3.53	Y
TEC	DKYGNEGpYIPSNYVTa	Y228	2.89	Y
TEC	WWRARDKpYGNEGYIPa	Y223	2.84	Y
TEC	PTTAGFSpYWEINPa	Y360	2.24	Y
TEC	KSNLDOpYEWYCRNMa	Y245	2.12	Y
TEC	EGYIPSNpYVTGKKSNa	Y233	2.05	Y
TEC	RYVLDDOpYTSSGAKa	Y519	1.6	Y
TEC	VHDANTLpYIFAPSPQa	Y90	1.58	Y
TEC	GLVTRLRpYPVSVKGGKa	Y343	1.03	Y
TEC	KFWTDGSpYQCCRQTEa	Y130	0.31	Y
TIE2	TYVNTTLpYEEKFTYAGa	Y1108	3.25	Y
TIE2	CEHRGYLpYLAIEYAPa	Y899	3.22	Y
TIE2	MLEERKTPYVNTTLYEa	Y1102	2.91	Y
TIE2	GACEHRGpYLYLAIEYa	Y897	2.76	Y
TIE2	TYEKFTpYAGIDCSAa	Y1113	2.1	Y
TIE2	NILVGENpYVAKIADFa	Y976	1.49	Y
TIE2	KNATITQpYQLKGLEPa	Y697	1.3	Y
TIE2	LSRQGEVpYVKKTMGRa	Y992	1.08	Y
TIE2	NNPDPTIpYPVLDWNDa	Y816	0.62	Y

TIE1	MAIESLNpYSVYTTKSa	Y1027	3.5	Y
TIE1	GACKNRGpYLYIAIEYa	Y912	3.24	Y
TIE1	RNCDEVPYELMRQCWa	Y1083	2.35	Y
TIE1	ESLNYSVpYTTKSDVWa	Y1030	1.8	Y
TIE1	LSRGEEVpYVKKTMGRA	Y1007	1.04	Y
TNK1	DLSAASRpYVLARPa	Y656	2.96	Y
TNK1	DLSAASRpYVLARPa	Y661	2.61	Y
TNK1	LGGARGRpYVMGGPRPa	Y277	1.94	Y
TNK1	PLCSRALpYSLALRCWa	Y353	1.43	Y
TNK1	CWRILEHpYQWDLAAa	Y651	1.19	Y
TNK1	QLAGAMApYLGARGLVa	Y235	1.11	Y
TNK1	GGPRPIpYAWCAPESa	Y287	0.34	Y
TXK	RYVLDDEpYVSSFGAKa	Y420	2.28	Y
TXK	KIQVKALpYDFLPREPa	Y91	2.12	Y
TYK2	PSEKEHFpYQRQHRLPa	Y827	2.98	Y
TYK2	FVSLVDGpYFRLTADSa	Y423	2.96	Y
TYK2	AVPEGHEpYYRVREDGa	Y1054	2.74	Y
TYK2	QGTRTNVpYEGRLRVEa	Y604	2.62	Y
TYK2	VPEGHEpYRVREDGDa	Y1055	2.04	Y
TYK2	QAEGEPcYIRDsgVAa	Y292	1.45	Y
TYK2	DKCPCVEpYHLMKNCWa	Y1145	1.21	Y
TYK2	LTADSSHpYLCHEVAPa	Y433	0.79	Y
TYRO3	FGLSRKIpYSGDYRQa	Y681	1.52	Y
TYRO3	RKIYSGDpYYROGCASa	Y685	1.41	Y
TYRO3	KIYSGDYpYRQGCASKa	Y686	1.2	Y
UFO	GVENSEIpYDYLRQGNa	Y759	3.13	Y
UFO	EVHPAGRpYVLCPSTTa	Y866	2.55	Y
UFO	DLHSFLpYSRLGDQPa	Y634	1.74	Y
UFO	KKIYNGDpYYRQGRIa	Y702	1.68	Y
UFO	ADCLDGLpYALMSRCWa	Y779	1.6	Y
UFO	RRKKETRpYGEVFEPTa	Y481	1.22	Y
UFO	RLGDQVPpYLPQMLVa	Y643	1.13	Y
UFO	KIYNGDYpYROGRIAKa	Y703	1.12	Y
UFO	FGLSKKIpYNGDYRQa	Y698	1.08	Y
VEGFR1	ARYLTRGpYSLIIKDVa	Y388	3.71	Y
VEGFR1	GSSDDVRpYVNAFKFMa	Y1213	3.52	Y
VEGFR1	SSEIKTDpYLSIIMDPa	Y794	2.53	Y
VEGFR1	CCSPPPDpYNSVVLYSa	Y1327	2.38	Y
VEGFR1	GSVESSApYLTVQGTsa	Y745	2.12	Y
VEGFR1	VIVEYCKpYGNLSNYLa	Y914	2.11	Y
VEGFR1	DYNSVVLpYSTPPIaaa	Y1333	1.93	Y
VEGFR1	EKKRRFTpYDHAELERa	Y1309	1.91	Y
VEGFR1	PLMVIVEpYCKYGNLSa	Y911	1.53	Y
VEGFR1	KYGNLSNpYLSKRDLa	Y920	1.12	Y
VEGFR1	DIYKNPDpYVRKGDTRa	Y1053	0.97	Y

VEGFR1	EOCERLPpYDASKWEFa	Y815	0.82	Y
VEGFR2	GGELKKTGpYLSIVMDPa	Y801	2.46	Y
VEGFR2	RFRQGGKpYVGAIPVDa	Y951	2.14	Y
VEGFR2	VCDPKFHpYDNTAGISa	Y1214	2.07	Y
VEGFR2	DIYKDPDpYVRKGDARa	Y1059	1.11	Y
VEGFR2	NTAGISQpYLQNSKRKa	Y1223	0.85	Y
VEGFR2	EEAPEDLpYKDFLTLEa	Y996	0.73	Y
VEGFR3	RHSLAARpYYNWVSFPa	Y1230	2.49	Y
VEGFR3	HSLAARYpYNNWVSFGa	Y1231	2.48	Y
VEGFR3	DIYKDPDpYVRKGSARa	Y1068	1.36	Y
VEGFR3	HLGRVLGpYGAFGKVVa	Y853	1.33	Y
VEGFR3	FPMTPTTpYKGSVDNQa	Y1265	0.4	Y
VEGFR3	NANVSAMpYKCVVSNKa	Y532	0.35	Y
YES1	HDKLVPLpYAVVSEEPa	Y336	3.79	Y
YES1	VVSEEPpYIVTEFMSa	Y345	3.55	Y
YES1	RKLDNGGpYYITTRA0a	Y222	3.46	Y
YES1	KLDNGGYpYITTRAQFa	Y223	2.67	Y
YES1	SETTKGApYSLSIRDWa	Y194	1.95	Y
YES1	TAPEAALpYGRFTIKSa	Y446	1.39	Y
YES1	RLIEDNEpYTARQGAKa	Y426	0.96	Y
ZAP70	LIYGKTVpYHYLISQDa	Y209	3.97	Y
ZAP70	PRKEQGTpYALSLIYGa	Y198	3.63	Y
ZAP70	YGKTVYHpY LISQDKAa	Y211	3.58	Y
ZAP70	MHOLDNpYIVRLIGVa	Y397	3.34	Y
ZAP70	EQRMRACpY YSLASKVa	Y597	3.32	Y
ZAP70	QRMRACTpY YSLASKVEa	Y598	2.95	Y
ZAP70	CLRSLGGpYVLSLVHDa	Y46	2.62	Y
ZAP70	ALGADDSpYYTARSAGa	Y492	2.55	Y
ZAP70	AHERMPWpYHSSLTREa	Y164	2.52	Y
ZAP70	TYALSLIpYGKTVYHYa	Y204	2.17	Y
ZAP70	EROLNGTpYAIAGGKAa	Y69	2.12	Y
ZAP70	EEAERKLpYSGAQTDGa	Y178	1.78	Y
ZAP70	PAELCEFPYSRDPDGLa	Y87	1.57	Y
ZAP70	DTLNSDGpYTPEPARIa	Y292	1.43	Y
ZAP70	PECPPELpYALMSDCWa	Y569	1.22	Y
ZAP70	LGADDSYpYTARSAGKa	Y493	0.88	Y
ZAP70	GKWPLKWpYAPECINFa	Y506	0.62	Y
ZAP70	TMWEALSpYQKPYKKa	Y535	0.54	Y
ZAP70	SQDKAGKpYCIPEGTKa	Y221	0.52	Y
ZAP70	LKADGLIpYCLKEACP a	Y248	0.28	Y
ABL1	PNLFVALpYDFVASGDa	Y70	1.92	N
ABL1	KRNKPTVpYGVSPNYDa	Y245	1.76	N
ABL1	TASDGKLpYVSSSRFa	Y204	1.76	N
ABL1	HKLGGGQpYGEVYEGVa	Y272	1.58	N
ABL1	LRYEGRVpYHYRINTAa	Y172	1.48	N

ABL1	YEGRVYH _p YRINTASDa	Y174	1.42	N
ABL1	QRSISLR _p YEGRVYHYa	Y167	1.27	N
ABL1	EGCPEKV _p YELMRACWa	Y488	1.15	N
ABL1	YELLEKD _p YRMERPEGa	Y456	0.97	N
ABL1	GLITTLH _p YPAPKRNKa	Y215	0.47	N
ABL2	PNL _p FVAL _p YDFVASGDa	Y80	3.21	N
ABL2	ENQPHKK _p YELTGNFSa	Y683	2.41	N
ABL2	LRYEGRV _p YHYRINTTa	Y218	2.32	N
ABL2	PNL _p FVAL _p YDFVASGDa	Y116	1.9	N
ABL2	QLSISLR _p YEGRVYHYa	Y213	1.57	N
ABL2	NLVPPKC _p YGG _p SFAQRa	Y682	1.29	N
ABL2	HEALHRP _p YGCDVEPQa	Y59	0.79	N
ABL2	PEALHRP _p YGCDVEPQa	Y80	0.5	N
ABL2	GLV _p TTLH _p YPAPKC _p NKa	Y261	0.35	N
ACK1	KVSS _p THY _p YLLPERPSa	Y938	2.88	N
ACK1	SFASDPK _p YATPOVIOa	Y905	2.28	N
ACK1	RPSYLER _p YQRFLEAa	Y872	2.02	N
ACK1	LPQND _p DH _p YVMQEHRKa	Y347	1.29	N
ACK1	FFTQK _p PT _p YDPVSEDQa	Y596	1.13	N
ACK1	PLPPP _p A _p YDDVAQDEa	Y635	0.66	N
ALK	CGNV _p NYG _p YQQGLPLa	Y1586	1.98	N
ALK	TAPGAGH _p YEDTILKSa	Y1604	1.84	N
ALK	HGAFGEV _p YEGQVSGMa	Y1131	1.77	N
ALK	FPCGNV _p NYGYOOGLa	Y1584	1.58	N
ALK	NTALPIE _p YGLVEEEa	Y1401	1.35	N
ALK	RDIYRAS _p Y _p YRKG _p GCAa	Y1282	0.92	N
ALK	FGMARD _p YRAS _p Y _p YRKa	Y1278	0.64	N
ALK	DIYRAS _p Y _p YRKG _p GCAa	Y1283	0.55	N
BLK	QSVLEDF _p YTATERQYa	Y494	1.4	N
BTK	DKNGQEG _p YIPSN _p YVTa	Y263	1.75	N
BTK	AEDSIEM _p YEWY _p SKHMa	Y279	1.59	N
BTK	TIPELIN _p YHQHNSAGa	Y361	1.46	N
CSF1R	ESYEGNS _p YTFIDPTOa	Y561	3.62	N
CSF1R	RWKIIES _p YEGNS _p YTFa	Y556	2.38	N
CSF1R	IDPTQLP _p YNEKWEFPa	Y571	1.48	N
CSF1R	KYKQKPK _p YQVRWKIIa	Y546	1.3	N
CSF1R	SSQGVDT _p YVEMRPV _p Sa	Y723	1.01	N
CSF1R	PLLQPNN _p YQFCaaaa	Y969	0.97	N
CSF1R	NIHLEKK _p YVRRDSGFa	Y708	0.44	N
DDR1	LLLSNPA _p YRLLLATY _p a	Y513	1.33	N
DDR1	AQGPTIS _p YPMLLHV _p Aa	Y740	0.87	N
DDR1	PLCMITD _p YMENGDLNa	Y703	0.74	N
DDR2	GPEGVPH _p YAEADIVNa	Y521	1.82	N
EGFR	MTFGSKP _p YDGIPASEa	Y915	1.83	N
EGFR	TAVGNPE _p YLNTVQPTa	Y1138	1.37	N

EGFR	DVVDADE _p YLIPOOGFa	Y1016	1.34	N
EGFR	PFGCLLD _p YVREHKDNa	Y801	1.31	N
EGFR	TFLPVPE _p YINQSVPKa	Y1092	1.27	N
EGFR	ESILHRI _p YTHQSDVWa	Y891	0.91	N
EGFR	EDSFLQR _p YSSDPTGAa	Y1069	0.67	N
EGFR	APSRDPH _p YQDPHSTAa	Y1125	0.67	N
EPHA1	ESIRMKR _p YILHFHSAa	Y930	2.96	N
EPHA1	DKLWLK _p YVDLQAYEa	Y599	1.95	N
EPHA1	PYVDLOA _p YEDPAOGAa	Y605	1.19	N
EPHA2	NDMPHYM _p YVVCNVMSa	Y67	0.88	N
EPHA3	ILLTVV _p YVLIGRFCa	Y561	2.29	N
EPHA3	LIGRFCG _p YKSKHGADa	Y570	0.61	N
EPHA4	QAIKMDR _p YKDNFTAAa	Y928	0.85	N
EPHA5	EAIKMGR _p YTEIFMENA	Y982	1.89	N
EPHA6	PFQVTKL _p YWLNEKWDa	Y12	0.71	N
EPHA6	DSIKMGO _p YKNNFVAa	Y978	0.66	N
EPHA7	QAIKMER _p YKDNFTAAa	Y940	0.66	N
EPHA7	ALVSVKV _p YYKCCWSIa	Y201	0.52	N
EPHA7	LVSVKV _p YKCCWSIIa	Y202	0.52	N
EPHA8	LAYGERP _p YWNMTNRDa	Y839	1.87	N
EPHA8	LEYEIKY _p YEKDKEMQa	Y478	1.34	N
EPHB1	SAIKMVQ _p YRDSFLTAa	Y928	0.37	N
EPHB2	EAIKMGQ _p YKESFANAa	Y930	0.47	N
EPHB2	EAIKMGQ _p YKESFANAa	Y931	0.47	N
EPHB2	LIAVRVF _p YRKCPRIIa	Y194	0.43	N
EPHB4	RAIKMGR _p YEEESFAAAa	Y924	2.36	N
ERBB2	MTFGAKP _p YDGIPAREa	Y923	1.88	N
ERBB2	TCSQPE _p YVNPQDVRa	Y1139	1.36	N
ERBB2	GAVENPE _p YLTPOGGAA	Y1196	1.35	N
ERBB2	DLVDAEE _p YLVPPQGFa	Y1023	1.3	N
ERBB2	SPAFDNL _p YWDODPPa	Y1221	1.26	N
ERBB2	LPSETDG _p YVAPLTCsa	Y1127	1.22	N
ERBB2	DPSPLOR _p YSEDPTVPa	Y1112	0.61	N
ERBB2	PAFDNLY _p YWDQDPPEa	Y1222	0.4	N
ERBB3	SSLEELG _p YEYMDVGSa	Y1222	3.09	N
ERBB3	EEEDVNG _p YVMPDTHLa	Y1159	2.72	N
ERBB3	GTTPEDED _p YEYMNQRa	Y1260	2.51	N
ERBB3	EEDEDEE _p YEYMNRRRa	Y1197	2.19	N
ERBB3	CPASEQG _p YEEMRAFQa	Y1289	2.05	N
ERBB3	PDDKOLL _p YSEAKTPIa	Y868	1.83	N
ERBB3	TPDEDYE _p YMNQRDGA	Y1262	1.43	N
ERBB3	DEDEEYE _p YMNRRRRHa	Y1199	1.39	N
ERBB3	NKRAMRR _p YLERGESIa	Y680	1.37	N
ERBB3	GGPGGD _p YAAMGACPa	Y1276	0.86	N
ERBB3	LLSPSSG _p YMPMNQGNa	Y1054	0.71	N

ERBB4	DMMDAEEpYLVPOAFNa	Y1022	3.07	N
ERBB4	FNIPPIpYTSRARIDa	Y1035	2.08	N
ERBB4	IVAENPEpYLSEFSLKa	Y1284	1.34	N
ERBB4	LQEYSTKpYFYKQNGRa	Y1266	1.01	N
ERBB4	NTLGKAEpYLNKNNLSa	Y1221	0.86	N
ERBB4	EYSTKYFpYKQNGRIRa	Y1268	0.8	N
ERBB4	TVLPPPpYRHRNTVVa	Y1301	0.78	N
FAK1	HMVQTNHpYQVSGYPGa	Y742	3.09	N
FAK1	SVSETDDpYAEIIDEEa	Y397	2.63	N
FAK1	PIGNQHIpYQPVGKPDa	Y883	2.5	N
FAK1	PIGNQHIpYQPVGKPDa	Y861	2.44	N
FAK1	SVSETDDpYAEIIDEEa	Y419	2.32	N
FAK1	PIGNQHIpYQPVGKPGa	Y861	2.25	N
FAK1	IIDEEDTpYTMPSTRDa	Y429	1.63	N
FAK1	IIDEEDTpYTMPSTRDa	Y407	1.52	N
FAK1	GDVHOGIpYMSPENPAa	Y441	1.15	N
FAK1	aaaMAAApYLDPNLNHa	Y5	1.06	N
FAK1	RYMEDSTpYKASKGKa	Y598	1.04	N
FAK1	YMEDSTpYKASKGKLa	Y599	1.01	N
FAK1	LSSPADSpYNEGVKLQa	Y898	0.96	N
FAK1	MADLIDGpYCRLVNGTa	Y347	0.91	N
FAK1	PKPSRPGpYSPRSSEa	Y720	0.75	N
FAK1	TAMAGSIpYPGQASLLa	Y761	0.59	N
FAK2	CSIESDIpYAEIPDETa	Y402	3.68	N
FAK2	EQERNARpYRTPKILEa	Y699	1.66	N
FAK2	TLTSPMEpYSPVNSLa	Y756	0.67	N
FER	AQLHQNQpYYDITLPLa	Y199	2.91	N
FER	QLHQNQpYYDITLPLLa	Y200	2.64	N
FER	PLAEQDWpYHGAIPIRa	Y461	1.9	N
FES	RPSFSTIpYQELQSIRa	Y811	1.96	N
FGFR1	LSMPLDOpYSPSPDTPa	Y776	1.43	N
FGFR1	EALFDRIpYTHQSDVWa	Y677	1.27	N
FGFR1	ALTSNOEpYLDLSMPLa	Y766	1.17	N
FGFR1	FTLGGSpYPGVPVEEa	Y701	0.52	N
FGFR2	MLAGVSEpYELPEDPKa	Y466	2.01	N
FGFR2	LSQPLEQpYSPSPDTPa	Y779	1.6	N
FGFR2	TLTTNEEpYLDLSQPLa	Y769	1.17	N
FGFR2	FSPDMPpYEPCLPQYa	Y805	0.91	N
FGFR2	YEPCLQpYPHINGSVa	Y812	0.74	N
FGFR2	LEOYSPSpYDPTRSSCa	Y783	0.5	N
FGFR3	RDVHNLDPYKKTNGa	Y535	1.72	N
FGFR3	TVTSTDEpYLDLSAPFa	Y760	1.34	N
FGFR3	DVHNLDPYKKTNGRa	Y536	1.33	N
FGFR3	LSAPFEQpYSPGGQDTa	Y770	1.3	N
FGFR3	ANCTHDLpYMIMRECWa	Y612	1.21	N

FGFR3	LSAPFEOpYSPGGODTa	Y658	0.96	N
FGFR3	RRPPGLDpYSFDTCKPa	Y465	0.57	N
FGR	HDKLVQLpYAVVSEEPa	Y322	3.88	N
FGR	VVSEEPpYIVTEFMCa	Y331	3.35	N
FGR	PGCPASLpYEAMEQTWa	Y488	1.21	N
FGR	LEQVEQGpYHMPCPPGa	Y475	0.44	N
FGR	FTSAEPQpYQPGDQTaa	Y523	0.4	N
FLT3	KYKKQFRpYESQLQMVa	Y572	3.58	N
FLT3	TGSSDNEpYFYVDFREa	Y589	3.37	N
FLT3	ADAEAMpYQNVDGRVa	Y955	2.58	N
FLT3	SSDNEYFpYVDFREYEa	Y591	2.55	N
FLT3	HSEDEIEpYENQKREa	Y768	1.71	N
FLT3	EDLLCFApYQVAKGMEa	Y793	1.41	N
FYN	TDPTQHpYPSFGVTSa	Y39	1.89	N
FYN	SLNQSSGpYRYGTDPTa	Y28	1.27	N
FYN	NOSSGYRpYGTDPPTPa	Y30	1.07	N
FYN	FTATEPQpYQPGENLaa	Y528	1.03	N
FYN	FTATEPQpYQPGENLaa	Y531	1.01	N
FYN	LEQVERGpYRMPCQDa	Y483	0.32	N
HCK	IVVALYDpYEAHHEDa	Y89	4.89	N
HCK	QSVLDDFpYTATESQYa	Y515	2.63	N
HCK	YTATESQpYQQPaaaa	Y522	1.94	N
HCK	ASPHCPVpYVPDPTSTa	Y51	0.99	N
IGF1R	RLGNGVLpYASVNPEYa	Y973	2.34	N
IGF1R	YASVNPEpYFSAADVYa	Y980	1.83	N
INSR	YASSNPEpYLSASDVFa	Y987	2.87	N
INSR	DGPLGLpYASSNPEYa	Y992	2.5	N
INSR	YASSNPEpYLSASDVFa	Y999	1.74	N
INSR	EIADGMApYLNAKKFVa	Y1149	1.12	N
ITK	ETVVIAlpYDYQTNDPa	Y180	2.04	N
ITK	PVTAGLRpYGKWVIDPa	Y353	1.31	N
ITK	VVIALYDpYQTNDPQEa	Y182	1.18	N
JAK1	aaaaaMOpYLNKEDCa	Y3	2.19	N
JAK1	ELPKDISpYKRYIPETa	Y217	1.92	N
JAK1	PSGSLKEpYLPKNKNKa	Y967	0.57	N
JAK2	NSLFTPDpYELLTENDa	Y813	3.18	N
JAK2	VLPQDKEpYKVKKEPGa	Y1007	2.58	N
JAK2	LINNCMDpYEPDFRPSa	Y790	1.89	N
JAK2	EYLGTKRpYIHRDLATa	Y972	1.5	N
JAK2	VLYRIRFpYFPRWYCSa	Y119	1.47	N
JAK2	LPQDKEYpYKVKKEPGEa	Y1008	1	N
JAK2	PYGSLRDpYLQKHKERA	Y940	0.83	N
JAK3	NSLISSDpYELLSDPa	Y785	3.9	N
JAK3	LVQPOSQpYQLSQMTFa	Y506	2.77	N
JAK3	QICKGMEpYLGSRRCVa	Y939	0.93	N

JAK3	HGSFTKI _p YRGCHEV _a	Y536	0.48	N
KIT	EEINGNN _p YVYIDPTQ _a	Y568	2.85	N
KIT	DMKPGV _S _p YVVPTKAD _a	Y730	2.72	N
KIT	INGNNY _V _p YIDPTQLP _a	Y570	2.17	N
KIT	KYLQKPM _p YEVQWKV _V _a	Y553	1.76	N
KIT	IIVMLT _p YKYLQKPM _a	Y545	1.57	N
KIT	IDPTQLP _p YDHKWEFP _a	Y578	0.78	N
KIT	CSDSTNE _p YMDMKPGV _a	Y721	0.44	N
KSYK	LPMDTEV _p YESPYADP _a	Y348	3.01	N
KSYK	KENLIRE _p YVKQTWNL _a	Y131	1.76	N
KSYK	SPADLCH _p YHSQESDG _a	Y91	1.64	N
KSYK	TREEAED _p YLVQGGMS _a	Y28	1.37	N
KSYK	TEVYESP _p YADPEEIR _a	Y352	0.73	N
LCK	HQRLVRL _p YAVVTQEP _a	Y304	3.38	N
LCK	VVTQEP _p YIITEYME _a	Y313	3	N
LCK	VRDPLV _T _p YEGSNPPA _a	Y51	1.39	N
LCK	DVCENCH _p YPIVPLDG _a	Y25	1.11	N
LCK	QGEVVKH _p YKIRNLDN _a	Y181	0.89	N
LCK	IQNLERG _p YRMVRPDN _a	Y457	0.77	N
LMTK2	HLDEGLS _p YTSIFYPV _a	Y500	2.8	N
LMTK2	SQGLSFE _p YVWEAAKH _a	Y476	1.62	N
LTK	RDIYRAS _p YRRGRDRA _a	Y676	1.56	N
LTK	FGMARDI _p YRASYYRR _a	Y672	1.46	N
LTK	DIYRAS _p YRRGDRAL _a	Y677	1.24	N
LYN	QSVLDDF _p YTATEGQY _a	Y501	3.25	N
LYN	YTATEGQ _p YQQQPaaaa	Y508	2.02	N
LYN	YTATEGQ _p YQQQPaaaa	Y487	2.01	N
LYN	EERPTFD _p YLQSVLDD _a	Y492	1.36	N
LYN	RNTERTI _p YVRDPTSN _a	Y32	0.75	N
MATK	ACENKSW _p YRVKHHTS _a	Y87	1.16	N
MERTK	RNOADV _I _p YVNTOLLE _a	Y872	3.3	N
MERTK	SKPHEGR _p YILNGGSE _a	Y929	2.19	N
MET	YVHVNAT _p YVNVKCV _A _a	Y1356	3.66	N
MET	STFIGEH _p YVHVNATY _a	Y1349	2.9	N
MET	FGLARDM _p YDKEYYSV _a	Y1230	2.67	N
MET	LDGILSK _p YFDLIYVH _a	Y830	2.09	N
MET	LGSELVR _p YDARVHTP _a	Y971	1.74	N
MET	NVKCVAP _p YPSLLSSE _a	Y1365	1.05	N
MET	QVAKGMK _p YLASKKFV _a	Y1194	0.78	N
MET	GSCROVO _p YPLTDMSP _a	Y1026	0.57	N
MUSK	MAHEEVI _p YYVRDGN _a	Y813	2.04	N
NTRK1	FGMSRDI _p YSTDYRRV _a	Y640	2.69	N
NTRK1	QVAAGMV _p YLAGLHFV _a	Y640	2.64	N
NTRK1	RDIYSTD _p YRVGGRT _a	Y644	2.57	N
NTRK1	DIYSTDY _p YRVGGRTM _a	Y645	1.9	N

NTRK1	HIIENPOpYFSDACVHa	Y490	1.33	N
NTRK1	HIIENPQpYFSDACVHa	Y496	1.31	N
NTRK1	HIIENPQpYFSDACVHa	Y460	1.08	N
NTRK2	PVIENPQpYFGITNSQa	Y516	2.89	N
PDGFRA	PGQYKKS _p YEKIHLDFa	Y962	3.54	N
PDGFRA	ISPDGHE _p YIYVDPMQa	Y572	3.35	N
PDGFRA	RLSADSG _p YIIPLPDIa	Y1018	3.34	N
PDGFRA	IWKQKPR _p YEIRWRVla	Y555	3.12	N
PDGFRA	PDGHEY _p YVDPMOLPa	Y574	2.03	N
PDGFRA	VDPMLP _p YDSRWEFPa	Y582	0.96	N
PDGFRB	RPPSAEL _p YSNALPVGa	Y716	2.96	N
PDGFRB	SSNYMAP _p YDNYVPSAa	Y775	2.78	N
PDGFRB	PNEGDND _p YIIPLPDPa	Y1021	2.5	N
PDGFRB	VSSDGHE _p YIYVDPMQa	Y579	2.43	N
PDGFRB	LDTSSVL _p YTAVQPNEa	Y1009	2.12	N
PDGFRB	LWOKKPR _p YEIRWKVla	Y562	2.04	N
PDGFRB	VDPMLP _p YDSTWELPa	Y589	1.95	N
PDGFRB	YMAPYDN _p YVPSAPERa	Y778	1.91	N
PDGFRB	SDGHEY _p YVDPMQLPa	Y581	1.65	N
PDGFRB	YNAIKRG _p YRMAQPAHa	Y921	1.29	N
PDGFRB	ADIESSN _p YMAPYDNYa	Y771	1.07	N
PDGFRB	DMKGDVK _p YADIESSNa	Y763	0.83	N
PDGFRB	TGESDGG _p YMDMSKDEa	Y740	0.45	N
PTK6	GGAVAOG _p YVPHNYLaa	Y61	2.56	N
PTK6	QAHLGPK _p YVGLWDFKa	Y13	1.7	N
PTK6	DTQAVRH _p YKIWRRAGa	Y127	1.29	N
PTK6	QGYVPHN _p YLAERETVa	Y66	1.26	N
RET	ESLFDHI _p YTTQSDVWa	Y928	1.61	N
RET	LIVEYAK _p YGSRLRGLa	Y809	1.6	N
RET	MMVKRRD _p YLDLAASTa	Y1015	1.05	N
RET	VTLGGNP _p YPGIPPERa	Y952	0.77	N
RET	QISQGMQ _p YLAEMKLVa	Y864	0.68	N
RET	TPSDSLI _p YDDGLSEa	Y1029	0.57	N
RET	TWIENKL _p YGMSPDNWa	Y1062	0.4	N
RON	YVQLPAT _p YMNLGPSa	Y1360	2.69	N
RON	SALLGDH _p YVQLPATYa	Y1353	2.42	N
RON	ATPLPIL _p YSGSDYRSa	Y1012	1.84	N
RON	EYCPDSL _p YQVMQQCWaa	Y1317	1.75	N
RON	ILYSGSD _p YRSGLALPa	Y1017	1.23	N
ROR1	SNLSNPR _p YPNYMFPSa	Y786	3.27	N
ROR1	SNPRYPN _p YMFPSQGIa	Y789	2.3	N
ROR1	GYPIPPG _p YAAFPAaHa	Y828	2.15	N
ROR1	AAFPAAH _p YQPTGPPRa	Y836	2.04	N
ROR1	PPTASPG _p YSDEYEEDa	Y160	1.68	N
ROR1	EDGFCQP _p YRGIACARa	Y173	0.95	N

ROR2	LYVPVNG _D YQVPVAYGa	Y824	2.55	N
ROR2	SGSTSTG _P YVTTAPSNa	Y873	2.18	N
ROR2	AWGNLSN _P YNSSAQTSa	Y755	1.01	N
ROS1	CLLNEPQ _P YIILELMEa	Y2023	3.77	N
ROS1	VGLANAC _P YAIHTLPTa	Y1923	2.71	N
ROS1	YLYWTTL _P YSVESTRLa	Y807	2.69	N
ROS1	SNLDVLN _P YVQTGGRLa	Y2173	2.54	N
ROS1	DSVGGYL _P YWTTLYSVa	Y802	2.17	N
ROS1	VVDSVGG _D YLYWTTLYa	Y800	1.8	N
ROS1	RDIYKND _P YRKRGEGa	Y2114	1.33	N
ROS1	DIYKNDY _P YRKRGEGLa	Y2115	1.14	N
ROS1	FGLARDI _P YKNDYRKa	Y2110	1.05	N
ROS1	ACLTHSG _P YGDGSDaaa	Y2342	0.41	N
ROS1	NFFLNSI _P YKSRDEANa	Y2227	0.36	N
ROS1	CQEKQV _A PYCPGKPEa	Y2323	0.27	N
SRC	LOAFLE _D PYFTSTEOa	Y522	2.26	N
SRC	FTSTEPQ _P YQGENLaa	Y530	1.55	N
TEC	EEIVVAM _P YDFQAAEGa	Y188	0.84	N
TEC	NNNIMIK _P YHPKFWTDa	Y120	0.45	N
TIE2	GMTCAEL _P YEKLPQGYa	Y1048	3.54	N
TIE2	AIKRMKE _P YASKDDHRa	Y860	0.51	N
TNK1	PKSKNWV _P YKILGGFAa	Y77	2.42	N
TYK2	LTSQCLT _P YEPTQRPSa	Y851	1.8	N
TYRO3	SASODPL _P YINIERAEa	Y804	4.47	N
TYRO3	GTPSDCR _P YILTPGGLa	Y849	3.23	N
TYRO3	LPGRDQP _P YSGAGDGSa	Y828	1.8	N
UFO	QEPDEIL _P YVNMDEGGa	Y821	1.38	N
UFO	ESLADR _V PYTSKSDVWa	Y726	0.76	N
VEGFR1	VQQDGKD _P YIPINAILa	Y1169	2.7	N
VEGFR1	ATEKSAR _P YLTRGYSLa	Y383	1.96	N
VEGFR1	ATSMFDD _P YOGDSSTLa	Y1242	1.16	N
VEGFR1	FGLARDI _P YKNPDYVRa	Y1048	1.03	N
VEGFR2	AODGKD _D YIVLPISEa	Y1175	3.42	N
VEGFR2	GSNQTSG _P YQSGYHSDa	Y1305	2.4	N
VEGFR2	FGLARDI _P YKDPDYVRa	Y1054	1.11	N
VEGFR2	DDTDTT _V PYSSEAELa	Y1319	0.89	N
VEGFR2	TSGYQSG _P YHSDDTDTa	Y1309	0.71	N
VEGFR3	ARGGQVF _P YNSEYGELa	Y1333	1.77	N
VEGFR3	EQCEYLS _P YDASQWEFa	Y833	1.66	N
VEGFR3	PLEEOCE _P YLSYDASOa	Y830	1.34	N
VEGFR3	QVFYNSE _P YGELSEPSa	Y1337	1.2	N
VEGFR3	FGLARDI _P YKDPDYVRa	Y1063	0.95	N
VEGFR3	TFFTDNS _P Yaaaaaaaa	Y1363	0.79	N
YES1	VTIFVAL _P YDYEARTTa	Y100	2.71	N
YES1	IATGKNG _P YIPSNYVAa	Y141	2.05	N

YES1	NGYIPSN _D YVAPADSI _a	Y146	1.95	N
YES1	FTATEPQ _P YQPGENL _{aa}	Y537	1.44	N
YES1	VSTSVSH _P YGAEPPTV _a	Y32	1.13	N
YES1	SIQAEEW _P YFGKMGRK _a	Y159	0.69	N
YES1	LEQVERG _P YRMPCQGa	Y489	0.43	N
YES1	NKSPAIK _P YRPENTPE _a	Y16	0.32	N
ZAP70	MPMDTSV _P YESPYSDP _a	Y315	4.14	N
ZAP70	AAHLPF _F YGSISRAE _a	Y12	2.04	N
ZAP70	VLLVNRH _D YAKISDFG _a	Y474	2	N
ZAP70	RDAMVRD _P YVRQTWKL _a	Y126	1.46	N
ZAP70	TSVYESP _P YSDPEELK _a	Y319	0.96	N
ZAP70	QVSMGMK _P YLEEKNFV _a	Y451	0.85	N

Suppl. 2.4 Loop panel for PRM

m/z	charge	Site	Sequence
506.22157	3	ABL1_2_393_439	LMTGDTY[Pho]TAHAGAK
644.94013	3	ACK1_284	ALPONDDHY[Pho]VMOEHR
997.44022	2	ALK_1507(nonloop)	PTSLWNPTY[Pho]GSWFTEK
752.83199	2	BLK_389	IIDSEY[Pho]TAQEGAK
827.37402	2	BMX_566	YVLDDQY[Pho]VSSVGTGK
821.84783	2	BTK_551	YVLDDQY[Pho]TSSVGSK
464.53527	3	CSFIR_809	DIMNDSNY[Pho]IVK
848.35785	2	CSK_184(nonloop)	VMEGTVAQADEFY[Pho]R
647.73069	2	DDR1_796_797	NLYAGDY[Pho]Y[Pho]R
655.72815	2	DDR2_740_741	NLYSGDY[Pho]Y[Pho]R
869.86402	2	EPHA1_781	LLDDFDGTY[Pho]ETQGGK
881.87458	2	EPHA2_772	VLEDDPEATY[Pho]TSSGGK
780.33489	2	EPHA3_4_5_779_779_883	VLEDDPEAAY[Pho]TTR
873.87712	2	EPHA6_7_830_791	VLEDDPEAAY[Pho]TTTGGK
866.8693	2	EPHA8_793	VLEDDPEAAY[Pho]TTTGGK
1014.4277	2	EPHB1_778	YLQDDTSDPTY[Pho]TSSLGGK
998.9248	2	EPHB2_780	FLEDDTSDPTY[Pho]TSALGGK
1004.9248	2	EPHB3_792	FLEDDPSDPTY[Pho]TSSLGGK
1006.4303	2	EPHB4_774	FLEENSSDPTY[Pho]TSSLGGK
1035.9294	2	EPHB6_651(nonloop)	YYIDPSTY[Pho]EDPC[CAM]QAIR
485.68694	2	ErbB1(EGFR)_869	EY[Pho]HAEGGK
878.37729	2	ERBB2_877	LLDIDETAY[Pho]HADGGK
585.92062	3	ERBB2_877	LLDIDETAY[Pho]HADGGK
516.24409	2	ERBB3_866	OLLY[Pho]SEAK
467.17112	2	ERBB4_875	EY[Pho]NADGGK
680.21623	2	FAK1_576_577	YMEDSTY[Pho]Y[Pho]K
699.23293	2	FAK2_579_580	YIEDEDY[Pho]Y[Pho]K
703.7954	2	FER_714	QEDGGVY[Pho]SSSGLK
737.81413	2	FES_713	EEADGVY[Pho]AASGGLR
682.25962	2	FGFR1_653_654	DIHHIDY[Pho]Y[Pho]K
455.1755	3	FGFR1_653_654	DIHHIDY[Pho]Y[Pho]K
659.24363	2	FGFR2_656_657	DINNIDY[Pho]Y[Pho]K
663.7438	2	FGFR3_647_648	DVHNLDY[Pho]Y[Pho]K
646.24905	2	FGFR4_642_643	GVHHIDY[Pho]Y[Pho]K
431.16846	3	FGFR4_642_643	GVHHIDY[Pho]Y[Pho]K
464.83064	3	FGR_412	DDEY[Pho]NPC[CAM]QGSK
689.78907	2	FLT3_842	DIMSDSNY[Pho]VVR
660.2612	2	FRK_387	VNEDIY[Pho]ESR
645.27411	2	HCK_LYN_411_397	VIEDNEY[Pho]TAR
466.49479	3	IGFIR_INSR_1165_1166_1189_1190	DIYETDY[Pho]Y[Pho]R
692.23072	2	INSRR_1145_1146	DVYETDY[Pho]Y[Pho]R
821.35583	2	ITK_512	FVLDDQY[Pho]TSSGTGK
481.66904	2	JAK1_1034_1035	EY[Pho]Y[Pho]TVK

619.8001	2	JAK2_221(nonloop)	IODY[Pho]HILTR
637.30295	3	JAK2_570(nonloop)	EVGDY[Pho]GQLHETEVLLK
487.67466	2	JAK3_980_981	DY[Pho]Y[Pho]VVR
509.7157	2	KIT_823	NDSNY[Pho]VVK
531.66449	2	KSYK_525_526	ADENY[Pho]Y[Pho]K
966.45059	2	LMTK1_283	EDY[Pho]FVTADQLWVPLR
644.63615	3	LMTK1_283	EDY[Pho]FVTADQLWVPLR
604.22375	2	LMTK2_295	EDY[Pho]IETDDK
673.24109	2	LMTK3_296_297	EDY[Pho]Y[Pho]LTPER
598.70669	2	MERTK_TYRO3_753_754_685_686	IYSGDY[Pho]Y[Pho]R
600.21214	2	MET_1234_1235	EY[Pho]Y[Pho]SVHNK
648.7329	2	MUSK_755_756	NIYSADY[Pho]Y[Pho]K
678.23327	2	NTRK1_680_681	DIYSTDY[Pho]Y[Pho]R
671.22544	2	NTRK2_3_706_707_709_710	DVYSTDY[Pho]Y[Pho]R
463.52325	3	PGFRA_849	DIMHDSNY[Pho]VSK
453.68387	2	PGFRB_857	DSNY[Pho]ISK
603.93297	3	PTK6_342	EDVY[Pho]LSHDHNIPYK
826.79455	2	PTK7_960_961	DVYNSEY[Pho]Y[Pho]HFR
551.53213	3	PTK7_960_961	DVYNSEY[Pho]Y[Pho]HFR
663.7605	2	RET_905	DVYEEDSY[Pho]VK
457.17064	3	RON_1238_1239	EY[Pho]Y[Pho]SVQOHR
670.23581	2	ROR1_645_646	EIYSADY[Pho]Y[Pho]R
641.22745	2	ROR2_645_646	EVYAADY[Pho]Y[Pho]K
703.29525	3	ROS1_2274(nonloop)	EGLNY[Pho]MVLATECICAMIGOGEEK
652.28193	2	SRC_YES_FYN_LCK_419_426_420_394	LIEDNEY[Pho]TAR
633.2503	2	SRMS_380	DDIY[Pho]SPSSSSK
807.34018	2	TEC_519	YVLDDQY[Pho]TSSSGAK
452.19661	2	TIE1_1007	GEEVY[Pho]VK
451.7046	2	TIE2_992	GQEVY[Pho]VK
836.86074	2	TXK_420	YVLDDEY[Pho]VSSFGAK
460.83889	3	TYK2_1054_1055	AVPEGHEY[Pho]Y[Pho]R
612.21214	2	UFO_702_703	IYNGDY[Pho]Y[Pho]R
422.17347	2	VGFR1_1053	NPDY[Pho]VR
422.66548	2	VGFR2_3_1059_1068	DPDY[Pho]VR
731.76801	2	ZAP70_492_493	ALGADDY[Pho]Y[Pho]TAR
681.28141	2	GSK3_279_216	GEPNVSY[Pho]IC[CAM]SR
652.77068	2	GSK3_279_216	GEPNVSY[Pho]ICSR
777.99428	3	MAPK3	IADPEHDHTGFLT[Pho]EY[Pho]VATR
768.65051	3	MAPK1	VADPDHDHTGFLT[Pho]EY[Pho]VATR

Suppl. 2.5 Full panel for MRM

MS1	MS2	Fragments	DP	CE
506.2216	346.1795	ABL1_2_393_439(loop).LMTGDTY[Pho]TAHAGAK.+3b3	68	25.1
506.2216	619.2756	ABL1_2_393_439(loop).LMTGDTY[Pho]TAHAGAK.+3b6	68	25.1
506.2216	346.2085	ABL1_2_393_439(loop).LMTGDTY[Pho]TAHAGAK.+3y4	68	25.1
506.2216	483.2674	ABL1_2_393_439(loop).LMTGDTY[Pho]TAHAGAK.+3y5	68	25.1
506.2216	554.3045	ABL1_2_393_439(loop).LMTGDTY[Pho]TAHAGAK.+3y6	68	25.1
506.2216	655.3522	ABL1_2_393_439(loop).LMTGDTY[Pho]TAHAGAK.+3y7	68	25.1
506.2216	898.3819	ABL1_2_393_439(loop).LMTGDTY[Pho]TAHAGAK.+3y8	68	25.1
506.2216	999.4295	ABL1_2_393_439(loop).LMTGDTY[Pho]TAHAGAK.+3y9	68	25.1
554.5905	441.2456	ABL1_226.NKPTVY[Pho]GVSPNYDK.+3b4	71.5	27.8
554.5905	540.314	ABL1_226.NKPTVY[Pho]GVSPNYDK.+3b5	71.5	27.8
554.5905	783.3437	ABL1_226.NKPTVY[Pho]GVSPNYDK.+3b6	71.5	27.8
554.5905	840.3651	ABL1_226.NKPTVY[Pho]GVSPNYDK.+3b7	71.5	27.8
554.5905	939.4336	ABL1_226.NKPTVY[Pho]GVSPNYDK.+3b8	71.5	27.8
554.5905	539.246	ABL1_226.NKPTVY[Pho]GVSPNYDK.+3y4	71.5	27.8
554.5905	636.2988	ABL1_226.NKPTVY[Pho]GVSPNYDK.+3y5	71.5	27.8
554.5905	723.3308	ABL1_226.NKPTVY[Pho]GVSPNYDK.+3y6	71.5	27.8
861.3822	413.2143	ABL1_253.LGGGQY[Pho]GEVYEGVWK.+2b5	93.9	39.9
861.3822	656.244	ABL1_253.LGGGQY[Pho]GEVYEGVWK.+2b6	93.9	39.9
861.3822	941.3764	ABL1_253.LGGGQY[Pho]GEVYEGVWK.+2b9	93.9	39.9
861.3822	489.282	ABL1_253.LGGGQY[Pho]GEVYEGVWK.+2y4	93.9	39.9
861.3822	618.3246	ABL1_253.LGGGQY[Pho]GEVYEGVWK.+2y5	93.9	39.9
861.3822	781.3879	ABL1_253.LGGGQY[Pho]GEVYEGVWK.+2y6	93.9	39.9
861.3822	880.4563	ABL1_253.LGGGQY[Pho]GEVYEGVWK.+2y7	93.9	39.9
861.3822	1066.52	ABL1_253.LGGGQY[Pho]GEVYEGVWK.+2y9	93.9	39.9
1092.012	1183.457	ABL2_161.NGQGWVPSNY[Pho]ITPVNSLEK.+2b10	110.7	48.2
1092.012	543.231	ABL2_161.NGQGWVPSNY[Pho]ITPVNSLEK.+2b5	110.7	48.2
1092.012	642.2994	ABL2_161.NGQGWVPSNY[Pho]ITPVNSLEK.+2b6	110.7	48.2
1092.012	940.4272	ABL2_161.NGQGWVPSNY[Pho]ITPVNSLEK.+2b9	110.7	48.2
1092.012	389.2395	ABL2_161.NGQGWVPSNY[Pho]ITPVNSLEK.+2y3	110.7	48.2
1092.012	590.3144	ABL2_161.NGQGWVPSNY[Pho]ITPVNSLEK.+2y5	110.7	48.2
1092.012	786.4356	ABL2_161.NGQGWVPSNY[Pho]ITPVNSLEK.+2y7	110.7	48.2
1092.012	887.4833	ABL2_161.NGQGWVPSNY[Pho]ITPVNSLEK.+2y8	110.7	48.2
435.8557	411.1775	ABL2_174.HSWY[Pho]HGPVSR.+3b3	62.9	21.3
435.8557	654.2072	ABL2_174.HSWY[Pho]HGPVSR.+3b4	62.9	21.3
435.8557	361.2194	ABL2_174.HSWY[Pho]HGPVSR.+3y3	62.9	21.3
435.8557	458.2722	ABL2_174.HSWY[Pho]HGPVSR.+3y4	62.9	21.3
435.8557	515.2936	ABL2_174.HSWY[Pho]HGPVSR.+3y5	62.9	21.3
435.8557	652.3525	ABL2_174.HSWY[Pho]HGPVSR.+3y6	62.9	21.3
644.9401	754.3366	ACK1_284(loop).ALPQNDHXY[Pho]VMQEHR.+3b7	78.1	32.7
644.9401	441.2205	ACK1_284(loop).ALPQNDHXY[Pho]VMQEHR.+3y3	78.1	32.7
644.9401	569.279	ACK1_284(loop).ALPQNDHXY[Pho]VMQEHR.+3y4	78.1	32.7
644.9401	700.3195	ACK1_284(loop).ALPQNDHXY[Pho]VMQEHR.+3y5	78.1	32.7
644.9401	1042.418	ACK1_284(loop).ALPQNDHXY[Pho]VMQEHR.+3y7	78.1	32.7

644.9401	1179.477	ACK1_284(loop).ALPONDDHY[Pho]VMOEHR.+3v8	78.1	32.7
997.4402	399.2238	ALK_1507.PTSLWNPTY[Pho]GSWFTEK.+2b4	103.8	44.8
997.4402	585.3031	ALK_1507.PTSLWNPTY[Pho]GSWFTEK.+2b5	103.8	44.8
997.4402	699.3461	ALK_1507.PTSLWNPTY[Pho]GSWFTEK.+2b6	103.8	44.8
997.4402	524.2715	ALK_1507.PTSLWNPTY[Pho]GSWFTEK.+2y4	103.8	44.8
997.4402	710.3508	ALK_1507.PTSLWNPTY[Pho]GSWFTEK.+2y5	103.8	44.8
997.4402	854.4043	ALK_1507.PTSLWNPTY[Pho]GSWFTEK.+2y7	103.8	44.8
997.4402	1097.434	ALK_1507.PTSLWNPTY[Pho]GSWFTEK.+2y8	103.8	44.8
997.4402	1198.482	ALK_1507.PTSLWNPTY[Pho]GSWFTEK.+2y9	103.8	44.8
752.832	429.2344	BLK_389(loop).IIDSEY[Pho]TAQEGAK.+2b4	86	36
752.832	558.277	BLK_389(loop).IIDSEY[Pho]TAQEGAK.+2b5	86	36
752.832	801.3066	BLK_389(loop).IIDSEY[Pho]TAQEGAK.+2b6	86	36
752.832	1163.462	BLK_389(loop).IIDSEY[Pho]TAQEGAK.+2y10	86	36
752.832	603.3097	BLK_389(loop).IIDSEY[Pho]TAQEGAK.+2y6	86	36
752.832	704.3573	BLK_389(loop).IIDSEY[Pho]TAQEGAK.+2y7	86	36
752.832	947.387	BLK_389(loop).IIDSEY[Pho]TAQEGAK.+2y8	86	36
752.832	1076.43	BLK_389(loop).IIDSEY[Pho]TAQEGAK.+2y9	86	36
688.2763	416.214	BMX_40.TNLSY[Pho]YEYDK.+2b4	81.3	33.6
688.2763	822.307	BMX_40.TNLSY[Pho]YEYDK.+2b6	81.3	33.6
688.2763	425.2031	BMX_40.TNLSY[Pho]YEYDK.+2y3	81.3	33.6
688.2763	554.2457	BMX_40.TNLSY[Pho]YEYDK.+2y4	81.3	33.6
688.2763	717.309	BMX_40.TNLSY[Pho]YEYDK.+2y5	81.3	33.6
688.2763	960.3387	BMX_40.TNLSY[Pho]YEYDK.+2y6	81.3	33.6
688.2763	1047.371	BMX_40.TNLSY[Pho]YEYDK.+2y7	81.3	33.6
688.2763	1160.455	BMX_40.TNLSY[Pho]YEYDK.+2y8	81.3	33.6
827.374	491.25	BMX_566(loop).YVLDDQY[Pho]VSSVGTK.+2b4	91.4	38.6
827.374	606.277	BMX_566(loop).YVLDDQY[Pho]VSSVGTK.+2b5	91.4	38.6
827.374	977.3652	BMX_566(loop).YVLDDQY[Pho]VSSVGTK.+2b7	91.4	38.6
827.374	1163.466	BMX_566(loop).YVLDDQY[Pho]VSSVGTK.+2b9	91.4	38.6
827.374	491.2824	BMX_566(loop).YVLDDQY[Pho]VSSVGTK.+2y5	91.4	38.6
827.374	578.3144	BMX_566(loop).YVLDDQY[Pho]VSSVGTK.+2y6	91.4	38.6
827.374	677.3828	BMX_566(loop).YVLDDQY[Pho]VSSVGTK.+2y7	91.4	38.6
827.374	920.4125	BMX_566(loop).YVLDDQY[Pho]VSSVGTK.+2y8	91.4	38.6
821.8478	491.25	BTK_551(loop).YVLDDQY[Pho]TSSVGSK.+2b4	91	38.4
821.8478	735.3196	BTK_551(loop).YVLDDQY[Pho]TSSVGSK.+2b6	91	38.4
821.8478	978.3492	BTK_551(loop).YVLDDQY[Pho]TSSVGSK.+2b7	91	38.4
821.8478	1079.397	BTK_551(loop).YVLDDQY[Pho]TSSVGSK.+2b8	91	38.4
821.8478	477.2667	BTK_551(loop).YVLDDQY[Pho]TSSVGSK.+2y5	91	38.4
821.8478	564.2988	BTK_551(loop).YVLDDQY[Pho]TSSVGSK.+2y6	91	38.4
821.8478	665.3464	BTK_551(loop).YVLDDQY[Pho]TSSVGSK.+2y7	91	38.4
821.8478	908.3761	BTK_551(loop).YVLDDQY[Pho]TSSVGSK.+2y8	91	38.4
696.2993	360.1588	CSFIR_809(loop).DIMNDSNY[Pho]IVK.+2b3	81.9	33.9
696.2993	1146.417	CSFIR_809(loop).DIMNDSNY[Pho]IVK.+2b9	81.9	33.9
696.2993	602.2949	CSFIR_809(loop).DIMNDSNY[Pho]IVK.+2y4	81.9	33.9
696.2993	716.3379	CSFIR_809(loop).DIMNDSNY[Pho]IVK.+2y5	81.9	33.9

696.2993	803.3699	CSF1R_809(loop).DIMNDSNY[Pho]IVK.+2v6	81.9	33.9
696.2993	918.3968	CSF1R_809(loop).DIMNDSNY[Pho]IVK.+2v7	81.9	33.9
696.2993	1032.44	CSF1R_809(loop).DIMNDSNY[Pho]IVK.+2y8	81.9	33.9
696.2993	1163.48	CSF1R_809(loop).DIMNDSNY[Pho]IVK.+2y9	81.9	33.9
848.3578	360.1588	CSK_184.VMEGTVAQADEFY[Pho]R.+2b3	93	39.4
848.3578	518.2279	CSK_184.VMEGTVAQADEFY[Pho]R.+2b5	93	39.4
848.3578	617.2963	CSK_184.VMEGTVAQADEFY[Pho]R.+2b6	93	39.4
848.3578	565.217	CSK_184.VMEGTVAQADEFY[Pho]R.+2y3	93	39.4
848.3578	809.2866	CSK_184.VMEGTVAQADEFY[Pho]R.+2y5	93	39.4
848.3578	1008.382	CSK_184.VMEGTVAQADEFY[Pho]R.+2y7	93	39.4
848.3578	1178.488	CSK_184.VMEGTVAQADEFY[Pho]R.+2y9	93	39.4
647.7307	391.1976	DDR1_796_797(loop).NLYAGDY[Pho]Y[Pho]R.+2b3	78.3	32.2
647.7307	462.2347	DDR1_796_797(loop).NLYAGDY[Pho]Y[Pho]R.+2b4	78.3	32.2
647.7307	519.2562	DDR1_796_797(loop).NLYAGDY[Pho]Y[Pho]R.+2b5	78.3	32.2
647.7307	661.1783	DDR1_796_797(loop).NLYAGDY[Pho]Y[Pho]R.+2y3	78.3	32.2
647.7307	776.2052	DDR1_796_797(loop).NLYAGDY[Pho]Y[Pho]R.+2y4	78.3	32.2
647.7307	833.2267	DDR1_796_797(loop).NLYAGDY[Pho]Y[Pho]R.+2y5	78.3	32.2
647.7307	904.2638	DDR1_796_797(loop).NLYAGDY[Pho]Y[Pho]R.+2y6	78.3	32.2
647.7307	1067.327	DDR1_796_797(loop).NLYAGDY[Pho]Y[Pho]R.+2y7	78.3	32.2
655.7282	391.1976	DDR2_740_741(loop).NLYSGDY[Pho]Y[Pho]R.+2b3	78.9	32.5
655.7282	478.2296	DDR2_740_741(loop).NLYSGDY[Pho]Y[Pho]R.+2b4	78.9	32.5
655.7282	535.2511	DDR2_740_741(loop).NLYSGDY[Pho]Y[Pho]R.+2b5	78.9	32.5
655.7282	661.1783	DDR2_740_741(loop).NLYSGDY[Pho]Y[Pho]R.+2y3	78.9	32.5
655.7282	776.2052	DDR2_740_741(loop).NLYSGDY[Pho]Y[Pho]R.+2y4	78.9	32.5
655.7282	833.2267	DDR2_740_741(loop).NLYSGDY[Pho]Y[Pho]R.+2y5	78.9	32.5
655.7282	920.2587	DDR2_740_741(loop).NLYSGDY[Pho]Y[Pho]R.+2y6	78.9	32.5
655.7282	1083.322	DDR2_740_741(loop).NLYSGDY[Pho]Y[Pho]R.+2y7	78.9	32.5
645.7717	317.1456	EGFR_1197.GSTAENAEY[Pho]LR.+2b4	78.2	32.1
645.7717	446.1882	EGFR_1197.GSTAENAEY[Pho]LR.+2b5	78.2	32.1
645.7717	531.2327	EGFR_1197.GSTAENAEY[Pho]LR.+2y3	78.2	32.1
645.7717	660.2753	EGFR_1197.GSTAENAEY[Pho]LR.+2y4	78.2	32.1
645.7717	731.3124	EGFR_1197.GSTAENAEY[Pho]LR.+2y5	78.2	32.1
645.7717	845.3553	EGFR_1197.GSTAENAEY[Pho]LR.+2y6	78.2	32.1
645.7717	974.3979	EGFR_1197.GSTAENAEY[Pho]LR.+2y7	78.2	32.1
645.7717	1045.435	EGFR_1197.GSTAENAEY[Pho]LR.+2y8	78.2	32.1
822.8474	566.2755	EGFR_998.MHLPSTDSNFY[Pho]R.+2b5	91.1	38.5
822.8474	879.4029	EGFR_998.MHLPSTDSNFY[Pho]R.+2b8	91.1	38.5
822.8474	966.4349	EGFR_998.MHLPSTDSNFY[Pho]R.+2b9	91.1	38.5
822.8474	766.292	EGFR_998.MHLPSTDSNFY[Pho]R.+2y5	91.1	38.5
822.8474	881.3189	EGFR_998.MHLPSTDSNFY[Pho]R.+2y6	91.1	38.5
822.8474	982.3666	EGFR_998.MHLPSTDSNFY[Pho]R.+2y7	91.1	38.5
822.8474	1166.451	EGFR_998.MHLPSTDSNFY[Pho]R.+2y9	91.1	38.5
772.6705	410.1783	EGFR_Y1172.GSHQISLNDPDIY[Pho]QQDFFPK.+3b4	87.4	39.6
772.6705	523.2623	EGFR_Y1172.GSHQISLNDPDIY[Pho]QQDFFPK.+3b5	87.4	39.6
772.6705	838.4054	EGFR_Y1172.GSHQISLNDPDIY[Pho]QQDFFPK.+3b8	87.4	39.6

772.6705	952.4483	EGFR_Y1172.GSHQISLDNPDY[Pho]OODFFPK.+3b9	87.4	39.6
772.6705	538.3024	EGFR_Y1172.GSHQISLDNPDY[Pho]QQDFFPK.+3y4	87.4	39.6
772.6705	653.3293	EGFR_Y1172.GSHQISLDNPDY[Pho]QQDFFPK.+3y5	87.4	39.6
772.6705	909.4465	EGFR_Y1172.GSHQISLDNPDY[Pho]QQDFFPK.+3y7	87.4	39.6
772.6705	1152.476	EGFR_Y1172.GSHQISLDNPDY[Pho]QQDFFPK.+3y8	87.4	39.6
869.864	457.2293	EPHA1_781(loop).LLDDFDGTY[Pho]ETQGGK.+2b4	94.5	40.2
869.864	719.3246	EPHA1_781(loop).LLDDFDGTY[Pho]ETQGGK.+2b6	94.5	40.2
869.864	1135.43	EPHA1_781(loop).LLDDFDGTY[Pho]ETQGGK.+2y10	94.5	40.2
869.864	490.262	EPHA1_781(loop).LLDDFDGTY[Pho]ETQGGK.+2y5	94.5	40.2
869.864	619.3046	EPHA1_781(loop).LLDDFDGTY[Pho]ETQGGK.+2y6	94.5	40.2
869.864	862.3342	EPHA1_781(loop).LLDDFDGTY[Pho]ETQGGK.+2y7	94.5	40.2
869.864	963.3819	EPHA1_781(loop).LLDDFDGTY[Pho]ETQGGK.+2y8	94.5	40.2
869.864	1020.403	EPHA1_781(loop).LLDDFDGTY[Pho]ETQGGK.+2y9	94.5	40.2
881.8746	457.2293	EPHA2_772(loop).VLEDDPEATY[Pho]TTSGGK.+2b4	95.4	40.6
881.8746	572.2562	EPHA2_772(loop).VLEDDPEATY[Pho]TTSGGK.+2b5	95.4	40.6
881.8746	869.3887	EPHA2_772(loop).VLEDDPEATY[Pho]TTSGGK.+2b8	95.4	40.6
881.8746	1191.493	EPHA2_772(loop).VLEDDPEATY[Pho]TTSGGK.+2y11	95.4	40.6
881.8746	550.2831	EPHA2_772(loop).VLEDDPEATY[Pho]TTSGGK.+2y6	95.4	40.6
881.8746	793.3128	EPHA2_772(loop).VLEDDPEATY[Pho]TTSGGK.+2y7	95.4	40.6
881.8746	894.3605	EPHA2_772(loop).VLEDDPEATY[Pho]TTSGGK.+2y8	95.4	40.6
881.8746	965.3976	EPHA2_772(loop).VLEDDPEATY[Pho]TTSGGK.+2y9	95.4	40.6
780.3349	572.2562	EPHA3_4_5_779_779_883(loop).VLEDDPEAAY[Pho]TTR.+2b5	88	36.9
780.3349	1218.467	EPHA3_4_5_779_779_883(loop).VLEDDPEAAY[Pho]TTR.+2y10	88	36.9
780.3349	377.2143	EPHA3_4_5_779_779_883(loop).VLEDDPEAAY[Pho]TTR.+2y3	88	36.9
780.3349	620.244	EPHA3_4_5_779_779_883(loop).VLEDDPEAAY[Pho]TTR.+2y4	88	36.9
780.3349	691.2811	EPHA3_4_5_779_779_883(loop).VLEDDPEAAY[Pho]TTR.+2y5	88	36.9
780.3349	762.3182	EPHA3_4_5_779_779_883(loop).VLEDDPEAAY[Pho]TTR.+2y6	88	36.9
780.3349	988.4136	EPHA3_4_5_779_779_883(loop).VLEDDPEAAY[Pho]TTR.+2y8	88	36.9
780.3349	1103.44	EPHA3_4_5_779_779_883(loop).VLEDDPEAAY[Pho]TTR.+2y9	88	36.9
873.8771	457.2293	EPHA6_7_830_791(loop).VLEDDPEAAY[Pho]TTTGGK.+2b4	94.8	40.3
873.8771	572.2562	EPHA6_7_830_791(loop).VLEDDPEAAY[Pho]TTTGGK.+2b5	94.8	40.3
873.8771	798.3516	EPHA6_7_830_791(loop).VLEDDPEAAY[Pho]TTTGGK.+2b7	94.8	40.3
873.8771	869.3887	EPHA6_7_830_791(loop).VLEDDPEAAY[Pho]TTTGGK.+2b8	94.8	40.3
873.8771	564.2988	EPHA6_7_830_791(loop).VLEDDPEAAY[Pho]TTTGGK.+2y6	94.8	40.3
873.8771	807.3284	EPHA6_7_830_791(loop).VLEDDPEAAY[Pho]TTTGGK.+2y7	94.8	40.3
873.8771	878.3655	EPHA6_7_830_791(loop).VLEDDPEAAY[Pho]TTTGGK.+2y8	94.8	40.3
873.8771	949.4027	EPHA6_7_830_791(loop).VLEDDPEAAY[Pho]TTTGGK.+2y9	94.8	40.3
866.8693	342.2023	EPHA8_793(loop).VLEDDPDAAY[Pho]TTTGGK.+2b3	94.3	40.1
866.8693	457.2293	EPHA8_793(loop).VLEDDPDAAY[Pho]TTTGGK.+2b4	94.3	40.1
866.8693	572.2562	EPHA8_793(loop).VLEDDPDAAY[Pho]TTTGGK.+2b5	94.3	40.1
866.8693	1161.482	EPHA8_793(loop).VLEDDPDAAY[Pho]TTTGGK.+2y11	94.3	40.1
866.8693	564.2988	EPHA8_793(loop).VLEDDPDAAY[Pho]TTTGGK.+2y6	94.3	40.1
866.8693	807.3284	EPHA8_793(loop).VLEDDPDAAY[Pho]TTTGGK.+2y7	94.3	40.1
866.8693	878.3655	EPHA8_793(loop).VLEDDPDAAY[Pho]TTTGGK.+2y8	94.3	40.1
866.8693	949.4027	EPHA8_793(loop).VLEDDPDAAY[Pho]TTTGGK.+2y9	94.3	40.1

1014.428	635.2671	EPHB1_778(loop).YLQDDTSDPTY[Pho]TSSLGGK.+2b5	105.1	45.4
1014.428	938.3738	EPHB1_778(loop).YLQDDTSDPTY[Pho]TSSLGGK.+2b8	105.1	45.4
1014.428	1090.482	EPHB1_778(loop).YLQDDTSDPTY[Pho]TSSLGGK.+2y10	105.1	45.4
1014.428	1205.509	EPHB1_778(loop).YLQDDTSDPTY[Pho]TSSLGGK.+2y11	105.1	45.4
1014.428	461.2718	EPHB1_778(loop).YLQDDTSDPTY[Pho]TSSLGGK.+2y5	105.1	45.4
1014.428	548.3039	EPHB1_778(loop).YLQDDTSDPTY[Pho]TSSLGGK.+2y6	105.1	45.4
1014.428	649.3515	EPHB1_778(loop).YLQDDTSDPTY[Pho]TSSLGGK.+2y7	105.1	45.4
1014.428	892.3812	EPHB1_778(loop).YLQDDTSDPTY[Pho]TSSLGGK.+2y8	105.1	45.4
998.9248	620.2562	EPHB2_780(loop).FLEDDTSDPTY[Pho]TSALGGK.+2b5	103.9	44.8
998.9248	923.3629	EPHB2_780(loop).FLEDDTSDPTY[Pho]TSALGGK.+2b8	103.9	44.8
998.9248	1074.487	EPHB2_780(loop).FLEDDTSDPTY[Pho]TSALGGK.+2y10	103.9	44.8
998.9248	1189.514	EPHB2_780(loop).FLEDDTSDPTY[Pho]TSALGGK.+2y11	103.9	44.8
998.9248	374.2398	EPHB2_780(loop).FLEDDTSDPTY[Pho]TSALGGK.+2y4	103.9	44.8
998.9248	532.3089	EPHB2_780(loop).FLEDDTSDPTY[Pho]TSALGGK.+2y6	103.9	44.8
998.9248	633.3566	EPHB2_780(loop).FLEDDTSDPTY[Pho]TSALGGK.+2y7	103.9	44.8
998.9248	876.3863	EPHB2_780(loop).FLEDDTSDPTY[Pho]TSALGGK.+2y8	103.9	44.8
1004.925	620.2562	EPHB3_792(loop).FLEDDPSDPTY[Pho]TSSLGGK.+2b5	104.4	45
1004.925	804.341	EPHB3_792(loop).FLEDDPSDPTY[Pho]TSSLGGK.+2b7	104.4	45
1004.925	919.368	EPHB3_792(loop).FLEDDPSDPTY[Pho]TSSLGGK.+2b8	104.4	45
1004.925	1090.482	EPHB3_792(loop).FLEDDPSDPTY[Pho]TSSLGGK.+2y10	104.4	45
1004.925	1205.509	EPHB3_792(loop).FLEDDPSDPTY[Pho]TSSLGGK.+2y11	104.4	45
1004.925	548.3039	EPHB3_792(loop).FLEDDPSDPTY[Pho]TSSLGGK.+2y6	104.4	45
1004.925	649.3515	EPHB3_792(loop).FLEDDPSDPTY[Pho]TSSLGGK.+2y7	104.4	45
1004.925	892.3812	EPHB3_792(loop).FLEDDPSDPTY[Pho]TSSLGGK.+2y8	104.4	45
1006.43	1120.479	EPHB4_774(loop).FLEENSSDPTY[Pho]TSSLGGK.+2b10	104.5	45.1
1006.43	922.3789	EPHB4_774(loop).FLEENSSDPTY[Pho]TSSLGGK.+2b8	104.5	45.1
1006.43	1090.482	EPHB4_774(loop).FLEENSSDPTY[Pho]TSSLGGK.+2y10	104.5	45.1
1006.43	1205.509	EPHB4_774(loop).FLEENSSDPTY[Pho]TSSLGGK.+2y11	104.5	45.1
1006.43	461.2718	EPHB4_774(loop).FLEENSSDPTY[Pho]TSSLGGK.+2y5	104.5	45.1
1006.43	548.3039	EPHB4_774(loop).FLEENSSDPTY[Pho]TSSLGGK.+2y6	104.5	45.1
1006.43	649.3515	EPHB4_774(loop).FLEENSSDPTY[Pho]TSSLGGK.+2y7	104.5	45.1
1006.43	892.3812	EPHB4_774(loop).FLEENSSDPTY[Pho]TSSLGGK.+2y8	104.5	45.1
816.7209	1115.573	ERBB2_1005.FVVIQNE DLGPASPLDSTFY[Pho]R.+3b10	90.7	42
816.7209	666.2647	ERBB2_1005.FVVIQNE DLGPASPLDSTFY[Pho]R.+3y4	90.7	42
816.7209	753.2967	ERBB2_1005.FVVIQNE DLGPASPLDSTFY[Pho]R.+3y5	90.7	42
816.7209	868.3237	ERBB2_1005.FVVIQNE DLGPASPLDSTFY[Pho]R.+3y6	90.7	42
816.7209	981.4077	ERBB2_1005.FVVIQNE DLGPASPLDSTFY[Pho]R.+3y7	90.7	42
816.7209	1078.461	ERBB2_1005.FVVIQNE DLGPASPLDSTFY[Pho]R.+3y8	90.7	42
816.7209	1165.493	ERBB2_1005.FVVIQNE DLGPASPLDSTFY[Pho]R.+3y9	90.7	42
639.8101	1066.461	ERBB2_735_ERBB4_733.VLGSGAFGT VY[Pho]K.+2y10	77.8	31.9
639.8101	489.2109	ERBB2_735_ERBB4_733.VLGSGAFGT VY[Pho]K.+2y3	77.8	31.9
639.8101	590.2586	ERBB2_735_ERBB4_733.VLGSGAFGT VY[Pho]K.+2y4	77.8	31.9
639.8101	647.28	ERBB2_735_ERBB4_733.VLGSGAFGT VY[Pho]K.+2y5	77.8	31.9
639.8101	794.3484	ERBB2_735_ERBB4_733.VLGSGAFGT VY[Pho]K.+2y6	77.8	31.9
639.8101	865.3855	ERBB2_735_ERBB4_733.VLGSGAFGT VY[Pho]K.+2y7	77.8	31.9

639.8101	922.407	ERBB2_735_ERBB4_733.VLGSGAFGTVY[Pho]K.+2v8	77.8	31.9
639.8101	1009.439	ERBB2_735_ERBB4_733.VLGSGAFGTVY[Pho]K.+2y9	77.8	31.9
878.3773	570.3134	ERBB2_877(loop).LLDIDETEV[Pho]HADGGK.+2b5	95.2	40.5
878.3773	699.3559	ERBB2_877(loop).LLDIDETEV[Pho]HADGGK.+2b6	95.2	40.5
878.3773	1186.441	ERBB2_877(loop).LLDIDETEV[Pho]HADGGK.+2y10	95.2	40.5
878.3773	447.2198	ERBB2_877(loop).LLDIDETEV[Pho]HADGGK.+2y5	95.2	40.5
878.3773	584.2787	ERBB2_877(loop).LLDIDETEV[Pho]HADGGK.+2y6	95.2	40.5
878.3773	827.3084	ERBB2_877(loop).LLDIDETEV[Pho]HADGGK.+2y7	95.2	40.5
878.3773	956.351	ERBB2_877(loop).LLDIDETEV[Pho]HADGGK.+2v8	95.2	40.5
878.3773	1057.399	ERBB2_877(loop).LLDIDETEV[Pho]HADGGK.+2y9	95.2	40.5
585.9206	699.3559	ERBB2_877(loop).LLDIDETEV[Pho]HADGGK.+3b6	73.8	29.5
585.9206	376.1827	ERBB2_877(loop).LLDIDETEV[Pho]HADGGK.+3y4	73.8	29.5
585.9206	447.2198	ERBB2_877(loop).LLDIDETEV[Pho]HADGGK.+3y5	73.8	29.5
585.9206	584.2787	ERBB2_877(loop).LLDIDETEV[Pho]HADGGK.+3y6	73.8	29.5
585.9206	827.3084	ERBB2_877(loop).LLDIDETEV[Pho]HADGGK.+3y7	73.8	29.5
585.9206	956.351	ERBB2_877(loop).LLDIDETEV[Pho]HADGGK.+3v8	73.8	29.5
585.9206	1057.399	ERBB2_877(loop).LLDIDETEV[Pho]HADGGK.+3y9	73.8	29.5
730.9637	922.4153	ERBB3_1328.SLEATDSAFDNPDY[Pho]WHSR.+3b9	84.4	37.4
730.9637	585.2892	ERBB3_1328.SLEATDSAFDNPDY[Pho]WHSR.+3y4	84.4	37.4
730.9637	828.3189	ERBB3_1328.SLEATDSAFDNPDY[Pho]WHSR.+3y5	84.4	37.4
730.9637	943.3458	ERBB3_1328.SLEATDSAFDNPDY[Pho]WHSR.+3y6	84.4	37.4
730.9637	1040.399	ERBB3_1328.SLEATDSAFDNPDY[Pho]WHSR.+3y7	84.4	37.4
730.9637	1154.441	ERBB3_1328.SLEATDSAFDNPDY[Pho]WHSR.+3y8	84.4	37.4
516.2441	598.2636	ERBB3_866(loop).QLLY[Pho]SEAK.+2b4	68.8	27.4
516.2441	685.2957	ERBB3_866(loop).QLLY[Pho]SEAK.+2b5	68.8	27.4
516.2441	814.3383	ERBB3_866(loop).QLLY[Pho]SEAK.+2b6	68.8	27.4
516.2441	434.2245	ERBB3_866(loop).QLLY[Pho]SEAK.+2y4	68.8	27.4
516.2441	677.2542	ERBB3_866(loop).QLLY[Pho]SEAK.+2y5	68.8	27.4
516.2441	790.3383	ERBB3_866(loop).QLLY[Pho]SEAK.+2y6	68.8	27.4
630.6154	567.2885	ERBB4_1258.STLQHPDY[Pho]LQEYSTK.+3b5	77.1	31.9
630.6154	779.3682	ERBB4_1258.STLQHPDY[Pho]LQEYSTK.+3b7	77.1	31.9
630.6154	1022.398	ERBB4_1258.STLQHPDY[Pho]LQEYSTK.+3b8	77.1	31.9
630.6154	498.2558	ERBB4_1258.STLQHPDY[Pho]LQEYSTK.+3y4	77.1	31.9
630.6154	627.2984	ERBB4_1258.STLQHPDY[Pho]LQEYSTK.+3y5	77.1	31.9
630.6154	755.357	ERBB4_1258.STLQHPDY[Pho]LQEYSTK.+3y6	77.1	31.9
630.6154	868.4411	ERBB4_1258.STLQHPDY[Pho]LQEYSTK.+3y7	77.1	31.9
630.6154	1111.471	ERBB4_1258.STLQHPDY[Pho]LQEYSTK.+3y8	77.1	31.9
630.6154	430.2296	ERBB4_1262.STLQHPDY[LQEY][Pho]STK.+3b4	77.1	31.9
630.6154	567.2885	ERBB4_1262.STLQHPDY[LQEY][Pho]STK.+3b5	77.1	31.9
630.6154	664.3413	ERBB4_1262.STLQHPDY[LQEY][Pho]STK.+3b6	77.1	31.9
630.6154	779.3682	ERBB4_1262.STLQHPDY[LQEY][Pho]STK.+3b7	77.1	31.9
630.6154	335.1925	ERBB4_1262.STLQHPDY[LQEY][Pho]STK.+3y3	77.1	31.9
630.6154	1111.471	ERBB4_1262.STLQHPDY[LQEY][Pho]STK.+3y8	77.1	31.9
630.6154	1226.498	ERBB4_1262.STLQHPDY[LQEY][Pho]STK.+3y9	77.1	31.9
680.2162	539.1806	FAK1_576_577(loop).YMEDSTY[Pho]Y[Pho]K.+2b4	80.7	33.3

680.2162	626.2127	FAK1_576_577(loop).YMEDSTY[Pho]Y[Pho]K.+2b5	80.7	33.3
680.2162	633.1721	FAK1_576_577(loop).YMEDSTY[Pho]Y[Pho]K.+2y3	80.7	33.3
680.2162	734.2198	FAK1_576_577(loop).YMEDSTY[Pho]Y[Pho]K.+2y4	80.7	33.3
680.2162	821.2518	FAK1_576_577(loop).YMEDSTY[Pho]Y[Pho]K.+2y5	80.7	33.3
680.2162	936.2788	FAK1_576_577(loop).YMEDSTY[Pho]Y[Pho]K.+2y6	80.7	33.3
680.2162	1065.321	FAK1_576_577(loop).YMEDSTY[Pho]Y[Pho]K.+2y7	80.7	33.3
699.2329	650.2668	FAK2_579_580(loop).YIEDEDY[Pho]Y[Pho]K.+2b5	82.1	34
699.2329	765.2937	FAK2_579_580(loop).YIEDEDY[Pho]Y[Pho]K.+2b6	82.1	34
699.2329	633.1721	FAK2_579_580(loop).YIEDEDY[Pho]Y[Pho]K.+2y3	82.1	34
699.2329	748.1991	FAK2_579_580(loop).YIEDEDY[Pho]Y[Pho]K.+2y4	82.1	34
699.2329	992.2686	FAK2_579_580(loop).YIEDEDY[Pho]Y[Pho]K.+2y6	82.1	34
699.2329	1121.311	FAK2_579_580(loop).YIEDEDY[Pho]Y[Pho]K.+2y7	82.1	34
703.7954	1034.455	FER_714(loop).QEDGGVY[Pho]SSSGLK.+2y10	82.4	34.2
703.7954	1149.482	FER_714(loop).QEDGGVY[Pho]SSSGLK.+2y11	82.4	34.2
703.7954	491.2824	FER_714(loop).QEDGGVY[Pho]SSSGLK.+2y5	82.4	34.2
703.7954	578.3144	FER_714(loop).QEDGGVY[Pho]SSSGLK.+2y6	82.4	34.2
703.7954	821.3441	FER_714(loop).QEDGGVY[Pho]SSSGLK.+2y7	82.4	34.2
703.7954	920.4125	FER_714(loop).QEDGGVY[Pho]SSSGLK.+2y8	82.4	34.2
703.7954	977.434	FER_714(loop).QEDGGVY[Pho]SSSGLK.+2y9	82.4	34.2
737.8141	601.2464	FES_713(loop).EEADGVY[Pho]AASGLR.+2b6	84.9	35.4
737.8141	1030.472	FES_713(loop).EEADGVY[Pho]AASGLR.+2y10	84.9	35.4
737.8141	1145.499	FES_713(loop).EEADGVY[Pho]AASGLR.+2y11	84.9	35.4
737.8141	560.3151	FES_713(loop).EEADGVY[Pho]AASGLR.+2y6	84.9	35.4
737.8141	631.3522	FES_713(loop).EEADGVY[Pho]AASGLR.+2y7	84.9	35.4
737.8141	874.3819	FES_713(loop).EEADGVY[Pho]AASGLR.+2y8	84.9	35.4
737.8141	973.4503	FES_713(loop).EEADGVY[Pho]AASGLR.+2y9	84.9	35.4
775.4049	383.1925	FGFR1_307.IGPDNLPY[Pho]VQILK.+2b4	87.6	36.8
775.4049	497.2354	FGFR1_307.IGPDNLPY[Pho]VQILK.+2b5	87.6	36.8
775.4049	610.3195	FGFR1_307.IGPDNLPY[Pho]VQILK.+2b6	87.6	36.8
775.4049	843.4376	FGFR1_307.IGPDNLPY[Pho]VQILK.+2y6	87.6	36.8
775.4049	940.4903	FGFR1_307.IGPDNLPY[Pho]VQILK.+2y7	87.6	36.8
775.4049	1053.574	FGFR1_307.IGPDNLPY[Pho]VQILK.+2y8	87.6	36.8
775.4049	1167.617	FGFR1_307.IGPDNLPY[Pho]VQILK.+2y9	87.6	36.8
681.2996	415.2187	FGFR1_605_FGFR3_599.DLVSC[CAM]AY[Pho]QVAR.+2b4	80.8	33.4
681.2996	646.2865	FGFR1_605_FGFR3_599.DLVSC[CAM]AY[Pho]QVAR.+2b6	80.8	33.4
681.2996	345.2245	FGFR1_605_FGFR3_599.DLVSC[CAM]AY[Pho]QVAR.+2y3	80.8	33.4
681.2996	473.2831	FGFR1_605_FGFR3_599.DLVSC[CAM]AY[Pho]QVAR.+2y4	80.8	33.4
681.2996	716.3127	FGFR1_605_FGFR3_599.DLVSC[CAM]AY[Pho]QVAR.+2y5	80.8	33.4
681.2996	787.3498	FGFR1_605_FGFR3_599.DLVSC[CAM]AY[Pho]QVAR.+2y6	80.8	33.4
681.2996	947.3805	FGFR1_605_FGFR3_599.DLVSC[CAM]AY[Pho]QVAR.+2y7	80.8	33.4
681.2996	1034.413	FGFR1_605_FGFR3_599.DLVSC[CAM]AY[Pho]QVAR.+2y8	80.8	33.4
682.2596	503.2361	FGFR1_653_654(loop).DIHHIDY[Pho]Y[Pho]K.+2b4	80.9	33.4
682.2596	616.3202	FGFR1_653_654(loop).DIHHIDY[Pho]Y[Pho]K.+2b5	80.9	33.4
682.2596	731.3471	FGFR1_653_654(loop).DIHHIDY[Pho]Y[Pho]K.+2b6	80.9	33.4
682.2596	974.3768	FGFR1_653_654(loop).DIHHIDY[Pho]Y[Pho]K.+2b7	80.9	33.4

682.2596	748.1991	FGFR1_653_654(loop).DIHHIDY[Pho]Y[Pho]K.+2v4	80.9	33.4
682.2596	861.2831	FGFR1_653_654(loop).DIHHIDY[Pho]Y[Pho]K.+2y5	80.9	33.4
682.2596	998.342	FGFR1_653_654(loop).DIHHIDY[Pho]Y[Pho]K.+2y6	80.9	33.4
682.2596	1135.401	FGFR1_653_654(loop).DIHHIDY[Pho]Y[Pho]K.+2y7	80.9	33.4
455.1755	366.1772	FGFR1_653_654(loop).DIHHIDY[Pho]Y[Pho]K.+3b3	64.3	22.4
455.1755	503.2361	FGFR1_653_654(loop).DIHHIDY[Pho]Y[Pho]K.+3b4	64.3	22.4
455.1755	616.3202	FGFR1_653_654(loop).DIHHIDY[Pho]Y[Pho]K.+3b5	64.3	22.4
455.1755	731.3471	FGFR1_653_654(loop).DIHHIDY[Pho]Y[Pho]K.+3b6	64.3	22.4
455.1755	633.1721	FGFR1_653_654(loop).DIHHIDY[Pho]Y[Pho]K.+3v3	64.3	22.4
455.1755	748.1991	FGFR1_653_654(loop).DIHHIDY[Pho]Y[Pho]K.+3v4	64.3	22.4
455.1755	861.2831	FGFR1_653_654(loop).DIHHIDY[Pho]Y[Pho]K.+3v5	64.3	22.4
703.3127	415.2187	FGFR2_608.DLVSC[CAM]TY[Pho]QLAR.+2b4	82.4	34.2
703.3127	487.2987	FGFR2_608.DLVSC[CAM]TY[Pho]QLAR.+2y4	82.4	34.2
703.3127	730.3284	FGFR2_608.DLVSC[CAM]TY[Pho]QLAR.+2y5	82.4	34.2
703.3127	831.376	FGFR2_608.DLVSC[CAM]TY[Pho]QLAR.+2y6	82.4	34.2
703.3127	991.4067	FGFR2_608.DLVSC[CAM]TY[Pho]QLAR.+2y7	82.4	34.2
703.3127	1078.439	FGFR2_608.DLVSC[CAM]TY[Pho]QLAR.+2y8	82.4	34.2
703.3127	1177.507	FGFR2_608.DLVSC[CAM]TY[Pho]QLAR.+2y9	82.4	34.2
553.733	674.2255	FGFR2_616.GMEY[Pho]LASQK.+2b5	71.5	28.8
553.733	362.2034	FGFR2_616.GMEY[Pho]LASQK.+2v3	71.5	28.8
553.733	433.2405	FGFR2_616.GMEY[Pho]LASQK.+2v4	71.5	28.8
553.733	546.3246	FGFR2_616.GMEY[Pho]LASQK.+2v5	71.5	28.8
553.733	789.3542	FGFR2_616.GMEY[Pho]LASQK.+2v6	71.5	28.8
553.733	918.3968	FGFR2_616.GMEY[Pho]LASQK.+2v7	71.5	28.8
659.2436	457.2041	FGFR2_656_657(loop).DINNIDY[Pho]Y[Pho]K.+2b4	79.2	32.6
659.2436	570.2882	FGFR2_656_657(loop).DINNIDY[Pho]Y[Pho]K.+2b5	79.2	32.6
659.2436	748.1991	FGFR2_656_657(loop).DINNIDY[Pho]Y[Pho]K.+2y4	79.2	32.6
659.2436	861.2831	FGFR2_656_657(loop).DINNIDY[Pho]Y[Pho]K.+2y5	79.2	32.6
659.2436	975.3261	FGFR2_656_657(loop).DINNIDY[Pho]Y[Pho]K.+2y6	79.2	32.6
663.7438	466.2045	FGFR3_647_648(loop).DVHNLDY[Pho]Y[Pho]K.+2b4	79.5	32.8
663.7438	579.2885	FGFR3_647_648(loop).DVHNLDY[Pho]Y[Pho]K.+2b5	79.5	32.8
663.7438	694.3155	FGFR3_647_648(loop).DVHNLDY[Pho]Y[Pho]K.+2b6	79.5	32.8
663.7438	937.3451	FGFR3_647_648(loop).DVHNLDY[Pho]Y[Pho]K.+2b7	79.5	32.8
663.7438	748.1991	FGFR3_647_648(loop).DVHNLDY[Pho]Y[Pho]K.+2y4	79.5	32.8
663.7438	861.2831	FGFR3_647_648(loop).DVHNLDY[Pho]Y[Pho]K.+2y5	79.5	32.8
663.7438	975.3261	FGFR3_647_648(loop).DVHNLDY[Pho]Y[Pho]K.+2y6	79.5	32.8
800.4051	397.2809	FGFR4_754.VLLAVSEEY[Pho]LDLR.+2b4	89.5	37.7
800.4051	496.3493	FGFR4_754.VLLAVSEEY[Pho]LDLR.+2b5	89.5	37.7
800.4051	583.3814	FGFR4_754.VLLAVSEEY[Pho]LDLR.+2b6	89.5	37.7
800.4051	759.3437	FGFR4_754.VLLAVSEEY[Pho]LDLR.+2v5	89.5	37.7
800.4051	888.3863	FGFR4_754.VLLAVSEEY[Pho]LDLR.+2v6	89.5	37.7
800.4051	1104.461	FGFR4_754.VLLAVSEEY[Pho]LDLR.+2v8	89.5	37.7
800.4051	1203.529	FGFR4_754.VLLAVSEEY[Pho]LDLR.+2v9	89.5	37.7
473.7233	372.0955	FGR_180_FYN_185_YES_194.GAY[Pho]SLSIR.+2b3	65.7	25.9
473.7233	459.1275	FGR_180_FYN_185_YES_194.GAY[Pho]SLSIR.+2b4	65.7	25.9

473.7233	572.2116	FGR_180_FYN_185_YES_194.GAY[Pho]SLSIR.+2b5	65.7	25.9
473.7233	375.235	FGR_180_FYN_185_YES_194.GAY[Pho]SLSIR.+2y3	65.7	25.9
473.7233	488.3191	FGR_180_FYN_185_YES_194.GAY[Pho]SLSIR.+2y4	65.7	25.9
473.7233	575.3511	FGR_180_FYN_185_YES_194.GAY[Pho]SLSIR.+2y5	65.7	25.9
473.7233	818.3808	FGR_180_FYN_185_YES_194.GAY[Pho]SLSIR.+2y6	65.7	25.9
725.2797	490.2984	FGR_208.LDMGGY[Pho]Y[Pho]ITTR.+2y4	84	35
725.2797	733.328	FGR_208.LDMGGY[Pho]Y[Pho]ITTR.+2y5	84	35
725.2797	976.3577	FGR_208.LDMGGY[Pho]Y[Pho]ITTR.+2y6	84	35
725.2797	1033.379	FGR_208.LDMGGY[Pho]Y[Pho]ITTR.+2y7	84	35
725.2797	1090.401	FGR_208.LDMGGY[Pho]Y[Pho]ITTR.+2y8	84	35
725.2797	1221.441	FGR_208.LDMGGY[Pho]Y[Pho]ITTR.+2y9	84	35
696.7423	814.2291	FGR_412(loop).DDEY[Pho]NPC[CAM]QGSK.+2b6	81.9	33.9
696.7423	291.1663	FGR_412(loop).DDEY[Pho]NPC[CAM]QGSK.+2y3	81.9	33.9
696.7423	419.2249	FGR_412(loop).DDEY[Pho]NPC[CAM]QGSK.+2y4	81.9	33.9
696.7423	579.2555	FGR_412(loop).DDEY[Pho]NPC[CAM]QGSK.+2y5	81.9	33.9
696.7423	676.3083	FGR_412(loop).DDEY[Pho]NPC[CAM]QGSK.+2y6	81.9	33.9
696.7423	790.3512	FGR_412(loop).DDEY[Pho]NPC[CAM]QGSK.+2y7	81.9	33.9
520.2046	665.1855	FLT3_597.EY[Pho]EYDLK.+2b4	69	27.6
520.2046	780.2124	FLT3_597.EY[Pho]EYDLK.+2b5	69	27.6
520.2046	538.2871	FLT3_597.EY[Pho]EYDLK.+2y4	69	27.6
520.2046	667.3297	FLT3_597.EY[Pho]EYDLK.+2y5	69	27.6
520.2046	665.1855	FLT3_599.EY[Pho]DLK.+2b4	69	27.6
520.2046	780.2124	FLT3_599.EY[Pho]DLK.+2b5	69	27.6
520.2046	618.2535	FLT3_599.EY[Pho]DLK.+2y4	69	27.6
520.2046	747.2961	FLT3_599.EY[Pho]DLK.+2y5	69	27.6
689.7891	447.1908	FLT3_842(loop).DIMSDSNY[Pho]VVR.+2b4	81.4	33.7
689.7891	616.2854	FLT3_842(loop).DIMSDSNY[Pho]VVR.+2y4	81.4	33.7
689.7891	730.3284	FLT3_842(loop).DIMSDSNY[Pho]VVR.+2y5	81.4	33.7
689.7891	817.3604	FLT3_842(loop).DIMSDSNY[Pho]VVR.+2y6	81.4	33.7
689.7891	932.3873	FLT3_842(loop).DIMSDSNY[Pho]VVR.+2y7	81.4	33.7
689.7891	1019.419	FLT3_842(loop).DIMSDSNY[Pho]VVR.+2y8	81.4	33.7
689.7891	1150.46	FLT3_842(loop).DIMSDSNY[Pho]VVR.+2y9	81.4	33.7
660.2612	458.1882	FRK_387(loop).VDNEDIY[Pho]ESR.+2b4	79.3	32.6
660.2612	573.2151	FRK_387(loop).VDNEDIY[Pho]ESR.+2b5	79.3	32.6
660.2612	634.2232	FRK_387(loop).VDNEDIY[Pho]ESR.+2y4	79.3	32.6
660.2612	747.3073	FRK_387(loop).VDNEDIY[Pho]ESR.+2y5	79.3	32.6
660.2612	862.3342	FRK_387(loop).VDNEDIY[Pho]ESR.+2y6	79.3	32.6
660.2612	991.3768	FRK_387(loop).VDNEDIY[Pho]ESR.+2y7	79.3	32.6
660.2612	1105.42	FRK_387(loop).VDNEDIY[Pho]ESR.+2y8	79.3	32.6
716.7809	1056.348	FYN_213_214_YES_222_223.LDNGGY[Pho]Y[Pho]ITTR.+2b8	83.4	34.7
716.7809	1157.395	FYN_213_214_YES_222_223.LDNGGY[Pho]Y[Pho]ITTR.+2b9	83.4	34.7
716.7809	733.328	FYN_213_214_YES_222_223.LDNGGY[Pho]Y[Pho]ITTR.+2y5	83.4	34.7
716.7809	976.3577	FYN_213_214_YES_222_223.LDNGGY[Pho]Y[Pho]ITTR.+2y6	83.4	34.7
716.7809	1033.379	FYN_213_214_YES_222_223.LDNGGY[Pho]Y[Pho]ITTR.+2y7	83.4	34.7
716.7809	1090.401	FYN_213_214_YES_222_223.LDNGGY[Pho]Y[Pho]ITTR.+2y8	83.4	34.7

716.7809	1204.444	FYN_213_214_YES_222_223.LDNGGY[Pho]Y[Pho]ITTR.+2y9	83.4	34.7
657.7976	656.3039	FYN_440_SRC_439_YES_446.WTAPEAALY[Pho]GR.+2b6	79.1	32.5
657.7976	588.2541	FYN_440_SRC_439_YES_446.WTAPEAALY[Pho]GR.+2y4	79.1	32.5
657.7976	659.2913	FYN_440_SRC_439_YES_446.WTAPEAALY[Pho]GR.+2y5	79.1	32.5
657.7976	730.3284	FYN_440_SRC_439_YES_446.WTAPEAALY[Pho]GR.+2y6	79.1	32.5
657.7976	859.371	FYN_440_SRC_439_YES_446.WTAPEAALY[Pho]GR.+2y7	79.1	32.5
657.7976	956.4237	FYN_440_SRC_439_YES_446.WTAPEAALY[Pho]GR.+2y8	79.1	32.5
657.7976	1027.461	FYN_440_SRC_439_YES_446.WTAPEAALY[Pho]GR.+2y9	79.1	32.5
710.3188	444.2089	HCK_209.TLDNGGFY[Pho]ISPR.+2b4	82.9	34.4
710.3188	1205.499	HCK_209.TLDNGGFY[Pho]ISPR.+2y10	82.9	34.4
710.3188	472.2878	HCK_209.TLDNGGFY[Pho]ISPR.+2y4	82.9	34.4
710.3188	715.3175	HCK_209.TLDNGGFY[Pho]ISPR.+2y5	82.9	34.4
710.3188	862.3859	HCK_209.TLDNGGFY[Pho]ISPR.+2y6	82.9	34.4
710.3188	919.4073	HCK_209.TLDNGGFY[Pho]ISPR.+2y7	82.9	34.4
710.3188	976.4288	HCK_209.TLDNGGFY[Pho]ISPR.+2y8	82.9	34.4
645.2741	457.2293	HCK_LYN_411_397(loop).VIEDNEY[Pho]TAR.+2b4	78.2	32.1
645.2741	571.2722	HCK_LYN_411_397(loop).VIEDNEY[Pho]TAR.+2b5	78.2	32.1
645.2741	347.2037	HCK_LYN_411_397(loop).VIEDNEY[Pho]TAR.+2y3	78.2	32.1
645.2741	590.2334	HCK_LYN_411_397(loop).VIEDNEY[Pho]TAR.+2y4	78.2	32.1
645.2741	719.276	HCK_LYN_411_397(loop).VIEDNEY[Pho]TAR.+2y5	78.2	32.1
645.2741	833.3189	HCK_LYN_411_397(loop).VIEDNEY[Pho]TAR.+2y6	78.2	32.1
645.2741	948.3459	HCK_LYN_411_397(loop).VIEDNEY[Pho]TAR.+2y7	78.2	32.1
645.2741	1077.388	HCK_LYN_411_397(loop).VIEDNEY[Pho]TAR.+2y8	78.2	32.1
876.3891	428.214	IGF1R_1014.ELGQGSFGMVY[Pho]EGVAK.+2b4	95	40.4
876.3891	1180.511	IGF1R_1014.ELGQGSFGMVY[Pho]EGVAK.+2y10	95	40.4
876.3891	503.2824	IGF1R_1014.ELGQGSFGMVY[Pho]EGVAK.+2y5	95	40.4
876.3891	746.312	IGF1R_1014.ELGQGSFGMVY[Pho]EGVAK.+2y6	95	40.4
876.3891	845.3805	IGF1R_1014.ELGQGSFGMVY[Pho]EGVAK.+2y7	95	40.4
876.3891	976.4209	IGF1R_1014.ELGQGSFGMVY[Pho]EGVAK.+2y8	95	40.4
876.3891	1033.442	IGF1R_1014.ELGQGSFGMVY[Pho]EGVAK.+2y9	95	40.4
659.2554	601.1905	IGF1R_1161_INSR_1185.DIY[Pho]ETDYR.+2b4	79.2	32.6
659.2554	702.2382	IGF1R_1161_INSR_1185.DIY[Pho]ETDYR.+2b5	79.2	32.6
659.2554	817.2652	IGF1R_1161_INSR_1185.DIY[Pho]ETDYR.+2b6	79.2	32.6
659.2554	616.2726	IGF1R_1161_INSR_1185.DIY[Pho]ETDYR.+2y4	79.2	32.6
659.2554	846.3628	IGF1R_1161_INSR_1185.DIY[Pho]ETDYR.+2y6	79.2	32.6
659.2554	1089.392	IGF1R_1161_INSR_1185.DIY[Pho]ETDYR.+2y7	79.2	32.6
614.9221	726.2131	INSR_1355.SY[Pho]EEHIPYTHMNGGK.+3b5	75.9	31
614.9221	839.2971	INSR_1355.SY[Pho]EEHIPYTHMNGGK.+3b6	75.9	31
614.9221	643.2981	INSR_1355.SY[Pho]EEHIPYTHMNGGK.+3y6	75.9	31
614.9221	744.3457	INSR_1355.SY[Pho]EEHIPYTHMNGGK.+3y7	75.9	31
614.9221	907.4091	INSR_1355.SY[Pho]EEHIPYTHMNGGK.+3y8	75.9	31
614.9221	1004.462	INSR_1355.SY[Pho]EEHIPYTHMNGGK.+3y9	75.9	31
614.9221	509.1878	INSR_1361.SYEEHIPY[Pho]THMNGGK.+3b4	75.9	31
614.9221	759.3308	INSR_1361.SYEEHIPY[Pho]THMNGGK.+3b6	75.9	31
614.9221	375.1987	INSR_1361.SYEEHIPY[Pho]THMNGGK.+3y4	75.9	31

614.9221	506.2391	INSR_1361.SYEEHIPY[Pho]THMNGGK.+3v5	75.9	31
614.9221	643.2981	INSR_1361.SYEEHIPY[Pho]THMNGGK.+3v6	75.9	31
614.9221	744.3457	INSR_1361.SYEEHIPY[Pho]THMNGGK.+3v7	75.9	31
614.9221	1084.428	INSR_1361.SYEEHIPY[Pho]THMNGGK.+3v9	75.9	31
652.2476	688.2226	INSRR_1141.DVY[Pho]ETDYR.+2b5	78.7	32.3
652.2476	803.2495	INSRR_1141.DVY[Pho]ETDYR.+2b6	78.7	32.3
652.2476	966.3128	INSRR_1141.DVY[Pho]ETDYR.+2b7	78.7	32.3
652.2476	616.2726	INSRR_1141.DVY[Pho]ETDYR.+2y4	78.7	32.3
652.2476	717.3202	INSRR_1141.DVY[Pho]ETDYR.+2y5	78.7	32.3
652.2476	846.3628	INSRR_1141.DVY[Pho]ETDYR.+2y6	78.7	32.3
652.2476	1089.392	INSRR_1141.DVY[Pho]ETDYR.+2y7	78.7	32.3
821.3558	590.2821	ITK_512(loop).FVLDDQY[Pho]TSSTGTK.+2b5	91	38.4
821.3558	1167.457	ITK_512(loop).FVLDDQY[Pho]TSSTGTK.+2y10	91	38.4
821.3558	493.2617	ITK_512(loop).FVLDDQY[Pho]TSSTGTK.+2y5	91	38.4
821.3558	580.2937	ITK_512(loop).FVLDDQY[Pho]TSSTGTK.+2y6	91	38.4
821.3558	681.3414	ITK_512(loop).FVLDDQY[Pho]TSSTGTK.+2y7	91	38.4
821.3558	924.371	ITK_512(loop).FVLDDQY[Pho]TSSTGTK.+2y8	91	38.4
821.3558	1052.43	ITK_512(loop).FVLDDQY[Pho]TSSTGTK.+2y9	91	38.4
529.2519	583.2164	JAK1_220.Y[Pho]IPETLNK.+2b4	69.7	27.9
529.2519	684.264	JAK1_220.Y[Pho]IPETLNK.+2b5	69.7	27.9
529.2519	797.3481	JAK1_220.Y[Pho]IPETLNK.+2b6	69.7	27.9
529.2519	475.2875	JAK1_220.Y[Pho]IPETLNK.+2y4	69.7	27.9
529.2519	604.3301	JAK1_220.Y[Pho]IPETLNK.+2y5	69.7	27.9
529.2519	701.3828	JAK1_220.Y[Pho]IPETLNK.+2y6	69.7	27.9
489.6912	547.1258	JAK1_993.GMDY[Pho]LGSR.+2b4	66.8	26.5
489.6912	717.2314	JAK1_993.GMDY[Pho]LGSR.+2b6	66.8	26.5
489.6912	675.2862	JAK1_993.GMDY[Pho]LGSR.+2y5	66.8	26.5
489.6912	790.3131	JAK1_993.GMDY[Pho]LGSR.+2y6	66.8	26.5
968.4404	685.2788	JAK2_201.ENDQTPLAIY[Pho]NSISYK.+2b6	101.7	43.7
968.4404	798.3628	JAK2_201.ENDQTPLAIY[Pho]NSISYK.+2b7	101.7	43.7
968.4404	869.3999	JAK2_201.ENDQTPLAIY[Pho]NSISYK.+2b8	101.7	43.7
968.4404	982.484	JAK2_201.ENDQTPLAIY[Pho]NSISYK.+2b9	101.7	43.7
968.4404	711.3672	JAK2_201.ENDQTPLAIY[Pho]NSISYK.+2y6	101.7	43.7
968.4404	954.3968	JAK2_201.ENDQTPLAIY[Pho]NSISYK.+2y7	101.7	43.7
968.4404	1067.481	JAK2_201.ENDQTPLAIY[Pho]NSISYK.+2y8	101.7	43.7
968.4404	1138.518	JAK2_201.ENDQTPLAIY[Pho]NSISYK.+2y9	101.7	43.7
968.4404	869.3999	JAK2_206.ENDQTPLAIYNSISY[Pho]K.+2b8	101.7	43.7
968.4404	982.484	JAK2_206.ENDQTPLAIYNSISY[Pho]K.+2b9	101.7	43.7
968.4404	477.1745	JAK2_206.ENDQTPLAIYNSISY[Pho]K.+2y3	101.7	43.7
968.4404	677.2906	JAK2_206.ENDQTPLAIYNSISY[Pho]K.+2y5	101.7	43.7
968.4404	791.3335	JAK2_206.ENDQTPLAIYNSISY[Pho]K.+2y6	101.7	43.7
968.4404	954.3968	JAK2_206.ENDQTPLAIYNSISY[Pho]K.+2y7	101.7	43.7
968.4404	1067.481	JAK2_206.ENDQTPLAIYNSISY[Pho]K.+2y8	101.7	43.7
968.4404	1138.518	JAK2_206.ENDQTPLAIYNSISY[Pho]K.+2y9	101.7	43.7
619.8001	737.2654	JAK2_221.IQDY[Pho]HILTR.+2b5	76.3	31.2

619.8001	850.3495	JAK2_221.IQDY[Pho]HILTR.+2b6	76.3	31.2
619.8001	963.4336	JAK2_221.IQDY[Pho]HILTR.+2b7	76.3	31.2
619.8001	502.3348	JAK2_221.IQDY[Pho]HILTR.+2y4	76.3	31.2
619.8001	639.3937	JAK2_221.IQDY[Pho]HILTR.+2y5	76.3	31.2
619.8001	882.4233	JAK2_221.IQDY[Pho]HILTR.+2y6	76.3	31.2
619.8001	997.4503	JAK2_221.IQDY[Pho]HILTR.+2y7	76.3	31.2
637.303	401.1667	JAK2_570.EVG DY[Pho]GQLHETE VLLK.+3b4	77.6	32.3
637.303	644.1963	JAK2_570.EVG DY[Pho]GQLHETE VLLK.+3b5	77.6	32.3
637.303	1209.684	JAK2_570.EVG DY[Pho]GQLHETE VLLK.+3y10	77.6	32.3
637.303	601.3919	JAK2_570.EVG DY[Pho]GQLHETE VLLK.+3y5	77.6	32.3
637.303	702.4396	JAK2_570.EVG DY[Pho]GQLHETE VLLK.+3y6	77.6	32.3
637.303	831.4822	JAK2_570.EVG DY[Pho]GQLHETE VLLK.+3y7	77.6	32.3
637.303	968.5411	JAK2_570.EVG DY[Pho]GQLHETE VLLK.+3y8	77.6	32.3
637.303	1081.625	JAK2_570.EVG DY[Pho]GQLHETE VLLK.+3y9	77.6	32.3
767.8724	730.2881	JAK2_931.LIMEY[Pho]LPYGSLR.+2b5	87.1	36.5
767.8724	843.3722	JAK2_931.LIMEY[Pho]LPYGSLR.+2b6	87.1	36.5
767.8724	595.3198	JAK2_931.LIMEY[Pho]LPYGSLR.+2y5	87.1	36.5
767.8724	692.3726	JAK2_931.LIMEY[Pho]LPYGSLR.+2y6	87.1	36.5
767.8724	805.4567	JAK2_931.LIMEY[Pho]LPYGSLR.+2y7	87.1	36.5
767.8724	1048.486	JAK2_931.LIMEY[Pho]LPYGSLR.+2y8	87.1	36.5
767.8724	1177.529	JAK2_931.LIMEY[Pho]LPYGSLR.+2y9	87.1	36.5
807.8556	730.2881	JAK2_931_934.LIMEY[Pho]LPY[Pho]GSLR.+2b5	90	37.9
807.8556	843.3722	JAK2_931_934.LIMEY[Pho]LPY[Pho]GSLR.+2b6	90	37.9
807.8556	432.2565	JAK2_931_934.LIMEY[Pho]LPY[Pho]GSLR.+2y4	90	37.9
807.8556	675.2862	JAK2_931_934.LIMEY[Pho]LPY[Pho]GSLR.+2y5	90	37.9
807.8556	772.3389	JAK2_931_934.LIMEY[Pho]LPY[Pho]GSLR.+2y6	90	37.9
807.8556	885.423	JAK2_931_934.LIMEY[Pho]LPY[Pho]GSLR.+2y7	90	37.9
807.8556	1128.453	JAK2_931_934.LIMEY[Pho]LPY[Pho]GSLR.+2y8	90	37.9
767.8724	650.3218	JAK2_934.LIMEYLPY[Pho]GSLR.+2b5	87.1	36.5
767.8724	763.4059	JAK2_934.LIMEYLPY[Pho]GSLR.+2b6	87.1	36.5
767.8724	1103.488	JAK2_934.LIMEYLPY[Pho]GSLR.+2b8	87.1	36.5
767.8724	1160.51	JAK2_934.LIMEYLPY[Pho]GSLR.+2b9	87.1	36.5
767.8724	675.2862	JAK2_934.LIMEYLPY[Pho]GSLR.+2y5	87.1	36.5
767.8724	772.3389	JAK2_934.LIMEYLPY[Pho]GSLR.+2y6	87.1	36.5
767.8724	1048.486	JAK2_934.LIMEYLPY[Pho]GSLR.+2y8	87.1	36.5
767.8724	1177.529	JAK2_934.LIMEYLPY[Pho]GSLR.+2y9	87.1	36.5
759.3482	716.2725	JAK3_904.LVMEY[Pho]LPSGC[CAM]LR.+2b5	86.5	36.2
759.3482	829.3566	JAK3_904.LVMEY[Pho]LPSGC[CAM]LR.+2b6	86.5	36.2
759.3482	592.2872	JAK3_904.LVMEY[Pho]LPSGC[CAM]LR.+2y5	86.5	36.2
759.3482	689.3399	JAK3_904.LVMEY[Pho]LPSGC[CAM]LR.+2y6	86.5	36.2
759.3482	802.424	JAK3_904.LVMEY[Pho]LPSGC[CAM]LR.+2y7	86.5	36.2
759.3482	1045.454	JAK3_904.LVMEY[Pho]LPSGC[CAM]LR.+2y8	86.5	36.2
759.3482	1174.496	JAK3_904.LVMEY[Pho]LPSGC[CAM]LR.+2y9	86.5	36.2
652.8196	583.2891	JAK3_929.LLLY[Pho]SSQIC[CAM]K.+2b4	78.7	32.4
652.8196	670.3212	JAK3_929.LLLY[Pho]SSQIC[CAM]K.+2b5	78.7	32.4

652.8196	757.3532	JAK3_929.LLLY[Pho]SSQIC[CAM]K.+2b6	78.7	32.4
652.8196	885.4118	JAK3_929.LLLY[Pho]SSQIC[CAM]K.+2b7	78.7	32.4
652.8196	998.4958	JAK3_929.LLLY[Pho]SSQIC[CAM]K.+2b8	78.7	32.4
652.8196	635.3181	JAK3_929.LLLY[Pho]SSQIC[CAM]K.+2y5	78.7	32.4
652.8196	1078.464	JAK3_929.LLLY[Pho]SSQIC[CAM]K.+2y8	78.7	32.4
487.6747	602.0935	JAK3_980_981(loop).DY[Pho]Y[Pho]VVR.+2b3	66.7	26.4
487.6747	701.162	JAK3_980_981(loop).DY[Pho]Y[Pho]VVR.+2b4	66.7	26.4
487.6747	373.2558	JAK3_980_981(loop).DY[Pho]Y[Pho]VVR.+2y3	66.7	26.4
487.6747	616.2854	JAK3_980_981(loop).DY[Pho]Y[Pho]VVR.+2y4	66.7	26.4
564.9334	485.1796	KIT_547.Y[Pho]LQKPMYEVQWK.+3b3	72.3	28.3
564.9334	613.2745	KIT_547.Y[Pho]LQKPMYEVQWK.+3b4	72.3	28.3
564.9334	841.3678	KIT_547.Y[Pho]LQKPMYEVQWK.+3b6	72.3	28.3
564.9334	560.3191	KIT_547.Y[Pho]LQKPMYEVQWK.+3y4	72.3	28.3
564.9334	689.3617	KIT_547.Y[Pho]LQKPMYEVQWK.+3y5	72.3	28.3
564.9334	852.425	KIT_547.Y[Pho]LQKPMYEVQWK.+3y6	72.3	28.3
564.9334	1080.518	KIT_547.Y[Pho]LQKPMYEVQWK.+3y8	72.3	28.3
591.5888	613.2745	KIT_547_553.Y[Pho]LQKPMY[Pho]EVQWK.+3b4	74.2	29.8
591.5888	841.3678	KIT_547_553.Y[Pho]LQKPMY[Pho]EVQWK.+3b6	74.2	29.8
591.5888	1084.397	KIT_547_553.Y[Pho]LQKPMY[Pho]EVQWK.+3b7	74.2	29.8
591.5888	461.2507	KIT_547_553.Y[Pho]LQKPMY[Pho]EVQWK.+3y3	74.2	29.8
591.5888	560.3191	KIT_547_553.Y[Pho]LQKPMY[Pho]EVQWK.+3y4	74.2	29.8
591.5888	689.3617	KIT_547_553.Y[Pho]LQKPMY[Pho]EVQWK.+3y5	74.2	29.8
591.5888	932.3914	KIT_547_553.Y[Pho]LQKPMY[Pho]EVQWK.+3y6	74.2	29.8
591.5888	1160.485	KIT_547_553.Y[Pho]LQKPMY[Pho]EVQWK.+3y8	74.2	29.8
564.9334	405.2132	KIT_553.YLQKPMY[Pho]EVQWK.+3b3	72.3	28.3
564.9334	533.3082	KIT_553.YLQKPMY[Pho]EVQWK.+3b4	72.3	28.3
564.9334	761.4015	KIT_553.YLQKPMY[Pho]EVQWK.+3b6	72.3	28.3
564.9334	560.3191	KIT_553.YLQKPMY[Pho]EVQWK.+3y4	72.3	28.3
564.9334	689.3617	KIT_553.YLQKPMY[Pho]EVQWK.+3y5	72.3	28.3
564.9334	932.3914	KIT_553.YLQKPMY[Pho]EVQWK.+3y6	72.3	28.3
564.9334	1063.432	KIT_553.YLQKPMY[Pho]EVQWK.+3y7	72.3	28.3
622.3203	399.2238	KIT_609.VVEATAY[Pho]GLIK.+2b4	76.5	31.3
622.3203	500.2715	KIT_609.VVEATAY[Pho]GLIK.+2b5	76.5	31.3
622.3203	430.3024	KIT_609.VVEATAY[Pho]GLIK.+2y4	76.5	31.3
622.3203	673.3321	KIT_609.VVEATAY[Pho]GLIK.+2y5	76.5	31.3
622.3203	744.3692	KIT_609.VVEATAY[Pho]GLIK.+2y6	76.5	31.3
622.3203	845.4168	KIT_609.VVEATAY[Pho]GLIK.+2y7	76.5	31.3
622.3203	916.454	KIT_609.VVEATAY[Pho]GLIK.+2y8	76.5	31.3
622.3203	1045.497	KIT_609.VVEATAY[Pho]GLIK.+2y9	76.5	31.3
509.7157	431.1521	KIT_823(loop).NDSNY[Pho]VVK.+2b4	68.3	27.2
509.7157	674.1818	KIT_823(loop).NDSNY[Pho]VVK.+2b5	68.3	27.2
509.7157	773.2502	KIT_823(loop).NDSNY[Pho]VVK.+2b6	68.3	27.2
509.7157	588.2793	KIT_823(loop).NDSNY[Pho]VVK.+2y4	68.3	27.2
509.7157	702.3222	KIT_823(loop).NDSNY[Pho]VVK.+2y5	68.3	27.2
509.7157	789.3542	KIT_823(loop).NDSNY[Pho]VVK.+2y6	68.3	27.2

531.6645	430.1569	KSYK_525_526(loop).ADENY[Pho]Y[Pho]K.+2b4	69.9	28
531.6645	673.1865	KSYK_525_526(loop).ADENY[Pho]Y[Pho]K.+2b5	69.9	28
531.6645	633.1721	KSYK_525_526(loop).ADENY[Pho]Y[Pho]K.+2y3	69.9	28
531.6645	747.2151	KSYK_525_526(loop).ADENY[Pho]Y[Pho]K.+2y4	69.9	28
531.6645	876.2576	KSYK_525_526(loop).ADENY[Pho]Y[Pho]K.+2y5	69.9	28
651.2979	1059.462	KSYK_74.ELNGTY[Pho]AIAGGR.+2y10	78.6	32.3
651.2979	360.199	KSYK_74.ELNGTY[Pho]AIAGGR.+2y4	78.6	32.3
651.2979	473.2831	KSYK_74.ELNGTY[Pho]AIAGGR.+2y5	78.6	32.3
651.2979	544.3202	KSYK_74.ELNGTY[Pho]AIAGGR.+2y6	78.6	32.3
651.2979	787.3498	KSYK_74.ELNGTY[Pho]AIAGGR.+2y7	78.6	32.3
651.2979	888.3975	KSYK_74.ELNGTY[Pho]AIAGGR.+2y8	78.6	32.3
651.2979	945.419	KSYK_74.ELNGTY[Pho]AIAGGR.+2y9	78.6	32.3
732.3187	427.23	LCK_263.LGAGQFGEVWMGY[Pho]YNGHTK.+3b5	84.5	37.4
732.3187	760.3624	LCK_263.LGAGQFGEVWMGY[Pho]YNGHTK.+3b8	84.5	37.4
732.3187	859.4308	LCK_263.LGAGQFGEVWMGY[Pho]YNGHTK.+3b9	84.5	37.4
732.3187	442.2409	LCK_263.LGAGQFGEVWMGY[Pho]YNGHTK.+3v4	84.5	37.4
732.3187	556.2838	LCK_263.LGAGQFGEVWMGY[Pho]YNGHTK.+3v5	84.5	37.4
732.3187	719.3471	LCK_263.LGAGQFGEVWMGY[Pho]YNGHTK.+3v6	84.5	37.4
732.3187	962.3768	LCK_263.LGAGQFGEVWMGY[Pho]YNGHTK.+3v7	84.5	37.4
732.3187	1019.398	LCK_263.LGAGQFGEVWMGY[Pho]YNGHTK.+3v8	84.5	37.4
732.3187	427.23	LCK_264.LGAGQFGEVWMGY[Pho]NGHTK.+3b5	84.5	37.4
732.3187	760.3624	LCK_264.LGAGQFGEVWMGY[Pho]NGHTK.+3b8	84.5	37.4
732.3187	859.4308	LCK_264.LGAGQFGEVWMGY[Pho]NGHTK.+3b9	84.5	37.4
732.3187	442.2409	LCK_264.LGAGQFGEVWMGY[Pho]NGHTK.+3v4	84.5	37.4
732.3187	556.2838	LCK_264.LGAGQFGEVWMGY[Pho]NGHTK.+3v5	84.5	37.4
732.3187	799.3134	LCK_264.LGAGQFGEVWMGY[Pho]NGHTK.+3v6	84.5	37.4
732.3187	962.3768	LCK_264.LGAGQFGEVWMGY[Pho]NGHTK.+3v7	84.5	37.4
732.3187	1019.398	LCK_264.LGAGQFGEVWMGY[Pho]NGHTK.+3v8	84.5	37.4
896.4213	585.2667	LCK_414.WTAPEAINY[Pho]GTFTIK.+2b5	96.5	41.1
896.4213	656.3039	LCK_414.WTAPEAINY[Pho]GTFTIK.+2b6	96.5	41.1
896.4213	1207.576	LCK_414.WTAPEAINY[Pho]GTFTIK.+2v10	96.5	41.1
896.4213	508.313	LCK_414.WTAPEAINY[Pho]GTFTIK.+2y4	96.5	41.1
896.4213	666.3821	LCK_414.WTAPEAINY[Pho]GTFTIK.+2v6	96.5	41.1
896.4213	909.4118	LCK_414.WTAPEAINY[Pho]GTFTIK.+2y7	96.5	41.1
896.4213	1023.455	LCK_414.WTAPEAINY[Pho]GTFTIK.+2y8	96.5	41.1
896.4213	1136.539	LCK_414.WTAPEAINY[Pho]GTFTIK.+2y9	96.5	41.1
710.9772	599.297	LCK_470.MVRPDNC[CAM]PEELY[Pho]QLMR.+3b5	82.9	36.3
710.9772	713.3399	LCK_470.MVRPDNC[CAM]PEELY[Pho]QLMR.+3b6	82.9	36.3
710.9772	873.3706	LCK_470.MVRPDNC[CAM]PEELY[Pho]QLMR.+3b7	82.9	36.3
710.9772	1099.466	LCK_470.MVRPDNC[CAM]PEELY[Pho]QLMR.+3b9	82.9	36.3
710.9772	547.3021	LCK_470.MVRPDNC[CAM]PEELY[Pho]QLMR.+3y4	82.9	36.3
710.9772	790.3317	LCK_470.MVRPDNC[CAM]PEELY[Pho]QLMR.+3y5	82.9	36.3
710.9772	903.4158	LCK_470.MVRPDNC[CAM]PEELY[Pho]QLMR.+3y6	82.9	36.3
966.4506	635.1749	LMTK1_283(loop).EDY[Pho]FVTADQLWVPLR.+2b4	101.6	43.6
966.4506	734.2433	LMTK1_283(loop).EDY[Pho]FVTADQLWVPLR.+2b5	101.6	43.6

966.4506	1198.658	LMTK1_283(loop).EDY[Pho]FVTADQLWVPLR.+2v10	101.6	43.6
966.4506	484.3242	LMTK1_283(loop).EDY[Pho]FVTADQLWVPLR.+2y4	101.6	43.6
966.4506	670.4035	LMTK1_283(loop).EDY[Pho]FVTADQLWVPLR.+2y5	101.6	43.6
966.4506	1026.573	LMTK1_283(loop).EDY[Pho]FVTADQLWVPLR.+2y8	101.6	43.6
966.4506	1097.61	LMTK1_283(loop).EDY[Pho]FVTADQLWVPLR.+2y9	101.6	43.6
475.7046	432.2241	LMTK1_479.GLNFEY[Pho]K.+2b4	65.8	26
475.7046	561.2667	LMTK1_479.GLNFEY[Pho]K.+2b5	65.8	26
475.7046	519.1851	LMTK1_479.GLNFEY[Pho]K.+2y3	65.8	26
475.7046	666.2535	LMTK1_479.GLNFEY[Pho]K.+2y4	65.8	26
475.7046	780.2964	LMTK1_479.GLNFEY[Pho]K.+2y5	65.8	26
556.2523	478.1374	LMTK2_1448.Y[Pho]FSPPPPAR.+2b3	71.7	28.9
556.2523	575.1901	LMTK2_1448.Y[Pho]FSPPPPAR.+2b4	71.7	28.9
556.2523	672.2429	LMTK2_1448.Y[Pho]FSPPPPAR.+2b5	71.7	28.9
556.2523	440.2616	LMTK2_1448.Y[Pho]FSPPPPAR.+2y4	71.7	28.9
556.2523	537.3144	LMTK2_1448.Y[Pho]FSPPPPAR.+2y5	71.7	28.9
556.2523	634.3671	LMTK2_1448.Y[Pho]FSPPPPAR.+2y6	71.7	28.9
556.2523	721.3991	LMTK2_1448.Y[Pho]FSPPPPAR.+2y7	71.7	28.9
571.5737	505.1806	LMTK2_1468.STEQSWPHSAPY[Pho]SR.+3y3	72.8	28.7
571.5737	602.2334	LMTK2_1468.STEQSWPHSAPY[Pho]SR.+3y4	72.8	28.7
571.5737	673.2705	LMTK2_1468.STEQSWPHSAPY[Pho]SR.+3y5	72.8	28.7
571.5737	760.3025	LMTK2_1468.STEQSWPHSAPY[Pho]SR.+3y6	72.8	28.7
571.5737	897.3615	LMTK2_1468.STEQSWPHSAPY[Pho]SR.+3y7	72.8	28.7
571.5737	994.4142	LMTK2_1468.STEQSWPHSAPY[Pho]SR.+3y8	72.8	28.7
604.2237	488.1065	LMTK2_295(loop).EDY[Pho]IETDDK.+2b3	75.2	30.6
604.2237	601.1905	LMTK2_295(loop).EDY[Pho]IETDDK.+2b4	75.2	30.6
604.2237	730.2331	LMTK2_295(loop).EDY[Pho]IETDDK.+2b5	75.2	30.6
604.2237	478.2144	LMTK2_295(loop).EDY[Pho]IETDDK.+2y4	75.2	30.6
604.2237	607.257	LMTK2_295(loop).EDY[Pho]IETDDK.+2y5	75.2	30.6
604.2237	720.341	LMTK2_295(loop).EDY[Pho]IETDDK.+2y6	75.2	30.6
604.2237	963.3707	LMTK2_295(loop).EDY[Pho]IETDDK.+2y7	75.2	30.6
673.2411	844.2202	LMTK3_296_297(loop).EDY[Pho]Y[Pho]LTPER.+2b5	80.2	33.1
673.2411	502.262	LMTK3_296_297(loop).EDY[Pho]Y[Pho]LTPER.+2y4	80.2	33.1
673.2411	615.3461	LMTK3_296_297(loop).EDY[Pho]Y[Pho]LTPER.+2y5	80.2	33.1
673.2411	858.3757	LMTK3_296_297(loop).EDY[Pho]Y[Pho]LTPER.+2y6	80.2	33.1
673.2411	1101.405	LMTK3_296_297(loop).EDY[Pho]Y[Pho]LTPER.+2y7	80.2	33.1
833.8905	751.4097	LTK_862.GLOPQNLWNPTY[Pho]R.+2b7	91.9	38.9
833.8905	937.489	LTK_862.GLOPQNLWNPTY[Pho]R.+2b8	91.9	38.9
833.8905	1051.532	LTK_862.GLOPQNLWNPTY[Pho]R.+2b9	91.9	38.9
833.8905	616.2491	LTK_862.GLOPQNLWNPTY[Pho]R.+2y4	91.9	38.9
833.8905	730.292	LTK_862.GLOPQNLWNPTY[Pho]R.+2y5	91.9	38.9
833.8905	916.3713	LTK_862.GLOPQNLWNPTY[Pho]R.+2y6	91.9	38.9
833.8905	1029.455	LTK_862.GLOPQNLWNPTY[Pho]R.+2y7	91.9	38.9
833.8905	1143.498	LTK_862.GLOPQNLWNPTY[Pho]R.+2y8	91.9	38.9
711.3085	430.1932	LYN_193.SLDNGGY[Pho]YISPR.+2b4	83	34.5
711.3085	950.3292	LYN_193.SLDNGGY[Pho]YISPR.+2b8	83	34.5

711.3085	1221.494	LYN_193.SLDNGGY[Pho]YISPR.+2v10	83	34.5
711.3085	472.2878	LYN_193.SLDNGGY[Pho]YISPR.+2v4	83	34.5
711.3085	635.3511	LYN_193.SLDNGGY[Pho]YISPR.+2v5	83	34.5
711.3085	878.3808	LYN_193.SLDNGGY[Pho]YISPR.+2v6	83	34.5
711.3085	935.4023	LYN_193.SLDNGGY[Pho]YISPR.+2v7	83	34.5
711.3085	992.4237	LYN_193.SLDNGGY[Pho]YISPR.+2v8	83	34.5
711.3085	1106.467	LYN_193.SLDNGGY[Pho]YISPR.+2v9	83	34.5
751.2916	430.1932	LYN_193_194.SLDNGGY[Pho]Y[Pho]ISPR.+2b4	85.9	35.9
751.2916	487.2147	LYN_193_194.SLDNGGY[Pho]Y[Pho]ISPR.+2b5	85.9	35.9
751.2916	1143.38	LYN_193_194.SLDNGGY[Pho]Y[Pho]ISPR.+2b9	85.9	35.9
751.2916	715.3175	LYN_193_194.SLDNGGY[Pho]Y[Pho]ISPR.+2y5	85.9	35.9
751.2916	958.3471	LYN_193_194.SLDNGGY[Pho]Y[Pho]ISPR.+2y6	85.9	35.9
751.2916	1015.369	LYN_193_194.SLDNGGY[Pho]Y[Pho]ISPR.+2y7	85.9	35.9
751.2916	1072.39	LYN_193_194.SLDNGGY[Pho]Y[Pho]ISPR.+2y8	85.9	35.9
751.2916	1186.433	LYN_193_194.SLDNGGY[Pho]Y[Pho]ISPR.+2y9	85.9	35.9
711.3085	430.1932	LYN_194.SLDNGGY[Pho]ISPR.+2b4	83	34.5
711.3085	1221.494	LYN_194.SLDNGGY[Pho]ISPR.+2y10	83	34.5
711.3085	472.2878	LYN_194.SLDNGGY[Pho]ISPR.+2y4	83	34.5
711.3085	715.3175	LYN_194.SLDNGGY[Pho]ISPR.+2y5	83	34.5
711.3085	878.3808	LYN_194.SLDNGGY[Pho]ISPR.+2y6	83	34.5
711.3085	935.4023	LYN_194.SLDNGGY[Pho]ISPR.+2y7	83	34.5
711.3085	992.4237	LYN_194.SLDNGGY[Pho]ISPR.+2y8	83	34.5
711.3085	1106.467	LYN_194.SLDNGGY[Pho]ISPR.+2y9	83	34.5
853.3461	503.1919	LYN_473.VENC[CAM]PDELY[Pho]DIMK.+2b4	93.3	39.6
853.3461	844.3142	LYN_473.VENC[CAM]PDELY[Pho]DIMK.+2b7	93.3	39.6
853.3461	957.3982	LYN_473.VENC[CAM]PDELY[Pho]DIMK.+2b8	93.3	39.6
853.3461	506.2643	LYN_473.VENC[CAM]PDELY[Pho]DIMK.+2y4	93.3	39.6
853.3461	749.294	LYN_473.VENC[CAM]PDELY[Pho]DIMK.+2y5	93.3	39.6
853.3461	862.378	LYN_473.VENC[CAM]PDELY[Pho]DIMK.+2y6	93.3	39.6
853.3461	1106.448	LYN_473.VENC[CAM]PDELY[Pho]DIMK.+2y8	93.3	39.6
853.3461	1203.5	LYN_473.VENC[CAM]PDELY[Pho]DIMK.+2y9	93.3	39.6
768.6505	1045.433	MAPK1(loop).VADPDHDTGFLT[Pho]EY[Pho]VATR.+3b10	87.2	39.4
768.6505	635.2784	MAPK1(loop).VADPDHDTGFLT[Pho]EY[Pho]VATR.+3b6	87.2	39.4
768.6505	887.3642	MAPK1(loop).VADPDHDTGFLT[Pho]EY[Pho]VATR.+3b8	87.2	39.4
768.6505	347.2037	MAPK1(loop).VADPDHDTGFLT[Pho]EY[Pho]VATR.+3y3	87.2	39.4
768.6505	446.2722	MAPK1(loop).VADPDHDTGFLT[Pho]EY[Pho]VATR.+3y4	87.2	39.4
768.6505	689.3018	MAPK1(loop).VADPDHDTGFLT[Pho]EY[Pho]VATR.+3y5	87.2	39.4
768.6505	818.3444	MAPK1(loop).VADPDHDTGFLT[Pho]EY[Pho]VATR.+3y6	87.2	39.4
768.6505	999.3584	MAPK1(loop).VADPDHDTGFLT[Pho]EY[Pho]VATR.+3y7	87.2	39.4
777.9943	663.3097	MAPK3(loop).IADPEHDTGFLT[Pho]EY[Pho]VATR.+3b6	87.8	39.9
777.9943	915.3955	MAPK3(loop).IADPEHDTGFLT[Pho]EY[Pho]VATR.+3b8	87.8	39.9
777.9943	1016.443	MAPK3(loop).IADPEHDTGFLT[Pho]EY[Pho]VATR.+3b9	87.8	39.9
777.9943	446.2722	MAPK3(loop).IADPEHDTGFLT[Pho]EY[Pho]VATR.+3y4	87.8	39.9
777.9943	689.3018	MAPK3(loop).IADPEHDTGFLT[Pho]EY[Pho]VATR.+3y5	87.8	39.9
777.9943	818.3444	MAPK3(loop).IADPEHDTGFLT[Pho]EY[Pho]VATR.+3y6	87.8	39.9

777.9943	999.3584	MAPK3(loop).IADPEHDHTGFLT[Pho]EY[Pho]VATR.+3v7	87.8	39.9
638.6899	616.2014	MERTK_749_753_754_TYRO3_681_685_686.IY[Pho]SGDY[Pho]Y[Pho]R.+2b5	77.7	31.8
638.6899	859.2311	MERTK_749_753_754_TYRO3_681_685_686.IY[Pho]SGDY[Pho]Y[Pho]R.+2b6	77.7	31.8
638.6899	661.1783	MERTK_749_753_754_TYRO3_681_685_686.IY[Pho]SGDY[Pho]Y[Pho]R.+2y3	77.7	31.8
638.6899	776.2052	MERTK_749_753_754_TYRO3_681_685_686.IY[Pho]SGDY[Pho]Y[Pho]R.+2y4	77.7	31.8
638.6899	833.2267	MERTK_749_753_754_TYRO3_681_685_686.IY[Pho]SGDY[Pho]Y[Pho]R.+2y5	77.7	31.8
638.6899	920.2587	MERTK_749_753_754_TYRO3_681_685_686.IY[Pho]SGDY[Pho]Y[Pho]R.+2y6	77.7	31.8
598.7067	364.1867	MERTK_TYRO3_753_754_685_686(loop).IYSGDY[Pho]Y[Pho]R.+2b3	74.8	30.4
598.7067	421.2082	MERTK_TYRO3_753_754_685_686(loop).IYSGDY[Pho]Y[Pho]R.+2b4	74.8	30.4
598.7067	536.2351	MERTK_TYRO3_753_754_685_686(loop).IYSGDY[Pho]Y[Pho]R.+2b5	74.8	30.4
598.7067	779.2648	MERTK_TYRO3_753_754_685_686(loop).IYSGDY[Pho]Y[Pho]R.+2b6	74.8	30.4
598.7067	661.1783	MERTK_TYRO3_753_754_685_686(loop).IYSGDY[Pho]Y[Pho]R.+2y3	74.8	30.4
598.7067	776.2052	MERTK_TYRO3_753_754_685_686(loop).IYSGDY[Pho]Y[Pho]R.+2y4	74.8	30.4
598.7067	833.2267	MERTK_TYRO3_753_754_685_686(loop).IYSGDY[Pho]Y[Pho]R.+2y5	74.8	30.4
598.7067	920.2587	MERTK_TYRO3_753_754_685_686(loop).IYSGDY[Pho]Y[Pho]R.+2y6	74.8	30.4
657.2803	658.2766	MET_1093.GHFGC[CAM]IVY[Pho]HGTLNDNDGK.+3b6	79	33.3
657.2803	901.3063	MET_1093.GHFGC[CAM]IVY[Pho]HGTLNDNDGK.+3b7	79	33.3
657.2803	433.2041	MET_1093.GHFGC[CAM]IVY[Pho]HGTLNDNDGK.+3y4	79	33.3
657.2803	548.2311	MET_1093.GHFGC[CAM]IVY[Pho]HGTLNDNDGK.+3y5	79	33.3
657.2803	661.3151	MET_1093.GHFGC[CAM]IVY[Pho]HGTLNDNDGK.+3y6	79	33.3
657.2803	774.3992	MET_1093.GHFGC[CAM]IVY[Pho]HGTLNDNDGK.+3y7	79	33.3
657.2803	875.4469	MET_1093.GHFGC[CAM]IVY[Pho]HGTLNDNDGK.+3y8	79	33.3
657.2803	932.4684	MET_1093.GHFGC[CAM]IVY[Pho]HGTLNDNDGK.+3y9	79	33.3
648.7329	478.2296	MUSK_755_756(loop).NIYSADY[Pho]Y[Pho]K.+2b4	78.4	32.2
648.7329	549.2667	MUSK_755_756(loop).NIYSADY[Pho]Y[Pho]K.+2b5	78.4	32.2
648.7329	907.3233	MUSK_755_756(loop).NIYSADY[Pho]Y[Pho]K.+2b7	78.4	32.2
648.7329	633.1721	MUSK_755_756(loop).NIYSADY[Pho]Y[Pho]K.+2y3	78.4	32.2
648.7329	748.1991	MUSK_755_756(loop).NIYSADY[Pho]Y[Pho]K.+2y4	78.4	32.2
648.7329	819.2362	MUSK_755_756(loop).NIYSADY[Pho]Y[Pho]K.+2y5	78.4	32.2
648.7329	906.2682	MUSK_755_756(loop).NIYSADY[Pho]Y[Pho]K.+2y6	78.4	32.2
648.7329	1069.332	MUSK_755_756(loop).NIYSADY[Pho]Y[Pho]K.+2y7	78.4	32.2
638.2501	472.1479	NTRK1_676.DIY[Pho]STDYR.+2b3	77.6	31.8
638.2501	559.18	NTRK1_676.DIY[Pho]STDYR.+2b4	77.6	31.8
638.2501	775.2546	NTRK1_676.DIY[Pho]STDYR.+2b6	77.6	31.8
638.2501	616.2726	NTRK1_676.DIY[Pho]STDYR.+2y4	77.6	31.8
638.2501	717.3202	NTRK1_676.DIY[Pho]STDYR.+2y5	77.6	31.8
638.2501	804.3523	NTRK1_676.DIY[Pho]STDYR.+2y6	77.6	31.8
638.2501	1047.382	NTRK1_676.DIY[Pho]STDYR.+2y7	77.6	31.8
693.8009	426.1806	NTRK1_757.AC[CAM]PPEVY[Pho]AIMR.+2b4	81.7	33.8
693.8009	555.2232	NTRK1_757.AC[CAM]PPEVY[Pho]AIMR.+2b5	81.7	33.8
693.8009	654.2916	NTRK1_757.AC[CAM]PPEVY[Pho]AIMR.+2b6	81.7	33.8
693.8009	733.3103	NTRK1_757.AC[CAM]PPEVY[Pho]AIMR.+2y5	81.7	33.8
693.8009	832.3787	NTRK1_757.AC[CAM]PPEVY[Pho]AIMR.+2y6	81.7	33.8
693.8009	961.4213	NTRK1_757.AC[CAM]PPEVY[Pho]AIMR.+2y7	81.7	33.8
693.8009	1058.474	NTRK1_757.AC[CAM]PPEVY[Pho]AIMR.+2y8	81.7	33.8

693.8009	1155.527	NTRK1 757.ACICAMIPPEVY[Pho]AIMR.+2v9	81.7	33.8
671.2254	465.198	NTRK2_3_706_707_709_710(loop).DVYSTDY[Pho]Y[Pho]R.+2b4	80	33
671.2254	566.2457	NTRK2_3_706_707_709_710(loop).DVYSTDY[Pho]Y[Pho]R.+2b5	80	33
671.2254	681.2726	NTRK2_3_706_707_709_710(loop).DVYSTDY[Pho]Y[Pho]R.+2b6	80	33
671.2254	661.1783	NTRK2_3_706_707_709_710(loop).DVYSTDY[Pho]Y[Pho]R.+2y3	80	33
671.2254	776.2052	NTRK2_3_706_707_709_710(loop).DVYSTDY[Pho]Y[Pho]R.+2y4	80	33
671.2254	877.2529	NTRK2_3_706_707_709_710(loop).DVYSTDY[Pho]Y[Pho]R.+2y5	80	33
671.2254	964.2849	NTRK2_3_706_707_709_710(loop).DVYSTDY[Pho]Y[Pho]R.+2y6	80	33
983.4098	431.2653	NTRK2 558.VFLAEC[CAM]Y[Pho]NLC[CAM]PEODK.+2b4	102.8	44.3
983.4098	720.3385	NTRK2_558.VFLAEC[CAM]Y[Pho]NLC[CAM]PEODK.+2b6	102.8	44.3
983.4098	963.3682	NTRK2_558.VFLAEC[CAM]Y[Pho]NLC[CAM]PEODK.+2b7	102.8	44.3
983.4098	1190.495	NTRK2_558.VFLAEC[CAM]Y[Pho]NLC[CAM]PEODK.+2b9	102.8	44.3
983.4098	776.3243	NTRK2_558.VFLAEC[CAM]Y[Pho]NLC[CAM]PEODK.+2y6	102.8	44.3
983.4098	889.4084	NTRK2_558.VFLAEC[CAM]Y[Pho]NLC[CAM]PEODK.+2y7	102.8	44.3
983.4098	1003.451	NTRK2_558.VFLAEC[CAM]Y[Pho]NLC[CAM]PEODK.+2y8	102.8	44.3
631.2423	458.1323	NTRK2 702 NTRK3 705.DVY[Pho]STDYYR.+2b3	77.1	31.6
631.2423	545.1643	NTRK2_702_NTRK3_705.DVY[Pho]STDYYR.+2b4	77.1	31.6
631.2423	761.2389	NTRK2_702_NTRK3_705.DVY[Pho]STDYYR.+2b6	77.1	31.6
631.2423	717.3202	NTRK2_702_NTRK3_705.DVY[Pho]STDYYR.+2y5	77.1	31.6
631.2423	804.3523	NTRK2_702_NTRK3_705.DVY[Pho]STDYYR.+2y6	77.1	31.6
631.2423	1047.382	NTRK2_702_NTRK3_705.DVY[Pho]STDYYR.+2y7	77.1	31.6
728.3552	423.2966	NTRK3_516.IPVIENPQY[Pho]FR.+2b4	84.2	35.1
728.3552	552.3392	NTRK3_516.IPVIENPQY[Pho]FR.+2b5	84.2	35.1
728.3552	666.3821	NTRK3 516.IPVIENPQY[Pho]FR.+2b6	84.2	35.1
728.3552	790.3284	NTRK3_516.IPVIENPQY[Pho]FR.+2y5	84.2	35.1
728.3552	904.3713	NTRK3_516.IPVIENPQY[Pho]FR.+2y6	84.2	35.1
728.3552	1033.414	NTRK3_516.IPVIENPQY[Pho]FR.+2y7	84.2	35.1
728.3552	1146.498	NTRK3_516.IPVIENPQY[Pho]FR.+2y8	84.2	35.1
728.3552	1245.566	NTRK3_516.IPVIENPQY[Pho]FR.+2y9	84.2	35.1
811.3702	560.3079	NTRK3_558.VFLAEC[CAM]Y[Pho]NLSPTK.+2b5	90.3	38.1
811.3702	720.3385	NTRK3 558.VFLAEC[CAM]Y[Pho]NLSPTK.+2b6	90.3	38.1
811.3702	1190.495	NTRK3_558.VFLAEC[CAM]Y[Pho]NLSPTK.+2b9	90.3	38.1
811.3702	659.3723	NTRK3 558.VFLAEC[CAM]Y[Pho]NLSPTK.+2y6	90.3	38.1
811.3702	902.4019	NTRK3_558.VFLAEC[CAM]Y[Pho]NLSPTK.+2y7	90.3	38.1
811.3702	1062.433	NTRK3_558.VFLAEC[CAM]Y[Pho]NLSPTK.+2y8	90.3	38.1
816.3604	645.2838	PGFRA_742.QADTTQY[Pho]VPMLEP.+2b6	90.6	38.2
816.3604	987.3819	PGFRA_742.QADTTQY[Pho]VPMLEP.+2b8	90.6	38.2
816.3604	645.3389	PGFRA_742.QADTTQY[Pho]VPMLEP.+2y5	90.6	38.2
816.3604	744.4073	PGFRA_742.QADTTQY[Pho]VPMLEP.+2y6	90.6	38.2
816.3604	987.4369	PGFRA 742.OADTTQY[Pho]VPMLEP.+2y7	90.6	38.2
816.3604	1115.496	PGFRA_742.QADTTQY[Pho]VPMLEP.+2y8	90.6	38.2
816.3604	1216.543	PGFRA_742.QADTTQY[Pho]VPMLEP.+2y9	90.6	38.2
640.2896	715.2811	PGFRA_762.SLY[Pho]DRPASYK.+2b5	77.8	31.9
640.2896	883.371	PGFRA_762.SLY[Pho]DRPASYK.+2b7	77.8	31.9
640.2896	970.403	PGFRA_762.SLY[Pho]DRPASYK.+2b8	77.8	31.9

640.2896	565.298	PGFRA_762.SLY[Pho]DRPASYK.+2v5	77.8	31.9
640.2896	721.3991	PGFRA_762.SLY[Pho]DRPASYK.+2v6	77.8	31.9
640.2896	836.4261	PGFRA_762.SLY[Pho]DRPASYK.+2v7	77.8	31.9
640.2896	1079.456	PGFRA_762.SLY[Pho]DRPASYK.+2v8	77.8	31.9
453.8509	444.153	PGFRA_762_768.SLY[Pho]DRPASY[Pho]K.+3b3	64.2	22.3
453.8509	559.18	PGFRA_762_768.SLY[Pho]DRPASY[Pho]K.+3b4	64.2	22.3
453.8509	715.2811	PGFRA_762_768.SLY[Pho]DRPASY[Pho]K.+3b5	64.2	22.3
453.8509	812.3338	PGFRA_762_768.SLY[Pho]DRPASY[Pho]K.+3b6	64.2	22.3
453.8509	477.1745	PGFRA_762_768.SLY[Pho]DRPASY[Pho]K.+3v3	64.2	22.3
453.8509	548.2116	PGFRA_762_768.SLY[Pho]DRPASY[Pho]K.+3v4	64.2	22.3
453.8509	645.2644	PGFRA_762_768.SLY[Pho]DRPASY[Pho]K.+3v5	64.2	22.3
453.8509	801.3655	PGFRA_762_768.SLY[Pho]DRPASY[Pho]K.+3v6	64.2	22.3
640.2896	635.3148	PGFRA_768.SLYDRPASY[Pho]K.+2b5	77.8	31.9
640.2896	732.3675	PGFRA_768.SLYDRPASY[Pho]K.+2b6	77.8	31.9
640.2896	803.4046	PGFRA_768.SLYDRPASY[Pho]K.+2b7	77.8	31.9
640.2896	890.4367	PGFRA_768.SLYDRPASY[Pho]K.+2b8	77.8	31.9
640.2896	645.2644	PGFRA_768.SLYDRPASY[Pho]K.+2v5	77.8	31.9
640.2896	801.3655	PGFRA_768.SLYDRPASY[Pho]K.+2v6	77.8	31.9
640.2896	916.3924	PGFRA_768.SLYDRPASY[Pho]K.+2v7	77.8	31.9
694.7812	497.2177	PGFRA_849(loop).DIMHDSNY[Pho]VSK.+2b4	81.8	33.9
694.7812	612.2446	PGFRA_849(loop).DIMHDSNY[Pho]VSK.+2b5	81.8	33.9
694.7812	1056.349	PGFRA_849(loop).DIMHDSNY[Pho]VSK.+2b8	81.8	33.9
694.7812	333.2132	PGFRA_849(loop).DIMHDSNY[Pho]VSK.+2v3	81.8	33.9
694.7812	690.2858	PGFRA_849(loop).DIMHDSNY[Pho]VSK.+2v5	81.8	33.9
694.7812	777.3179	PGFRA_849(loop).DIMHDSNY[Pho]VSK.+2v6	81.8	33.9
694.7812	892.3448	PGFRA_849(loop).DIMHDSNY[Pho]VSK.+2v7	81.8	33.9
694.7812	1029.404	PGFRA_849(loop).DIMHDSNY[Pho]VSK.+2v8	81.8	33.9
463.5233	612.2446	PGFRA_849(loop).DIMHDSNY[Pho]VSK.+3b5	64.9	22.8
463.5233	699.2767	PGFRA_849(loop).DIMHDSNY[Pho]VSK.+3b6	64.9	22.8
463.5233	813.3196	PGFRA_849(loop).DIMHDSNY[Pho]VSK.+3b7	64.9	22.8
463.5233	333.2132	PGFRA_849(loop).DIMHDSNY[Pho]VSK.+3v3	64.9	22.8
463.5233	576.2429	PGFRA_849(loop).DIMHDSNY[Pho]VSK.+3v4	64.9	22.8
463.5233	690.2858	PGFRA_849(loop).DIMHDSNY[Pho]VSK.+3v5	64.9	22.8
463.5233	777.3179	PGFRA_849(loop).DIMHDSNY[Pho]VSK.+3v6	64.9	22.8
463.5233	892.3448	PGFRA_849(loop).DIMHDSNY[Pho]VSK.+3v7	64.9	22.8
665.795	416.0853	PGFRB_686.Y[Pho]GDLVDYLHR.+2b3	79.7	32.8
665.795	529.1694	PGFRB_686.Y[Pho]GDLVDYLHR.+2b4	79.7	32.8
665.795	628.2378	PGFRB_686.Y[Pho]GDLVDYLHR.+2b5	79.7	32.8
665.795	588.3253	PGFRB_686.Y[Pho]GDLVDYLHR.+2v4	79.7	32.8
665.795	703.3522	PGFRB_686.Y[Pho]GDLVDYLHR.+2v5	79.7	32.8
665.795	802.4206	PGFRB_686.Y[Pho]GDLVDYLHR.+2v6	79.7	32.8
665.795	915.5047	PGFRB_686.Y[Pho]GDLVDYLHR.+2v7	79.7	32.8
705.7782	416.0853	PGFRB_686_692.Y[Pho]GDLVDY[Pho]LHR.+2b3	82.6	34.3
705.7782	529.1694	PGFRB_686_692.Y[Pho]GDLVDY[Pho]LHR.+2b4	82.6	34.3
705.7782	628.2378	PGFRB_686_692.Y[Pho]GDLVDY[Pho]LHR.+2b5	82.6	34.3

705.7782	668.2916	PGFRB_686_692.Y[Pho]GDLVDY[Pho]LHR.+2v4	82.6	34.3
705.7782	783.3185	PGFRB_686_692.Y[Pho]GDLVDY[Pho]LHR.+2y5	82.6	34.3
705.7782	882.3869	PGFRB_686_692.Y[Pho]GDLVDY[Pho]LHR.+2y6	82.6	34.3
705.7782	995.471	PGFRB_686_692.Y[Pho]GDLVDY[Pho]LHR.+2y7	82.6	34.3
665.795	449.2031	PGFRB_692.YGDLVDY[Pho]LHR.+2b4	79.7	32.8
665.795	548.2715	PGFRB_692.YGDLVDY[Pho]LHR.+2b5	79.7	32.8
665.795	668.2916	PGFRB_692.YGDLVDY[Pho]LHR.+2y4	79.7	32.8
665.795	783.3185	PGFRB_692.YGDLVDY[Pho]LHR.+2y5	79.7	32.8
665.795	882.3869	PGFRB_692.YGDLVDY[Pho]LHR.+2y6	79.7	32.8
665.795	995.471	PGFRB_692.YGDLVDY[Pho]LHR.+2y7	79.7	32.8
665.795	1110.498	PGFRB_692.YGDLVDY[Pho]LHR.+2y8	79.7	32.8
444.1991	449.2031	PGFRB_692.YGDLVDY[Pho]LHR.+3b4	63.5	21.8
444.1991	548.2715	PGFRB_692.YGDLVDY[Pho]LHR.+3b5	63.5	21.8
444.1991	663.2984	PGFRB_692.YGDLVDY[Pho]LHR.+3b6	63.5	21.8
444.1991	668.2916	PGFRB_692.YGDLVDY[Pho]LHR.+3y4	63.5	21.8
444.1991	783.3185	PGFRB_692.YGDLVDY[Pho]LHR.+3y5	63.5	21.8
444.1991	882.3869	PGFRB_692.YGDLVDY[Pho]LHR.+3y6	63.5	21.8
811.3299	332.1088	PGFRB_751.DESVDY[Pho]VPMLDMK.+2b3	90.3	38.1
811.3299	789.2339	PGFRB_751.DESVDY[Pho]VPMLDMK.+2b6	90.3	38.1
811.3299	888.3023	PGFRB_751.DESVDY[Pho]VPMLDMK.+2b7	90.3	38.1
811.3299	506.2643	PGFRB_751.DESVDY[Pho]VPMLDMK.+2y4	90.3	38.1
811.3299	734.3575	PGFRB_751.DESVDY[Pho]VPMLDMK.+2y6	90.3	38.1
811.3299	833.426	PGFRB_751.DESVDY[Pho]VPMLDMK.+2y7	90.3	38.1
811.3299	1076.456	PGFRB_751.DESVDY[Pho]VPMLDMK.+2y8	90.3	38.1
811.3299	1191.483	PGFRB_751.DESVDY[Pho]VPMLDMK.+2y9	90.3	38.1
453.6839	317.1092	PGFRB_857(loop).DSNY[Pho]ISK.+2b3	64.2	25.2
453.6839	560.1388	PGFRB_857(loop).DSNY[Pho]ISK.+2b4	64.2	25.2
453.6839	673.2229	PGFRB_857(loop).DSNY[Pho]ISK.+2b5	64.2	25.2
453.6839	347.2289	PGFRB_857(loop).DSNY[Pho]ISK.+2y3	64.2	25.2
453.6839	590.2586	PGFRB_857(loop).DSNY[Pho]ISK.+2y4	64.2	25.2
453.6839	704.3015	PGFRB_857(loop).DSNY[Pho]ISK.+2y5	64.2	25.2
681.2968	1038.431	PGFRB_934.MAQPAHASDEIY[Pho]EIMQK.+3b10	80.8	34.7
681.2968	636.2922	PGFRB_934.MAQPAHASDEIY[Pho]EIMQK.+3b6	80.8	34.7
681.2968	909.3883	PGFRB_934.MAQPAHASDEIY[Pho]EIMQK.+3b9	80.8	34.7
681.2968	519.2959	PGFRB_934.MAQPAHASDEIY[Pho]EIMQK.+3y4	80.8	34.7
681.2968	648.3385	PGFRB_934.MAQPAHASDEIY[Pho]EIMQK.+3y5	80.8	34.7
681.2968	891.3682	PGFRB_934.MAQPAHASDEIY[Pho]EIMQK.+3y6	80.8	34.7
681.2968	1004.452	PGFRB_934.MAQPAHASDEIY[Pho]EIMQK.+3y7	80.8	34.7
603.933	587.1749	PTK6_342(loop).EDVY[Pho]LSHDHNIPYK.+3b4	75.1	30.4
603.933	787.291	PTK6_342(loop).EDVY[Pho]LSHDHNIPYK.+3b6	75.1	30.4
603.933	520.313	PTK6_342(loop).EDVY[Pho]LSHDHNIPYK.+3y4	75.1	30.4
603.933	634.3559	PTK6_342(loop).EDVY[Pho]LSHDHNIPYK.+3y5	75.1	30.4
603.933	771.4148	PTK6_342(loop).EDVY[Pho]LSHDHNIPYK.+3y6	75.1	30.4
603.933	886.4417	PTK6_342(loop).EDVY[Pho]LSHDHNIPYK.+3y7	75.1	30.4
603.933	1023.501	PTK6_342(loop).EDVY[Pho]LSHDHNIPYK.+3y8	75.1	30.4

603.933	1110.533	PTK6_342(loop).EDVY[Pho]LSHDHNIPYK.+3v9	75.1	30.4
826.7946	492.2089	PTK7_960_961(loop).DVYNSEY[Pho]Y[Pho]HFR.+2b4	91.4	38.6
826.7946	579.2409	PTK7_960_961(loop).DVYNSEY[Pho]Y[Pho]HFR.+2b5	91.4	38.6
826.7946	459.2463	PTK7_960_961(loop).DVYNSEY[Pho]Y[Pho]HFR.+2y3	91.4	38.6
826.7946	702.2759	PTK7_960_961(loop).DVYNSEY[Pho]Y[Pho]HFR.+2y4	91.4	38.6
826.7946	945.3056	PTK7_960_961(loop).DVYNSEY[Pho]Y[Pho]HFR.+2y5	91.4	38.6
826.7946	1074.348	PTK7_960_961(loop).DVYNSEY[Pho]Y[Pho]HFR.+2y6	91.4	38.6
826.7946	1161.38	PTK7_960_961(loop).DVYNSEY[Pho]Y[Pho]HFR.+2y7	91.4	38.6
551.5321	492.2089	PTK7_960_961(loop).DVYNSEY[Pho]Y[Pho]HFR.+3b4	71.3	27.6
551.5321	579.2409	PTK7_960_961(loop).DVYNSEY[Pho]Y[Pho]HFR.+3b5	71.3	27.6
551.5321	708.2835	PTK7_960_961(loop).DVYNSEY[Pho]Y[Pho]HFR.+3b6	71.3	27.6
551.5321	459.2463	PTK7_960_961(loop).DVYNSEY[Pho]Y[Pho]HFR.+3y3	71.3	27.6
551.5321	702.2759	PTK7_960_961(loop).DVYNSEY[Pho]Y[Pho]HFR.+3y4	71.3	27.6
551.5321	945.3056	PTK7_960_961(loop).DVYNSEY[Pho]Y[Pho]HFR.+3y5	71.3	27.6
551.5321	1074.348	PTK7_960_961(loop).DVYNSEY[Pho]Y[Pho]HFR.+3y6	71.3	27.6
593.7663	554.201	RET_826.VGPGY[Pho]LGSGGSR.+2b5	74.4	30.2
593.7663	667.2851	RET_826.VGPGY[Pho]LGSGGSR.+2b6	74.4	30.2
593.7663	463.2259	RET_826.VGPGY[Pho]LGSGGSR.+2y5	74.4	30.2
593.7663	520.2474	RET_826.VGPGY[Pho]LGSGGSR.+2y6	74.4	30.2
593.7663	633.3315	RET_826.VGPGY[Pho]LGSGGSR.+2y7	74.4	30.2
593.7663	876.3611	RET_826.VGPGY[Pho]LGSGGSR.+2y8	74.4	30.2
593.7663	933.3826	RET_826.VGPGY[Pho]LGSGGSR.+2y9	74.4	30.2
663.7605	458.1323	RET_900.DVY[Pho]EEDSYVK.+2b3	79.5	32.8
663.7605	587.1749	RET_900.DVY[Pho]EEDSYVK.+2b4	79.5	32.8
663.7605	716.2175	RET_900.DVY[Pho]EEDSYVK.+2b5	79.5	32.8
663.7605	496.2766	RET_900.DVY[Pho]EEDSYVK.+2y4	79.5	32.8
663.7605	611.3035	RET_900.DVY[Pho]EEDSYVK.+2y5	79.5	32.8
663.7605	740.3461	RET_900.DVY[Pho]EEDSYVK.+2y6	79.5	32.8
663.7605	869.3887	RET_900.DVY[Pho]EEDSYVK.+2y7	79.5	32.8
663.7605	1112.418	RET_900.DVY[Pho]EEDSYVK.+2y8	79.5	32.8
663.7605	507.2086	RET_905(loop).DVYEEDSY[Pho]VK.+2b4	79.5	32.8
663.7605	636.2511	RET_905(loop).DVYEEDSY[Pho]VK.+2b5	79.5	32.8
663.7605	489.2109	RET_905(loop).DVYEEDSY[Pho]VK.+2y3	79.5	32.8
663.7605	576.2429	RET_905(loop).DVYEEDSY[Pho]VK.+2y4	79.5	32.8
663.7605	691.2698	RET_905(loop).DVYEEDSY[Pho]VK.+2y5	79.5	32.8
663.7605	820.3124	RET_905(loop).DVYEEDSY[Pho]VK.+2y6	79.5	32.8
663.7605	949.355	RET_905(loop).DVYEEDSY[Pho]VK.+2y7	79.5	32.8
663.7605	1112.418	RET_905(loop).DVYEEDSY[Pho]VK.+2y8	79.5	32.8
685.2523	616.1092	RON_1238_1239(loop).EY[Pho]Y[Pho]SVQQHR.+2b3	81.1	33.5
685.2523	703.1412	RON_1238_1239(loop).EY[Pho]Y[Pho]SVQQHR.+2b4	81.1	33.5
685.2523	802.2096	RON_1238_1239(loop).EY[Pho]Y[Pho]SVQQHR.+2b5	81.1	33.5
685.2523	930.2682	RON_1238_1239(loop).EY[Pho]Y[Pho]SVQQHR.+2b6	81.1	33.5
685.2523	568.295	RON_1238_1239(loop).EY[Pho]Y[Pho]SVQQHR.+2y4	81.1	33.5
685.2523	997.4251	RON_1238_1239(loop).EY[Pho]Y[Pho]SVQQHR.+2y7	81.1	33.5
670.2358	493.2293	ROR1_645_646(loop).EIYSADY[Pho]Y[Pho]R.+2b4	80	33

670.2358	564.2664	ROR1_645_646(loop).EIYSADY[Pho]Y[Pho]R.+2b5	80	33
670.2358	661.1783	ROR1_645_646(loop).EIYSADY[Pho]Y[Pho]R.+2y3	80	33
670.2358	776.2052	ROR1_645_646(loop).EIYSADY[Pho]Y[Pho]R.+2y4	80	33
670.2358	847.2423	ROR1_645_646(loop).EIYSADY[Pho]Y[Pho]R.+2y5	80	33
670.2358	934.2744	ROR1_645_646(loop).EIYSADY[Pho]Y[Pho]R.+2y6	80	33
670.2358	1097.338	ROR1_645_646(loop).EIYSADY[Pho]Y[Pho]R.+2y7	80	33
641.2275	463.2187	ROR2_645_646(loop).EVYAADY[Pho]Y[Pho]K.+2b4	77.9	31.9
641.2275	534.2558	ROR2_645_646(loop).EVYAADY[Pho]Y[Pho]K.+2b5	77.9	31.9
641.2275	633.1721	ROR2_645_646(loop).EVYAADY[Pho]Y[Pho]K.+2y3	77.9	31.9
641.2275	748.1991	ROR2_645_646(loop).EVYAADY[Pho]Y[Pho]K.+2y4	77.9	31.9
641.2275	819.2362	ROR2_645_646(loop).EVYAADY[Pho]Y[Pho]K.+2y5	77.9	31.9
641.2275	890.2733	ROR2_645_646(loop).EVYAADY[Pho]Y[Pho]K.+2y6	77.9	31.9
641.2275	1053.337	ROR2_645_646(loop).EVYAADY[Pho]Y[Pho]K.+2y7	77.9	31.9
755.8525	443.1326	ROS1_135.Y[Pho]AQLLGSWTYTK.+2b3	86.2	36.1
755.8525	556.2167	ROS1_135.Y[Pho]AQLLGSWTYTK.+2b4	86.2	36.1
755.8525	669.3008	ROS1_135.Y[Pho]AQLLGSWTYTK.+2b5	86.2	36.1
755.8525	785.3828	ROS1_135.Y[Pho]AQLLGSWTYTK.+2y6	86.2	36.1
755.8525	842.4043	ROS1_135.Y[Pho]AQLLGSWTYTK.+2y7	86.2	36.1
755.8525	955.4884	ROS1_135.Y[Pho]AQLLGSWTYTK.+2y8	86.2	36.1
755.8525	1068.572	ROS1_135.Y[Pho]AQLLGSWTYTK.+2y9	86.2	36.1
795.8357	556.2167	ROS1_135_144.Y[Pho]AQLLGSWTY[Pho]TK.+2b4	89.1	37.5
795.8357	669.3008	ROS1_135_144.Y[Pho]AQLLGSWTY[Pho]TK.+2b5	89.1	37.5
795.8357	813.3542	ROS1_135_144.Y[Pho]AQLLGSWTY[Pho]TK.+2b7	89.1	37.5
795.8357	491.1901	ROS1_135_144.Y[Pho]AQLLGSWTY[Pho]TK.+2y3	89.1	37.5
795.8357	922.3706	ROS1_135_144.Y[Pho]AQLLGSWTY[Pho]TK.+2y7	89.1	37.5
795.8357	1035.455	ROS1_135_144.Y[Pho]AQLLGSWTY[Pho]TK.+2y8	89.1	37.5
795.8357	1148.539	ROS1_135_144.Y[Pho]AQLLGSWTY[Pho]TK.+2y9	89.1	37.5
755.8525	476.2504	ROS1_144.YAQLLGSWTY[Pho]TK.+2b4	86.2	36.1
755.8525	589.3344	ROS1_144.YAQLLGSWTY[Pho]TK.+2b5	86.2	36.1
755.8525	491.1901	ROS1_144.YAQLLGSWTY[Pho]TK.+2y3	86.2	36.1
755.8525	592.2378	ROS1_144.YAQLLGSWTY[Pho]TK.+2y4	86.2	36.1
755.8525	865.3492	ROS1_144.YAQLLGSWTY[Pho]TK.+2y6	86.2	36.1
755.8525	922.3706	ROS1_144.YAQLLGSWTY[Pho]TK.+2y7	86.2	36.1
755.8525	1035.455	ROS1_144.YAQLLGSWTY[Pho]TK.+2y8	86.2	36.1
755.8525	1148.539	ROS1_144.YAQLLGSWTY[Pho]TK.+2y9	86.2	36.1
488.7015	317.1278	ROS1_2069.GC[CAM]VY[Pho]LER.+2b3	66.7	26.5
488.7015	560.1575	ROS1_2069.GC[CAM]VY[Pho]LER.+2b4	66.7	26.5
488.7015	673.2415	ROS1_2069.GC[CAM]VY[Pho]LER.+2b5	66.7	26.5
488.7015	417.2456	ROS1_2069.GC[CAM]VY[Pho]LER.+2y3	66.7	26.5
488.7015	660.2753	ROS1_2069.GC[CAM]VY[Pho]LER.+2y4	66.7	26.5
488.7015	759.3437	ROS1_2069.GC[CAM]VY[Pho]LER.+2y5	66.7	26.5
703.2953	657.228	ROS1_2274.EGLNY[Pho]MVLATEC[CAM]GQGEEK.+3b5	82.4	35.8
703.2953	788.2685	ROS1_2274.EGLNY[Pho]MVLATEC[CAM]GQGEEK.+3b6	82.4	35.8
703.2953	887.3369	ROS1_2274.EGLNY[Pho]MVLATEC[CAM]GQGEEK.+3b7	82.4	35.8
703.2953	462.2195	ROS1_2274.EGLNY[Pho]MVLATEC[CAM]GQGEEK.+3y4	82.4	35.8

703.2953	647.2995	ROS1_2274.EGLNY[Pho]MVLATEC[CAM]IGOGEEK.+3v6	82.4	35.8
703.2953	807.3301	ROS1_2274.EGLNY[Pho]MVLATEC[CAM]IGOGEEK.+3v7	82.4	35.8
703.2953	936.3727	ROS1_2274.EGLNY[Pho]MVLATEC[CAM]IGOGEEK.+3v8	82.4	35.8
703.2953	1037.42	ROS1_2274.EGLNY[Pho]MVLATEC[CAM]IGOGEEK.+3v9	82.4	35.8
810.0118	1099.395	RYK_492(loop).DLFPMDY[Pho]HC[CAM]LGDNENRPVR.+3b8	90.2	41.7
810.0118	1169.602	RYK_492(loop).DLFPMDY[Pho]HC[CAM]LGDNENRPVR.+3v10	90.2	41.7
810.0118	641.3842	RYK_492(loop).DLFPMDY[Pho]HC[CAM]LGDNENRPVR.+3v5	90.2	41.7
810.0118	884.4697	RYK_492(loop).DLFPMDY[Pho]HC[CAM]LGDNENRPVR.+3v7	90.2	41.7
810.0118	999.4966	RYK_492(loop).DLFPMDY[Pho]HC[CAM]LGDNENRPVR.+3v8	90.2	41.7
810.0118	1056.518	RYK_492(loop).DLFPMDY[Pho]HC[CAM]LGDNENRPVR.+3v9	90.2	41.7
813.8289	372.0955	SRC_187.GAY[Pho]C[CAM]LSVSDFDNAK.+2b3	90.4	38.2
813.8289	645.2102	SRC_187.GAY[Pho]C[CAM]LSVSDFDNAK.+2b5	90.4	38.2
813.8289	732.2423	SRC_187.GAY[Pho]C[CAM]LSVSDFDNAK.+2b6	90.4	38.2
813.8289	1095.532	SRC_187.GAY[Pho]C[CAM]LSVSDFDNAK.+2v10	90.4	38.2
813.8289	594.2882	SRC_187.GAY[Pho]C[CAM]LSVSDFDNAK.+2v5	90.4	38.2
813.8289	796.3472	SRC_187.GAY[Pho]C[CAM]LSVSDFDNAK.+2v7	90.4	38.2
813.8289	895.4156	SRC_187.GAY[Pho]C[CAM]LSVSDFDNAK.+2v8	90.4	38.2
813.8289	982.4476	SRC_187.GAY[Pho]C[CAM]LSVSDFDNAK.+2v9	90.4	38.2
648.287	430.1932	SRC_216.LDSGGFY[Pho]ITSR.+2b5	78.4	32.2
648.287	476.2827	SRC_216.LDSGGFY[Pho]ITSR.+2v4	78.4	32.2
648.287	719.3124	SRC_216.LDSGGFY[Pho]ITSR.+2v5	78.4	32.2
648.287	866.3808	SRC_216.LDSGGFY[Pho]ITSR.+2v6	78.4	32.2
648.287	923.4023	SRC_216.LDSGGFY[Pho]ITSR.+2v7	78.4	32.2
648.287	980.4237	SRC_216.LDSGGFY[Pho]ITSR.+2v8	78.4	32.2
648.287	1067.456	SRC_216.LDSGGFY[Pho]ITSR.+2v9	78.4	32.2
652.2819	471.2449	SRC_YES_FYN_LCK_419_426_420_394(loop).LIEDNEY[Pho]TAR.+2b4	78.7	32.3
652.2819	714.3305	SRC_YES_FYN_LCK_419_426_420_394(loop).LIEDNEY[Pho]TAR.+2b6	78.7	32.3
652.2819	347.2037	SRC_YES_FYN_LCK_419_426_420_394(loop).LIEDNEY[Pho]TAR.+2v3	78.7	32.3
652.2819	590.2334	SRC_YES_FYN_LCK_419_426_420_394(loop).LIEDNEY[Pho]TAR.+2v4	78.7	32.3
652.2819	719.276	SRC_YES_FYN_LCK_419_426_420_394(loop).LIEDNEY[Pho]TAR.+2v5	78.7	32.3
652.2819	833.3189	SRC_YES_FYN_LCK_419_426_420_394(loop).LIEDNEY[Pho]TAR.+2v6	78.7	32.3
652.2819	948.3459	SRC_YES_FYN_LCK_419_426_420_394(loop).LIEDNEY[Pho]TAR.+2v7	78.7	32.3
652.2819	1077.388	SRC_YES_FYN_LCK_419_426_420_394(loop).LIEDNEY[Pho]TAR.+2v8	78.7	32.3
633.2503	344.1452	SRMS_380(loop).DDIY[Pho]SPSSSSK.+2b3	77.3	31.7
633.2503	587.1749	SRMS_380(loop).DDIY[Pho]SPSSSSK.+2b4	77.3	31.7
633.2503	408.2089	SRMS_380(loop).DDIY[Pho]SPSSSSK.+2v4	77.3	31.7
633.2503	495.2409	SRMS_380(loop).DDIY[Pho]SPSSSSK.+2v5	77.3	31.7
633.2503	592.2937	SRMS_380(loop).DDIY[Pho]SPSSSSK.+2v6	77.3	31.7
633.2503	679.3257	SRMS_380(loop).DDIY[Pho]SPSSSSK.+2v7	77.3	31.7
633.2503	922.3554	SRMS_380(loop).DDIY[Pho]SPSSSSK.+2v8	77.3	31.7
633.2503	1035.439	SRMS_380(loop).DDIY[Pho]SPSSSSK.+2v9	77.3	31.7
807.3402	491.25	TEC_519(loop).YVLDDQY[Pho]TSSSGAK.+2b4	90	37.9
807.3402	606.277	TEC_519(loop).YVLDDQY[Pho]TSSSGAK.+2b5	90	37.9
807.3402	1123.43	TEC_519(loop).YVLDDQY[Pho]TSSSGAK.+2v10	90	37.9
807.3402	1238.457	TEC_519(loop).YVLDDQY[Pho]TSSSGAK.+2v11	90	37.9

807.3402	536.2675	TEC_519(loop).YVLDDOY[Pho]TSSSGAK.+2v6	90	37.9
807.3402	637.3151	TEC_519(loop).YVLDDQY[Pho]TSSSGAK.+2y7	90	37.9
807.3402	880.3448	TEC_519(loop).YVLDDQY[Pho]TSSSGAK.+2y8	90	37.9
807.3402	1008.403	TEC_519(loop).YVLDDQY[Pho]TSSSGAK.+2y9	90	37.9
452.1966	316.1139	TIE1_1007(loop).GEEVY[Pho]VK.+2b3	64.1	25.1
452.1966	415.1823	TIE1_1007(loop).GEEVY[Pho]VK.+2b4	64.1	25.1
452.1966	658.212	TIE1_1007(loop).GEEVY[Pho]VK.+2b5	64.1	25.1
452.1966	489.2109	TIE1_1007(loop).GEEVY[Pho]VK.+2y3	64.1	25.1
452.1966	588.2793	TIE1_1007(loop).GEEVY[Pho]VK.+2y4	64.1	25.1
452.1966	717.3219	TIE1_1007(loop).GEEVY[Pho]VK.+2y5	64.1	25.1
451.7046	315.1299	TIE2_992(loop).GQEVY[Pho]VK.+2b3	64	25.1
451.7046	414.1983	TIE2_992(loop).GQEVY[Pho]VK.+2b4	64	25.1
451.7046	657.228	TIE2_992(loop).GQEVY[Pho]VK.+2b5	64	25.1
451.7046	489.2109	TIE2_992(loop).GQEVY[Pho]VK.+2y3	64	25.1
451.7046	588.2793	TIE2_992(loop).GQEVY[Pho]VK.+2y4	64	25.1
451.7046	717.3219	TIE2_992(loop).GQEVY[Pho]VK.+2y5	64	25.1
800.7058	1068.566	TNK1_277(loop).YVMGGPRPIPY[Pho]AWC[CAM]APESLR.+3b10	89.5	41.1
800.7058	761.3763	TNK1_277(loop).YVMGGPRPIPY[Pho]AWC[CAM]APESLR.+3b7	89.5	41.1
800.7058	971.5131	TNK1_277(loop).YVMGGPRPIPY[Pho]AWC[CAM]APESLR.+3b9	89.5	41.1
800.7058	504.2776	TNK1_277(loop).YVMGGPRPIPY[Pho]AWC[CAM]APESLR.+3y4	89.5	41.1
800.7058	601.3304	TNK1_277(loop).YVMGGPRPIPY[Pho]AWC[CAM]APESLR.+3y5	89.5	41.1
800.7058	672.3675	TNK1_277(loop).YVMGGPRPIPY[Pho]AWC[CAM]APESLR.+3y6	89.5	41.1
800.7058	832.3982	TNK1_277(loop).YVMGGPRPIPY[Pho]AWC[CAM]APESLR.+3y7	89.5	41.1
800.7058	1018.477	TNK1_277(loop).YVMGGPRPIPY[Pho]AWC[CAM]APESLR.+3y8	89.5	41.1
836.8607	491.25	TXK_420(loop).YVLDDOY[Pho]VSSFGAK.+2b4	92.1	39
836.8607	1182.471	TXK_420(loop).YVLDDOY[Pho]VSSFGAK.+2y10	92.1	39
836.8607	422.2398	TXK_420(loop).YVLDDOY[Pho]VSSFGAK.+2y4	92.1	39
836.8607	509.2718	TXK_420(loop).YVLDDOY[Pho]VSSFGAK.+2y5	92.1	39
836.8607	596.3039	TXK_420(loop).YVLDDOY[Pho]VSSFGAK.+2y6	92.1	39
836.8607	695.3723	TXK_420(loop).YVLDDOY[Pho]VSSFGAK.+2y7	92.1	39
836.8607	938.4019	TXK_420(loop).YVLDDOY[Pho]VSSFGAK.+2y8	92.1	39
836.8607	1067.445	TXK_420(loop).YVLDDOY[Pho]VSSFGAK.+2y9	92.1	39
690.7547	591.2885	TYK2_1054_1055(loop).AVPEGHEY[Pho]Y[Pho]R.+2b6	81.5	33.7
690.7547	720.3311	TYK2_1054_1055(loop).AVPEGHEY[Pho]Y[Pho]R.+2b7	81.5	33.7
690.7547	661.1783	TYK2_1054_1055(loop).AVPEGHEY[Pho]Y[Pho]R.+2y3	81.5	33.7
690.7547	790.2209	TYK2_1054_1055(loop).AVPEGHEY[Pho]Y[Pho]R.+2y4	81.5	33.7
690.7547	927.2798	TYK2_1054_1055(loop).AVPEGHEY[Pho]Y[Pho]R.+2y5	81.5	33.7
690.7547	984.3012	TYK2_1054_1055(loop).AVPEGHEY[Pho]Y[Pho]R.+2y6	81.5	33.7
690.7547	1113.344	TYK2_1054_1055(loop).AVPEGHEY[Pho]Y[Pho]R.+2y7	81.5	33.7
690.7547	1210.397	TYK2_1054_1055(loop).AVPEGHEY[Pho]Y[Pho]R.+2y8	81.5	33.7
508.9047	423.1987	UFO_634.HGDLHSFLLY[Pho]SR.+3b4	68.2	25.3
508.9047	560.2576	UFO_634.HGDLHSFLLY[Pho]SR.+3b5	68.2	25.3
508.9047	505.1806	UFO_634.HGDLHSFLLY[Pho]SR.+3y3	68.2	25.3
508.9047	618.2647	UFO_634.HGDLHSFLLY[Pho]SR.+3y4	68.2	25.3
508.9047	731.3488	UFO_634.HGDLHSFLLY[Pho]SR.+3y5	68.2	25.3

508.9047	878.4172	UFO_634.HGDLHSFLLY[Pho]SR.+3v6	68.2	25.3
508.9047	965.4492	UFO_634.HGDLHSFLLY[Pho]SR.+3y7	68.2	25.3
572.229	471.1639	UFO_698.IY[Pho]NGDYR.+2b3	72.8	29.5
572.229	528.1854	UFO_698.IY[Pho]NGDYR.+2b4	72.8	29.5
572.229	643.2123	UFO_698.IY[Pho]NGDYR.+2b5	72.8	29.5
572.229	806.2757	UFO_698.IY[Pho]NGDYR.+2b6	72.8	29.5
572.229	616.2726	UFO_698.IY[Pho]NGDYR.+2y4	72.8	29.5
572.229	673.294	UFO_698.IY[Pho]NGDYR.+2y5	72.8	29.5
572.229	787.3369	UFO_698.IY[Pho]NGDYR.+2y6	72.8	29.5
612.2121	448.2191	UFO_702_703(loop).IYNGDY[Pho]Y[Pho]R.+2b4	75.7	30.9
612.2121	563.246	UFO_702_703(loop).IYNGDY[Pho]Y[Pho]R.+2b5	75.7	30.9
612.2121	661.1783	UFO_702_703(loop).IYNGDY[Pho]Y[Pho]R.+2y3	75.7	30.9
612.2121	776.2052	UFO_702_703(loop).IYNGDY[Pho]Y[Pho]R.+2y4	75.7	30.9
612.2121	833.2267	UFO_702_703(loop).IYNGDY[Pho]Y[Pho]R.+2y5	75.7	30.9
612.2121	947.2696	UFO_702_703(loop).IYNGDY[Pho]Y[Pho]R.+2y6	75.7	30.9
787.3613	1024.55	VGFR1_911.QGGPLMVIVEY[Pho]C[CAM]K.+2b10	88.5	37.2
787.3613	683.3545	VGFR1_911.QGGPLMVIVEY[Pho]C[CAM]K.+2b7	88.5	37.2
787.3613	796.4386	VGFR1_911.QGGPLMVIVEY[Pho]C[CAM]K.+2b8	88.5	37.2
787.3613	895.507	VGFR1_911.QGGPLMVIVEY[Pho]C[CAM]K.+2b9	88.5	37.2
787.3613	550.1731	VGFR1_911.QGGPLMVIVEY[Pho]C[CAM]K.+2y3	88.5	37.2
787.3613	679.2157	VGFR1_911.QGGPLMVIVEY[Pho]C[CAM]K.+2y4	88.5	37.2
787.3613	778.2841	VGFR1_911.QGGPLMVIVEY[Pho]C[CAM]K.+2y5	88.5	37.2
787.3613	891.3682	VGFR1_911.QGGPLMVIVEY[Pho]C[CAM]K.+2y6	88.5	37.2
689.3054	643.1912	VGFR2_1214.FHY[Pho]DNTAGISQYLQNSK.+3b4	81.4	35.1
689.3054	757.2341	VGFR2_1214.FHY[Pho]DNTAGISQYLQNSK.+3b5	81.4	35.1
689.3054	858.2818	VGFR2_1214.FHY[Pho]DNTAGISQYLQNSK.+3b6	81.4	35.1
689.3054	929.3189	VGFR2_1214.FHY[Pho]DNTAGISQYLQNSK.+3b7	81.4	35.1
689.3054	986.3404	VGFR2_1214.FHY[Pho]DNTAGISQYLQNSK.+3b8	81.4	35.1
689.3054	589.3304	VGFR2_1214.FHY[Pho]DNTAGISQYLQNSK.+3y5	81.4	35.1
689.3054	752.3937	VGFR2_1214.FHY[Pho]DNTAGISQYLQNSK.+3y6	81.4	35.1
689.3054	967.4843	VGFR2_1214.FHY[Pho]DNTAGISQYLQNSK.+3y8	81.4	35.1
422.6655	328.1139	VGFR2_3_1059_1068(loop).DPDY[Pho]VR.+2b3	61.9	24.1
422.6655	571.1436	VGFR2_3_1059_1068(loop).DPDY[Pho]VR.+2b4	61.9	24.1
422.6655	517.217	VGFR2_3_1059_1068(loop).DPDY[Pho]VR.+2y3	61.9	24.1
422.6655	632.244	VGFR2_3_1059_1068(loop).DPDY[Pho]VR.+2y4	61.9	24.1
635.31	458.1323	VGFR2_951.DY[Pho]VGAIPVDLK.+2b3	77.4	31.7
635.31	586.1909	VGFR2_951.DY[Pho]VGAIPVDLK.+2b5	77.4	31.7
635.31	699.2749	VGFR2_951.DY[Pho]VGAIPVDLK.+2b6	77.4	31.7
635.31	571.345	VGFR2_951.DY[Pho]VGAIPVDLK.+2y5	77.4	31.7
635.31	684.4291	VGFR2_951.DY[Pho]VGAIPVDLK.+2y6	77.4	31.7
635.31	755.4662	VGFR2_951.DY[Pho]VGAIPVDLK.+2y7	77.4	31.7
635.31	812.4876	VGFR2_951.DY[Pho]VGAIPVDLK.+2y8	77.4	31.7
635.31	911.556	VGFR2_951.DY[Pho]VGAIPVDLK.+2y9	77.4	31.7
896.8513	787.1888	VGFR3_1230_1231.Y[Pho]Y[Pho]NWSVFGC[CAM]LAR.+2b4	96.5	41.1
896.8513	973.2893	VGFR3_1230_1231.Y[Pho]Y[Pho]NWSVFGC[CAM]LAR.+2b6	96.5	41.1

896.8513	1120.358	VGFR3_1230_1231.Y[Pho]Y[Pho]NWVSFPGC[CAM]LAR.+2b7	96.5	41.1
896.8513	1217.41	VGFR3_1230_1231.Y[Pho]Y[Pho]NWVSFPGC[CAM]LAR.+2b8	96.5	41.1
896.8513	1192.593	VGFR3_1230_1231.Y[Pho]Y[Pho]NWVSFPGC[CAM]LAR.+2y10	96.5	41.1
896.8513	1006.514	VGFR3_1230_1231.Y[Pho]Y[Pho]NWVSFPGC[CAM]LAR.+2y9	96.5	41.1
836.3542	1181.518	VGFR3_1265.TFEEFPMTPTTY[Pho]K.+2b10	92.1	39
836.3542	507.2086	VGFR3_1265.TFEEFPMTPTTY[Pho]K.+2b4	92.1	39
836.3542	1080.471	VGFR3_1265.TFEEFPMTPTTY[Pho]K.+2b9	92.1	39
836.3542	491.1901	VGFR3_1265.TFEEFPMTPTTY[Pho]K.+2y3	92.1	39
836.3542	592.2378	VGFR3_1265.TFEEFPMTPTTY[Pho]K.+2y4	92.1	39
836.3542	689.2906	VGFR3_1265.TFEEFPMTPTTY[Pho]K.+2y5	92.1	39
836.3542	1165.5	VGFR3_1265.TFEEFPMTPTTY[Pho]K.+2y9	92.1	39
496.2361	270.1812	VGFR3_853.VLGY[Pho]GAFGK.+2b3	67.3	26.7
496.2361	513.2109	VGFR3_853.VLGY[Pho]GAFGK.+2b4	67.3	26.7
496.2361	641.2695	VGFR3_853.VLGY[Pho]GAFGK.+2b6	67.3	26.7
496.2361	422.2398	VGFR3_853.VLGY[Pho]GAFGK.+2y4	67.3	26.7
496.2361	479.2613	VGFR3_853.VLGY[Pho]GAFGK.+2y5	67.3	26.7
496.2361	722.2909	VGFR3_853.VLGY[Pho]GAFGK.+2y6	67.3	26.7
496.2361	779.3124	VGFR3_853.VLGY[Pho]GAFGK.+2y7	67.3	26.7
679.2916	415.1798	ZAP70_164.MPWY[Pho]HSSLTR.+2b3	80.6	33.3
679.2916	658.2095	ZAP70_164.MPWY[Pho]HSSLTR.+2b4	80.6	33.3
679.2916	476.2827	ZAP70_164.MPWY[Pho]HSSLTR.+2y4	80.6	33.3
679.2916	563.3148	ZAP70_164.MPWY[Pho]HSSLTR.+2y5	80.6	33.3
679.2916	700.3737	ZAP70_164.MPWY[Pho]HSSLTR.+2y6	80.6	33.3
679.2916	943.4033	ZAP70_164.MPWY[Pho]HSSLTR.+2y7	80.6	33.3
679.2916	1129.483	ZAP70_164.MPWY[Pho]HSSLTR.+2y8	80.6	33.3
453.1968	415.1798	ZAP70_164.MPWY[Pho]HSSLTR.+3b3	64.2	22.2
453.1968	658.2095	ZAP70_164.MPWY[Pho]HSSLTR.+3b4	64.2	22.2
453.1968	795.2684	ZAP70_164.MPWY[Pho]HSSLTR.+3b5	64.2	22.2
453.1968	476.2827	ZAP70_164.MPWY[Pho]HSSLTR.+3y4	64.2	22.2
453.1968	563.3148	ZAP70_164.MPWY[Pho]HSSLTR.+3y5	64.2	22.2
453.1968	700.3737	ZAP70_164.MPWY[Pho]HSSLTR.+3y6	64.2	22.2
560.2395	444.153	ZAP70_178.LY[Pho]SGAQTGDK.+2b3	72	29
560.2395	501.1745	ZAP70_178.LY[Pho]SGAQTGDK.+2b4	72	29
560.2395	700.2702	ZAP70_178.LY[Pho]SGAQTGDK.+2b6	72	29
560.2395	619.3046	ZAP70_178.LY[Pho]SGAQTGDK.+2y6	72	29
560.2395	676.326	ZAP70_178.LY[Pho]SGAQTGDK.+2y7	72	29
560.2395	763.3581	ZAP70_178.LY[Pho]SGAQTGDK.+2y8	72	29
731.768	313.187	ZAP70_492_493(loop).ALGADDSY[Pho]Y[Pho]TAR.+2b4	84.5	35.2
731.768	428.214	ZAP70_492_493(loop).ALGADDSY[Pho]Y[Pho]TAR.+2b5	84.5	35.2
731.768	630.2729	ZAP70_492_493(loop).ALGADDSY[Pho]Y[Pho]TAR.+2b7	84.5	35.2
731.768	590.2334	ZAP70_492_493(loop).ALGADDSY[Pho]Y[Pho]TAR.+2y4	84.5	35.2
731.768	833.2631	ZAP70_492_493(loop).ALGADDSY[Pho]Y[Pho]TAR.+2y5	84.5	35.2
731.768	920.2951	ZAP70_492_493(loop).ALGADDSY[Pho]Y[Pho]TAR.+2y6	84.5	35.2
731.768	1035.322	ZAP70_492_493(loop).ALGADDSY[Pho]Y[Pho]TAR.+2y7	84.5	35.2
731.768	1150.349	ZAP70_492_493(loop).ALGADDSY[Pho]Y[Pho]TAR.+2y8	84.5	35.2

636.8028	514.262	ZAP70_69.QLNGTY[Pho]AIAGGK.+2b5	77.5	31.8
636.8028	1031.456	ZAP70_69.QLNGTY[Pho]AIAGGK.+2y10	77.5	31.8
636.8028	445.2769	ZAP70_69.QLNGTY[Pho]AIAGGK.+2y5	77.5	31.8
636.8028	516.314	ZAP70_69.QLNGTY[Pho]AIAGGK.+2y6	77.5	31.8
636.8028	759.3437	ZAP70_69.QLNGTY[Pho]AIAGGK.+2y7	77.5	31.8
636.8028	860.3914	ZAP70_69.QLNGTY[Pho]AIAGGK.+2y8	77.5	31.8
636.8028	917.4128	ZAP70_69.QLNGTY[Pho]AIAGGK.+2y9	77.5	31.8

Chapter 3

3 SH2 Superbinder Modified Yeast Two Hybrid System for Identifying Tyrosine Kinase Substrates

3.1 Abstract

TKs provide therapeutic targets in many different cancer types, as the pTyr- mediated signaling network plays a critical role in a wide range of cancer-related cellular activities. Tyrosine phosphorylation has been identified in over half of human proteins, but substrates for any given TK have not been systematically investigated, largely due to the lack of a reliable high-throughput *in vivo* approach. Here, a modified yeast two hybrid (Y2H) system is presented that is designed for screening for direct TK substrates in a high-precision and high-throughput manner. This system co-expresses a superbinder SH2 bait and a conditional promoter regulated TK for screening tyrosine phosphorylated preys. The superbinder SH2 greatly promotes the sensitivity of reporter output and the conditionally expressed TK allows reverse-screening for eliminating false positives. In a mid-scale Src tyrosine kinase substrate screening of a human cDNA library, 94 positive colonies were isolated from approximate 170,000 mated cells, which represented 48 proteins or protein fragments. Even without further *in vivo* validation, 9 proteins of these candidates are known Src substrates or direct interactors.

3.2 Introduction

TKs are attractive therapeutic targets because aberrant TK activations are hallmarks of many cancer types. TKs, as well as pTyr-mediated signal transduction, play a critical role in a wide range of cancer-related events including proliferation, differentiation, metastasis, and apoptosis (Hunter, 2009; Levitzki, 2013; Lim and Pawson, 2010; Manning et al., 2002; Seet et al., 2006). Our current understanding of the pTyr signaling cascade is primarily reliant on the study of TKs that phosphorylate specific tyrosine residues and SH2 proteins that recognize the TK substrates to mediate signal transduction. Recent advances of pTyr-peptide enrichment and MS approaches have revolutionized the study of the pTyr signaling network by allowing fast and comprehensive identification of pTyr sites. A preliminary study by our group reported over 10,000 pTyr sites from cultured cancer cells, of which approximately 3,000 sites are novel (Bian et al., 2016). In contrast to the rapidly growing number of pTyr sites, the kinome profile of TKs is slow to emerge mainly because of the promiscuous nature of TK kinase specificities, which makes conventional kinase-assay-based approaches not necessarily reliable. In addition, functional redundancy and cross-activation among these TKs also limit the application of MS-based *in vivo* approaches. For instance, the most well-studied Src tyrosine kinase, which is also the first described oncoprotein reported in 1979 (Oppermann et al., 1979; Sefton et al., 1980; Stehelin et al., 1977), has only 67 substrates verified both *in vitro* and *in vivo* as summarized in the PhosphoSitePlus database (Hornbeck et al., 2015). However, only a few of these substrates were identified by high-throughput approaches (Kanner et al., 1989; Kanner et al., 1990; Reynolds et al., 2014).

Here, a modified yeast two-hybrid (Y2H) system is reported, which is based on a superbinder SH2 that is engineered from the natural Src SH2 domain (Kaneko et al., 2012a; Kaneko et al., 2012b). This system can profile the TK-substrate pairings in a high-throughput and high-precision manner. Unlike mammalian cells, yeast cells do not have any functional TKs or SH2 domains (Castellanos and Mazon, 1985), thus providing a clean background for studying tyrosine phosphorylation. Previously, several groups made successful attempts in verifying pTyr-dependent protein-protein interactions (PPI) in yeast expressing different tyrosine kinases, by borrowing an identical strategy of co-expressing

an active tyrosine kinase with the bait (BD fusion SH2 containing proteins) and the prey (AD fusion TK substrates) (Fig.3.1 A), as summarized in (Grossmann et al., 2015). A similar Y2H system was established by introducing a bait containing the superbinder SH2 and a conditionally expressed Src tyrosine kinase. This greatly increased the readout sensitivity of reporter genes and made the system applicable for the screening of novel tyrosine kinase substrates from a conventional cDNA library. In a mid-scale ~170,000 colonies screening of a human cDNA library, 94 independent colonies were isolated which grew on the selection medium in a Src-dependent manner. 48 in-frame proteins or protein fragments larger than 150 amino acids were identified from these candidate positives, of which at least 9 proteins were known Src substrates or direct interactors. In addition, to further simplify the after-screening identification and expand the applicability of this Y2H system, a novel screening strategy was designed based on SH2-AP-MS. From a mixture of 48 candidate positive colonies, the AD proteins were immunoprecipitated then their tyrosine phosphorylated sites were analyzed by SH2-AP-MS. In the preliminary test, three pTyr peptides were identified among the 48 proteins. With proper optimization, this new strategy will in theory allow the enrichment of positive colonies in liquid culturing and the simultaneous identification of AD insertion proteins and phosphorylation sites from a mixture of positive colonies, therefore is suitable for large-scale cDNA library screening for TK substrates.

3.3 Materials and Methods

3.3.1 Cloning and transformation

All the backbone vectors were purchased from ClonTech along with the Matchmaker Gold yeast two hybrid system. The pBridge BD vector with two multiple cloning sites (MCSs) was used for expressing Src kinase and SH2 bait simultaneously. The Src kinase was integrated into the MCS2 using Not1 and Bgl2 restriction sites, the SH2 wild-type (WT) or triple mutant (TrM) was integrated into the MCS1 using EcoR1 and BamH1 restriction sites. All prey DNA fragments were synthesized *in vitro* and then integrated into pGADT7 AD vector using restriction sites Nde1/Xho1 (artificial substrate), Nde1/BamH1 (RACK1-Y228 and TNS3-Y1173 substrates), or Xho1/BamH1 (RACK1-Y246 and TNS3-Y1256 substrates). All plasmids were amplified in DH5 α *E. coli* strain with proper antibiotics and purified by miniprep following manufacturer's instructions.

To prepare competent yeast cells, the yeast strains Y2HGold and Y187 were first streaked on a YPDA agar plate from a frozen stock. The plate was incubated at 30°C for 3~4 days until colonies appeared. A fresh single colony (diameter 2~3 mm) was picked and incubated in 3 ml YPDA medium at 30 °C with shaking at 250 rpm for 8~12 hours. 5 μ l of the culture was transferred into 50 ml fresh YPDA medium and incubated overnight until the OD₆₀₀ reached 0.15~0.3. Cells were collected by centrifugation and resuspended in 100 ml fresh YPDA medium, then incubated until the OD₆₀₀ reached 0.4~0.5. Cells were collected by centrifugation again then washed by deionized water, and finally resuspended in 1.5 ml 1.1x TE/LiAc buffer.

To transform, 50 μ l of competent cells were gently mixed with 100 ng purified plasmid DNA, 5 μ l yeast carrier DNA (10 μ g/ μ l) and 500 μ l PEG/LiAc buffer. The mixture was incubated at 30 °C for 30 min with occasional vortexing. 20 μ l DMSO was added into the mixture which was then subjected to heat-shock in a 42 °C water bath for 15 min. Transformed cells were collected by centrifugation and incubated on appropriate selection agar at 30°C for 3~4 days until colonies appeared.

3.3.2 Optimization of Src kinase expression in yeast

The yeast mating, toxicity test, and self-activation test were carried out following the procedures described in the ClonTech Matchmaker Gold yeast two hybrid system user manual. To determine the Src activity, the yeast strains were cultured in liquid -Leu medium supplemented with different concentrations of methionine. Cells were lysed directly in SDS gel loading buffer, boiling for five minutes and identical amounts of lysate protein was loaded on an SDS gel for electrophoresis. Tyrosine phosphorylation was visualized by western blot using anti-pTyr antibody 4G10, anti-mouse-HRP (horseradish peroxidase) and peroxidase substrate for enhanced chemiluminescence (ECL). To determine a proper Src expression level, the mated yeast strains pBridge-TrM-Src/pGADT7-artificial and pBridge-WT-Src/pGADT7-artificial were cultured in -Leu/-Trp liquid medium. The same number of cells were collected then cultured in -Leu/-Trp/-His liquid medium supplemented with different concentrations of methionine. The relative yeast growth rate was determined by measuring OD₆₀₀ of the liquid culture.

3.3.3 Quantification of MEL1 reporter gene expression

The α -Galactosidase assay was used for quantifying the MEL1 reporter gene expression. The procedures were modified from the ClonTech Yeast Handbook. Briefly, fresh colonies of different yeast strains were firstly cultured in liquid -Leu/-Trp medium. Cells were collected and carefully washed with 0.9% sodium chloride to completely remove medium residue. The same number of cells were pre-cultured overnight in -Leu/-Trp/-His liquid medium supplemented with 100 μ M methionine. The OD₆₀₀ was determined, cells were pelleted by centrifugation and the clear supernatant was transferred into fresh microcentrifuge tubes. To measure the catalytic activity of the α -galactosidase, the supernatant was incubated with p-nitrophenyl- α -D-galactoside (PNP- α -Gal) substrate at 30°C for one hour, then the concentration of the hydrolysis product p-nitrophenol was determined by measuring the OD₄₁₀. The relative abundance of MEL1 was defined by OD_{410}/OD_{600} .

3.3.4 Human cDNA library screening

The Y2H Gold strain with pBridge-TrM-Src was used as bait, screening against the ClonTech Mate & Plate Library (Universal Human). The library was constructed from human cDNA derived from a few different tissues or organs. One fresh colony containing the bait was cultured in 50 ml -Trp liquid medium supplemented with 5 mM methionine overnight until the OD₆₀₀ reached 0.8. Cells were collected and re-suspended in 5 ml -Trp liquid medium. For yeast cell mating, the bait cells, 1 ml of the pre-made library and 45 ml of 2 x YPDA liquid medium (50 µg/µl kanamycin) were mixed together in a sterile 2 L flask and incubated at 30°C for 24 hours with slow shaking. All cells were collected by centrifugation and resuspended in 10 ml 0.5 x YPDA liquid medium. To count the number of mated cells, 100 µl of the mated culture was spread in 1/10, 1/100, 1/1000 and 1/10000 dilutions on 100 mm -Leu/-Trp (5 mM methionine) plates and cultured at 30°C for 5 days. The number of colonies were recorded to estimate total mated cells and mating efficiency. The remainder of the mated culture was spread in 50 150 mm -Leu/-Trp/-His (100 µM methionine) plates and cultured at 30°C for 5 days. All separable colonies (in any sizes) that grew on the -His plates were picked and replicated in -Leu/-Trp/-His (100 µM methionine) plates three times. The Src-dependency of these colonies were further validated by comparing their growth in -Leu/-Trp/-His medium with either 100 µM or 5 mM methionine.

3.3.5 SH2-AP-MS identification of AD insertions

48 positive colonies were cultured individually in liquid -Leu/-Trp medium containing 5 mM methionine. Cells were collected by centrifugation and resuspended in 0.9% NaCl. The same number of cells from each colony were mixed together and re-incubated in liquid -Leu/-Trp/-His medium containing 100 mM methionine at 30°C overnight. The total cell lysate was extracted using the CellLytic Y Cell Lysis Reagent (Sigma, C4482). Two milligrams total lysate was immuno-precipitated with 4 µg of GAL4-AD antibody (Santa Cruz, sc1663). The precipitated protein was digested by trypsin (Promega, V5111) following the procedures described in section 2.4.5, then the pTyr peptides were isolated by superbinder SH2 enrichment. A data-dependent acquisition scanning was carried out

using a Thermo QExactive MS system equipped with EasyLC1000 and the raw data was analyzed by MaxQuant software.

3.4 Results

3.4.1 Design of the SH2 superbinder modified Y2H system

Since the original GAL4-based Y2H system has been successfully modified to verify pTyr-dependent protein-protein interactions, a similar GAL4-based system from ClonTech was further modified by introducing the superbinder SH2 as the bait. A great advantage of this Matchmaker Gold Y2H system is the BD-compatible vector pBridge that has two multiple cloning sites (MCSs). pBridge can co-express two independent proteins: a BD-fusion bait, and an additional protein under control of the conditional promoter MET25, which is regulated by the presence of the methionine in the culture medium.

First, two baits were constructed in the pBridge vector containing the constitutively active Src kinase under MET25 promoter, with either superbinder SH2-TrM or its wild-type variant SH2-WT fused with the BD domain (BD-TrM-Src and BD-WT-Src). Also, one prey was constructed in the pGADT7 vector containing the four tandem repeats of an artificial TK substrate peptide AAYANAA fused with AD domain (AD-artificial) (Clark and Peterson, 2002). The DNA fragment of the artificial substrate was made by annealing two complementary oligonucleotides that were synthesized *in vitro*. Next, the baits and prey were transformed into yeast strain Y2HGold separately for toxicity and self-activation tests. Both baits were found to be toxic, but the toxicity was attenuated by adding methionine or Src kinase inhibitor-1 (SKI-1) into the culture medium, suggesting that Src expression inhibited yeast growth (Fig.3.1 B). Src kinase activity was determined by western blot using anti-pTyr antibody 4G10. As shown in Fig.3.1 C, strong tyrosine phosphorylation was observed in the total cell lysate from yeast grown without methionine. As well, the signal was still detectable from yeast grown with 1 mM methionine, a concentration normally suggested to be able to turn off MET25 promoter. This indicates that Src kinase is expressed and active within yeast, which is consistent with a previous report stating that the prey could be effectively phosphorylated by low-abundant TKs in a yeast two hybrid (Grossmann et al., 2015). In the toxicity and self-activation test, the AD-artificial did not alter the yeast growth, as expected, while none of these constructs self-activated the HIS3 reporter (Suppl.3.1).

Because Src was moderately toxic to yeast, its expression level was further adjusted to find the optimal expression that maximizes yeast growth rate in HIS3 selection medium. The prey plasmid pGADT7-AD-artificial was transformed into the yeast strain Y187 and mated with the two baits, pBridge-TrM-Src and pBridge-WT-Src, in Y2HGold strain separately. When cultured in the HIS3 selection medium containing different concentrations of methionine, 100 μ M methionine was determined to be the optimal condition for both colonies (Fig.3.1 D). In the on-plate screening for MEL1 and HIS3 reporters, both colonies were confirmed to be secreting α -galactosidase and resisting lack of histidine in the presence of 100 μ M but not 5 mM methionine (Fig.3.1 E). On the same plates, the positive colony (pGBKT7-53/pGADT7-T), but not the negative colony (pGBKT7-Lam/pGADT7-T), expressed MEL1 and HIS3. It was also observed that the control colonies grew much larger than the Src-expressing colonies with 100 μ M methionine. Next, a quantification of MEL1 expression was carried out in these colonies by determining the activity of secreted α -galactosidase. As shown in Fig.3.1 F, the TrM-containing colony exhibited comparable α -galactosidase activity to the positive colony, which was two-fold of that in the WT-containing colony. Overall, these data demonstrate that Src expression with 100 μ M methionine effectively phosphorylated the artificial substrate (AAYANAA)₄ *in vivo* and the superbinder SH2 increased the readout sensitivity of the reporter genes. The interaction between SH2-TrM and phosphorylated (AAYANAA)₄ could be defined, by the high yield of α -galactosidase, as strong, but the overall growth rate of the yeast colony was much slower than the positive control colony due to the toxicity of Src expression. Therefore, the strategy and stringency of large-scale cDNA library screening might require further optimization for this modified Y2H system.

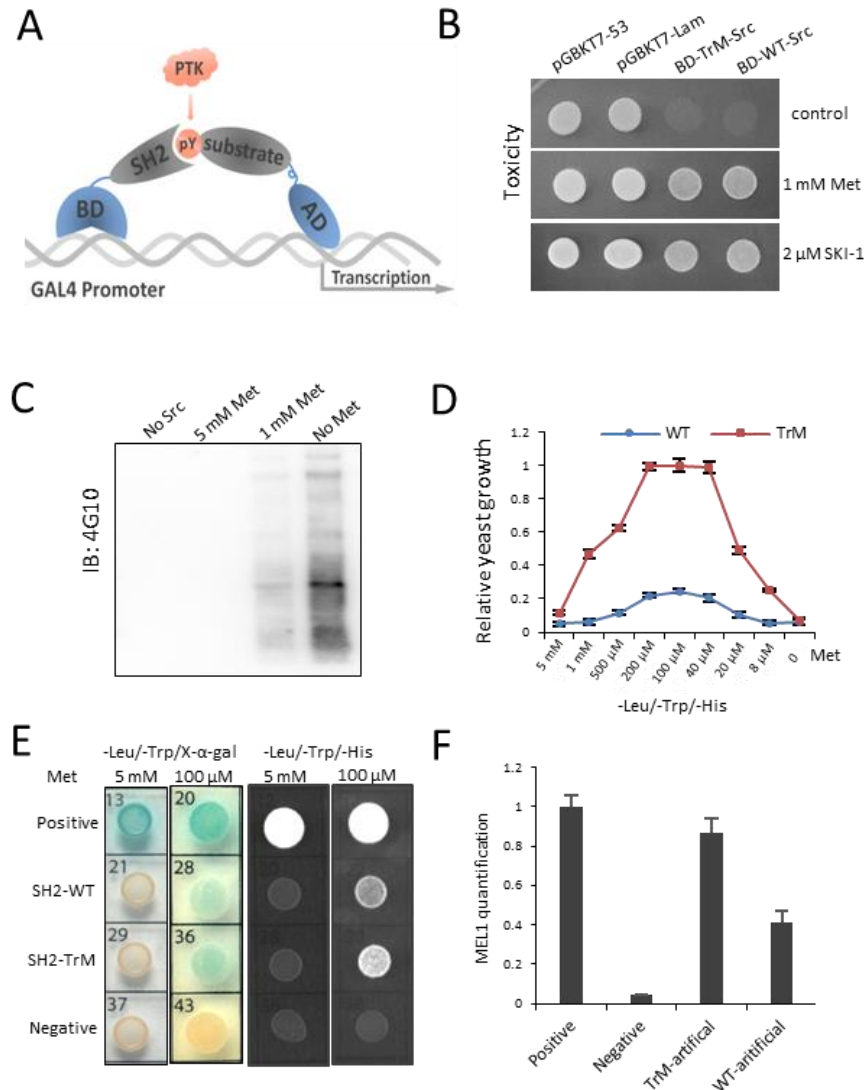


Figure 3.1 SH2 superbinder based Y2H for validating TK-substrate pairing

A) The design of the modified Y2H system with superbinder SH2 bait. The superbinder SH2 (bait) interacts with the phosphorylated substrate (prey) with a tyrosine kinase co-expressed in yeast; B) Src kinase is toxic to yeast growth. In Y2HGOLD strains transformed by pBridge-WT-Src or pBridge-TrM-Src, the yeast growth was greatly inhibited with the Src expression in the absence of methionine in the medium. Yeast growth was recovered in media supplemented with either 1 mM methionine or 2 μ M Src kinase inhibitor SKI-1 that inhibited the Src kinase expression or activity; C) Src kinase was active and effectively phosphorylated proteins in yeast. The lysates of Y2HGOLD-pBridge and Y2HGOLD-pBridge-WT-Src cultured with different concentrations of methionine were analyzed by western blot using anti-pTyr monoclonal antibody 4G10. 5 mM methionine, but not 1 mM methionine, was found to completely turn off the Src expression. D) Optimization of Src

expression in yeast. Two baits pBridge-WT-Src and pBridge-TrM-Src in Y2Hgold were mated with the artificial Src kinase substrate prey pGADT7-artificial in Y187 and then grown in liquid – Leu/-Trp/-His medium containing different concentrations of methionine. Maximum growth of both mated cells was observed under 100 μ M methionine condition, TrM containing cells grew faster than WT containing cells in all conditions; E) Both mated cells exhibited Src-dependent expression of MEL1 and HIS3 reporters. The positive control is pGBKT7-53 x pGADT7-T, the negative control is pGBKT7-Lam x pGADT7-T; F) TrM greatly increased the expression of the MEL1 reporter. The activities of α -galactosidase were normalized to cell numbers, n=3.

3.4.2 System evaluation with known peptide substrates of Src kinase

The modified system was further evaluated using a few peptide preys generated from known Src substrate proteins. Ten known Src-Phosphorylated peptides whose binding affinities (dissociation constant, K_d) to SH2-TrM or SH2-WT were determined individually by fluorescence polarization (FP) assay were synthesized *in vitro*. SH2-TrM exhibited overall stronger binding affinities to these peptides than SH2-WT (Suppl.3.2). Four peptides, RACK1-Y228, RACK1-Y246, TNS3 (tensin3)-Y1173 and TNS3-Y1256 were selected which exhibited a wide range of binding affinity to the SH2-TrM and SH2-WT (Fig.3.2 A; Suppl.3.2). The DNA fragments with four tandem repeats of these peptides were synthesized by annealing two complementary oligonucleotides *in vitro*, which were then integrated into the pGADT7 vector and transformed into the Y2HGold and Y187 strains. No toxicity or self-activation was observed in these prey-Y2HGold strains (Fig.3.2 B). The prey-Y187 strains were then mated with the two bait colonies pBridge-Src-TrM and pBridge-Src-WT in Y2HGold. In HIS3 selection medium (-Leu/-Trp/-His + 100 μ M methionine), three SH2-TrM containing colonies grew out after 5 days, including RACK1-Y228-TrM, RACK1-Y246-TrM, and TNS3-Y1173-TrM. As expected, none of these colonies grew out in similar selection medium containing 5 mM methionine (Fig.3.2 C). It was observed that all three colonies were much smaller in diameter compared to the positive control pGBKT7-53/pGADT7-T. In addition, the TNS3-Y1173 colony tended to grow faster than the RACK1-Y228 and RACK1-Y246 colonies even though the TNS3-Y1173 peptide had the weakest binding affinity to SH2-TrM by FP. The expression of the MEL1 reporter was quantified by α -galactosidase assay. As shown in Fig.3.2 D, the TNS3-Y1173-TrM indeed exhibited the highest MEL expression in all eight colonies, even though its affinity to SH2-TrM (12.9 μ M) was determined to be weak or moderate. This finding is consistent with an early Y2H study reporting that there is no linear correlation between reporter expression and the bait-prey binding affinity (Estojak et al., 1995). For individual substrate peptides, the SH2-TrM colonies always had higher MEL1 expression compared to the SH2-WT colonies. In conclusion, the superbinder SH2 modified Y2H exhibited good sensitivity in detecting tyrosine phosphorylation in these preys and have potential application in profiling the TK-substrate pairing on a library scale.

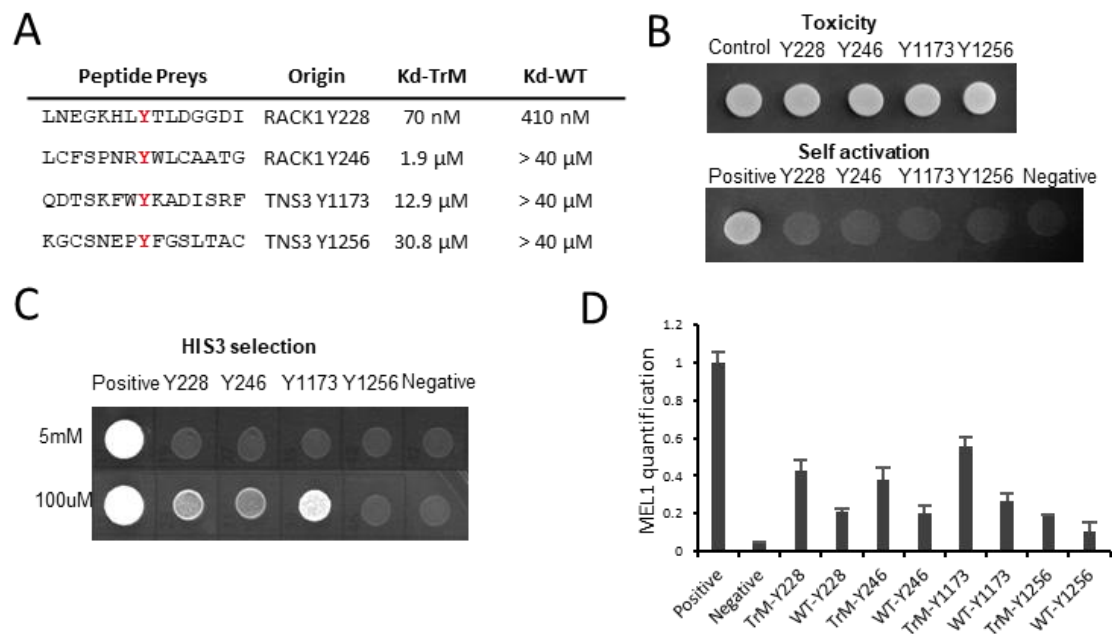


Figure 3.2 Evaluation of the Y2H system in recognizing Src kinase substrates

A) Four known substrate peptides of Src kinase with different binding affinities to SH2-WT and SH2-TrM; B) None of the substrate preys exhibited toxicity or self-activation; C) SH2-TrM promoted the cell growth in HIS3 selection medium. Three of the four substrate prey strains grew out in HIS3 selection medium when mated with SH2-TrM bait but not SH2-WT bait; D) SH2-TrM-containing strains in general exhibited higher MEL1 expression levels than SH2-WT-containing strains.

3.4.3 cDNA library screening for Src kinase substrate

A mid-scale library screening was performed using a universal human cDNA library that was made from a mixture of mRNA extracted from cell lines derived from different human tissues or organs (ClonTech). A high-stringency screening strategy was designed including both forward and reverse screening procedures (Tab.3.1). First, the pBridge-TrM-Src Y2HGold strain was mated with the cDNA library in the Y187 strain. Approximately 170,000 mated cells were spread on the HIS3 selection plates (-Trp/-Leu/-His/100 μ M methionine). Considering that Src expression is toxic and inhibits yeast cell growth, all separable colonies were picked after 5 days of incubation. Around 600 candidate colonies exhibited stable growth on the HIS3 selection medium after streaking three times on fresh medium. Next, these colonies were replicated on HIS3 selection plates with either 100 μ M or 5mM methionine to eliminate false positives exhibiting no obvious growth differences. Finally, the Src-dependency was further validated by determining the colony growth rates in liquid culture with either 100 μ M or 5 mM methionine. 94 colonies were isolated as candidate positives.

The AD-insertion were PCR amplified from plasmids extracted from the positive candidates. Based on the size of the PCR products, there should be few duplicates in these AD-insertions (Suppl.3.3). Therefore, the conventional analysis by restriction enzyme digestion was skipped, and the AD-insertions were sent for DNA sequencing directly. 72 different DNA fragments were identified from 94 candidate positives, including 17 full-length proteins and 31 protein fragments larger than 150 amino acids that are in frame. It is intriguing that this short list contains at least nine verified Src substrates or direct interactors, as well as several known Src partners that are functionally related, and most these AD-insertions contain reported tyrosine phosphorylation sites (Tab.3.2, Suppl.3.4).

Table 3.1 Library-scale screening for Src kinase substrates

	Human cDNA library screening strategy	Number of colonies
Mid-scale library screening	• Mate bait and cDNA library	~170,000
1 st round forward screening	• Grow 5 days on –His/100 μ M Met plate	~800
	• 3X streaking on –His/100 μ M Met plate	~600
2 nd round reverse screening	• 2X streaking on –His/100 μ M or 5 mM Met plates	120
	• 1X culturing on –His/100 μ M or 5 mM Met liquid medium	94
Sequencing	• Insertion PCR and sequencing	72 insertions: - 17 full length proteins - 31 fragments > 150aa

Quick facts of a mid-scale human cDNA library screening. The pBridge-TrM-Src Y2HGold strain was mated with the human cDNA library in the Y187 strain. Around 170,000 mated cells were spread on HIS3 selection plates with 100 μ M methionine for 5 days incubation. About 800 grown-out colonies were isolated for subsequent forward and reverse screenings to confirm the HIS3 reporter expression and Src-dependency. 94 candidate positive colonies were isolated for AD-insertion sequencing, which contains 72 different AD-insertions representing 17 in-frame full-length proteins and 31 protein fragments larger than 150 amino acids.

Table 3.2 Selected Src substrates and functional partners in candidate positives

Entry	Function	Insertion	Known pTyr	Refs
AT1B1	Substrate	340bp to end	3	(Tian et al., 2006)
AT1B3	Substrate	682bp to end	N/A	(Tian et al., 2006)
CAN3	Interactor	full length	N/A	(Hossain et al., 2013)
CBLB	Substrate	2449bp to end	1	(Sanjay et al., 2001; Yokouchi et al., 2001)
DAAM1	Interactor	2593bp to end	1	(Aspenstrom et al., 2006)
GRDN	Substrate	2131bp+0.9kb	1	(Lin et al., 2011; Nakai et al., 2014; Omori et al., 2015)
ROCK1	Substrate	1240bp+1.2kb	2	(Lee et al., 2010)
SDC2	Interactor	142bp to end	3	(Afratis et al., 2017; Ott and Rapraeger, 1998)
SHLB1	Substrate	505bp to end	N/A	(Yamaguchi et al., 2008)
TS101	Essential for Src mobility	full length	4	(Tu et al., 2010)

Selected candidate positives that include known Src substrates, interactors or functional partners. Most of these proteins or protein fragments have known tyrosine phosphorylation sites, while a few are highly tyrosine phosphorylated (Hornbeck et al., 2015).

3.4.4 SH2-AP-MS for after-screening prey identification

The Y2H is the most cost-efficient high-throughput *in vivo* assay for identifying protein-protein interactions. As presented above, the superbinder SH2 modified Y2H system is capable of screening for tyrosine kinase substrates on a library scale. The reverse screening largely contributes to the high genuine-positive rate, which eliminated approximately 80% of false positives isolated from the forward screening (Tab.3.1). However, the strategy seems highly time-inefficient because of the time-consuming on-plates screening and after-screening validation even for this mid-scale screening. It could be expected that a conventional million-colony screening might isolate over one thousand candidate positives due to duplicates and the relatively broad specificity of tyrosine kinases. Therefore, a new AD identification strategy was tested by introducing SH2-AP-MS to analyze tyrosine phosphorylation on AD proteins, which in theory would allow a quick identification of AD insertion proteins and pTyr sites from a matrix of positive colonies.

48 candidate positives were cultured individually in liquid -Leu/-Trp medium containing 5 mM methionine, which inhibits Src expression to maximize cell growth. An equal number of cells were mixed together and re-incubated overnight in -Leu/-Trp/-His medium containing 100 μ M methionine, which promotes Src expression to allow prey phosphorylation. The total cell lysate was extracted for immuno-precipitation (IP) using a GAL4-AD antibody. The precipitated protein was tryptic-digested, then the tyrosine phosphorylation peptides were enriched by superbinder SH2 and profiled by MS. However, only three pTyr sites were identified from 2 mg of total yeast lysate precipitated by 4 μ g GAL4-AD antibody, including HINFP_Y333 (Histone 4 transcription factor, Q9BQA5), OCAD1_Y87 (OCIA domain-containing protein 1, Q9NX40) and SPZ1_Y358 (Spermatogenic leucine zipper protein 1, Q9BXG8), of which the HINFP-Y333 phosphorylation was identified in an acute myelogenous leukemia cell previously (Hornbeck et al., 2015).

3.5 Discussion

Over the last two decades, TKs have emerged as attractive therapeutic targets, and TK inhibitors have played an increasingly prominent role in the treatment of cancer and other diseases. TKs and the pTyr-binding proteins have been globally profiled in humans. But our understanding of TK specificities lags when the number of identified pTyr sites expands rapidly along with the advance of mass spectrometry. This is largely due to the lack of a reliable and high-throughput *in vivo* assay for TK-substrate profiling. Even though TKs provide direct therapeutic targets in cancer, seeking more tractable therapeutic targets among the TK associated proteins are of great value in the clinic. For instance, there is a plethora of information about Src activation in preclinical models of many different cancer types, but the efficacy of multiple Src inhibitors are not highly promising in clinical applications or trials (Mayer and Krop, 2010). The reasons for failure of Src inhibitors in the clinic are not well understood but it is likely due to the inhibition of Src kinase family members in immune cells, which could inhibit host immune resistance against tumor cells or even render patients vulnerable to infections (Elias and Ditzel, 2015; Kreutzman et al., 2011). Therefore, profiling TK substrates that act downstream in tumorigenesis might offer excellent opportunities to identify promising therapeutic targets with a more desired effect.

The pioneer study of high-throughput screening for Src kinase substrates was carried out shortly after the discovery of pTyr-specific antibodies. A shotgun-based approach led to the cDNA cloning and functional characterization of a few substrates which are now well known and rigorously validated by other studies (Kanner et al., 1989; Kanner et al., 1990; Reynolds et al., 2014). Other than that, most reported Src substrates were identified from individual low-throughput studies (Lee et al., 2010; Lin et al., 2011; Nakai et al., 2014; Omori et al., 2015; Tian et al., 2006; Yamaguchi et al., 2008; Yokouchi et al., 2001). Taking advantage of the superbinder SH2 bait, our modified Y2H is capable of screening for substrates of Src tyrosine kinase in a high-throughput manner. As a proof of concept, the cDNA library screening exhibited a low duplication rate as expected for this mid-scale screening. Even though not fully validated, the short list of 48 candidate positives contains at least 9 known Src substrates or direct interactors. Here the reverse screening largely contributes to the high genuine positive rate because ~ 80% HIS3 expressing colonies were

determined to be false positives. According to the PhosphositePlus database, these AD insertions have 77 potential tyrosine phosphorylation sites while the entire human proteome contains approximately 10,000 pTyr sites from proteins encoded by 20,000 genes (Suppl.3.4) (Hornbeck et al., 2015). Even though a stringent screening strategy was performed, and the reverse screening seemed highly effective, false positives might still exist among these 48 colonies. To further validate the Src substrates, more tests should be carried out in yeast, including the re-transformation of bait and positive AD plasmids and switch of vectors.

This modified Y2H system can be immediately applied for the validation of individual TK-substrate pairing. More adjustments on the experimental pipeline are necessary if aiming for a global TK substrate profiling. The cDNA library is not optimal for this purpose due to imperfect cDNA synthesis. The ClonTech human general cDNA library has AD insertions 1.3 kb size on average, and consistently we failed to identify many full-length proteins (Tab.2, Suppl.34). The human ORFeome library could be superior. This library now includes full-length ORF constructs for over 15,000 genes, and has been successfully used in Y2H for a mega-scale library against library screening, representing so far the most comprehensive human protein-protein interaction network to date (Rolland et al., 2014; Rual et al., 2005). To improve the efficiency of after-screening work, the SH2-AP-MS was tested for fast identification of AD insertions, however, the preliminary result was not highly encouraging. Three pTyr sites were identified from a matrix of 48 positive colonies, with only one previously reported site. Increasing the amount of lysate and antibody or reducing the complexity of the matrix may immediately help to identify more pTyr sites. However, the low abundance of bait/prey expression in this GAL4 system could be another cause for the poor MS detection. Using a membrane-based (split-ubiquitin) Y2H system may result in better MS detection for higher bait/prey expression levels (Stagljar et al., 1998). Compared to the GAL4 system, the split-ubiquitin system also allows the expression of receptor tyrosine kinase with a highly hydrophobic region. Additionally, the cytosol tyrosine phosphorylation of prey proteins could be more efficient in the split-ubiquitin system, which will bring less toxicity to yeast growth, and therefore, facilitating the forward screening as well.

3.6 References

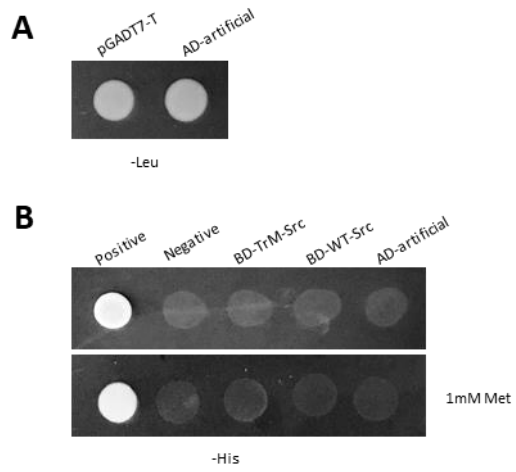
- Afratis, N.A., Nikitovic, D., Multhaupt, H.A., Theocharis, A.D., Couchman, J.R., and Karamanos, N.K. (2017). Syndecans - key regulators of cell signaling and biological functions. *The FEBS journal* 284, 27-41.
- Aspenstrom, P., Richnau, N., and Johansson, A.S. (2006). The diaphanous-related formin DAAM1 collaborates with the Rho GTPases RhoA and Cdc42, CIP4 and Src in regulating cell morphogenesis and actin dynamics. *Experimental cell research* 312, 2180-2194.
- Bian, Y., Li, L., Dong, M., Liu, X., Kaneko, T., Cheng, K., Liu, H., Voss, C., Cao, X., Wang, Y., *et al.* (2016). Ultra-deep tyrosine phosphoproteomics enabled by a phosphotyrosine superbinder. *Nat Chem Biol* 12, 959-966.
- Castellanos, R.M., and Mazon, M.J. (1985). Identification of phosphotyrosine in yeast proteins and of a protein tyrosine kinase associated with the plasma membrane. *J Biol Chem* 260, 8240-8242.
- Clark, D.D., and Peterson, B.R. (2002). Rapid Detection of Protein Tyrosine Kinase Activity in Recombinant Yeast Expressing a Universal Substrate. *J Proteome Res* 1, 207-209.
- Elias, D., and Ditzel, H.J. (2015). The potential of Src inhibitors. *Aging (Albany NY)* 7, 734-735.
- Estojak, J., Brent, R., and Golemis, E.A. (1995). Correlation of two-hybrid affinity data with in vitro measurements. *Mol Cell Biol* 15, 5820-5829.
- Grossmann, A., Benlasfer, N., Birth, P., Hegele, A., Wachsmuth, F., Apelt, L., and Stelzl, U. (2015). Phospho-tyrosine dependent protein-protein interaction network. *Molecular systems biology* 11, 794.
- Hornbeck, P.V., Zhang, B., Murray, B., Kornhauser, J.M., Latham, V., and Skrzypek, E. (2015). PhosphoSitePlus, 2014: mutations, PTMs and recalibrations. *Nucleic Acids Res* 43, D512-520.
- Hossain, M.I., Roulston, C.L., Kamaruddin, M.A., Chu, P.W., Ng, D.C., Dusting, G.J., Bjorge, J.D., Williamson, N.A., Fujita, D.J., Cheung, S.N., *et al.* (2013). A truncated fragment of Src protein kinase generated by calpain-mediated cleavage is a mediator of neuronal death in excitotoxicity. *The Journal of biological chemistry* 288, 9696-9709.
- Hunter, T. (2009). Tyrosine phosphorylation: thirty years and counting. *Curr Opin Cell Biol* 21, 140-146.
- Kaneko, T., Huang, H., Cao, X., Li, X., Li, C., Voss, C., Sidhu, S.S., and Li, S.S. (2012a). Superbinder SH2 domains act as antagonists of cell signaling. *Sci Signal* 5, ra68.
- Kaneko, T., Joshi, R., Feller, S.M., and Li, S.S. (2012b). Phosphotyrosine recognition domains: the typical, the atypical and the versatile. *Cell Commun Signal* 10, 32.

- Kanner, S.B., Reynolds, A.B., and Parsons, J.T. (1989). Immunoaffinity purification of tyrosine-phosphorylated cellular proteins. *J Immunol Methods* *120*, 115-124.
- Kanner, S.B., Reynolds, A.B., Vines, R.R., and Parsons, J.T. (1990). Monoclonal antibodies to individual tyrosine-phosphorylated protein substrates of oncogene-encoded tyrosine kinases. *Proc Natl Acad Sci U S A* *87*, 3328-3332.
- Kreutzman, A., Ladell, K., Koechel, C., Gostick, E., Ekblom, M., Stenke, L., Melo, T., Einsele, H., Porkka, K., Price, D.A., *et al.* (2011). Expansion of highly differentiated CD8+ T-cells or NK-cells in patients treated with dasatinib is associated with cytomegalovirus reactivation. *Leukemia* *25*, 1587-1597.
- Lee, H.H., Tien, S.C., Jou, T.S., Chang, Y.C., Jhong, J.G., and Chang, Z.F. (2010). Src-dependent phosphorylation of ROCK participates in regulation of focal adhesion dynamics. *Journal of cell science* *123*, 3368-3377.
- Levitzki, A. (2013). Tyrosine kinase inhibitors: views of selectivity, sensitivity, and clinical performance. *Annu Rev Pharmacol Toxicol* *53*, 161-185.
- Lim, W.A., and Pawson, T. (2010). Phosphotyrosine signaling: evolving a new cellular communication system. *Cell* *142*, 661-667.
- Lin, C., Ear, J., Pavlova, Y., Mittal, Y., Kufareva, I., Ghassemian, M., Abagyan, R., Garcia-Marcos, M., and Ghosh, P. (2011). Tyrosine phosphorylation of the Galpha-interacting protein GIV promotes activation of phosphoinositide 3-kinase during cell migration. *Sci Signal* *4*, ra64.
- Manning, G., Whyte, D.B., Martinez, R., Hunter, T., and Sudarsanam, S. (2002). The protein kinase complement of the human genome. *Science* *298*, 1912-1934.
- Mayer, E.L., and Krop, I.E. (2010). Advances in targeting SRC in the treatment of breast cancer and other solid malignancies. *Clin Cancer Res* *16*, 3526-3532.
- Nakai, T., Nagai, T., Tanaka, M., Itoh, N., Asai, N., Enomoto, A., Asai, M., Yamada, S., Saifullah, A.B., Sokabe, M., *et al.* (2014). Girdin phosphorylation is crucial for synaptic plasticity and memory: a potential role in the interaction of BDNF/TrkB/Akt signaling with NMDA receptor. *The Journal of neuroscience : the official journal of the Society for Neuroscience* *34*, 14995-15008.
- Omori, K., Asai, M., Kuga, D., Ushida, K., Izuchi, T., Mii, S., Enomoto, A., Asai, N., Nagino, M., and Takahashi, M. (2015). Girdin is phosphorylated on tyrosine 1798 when associated with structures required for migration. *Biochemical and biophysical research communications* *458*, 934-940.
- Oppermann, H., Levinson, A.D., Varmus, H.E., Levintow, L., and Bishop, J.M. (1979). Uninfected vertebrate cells contain a protein that is closely related to the product of the avian sarcoma virus transforming gene (src). *Proc Natl Acad Sci U S A* *76*, 1804-1808.
- Ott, V.L., and Rapraeger, A.C. (1998). Tyrosine phosphorylation of syndecan-1 and -4 cytoplasmic domains in adherent B82 fibroblasts. *The Journal of biological chemistry* *273*, 35291-35298.

- Reynolds, A.B., Kanner, S.B., Bouton, A.H., Schaller, M.D., Weed, S.A., Flynn, D.C., and Parsons, J.T. (2014). SRChing for the substrates of Src. *Oncogene* 33, 4537-4547.
- Rolland, T., Tasan, M., Charlotheaux, B., Pevzner, S.J., Zhong, Q., Sahni, N., Yi, S., Lemmens, I., Fontanillo, C., Mosca, R., *et al.* (2014). A proteome-scale map of the human interactome network. *Cell* 159, 1212-1226.
- Rual, J.F., Venkatesan, K., Hao, T., Hirozane-Kishikawa, T., Dricot, A., Li, N., Berriz, G.F., Gibbons, F.D., Dreze, M., Ayivi-Guedehoussou, N., *et al.* (2005). Towards a proteome-scale map of the human protein-protein interaction network. *Nature* 437, 1173-1178.
- Sanjay, A., Houghton, A., Neff, L., DiDomenico, E., Bardelay, C., Antoine, E., Levy, J., Gailit, J., Bowtell, D., Horne, W.C., *et al.* (2001). Cbl associates with Pyk2 and Src to regulate Src kinase activity, alpha(v)beta(3) integrin-mediated signaling, cell adhesion, and osteoclast motility. *The Journal of cell biology* 152, 181-195.
- Seet, B.T., Dikic, I., Zhou, M.M., and Pawson, T. (2006). Reading protein modifications with interaction domains. *Nat Rev Mol Cell Biol* 7, 473-483.
- Sefton, B.M., Hunter, T., Beemon, K., and Eckhart, W. (1980). Evidence that the phosphorylation of tyrosine is essential for cellular transformation by Rous sarcoma virus. *Cell* 20, 807-816.
- Stagljar, I., Korostensky, C., Johnsson, N., and te Heesen, S. (1998). A genetic system based on split-ubiquitin for the analysis of interactions between membrane proteins in vivo. *Proc Natl Acad Sci U S A* 95, 5187-5192.
- Stehelin, D., Fujita, D.J., Padgett, T., Varmus, H.E., and Bishop, J.M. (1977). Detection and enumeration of transformation-defective strains of avian sarcoma virus with molecular hybridization. *Virology* 76, 675-684.
- Tian, J., Cai, T., Yuan, Z., Wang, H., Liu, L., Haas, M., Maksimova, E., Huang, X.Y., and Xie, Z.J. (2006). Binding of Src to Na⁺/K⁺-ATPase forms a functional signaling complex. *Molecular biology of the cell* 17, 317-326.
- Tu, C., Ortega-Cava, C.F., Winograd, P., Stanton, M.J., Reddi, A.L., Dodge, I., Arya, R., Dimri, M., Clubb, R.J., Naramura, M., *et al.* (2010). Endosomal-sorting complexes required for transport (ESCRT) pathway-dependent endosomal traffic regulates the localization of active Src at focal adhesions. *Proceedings of the National Academy of Sciences of the United States of America* 107, 16107-16112.
- Yamaguchi, H., Woods, N.T., Dorsey, J.F., Takahashi, Y., Gjertsen, N.R., Yeatman, T., Wu, J., and Wang, H.G. (2008). SRC directly phosphorylates Bif-1 and prevents its interaction with Bax and the initiation of anoikis. *The Journal of biological chemistry* 283, 19112-19118.
- Yokouchi, M., Kondo, T., Sanjay, A., Houghton, A., Yoshimura, A., Komiya, S., Zhang, H., and Baron, R. (2001). Src-catalyzed phosphorylation of c-Cbl leads to the interdependent ubiquitination of both proteins. *The Journal of biological chemistry* 276, 35185-35193.

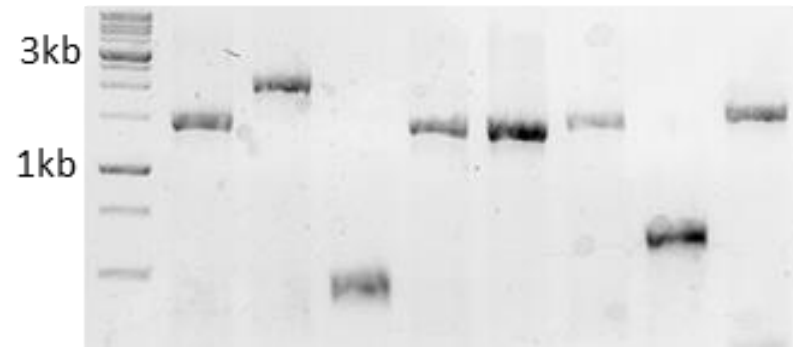
3.7 Supplemental data

Suppl. 3.1 Yeast toxicity and self-activation tests



Suppl. 3.2 SH2 binding affinities of selected Src phosphorylated peptides

Kd-TrM (μM)	Kd-WT (μM)	Gene	ID	pY site	Site sequence
0.08	0.05	Casp8	Q14790	Y380	TDSEEQPyLEMDLSS
0.07	0.41	RACK1	P63244	Y228	LNEGKHLyTLDGGDI
1.88	> 40	RACK1	P63244	Y246	LCFSPNRyWLCAATG
> 40	> 40	hnRNP K	P61978	Y72	IKALRTDyNASVSVP
0.67	3.08	hnRNP K	P61978	Y380	YAGGRGSyGDLGGPI
2.00	39.01	Src	P12931	Y419	RLIEDNEyTARQGAK
0.18	0.64	Src	P12931	Y530	FTSTEPQyQPGENL
12.89	> 40	tensin 3	Q68CZ2	Y1173	QDTSKFWyKADISRE
> 40	> 40	tensin 3	Q68CZ2	Y1206	SHSFRGyGLAMKVA
30.80	> 40	tensin 3	Q68CZ2	Y1256	KGCSNEPyFGSLTAL

Suppl. 3.3 AD insertion amplification in eight candidate positives

Suppl. 3.4 Protein IDs of candidate positive colonies

Entry name	Insertion size	Known pY site
ACO13_HUMAN	full length	N/A
AGR2_HUMAN	full length	4
AGR3_HUMAN	full length	1
ATP1B1_HUMAN	340bp to end	3
ATP1B3_HUMAN	682bp to end	N/A
CAN3_HUMAN	full length	N/A
CBLB_HUMAN	2449bp to end	1
CC112_HUMAN	343bp to end	N/A
CDC5L_HUMAN	1579bp to end	2
CH10_HUMAN	full length	2
CNTRL_HUMAN	349bp +1.1kb	4
DAAM1_HUMAN	2593bp to end	1
DERL2_HUMAN	full length	1
DNJC7_HUMAN	from 130bp to end	2
F118B_HUMAN	full length	2
FUND1_HUMAN	full length	2
GRDN_Human	2131bp+0.9kb	1
HINFP_HUMAN	205bp to end	2
HMMR_HUMAN	1690bp to end	1
HOME1_HUMAN	139bp to end	N/A
ID2_HUMAN	70bp to end	1
IFT81_HUMAN	1324bp to end	1
KCTD6_HUMAN	full length	N/A
MYCB2_HUMAN	7822bp +2kb	3
NIF3L_HUMAN	full length	2
OCAD1_HUMAN	208bp to end	5
ODF2L_HUMAN	802bp to end	N/A
PIMT_HUMAN	322bp/448bp to end	3
PNISR_HUMAN	1398bp to end	N/A
PSME2_HUMAN	full length	3
Q95HA6_HUMAN	full length	8
RBY1B_HUMAN	406bp to end	N/A
RM36_HUMAN	full length	N/A
ROCK1_HUMAN	1240bp+1.2kb	2
SDC2_HUMAN	142bp to end	3
SEPT7_HUMAN	535bp to end	3
SHLB1_HUMAN	505bp to end	N/A
SLFN5_HUMAN	full length	3
SPAT4_HUMAN	full length	N/A
SPRL1_HUMAN	1669 to end	N/A
SPZ1_HUMAN	559bp to end	N/A
SRPX_HUMAN	523bp to end	N/A
SUMO1_HUMAN	full length	N/A
TS101_HUMAN	full length	4
UACA_HUMAN	3050bp to end	1
UBP48_HUMAN	1120bp +1.2kb	1
UBR4_HUMAN	11248bp +2kb	3
XAGE1_HUMAN	full length	N/A
ZN266_HUMAN	667bp to end	2

Chapter 4

4 Summary and Perspectives

The human genome encodes around 500 protein kinases (Manning et al., 2002). The TK family consists of 90 members and tyrosine phosphorylation only contributes to around 5% of all protein phosphorylation (Ushiro and Cohen, 1980). However, the significance of TKs and pTyr-mediated signaling is not reflected by the abundance, particularly regarding cellular activities related to tumorigenesis and cancer malignance (Lim and Pawson, 2010). TKs are a major type of biomarker in many cancer types (Gharwan and Groninger, 2016; Hunter, 2009; Wu et al., 2015), and TK deregulation can occur in multiple ways: gene fusion (chromosomal translocation), gene amplification, mutation, truncation and overexpression. Moreover, abnormalities in other components within the pTyr-mediated signaling network also can alter the signaling outcome (Du and Lovly, 2018). Over the last two decades, more than half of all FDA approved anti-cancer targeted therapeutics are either small molecule TK inhibitors or RTK inhibition antibodies (Bhullar et al., 2018; Gharwan and Groninger, 2016; Twomey et al., 2017; Wu et al., 2015; Zhang et al., 2009). As introduced earlier, some TKs are well known biomarkers in specific cancer types, for example, ABL in leukemia, EGFR and ALK in lung cancer, and HER2 in breast cancer. It is intriguing that ABL, EGFR and ALK are also reported to be oncogenic in breast cancer, even though the corresponding frequencies are much lower, indicating these may not be the dominant TKs in driving tumorigenesis in breast tissue (Greuber et al., 2013; Hanna et al., 2015; Masuda et al., 2012; Siraj et al., 2015; Srinivasan and Plattner, 2006). Because many TKs stimulate cancer-related cellular activities via the same signaling pathways (MAPK/PI3K), it is not surprising that TK deregulation is able to transform cells in general. In TK inhibition therapy, functional redundancy likely contributes to intrinsic drug resistance and fast-developing acquired resistance in many cases reported in the clinic, as the inhibition of the primary TK biomarker could be compensated by the deregulation of non-target TKs (Lin and Shaw, 2016).

Targeted therapy experienced two breakthroughs in oncology in recent years. Unlike all previous approvals which limited the application of a targeted therapeutic to one or a few tumor types, the Trk inhibitor larotrectinib and a few PD-1 antibodies were approved as

tumor-type-agnostic therapeutics. Larotrectinib is the first selective small molecule pan-Trk (tropomyosin receptor kinases) inhibitor, which blocks the ATP-binding site of Trk receptors encoded by the NTRK (neurotrophic receptor tyrosine kinase) gene family (Drilon et al., 2018). Similar to ALK, Trks are normally expressed in human neuronal tissue and functions in the physiology of nervous system development, and the deregulation of Trks is mainly caused by gene fusions with many different fusion partners (Amatu et al., 2016). Trk gene fusions have been identified at high frequencies (up to or greater than 90%) in some rare cancer types, such as ETV6-NRTRK3 fusion in secretory breast carcinoma (Drilon et al., 2016), but at very low frequencies (commonly < 1%) in a wide variety of common cancer types (Amatu et al., 2016). It is estimated that 1,500 to 5,000 patients may carry a Trk gene fusion out of the 500,000 U.S. cancer patients diagnosed each year (Cocco et al., 2018; Khotskaya et al., 2017). The gold standard FISH assay has already been developed for the examination of Trk fusion, but the cost-to-benefit ratio is obviously not ideal due to the low frequency. In addition, FISH will require different sets of probes for different fusion partners, therefore NGS seems to be a more practical assay for examining Trk fusion, which could easily look for the genomic alternations of all TKs in a single test.

Although NGS is superior to IHC/FISH in multiplexing, the choice of examination methodology in clinical practice remains a matter of debate. Previously, the accuracy of IHC, FISH and NGS were investigated in the determination of ALK status in lung cancer. The conclusion was that NGS should be considered a supplementary test associated with IHC/FISH combined ALK testing, rather than the new gold standard method (Cabillic et al., 2014; Ilie et al., 2015; Niu et al., 2017; Pekar-Zlotin et al., 2015; Uguen et al., 2015). It is interesting that single-test-positive cases were reported in these studies (IHC⁺FISH⁻NGS⁻, IHC⁻FISH⁺NGS⁻, or IHC⁻FISH⁻NGS⁺), and ALK inhibition efficacy varied in the same subtype. This observation may not be simply due to the differential criteria or reproducibility of these assays, but also related to the imperfect correlation between mRNA/protein abundance and kinase signaling outcome. The ALK locus is a hotspot of chromosomal translocation, although the reason remains unclear. Over 30 ALK kinase domain-containing fusion proteins with at least 22 fusion partners have been reported in different cancer types (Hallberg and Palmer, 2013), but the most common FISH assay is

designed for EML-ALK which is frequent in lung cancer (Sasaki et al., 2010; Soda et al., 2007). At the protein level, the on-membrane ALK protein level can be regulated by a few proteins, including the oncogenic adaptor protein Numb, and two Numb isoforms act antagonistically to promote/inhibit ALK activity (Wei et al., 2019). In addition, it is expected that the presence of PTPs that decrease ALK phosphorylation, the adaptor SH2 proteins that mediate signaling transduction, and other components in MAPK/PI3K pathways would all be involved in the regulation of the ALK signaling outcome.

The SH2-AP-MS assay is an orthogonal method to current approaches, designed for the comprehensive evaluation of TK status. Compared to gene copy number or mRNA/protein abundance, the phosphorylation on activity-determining tyrosine residues could be a direct and more reliable indicator of TK activity. The loop-panel already contains two Trk activation loops (TrkA and TrkB/TrkC) and the full-panel adds four other non-loop pTyr sites from TrkA and TrkC. This assay could detect all types of TK deregulations in theory, which may be more accurate in examining TK biomarkers in some cases, for instance, when multiple TKs cooperate in driving tumorigenesis or a TK is deregulated at the post-translational level. To better evaluate TK status and signaling outcome, the MS detection panel may be further expanded, by including pTyr sites in adaptor and scaffold proteins (Good et al., 2011; Scott et al., 2005; Waterman et al., 2002), or pSer/pThr sites in TK downstream effectors (Cargnello and Roux, 2011).

With the advance in peptide separation and MS techniques, the SH2-AP-MS assay could become more sensitive and robust. The LC-MS tandem system is widely used in both targeted and discovery proteomics studies (Gross, 2004). However, liquid chromatography is powerful but imperfect for peptide separation, if this assay is applied for the examination of TK biomarker in the clinic. Many hydrophilic and hydrophobic peptides generated from enzymatic fragmentation of proteins are difficult to purify or separate, because they are either unretained or irreversibly bound by the reversed phase C18 sorbent. In generating the full-TK panel (Suppl.2.5), a few activation loops were eliminated from the list due to exceptional hydrophobicity. Considering that the activation loops are usually among the most intensively phosphorylated regions in TKs (Hornbeck et al., 2015), this could result in miss detection or false evaluation of TK status which is unacceptable in the clinic. Because the thoroughly optimized SH2-AP yields an uncomplicated peptide matrix,

commonly containing only tens or a few hundreds of peptides enriched from a minute amount of tissue, some other low-capacity peptide separation techniques could be used in the front end. Capillary electrophoresis (CE)-MS takes advantage of the high resolving power, sensitivity, robustness and fast separation speed of electrophoresis (Cai and Henion, 1995; Loo et al., 1989), which in theory will be more suitable in analyzing the SH2-AP enriched samples in the clinic.

In the SH2 superbinder modified Y2H, once the SH2-AP-MS is properly integrated for the identification of candidate positives, this system can be more practical and efficient in identifying direct TK substrates systematically. The comprehensive substrate profiling will not only expand our understanding of the pTyr-mediated signaling network, but also provide great opportunity in finding novel drug targets for some TKs previously considered as “less-druggable”. The success of mechanism-based drug development is reliant on the definition of the drug target. In cancer, the drug targets are typically proteins that are specific in cancer cells and function more significantly in tumorigenesis and malignance (Santos et al., 2016). As introduced, many TKs are ideal drug targets and the development of kinase inhibition therapeutics is straight forward and well-established. Some TK inhibition therapies are exceptionally successful in the clinic. For example, CML patients treated by imatinib have a striking 10-year survival rate of 83.3%, while the 5-year survival rate was less than 30% before imatinib was approved (Hochhaus et al., 2017; Moen et al., 2007). In contrast, the inhibitors of the Src kinase, the first described oncogene which is determined to be highly oncogenic in many solid tumors, only exhibit promising efficacies in pre-clinical models (Hunter and Sefton, 1980; Mayer and Krop, 2010; Sefton et al., 1980). The poor clinical performance is likely related to high protein similarity within the Src family. The application of Src inhibitors usually also blocks Src family members which are active in immune cells, resulting in the inhibition of patient immune resistance against tumor cells or even rendering patients vulnerable to infections (Elias and Ditzel, 2015; Kreutzman et al., 2011). In theory, the efficacy of these less-selective therapeutics can be dramatically improved by targeted drug delivery. In the case of Src inhibition in solid tumors, one possible strategy is nanonizing the inhibitor or conjugate the inhibitor to nano-sized carrier. Taking advantage of the enhanced permeability and retention (EPR) effect, the intravenously administered nano-sized drug could passively accumulate in the

advanced-stage solid tumors via passing the “leaky” vessels (Matsumura and Maeda, 1986). However, the efficiency of EPR is still controversial and drug nanonization strategy is not well established (Danhier, 2016; Nichols and Bae, 2014). Alternatively, since the development of a highly selective Src inhibitor remains challenging, it is perhaps more practical to look for “druggable” targets from Src direct substrates or associated proteins which are more specific in cancer cells and essential for Src transformation ability.

4.1 References

- Amatu, A., Sartore-Bianchi, A., and Siena, S. (2016). NTRK gene fusions as novel targets of cancer therapy across multiple tumour types. *ESMO Open* 1, e000023.
- Bhullar, K.S., Lagaron, N.O., McGowan, E.M., Parmar, I., Jha, A., Hubbard, B.P., and Rupasinghe, H.P.V. (2018). Kinase-targeted cancer therapies: progress, challenges and future directions. *Mol Cancer* 17, 48.
- Cabillic, F., Gros, A., Dugay, F., Begueret, H., Mesturoux, L., Chiforeanu, D.C., Dufrenot, L., Jauffret, V., Dachary, D., Corre, R., *et al.* (2014). Parallel FISH and immunohistochemical studies of ALK status in 3244 non-small-cell lung cancers reveal major discordances. *J Thorac Oncol* 9, 295-306.
- Cai, J., and Henion, J. (1995). Capillary electrophoresis-mass spectrometry. *Journal of Chromatography A* 703, 667-692.
- Cargnello, M., and Roux, P.P. (2011). Activation and function of the MAPKs and their substrates, the MAPK-activated protein kinases. *Microbiol Mol Biol Rev* 75, 50-83.
- Cocco, E., Scaltriti, M., and Drilon, A. (2018). NTRK fusion-positive cancers and TRK inhibitor therapy. *Nat Rev Clin Oncol* 15, 731-747.
- Danhier, F. (2016). To exploit the tumor microenvironment: Since the EPR effect fails in the clinic, what is the future of nanomedicine? *J Control Release* 244, 108-121.
- Drilon, A., Laetsch, T.W., Kummar, S., DuBois, S.G., Lassen, U.N., Demetri, G.D., Nathanson, M., Doebele, R.C., Farago, A.F., Pappo, A.S., *et al.* (2018). Efficacy of Larotrectinib in TRK Fusion-Positive Cancers in Adults and Children. *N Engl J Med* 378, 731-739.
- Drilon, A., Li, G., Dogan, S., Gounder, M., Shen, R., Arcila, M., Wang, L., Hyman, D.M., Hechtman, J., Wei, G., *et al.* (2016). What hides behind the MASC: clinical response and acquired resistance to entrectinib after ETV6-NTRK3 identification in a mammary analogue secretory carcinoma (MASC). *Ann Oncol* 27, 920-926.
- Du, Z., and Lovly, C.M. (2018). Mechanisms of receptor tyrosine kinase activation in cancer. *Mol Cancer* 17, 58.
- Elias, D., and Ditzel, H.J. (2015). The potential of Src inhibitors. *Aging (Albany NY)* 7, 734-735.
- Gharwan, H., and Groninger, H. (2016). Kinase inhibitors and monoclonal antibodies in oncology: clinical implications. *Nat Rev Clin Oncol* 13, 209-227.
- Good, M.C., Zalatan, J.G., and Lim, W.A. (2011). Scaffold proteins: hubs for controlling the flow of cellular information. *Science* 332, 680-686.
- Greuber, E.K., Smith-Pearson, P., Wang, J., and Pendergast, A.M. (2013). Role of ABL family kinases in cancer: from leukaemia to solid tumours. *Nat Rev Cancer* 13, 559-571.
- Gross, J.r.H. (2004). *Mass spectrometry : a textbook* (Berlin ; New York: Springer).
- Hallberg, B., and Palmer, R.H. (2013). Mechanistic insight into ALK receptor tyrosine kinase in human cancer biology. *Nat Rev Cancer* 13, 685-700.

- Hanna, M.G., Najfeld, V., Irie, H.Y., Tripodi, J., and Nayak, A. (2015). Analysis of ALK gene in 133 patients with breast cancer revealed polysomy of chromosome 2 and no ALK amplification. *Springerplus* 4, 439.
- Hochhaus, A., Larson, R.A., Guilhot, F., Radich, J.P., Branford, S., Hughes, T.P., Baccarani, M., Deininger, M.W., Cervantes, F., Fujihara, S., *et al.* (2017). Long-Term Outcomes of Imatinib Treatment for Chronic Myeloid Leukemia. *N Engl J Med* 376, 917-927.
- Hornbeck, P.V., Zhang, B., Murray, B., Kornhauser, J.M., Latham, V., and Skrzypek, E. (2015). PhosphoSitePlus, 2014: mutations, PTMs and recalibrations. *Nucleic Acids Res* 43, D512-520.
- Hunter, T. (2009). Tyrosine phosphorylation: thirty years and counting. *Curr Opin Cell Biol* 21, 140-146.
- Hunter, T., and Sefton, B.M. (1980). Transforming gene product of Rous sarcoma virus phosphorylates tyrosine. *Proc Natl Acad Sci U S A* 77, 1311-1315.
- Ilie, M.I., Bence, C., Hofman, V., Long-Mira, E., Butori, C., Bouhleb, L., Lalvee, S., Mouroux, J., Poudenx, M., Otto, J., *et al.* (2015). Discrepancies between FISH and immunohistochemistry for assessment of the ALK status are associated with ALK 'borderline'-positive rearrangements or a high copy number: a potential major issue for anti-ALK therapeutic strategies. *Ann Oncol* 26, 238-244.
- Khotskaya, Y.B., Holla, V.R., Farago, A.F., Mills Shaw, K.R., Meric-Bernstam, F., and Hong, D.S. (2017). Targeting TRK family proteins in cancer. *Pharmacol Ther* 173, 58-66.
- Kreutzman, A., Ladell, K., Koechel, C., Gostick, E., Ekblom, M., Stenke, L., Melo, T., Einsele, H., Porkka, K., Price, D.A., *et al.* (2011). Expansion of highly differentiated CD8+ T-cells or NK-cells in patients treated with dasatinib is associated with cytomegalovirus reactivation. *Leukemia* 25, 1587-1597.
- Lim, W.A., and Pawson, T. (2010). Phosphotyrosine signaling: evolving a new cellular communication system. *Cell* 142, 661-667.
- Lin, J.J., and Shaw, A.T. (2016). Resisting Resistance: Targeted Therapies in Lung Cancer. *Trends Cancer* 2, 350-364.
- Loo, J.A., Udseth, H.R., and Smith, R.D. (1989). Peptide and protein analysis by electrospray ionization-mass spectrometry and capillary electrophoresis-mass spectrometry. *Anal Biochem* 179, 404-412.
- Manning, G., Whyte, D.B., Martinez, R., Hunter, T., and Sudarsanam, S. (2002). The protein kinase complement of the human genome. *Science* 298, 1912-1934.
- Masuda, H., Zhang, D., Bartholomeusz, C., Doihara, H., Hortobagyi, G.N., and Ueno, N.T. (2012). Role of epidermal growth factor receptor in breast cancer. *Breast Cancer Res Treat* 136, 331-345.
- Matsumura, Y., and Maeda, H. (1986). A new concept for macromolecular therapeutics in cancer chemotherapy: mechanism of tumorotropic accumulation of proteins and the antitumor agent smancs. *Cancer Res* 46, 6387-6392.

- Mayer, E.L., and Krop, I.E. (2010). Advances in targeting SRC in the treatment of breast cancer and other solid malignancies. *Clin Cancer Res* 16, 3526-3532.
- Moen, M.D., McKeage, K., Plosker, G.L., and Siddiqui, M.A. (2007). Imatinib: a review of its use in chronic myeloid leukaemia. *Drugs* 67, 299-320.
- Nichols, J.W., and Bae, Y.H. (2014). EPR: Evidence and fallacy. *J Control Release* 190, 451-464.
- Niu, X., Chuang, J.C., Berry, G.J., and Wakelee, H.A. (2017). Anaplastic Lymphoma Kinase Testing: IHC vs. FISH vs. NGS. *Curr Treat Options Oncol* 18, 71.
- Pekar-Zlotin, M., Hirsch, F.R., Soussan-Gutman, L., Ilouze, M., Dvir, A., Boyle, T., Wynes, M., Miller, V.A., Lipson, D., Palmer, G.A., *et al.* (2015). Fluorescence in situ hybridization, immunohistochemistry, and next-generation sequencing for detection of EML4-ALK rearrangement in lung cancer. *Oncologist* 20, 316-322.
- Santos, R., Ursu, O., Gaulton, A., Bento, A.P., Donadi, R.S., Bologa, C.G., Karlsson, A., Al-Lazikani, B., Hersey, A., Oprea, T.I., *et al.* (2016). A comprehensive map of molecular drug targets. *Nature Reviews Drug Discovery* 16, 19.
- Sasaki, T., Rodig, S.J., Chirieac, L.R., and Janne, P.A. (2010). The biology and treatment of EML4-ALK non-small cell lung cancer. *Eur J Cancer* 46, 1773-1780.
- Scott, R.P., Eketjall, S., Aineskog, H., and Ibanez, C.F. (2005). Distinct turnover of alternatively spliced isoforms of the RET kinase receptor mediated by differential recruitment of the Cbl ubiquitin ligase. *J Biol Chem* 280, 13442-13449.
- Sefton, B.M., Hunter, T., Beemon, K., and Eckhart, W. (1980). Evidence that the phosphorylation of tyrosine is essential for cellular transformation by Rous sarcoma virus. *Cell* 20, 807-816.
- Siraj, A.K., Beg, S., Jehan, Z., Prabhakaran, S., Ahmed, M., A, R.H., Al-Dayel, F., Tulbah, A., Ajarim, D., and Al-Kuraya, K.S. (2015). ALK alteration is a frequent event in aggressive breast cancers. *Breast Cancer Res* 17, 127.
- Soda, M., Choi, Y.L., Enomoto, M., Takada, S., Yamashita, Y., Ishikawa, S., Fujiwara, S., Watanabe, H., Kurashina, K., Hatanaka, H., *et al.* (2007). Identification of the transforming EML4-ALK fusion gene in non-small-cell lung cancer. *Nature* 448, 561-566.
- Srinivasan, D., and Plattner, R. (2006). Activation of Abl tyrosine kinases promotes invasion of aggressive breast cancer cells. *Cancer Res* 66, 5648-5655.
- Twomey, J.D., Brahme, N.N., and Zhang, B. (2017). Drug-biomarker co-development in oncology - 20 years and counting. *Drug Resist Updat* 30, 48-62.
- Uguen, A., Talagas, M., Marcorelles, P., Gueguen, P., Costa, S., Andrieu-Key, S., and De Braekeleer, M. (2015). Next-Generation Sequencing and Immunohistochemistry as Future Gold Standard of ALK Testing in Lung Cancer? *Oncologist* 20, e24.
- Ushiro, H., and Cohen, S. (1980). Identification of phosphotyrosine as a product of epidermal growth factor-activated protein kinase in A-431 cell membranes. *J Biol Chem* 255, 8363-8365.

Waterman, H., Katz, M., Rubin, C., Shtiegman, K., Lavi, S., Elson, A., Jovin, T., and Yarden, Y. (2002). A mutant EGF-receptor defective in ubiquitylation and endocytosis unveils a role for Grb2 in negative signaling. *EMBO J* 21, 303-313.

Wei, R., Liu, X., Voss, C., Qin, W., Dagnino, L., Li, L., Vigny, M., and Li, S.S. (2019). NUMB regulates the endocytosis and activity of the anaplastic lymphoma kinase in an isoform-specific manner. *J Mol Cell Biol*.

Wu, P., Nielsen, T.E., and Clausen, M.H. (2015). FDA-approved small-molecule kinase inhibitors. *Trends Pharmacol Sci* 36, 422-439.

Zhang, J., Yang, P.L., and Gray, N.S. (2009). Targeting cancer with small molecule kinase inhibitors. *Nat Rev Cancer* 9, 28-39.

Curriculum Vitae

Xuguang Liu

Education

2012-2018 Ph.D Candidate, Biochemistry Department, Western University

2007-2010 MSc., Botany Department, The University of British Columbia

2001-2007 BSc/MSc., Life Science College, Wuhan University

Awards Received

1. 2018: Mitacs Accelerate Internship
2. 2015: Translation Breast Cancer Research Unit Scholarship
3. 2014: Translation Breast Cancer Research Unit Scholarship
4. 2013: Translation Breast Cancer Research Unit Scholarship
5. 2012: Translation Breast Cancer Research Unit Scholarship,

Publications

Wei, R., Kaneko, T., Liu, X., Liu, H., Li, L., Voss, C., Liu, E., He, N., and Li, S.S. (2018). Interactome Mapping Uncovers a General Role for Numb in Protein Kinase Regulation. *Mol Cell Proteomics* 17, 2216-2228.

Balasuriya, N., Kunkel, M.T., Liu, X., Biggar, K.K., Li, S.S., Newton, A.C., and O'Donoghue, P. (2018a). Genetic code expansion and live cell imaging reveal that Thr-308 phosphorylation is irreplaceable and sufficient for Akt1 activity. *J Biol Chem* 293, 10744-10756.

Balasuriya, N., McKenna, M., Liu, X., Li, S.S.C., and O'Donoghue, P. (2018b). Phosphorylation-Dependent Inhibition of Akt1. *Genes (Basel)* 9.

Bian, Y., Li, L., Dong, M., Liu, X., Kaneko, T., Cheng, K., Liu, H., Voss, C., Cao, X., Wang, Y., *et al.* (2016). Ultra-deep tyrosine phosphoproteomics enabled by a phosphotyrosine superbinder. *Nat Chem Biol* 12, 959-966.

Le, J., Liu, X., Yang, K.Z., Chen, X.L., Zou, J.J., Wang, H.Z., Wang, M., Vanneste, S., Morita, M., Tasaka, M., *et al.* (2014). Auxin transport and activity regulate stomatal patterning and development. *Nat Commun* 5, 3090.

Lee, E., Liu, X (co first)., Eglit, Y., and Sack, F. (2013). FOUR LIPS and MYB88 conditionally restrict the G1/S transition during stomatal formation. *J Exp Bot* 64, 5207-5219.

Liu, H., Galka, M., Mori, E., Liu, X., Lin, Y.F., Wei, R., Pittock, P., Voss, C., Dhami, G., Li, X., *et al.* (2013). A method for systematic mapping of protein lysine methylation identifies functions for HP1beta in DNA damage response. *Mol Cell* 50, 723-735.